The International PhD programme in Cardiovascular Pathophysiology and Therapeutics

MODI-AF

Echocardiography Markers Of myocardial tissue Deformation as Independent predictors of rhythm outcome after catheter ablation for Atrial Fibrillation

Left Atrial Structural and Functional Remodeling in Atrial Fibrillation

PhD thesis

Asim Katbeh. MD. FESC

MODI-AF

Echocardiography Markers Of myocardial tissue Deformation as Independent predictors of rhythm outcome after catheter ablation for Atrial Fibrillation

Left Atrial Structural and Functional Remodeling in Atrial Fibrillation

Asim Katbeh. MD. FESC

12/04/1983 Damascus, Syria

Promotor. Martin Penicka. MD. PhD. FESC

Cardiovascular Center OLV Aalst, Moorselbaan 164, Aalst 9300, Belgium

University Federico II of Naples, Faculty of Medicine, Via Pansini n. 5, 80131 Naples, Italy

Contents

Part 1

MODI-AF project

Chapter 1

Introduction and study protocol

Atrial fibrillation

For a long time, the pulse of patients was the only way to reach the heart. Irregular pulse was first described by the Andalusian Philosopher Moses Maimonides ten centuries ago. After him, William Stokes, Karel Frederik Wenckebach, and J. McKenckie described what we would today consider atrial fibrillation (AF) [1]. With the introduction of electrocardiogram by Willem Einthoven in 1901, AF was later clearly defined by him and Sir Thomas Lewis [1].

At present, AF is the most common cardiac arrhythmia with an estimated worldwide prevalence of 1.5–2.0% in the general population [2]. The incidence of AF is further predicted to increase twofold over the next decades owing mainly to a steadily aging population with growing burden of cardiovascular comorbidities [3]. Atrial arrhythmias, especially AF, are often associated with complex electrical and structural remodeling of the heart, which often lead to a deterioration in cardiac performance [4].

Catheter Ablation

The use of catheter ablation (CA) was first introduced in the late 1960s; it was designed first for recording, where the surgical treatment of the cardiac arrhythmia was the main concept [5]. In 1981, the concept of the transvenous catheter was first defined when a patient that was undergoing an electrophysiological recording following defibrillation, where a high-voltage discharge was emitted when the defibrillator electrode hit the catheter electrode at His. Direct current cardioversion was first used in AF ablation. The direct current was delivered to the distal electrode and a surface electrode; this led to uncontrollable tissue damage. In the 1990s, radiofrequency CA replaced the direct current [5].

Nowadays, the CA is a widely used therapy option for patients with symptomatic AF and it can safely performed with a higher success rate and results in significant clinical and functional improvements. However, management of patients undergoing AF ablation varies in daily practice and is incompletely defined by current guidelines [6]. Also, with the increasing number of ablation modalities available, the CA practices may further vary between centres [6].

Left atrial mechanics

Myocardial atrial contraction is a complex process that involves shortening and thickening of atrial cardiomyocytes. Left atrium (LA) is the most posterior of the cardiac chambers. Blood coming from the lungs enters the posterior part of the LA by the four pulmonary veins, then

passes in the vestibule, which is the outlet part of the atrial chamber surrounding the mitral orifice [7]. The LA function shows phasic variations during different periods of the cardiac cycle. The LA function as a receiving and dilating chamber during ventricular systole, allowing uninterrupted flow to arrive into the atrium even when the mitral valve is closed. In early diastole, blood flow rotation ceases in the LA as the body of blood drops into the left ventricule (LV) cavity. In late diastole, the onset of atrial contraction redirects LA flow toward the LV outflow region [7].

Myocardial functional imaging markers

For many decades, standard echocardiography has still been considered the first-line tool for myocardial function description. Nowadays, Speckle Tracking Echocardiography (STE) is a non-invasive method that allows the assessment of the global and regional function of both the ventricles and the atria, independently of the angle of insonation [8,9] STE is based on the observation that the interaction between the ultrasound beam and the myocardium generates acoustic markers, defined speckle, which can be tracked in their displacement during the cardiac cycle. Atrial strain measured by SLE is angle-independent, thus overcoming Doppler limitations. 2D-STE is performed from 4- and 2-chamber apical views and evaluated in accordance to the recommendations described in the consensus document of the EACVI/ASE/Industry task force [10]. Importantly, two longitudinal strain parameters of the LA are recognized: the atrial reservoir strain, measured at the end of the atrial reservoir phase, and the atrial contraction strain, identified just before the start of the active atrial contraction [10]. Strain is calculated as the average value from all LA segments.

The assessment of atrial remodeling by SLE adds a clincial value, especially in patients with atrial arrhythmias and diastolic dysfunction [7-9]. Furthermore, a great effort is made to classify atrial cardiomyopathy based on strain derived indices to provide enhanced diagnostic accuracy beyond conventional echocardiographic measures [7-9]. Focucing on patterns of atrial longitudinal strain beyond volume is the key factor to define phyentypes of atrial mechanics and to determine stages of atrial cardiomyopathy [8,9]. Many studies demonstrating that LA strain can detect impairment of LA function without LA enlargement and has incremental predictive value for AF over LA enlargement in a variety of cardiac conditions [11-13].

LA strain has been proposed as more sensitive measure to detect subtle atrial dysfunction as compared with volume derived indices and it is preload dependent but to a lesser degree than LA volume [14,15]. Recently, it is proposed as an additional parameter to improve risk scoring systems for AF and other cardiac comorbidities [16-18]. Furthermore, recent studies reported that it may provide an overall better estimation of LV filling pressures than other non-invasive LV filling pressure ratios such as mitral E/e' average septal-lateral ratio [19-21]. Importantly, in patients with normal LV ejection fraction, LA strain presents a good correlation with LV end-diastolic pressure and demonstrate better agreement with the invasive reference than E/e' [22]. However, LA strain is determined not only by LV diastolic

function but also to a large degree by LV systolic function and the interaction between LA strain and LV global longitudinal strain should be considered [19]. On the other hand, atrial deformation analysis brings some difficulties compared to ventricles and many considerations should be given to improve the functional quantification of the atrial myocardium [10,22]. Today, the measurement of LA phasic strain becomes an automatic process which keeps the benefits continuous in this clinical field [23,26].

It has been hypothesized that the use of multiple bio-imaging markers, specifically in patients with cardiac comorbidities such as heart failure (HF), could be more beneficial than the use of a single parameter. Pulsed and tissue Doppler assessments are useful tools to estimate LV filling pressure and diastolic dysfunction but these tools need to be enriched with LA evaluation in terms of morphology and function [24]. Recently, LA reservoir strain is proposed as an additional parameter to improve the European Society of Cardiology HFA-PEFF risk scoring system for the diagnosis of HF with preserved ejection fraction (HFpEF) in the presence of AF versus the absence of AF [25]. Furthermore, the combination of Tissue Doppler indices, LV gloabl strain and LA phasic strian could bring more benefits for risk stratification and patient selection for early treatment of AF [26,27].

In the same context, it has been hypothesized that not only an increased LA volume but also LA functional changes, as a consequence of myocardial fibrosis induced by chronic disorders or procedure-related factors might contribute to a reduction in LA reverse remodeling following sinus rhythm restoration [14]. Little is known, however, about how myocardial fibrosis occurring in chronic AF and/or HF are related to measurable functional changes by SLE and to which extent LA functional parameters have prognostic and diagnostic value.

Many studies have been investigated the association of AF recurrence with LA strain [28-30]. In all of these studies, there was a close relationship between AF recurrence and decreased LA strain and patients with non-severe imapired LA strain would benefit more from AF ablation [28-30]. Recent meta-analysises have suggested that LA enlargement and reduced LA function in the form of strain and emptying fraction are powerful predictors of AF ablation failure [31,32]. The pooled analysis showed that patients with reduced LA function at the time of CA had more AF recurrence during follow-up compared to those with preserved LA function, and LA strain and LA emptying fraction were significantly lower in the AF recurrence group compared with the no recurrence group [32]. However, in current clinical practice there are no predefined cut-offs of LA dimension and function able to guide physicians in selection of patients for CA.

In the last decade, several studies have reported that, in the case of failing recovery of atrial function, there is an increased risk of AF recurrence [33-35]. Furthermore, a recent study has shown that inhomogeneous timing of LA contraction, presented as mechanical dispersion which can be detected by strain curve, may be more sensitive than LA strian to predict AF recurrence after CA [36]. Moreover, this parameter could be used to describe the complex myocardial changes associated with AF or related to ablation technics. However, it remains

unclear if LA strain will add a clinical value over the traditional echocardiographic markers to predict the outcome in this clinical scenario. In fact, the impact of earlier markers of LA reverse remodeling on post-ablation outcome requires further research.

The reference values for atrial strain are determined in several studies [37-39]. According to EACVI NORRE study, the lowest expected values of LA function were 26.1%, 12.0% and 7.7% for LA reservoir, conduit and contraction strain respectively [37]. Other recent published systematic review reported that normal reference range for reservoir strain of 39% (95% CI, 38%-41%), for conduit strain of 23% (95% CI, 21%-25%), and for contractile strain of 17% (95% CI, 16%-19%) [38]. On the other hand, LA strain across vendors was investigated in two recent studies [40,41]. Both studies demonstrated that the LAS across vender platforms are not recommended and although the variation among multi vendors was small, it should be considered in performing serial studies [40,41]. Since the current lack of consensus on normal reference values and vendor independence remains, more attention should be considered when we describe the SLE-derived strain as a part of echocardiographic atrial assessment.

Study background and protocol

AF recurrence is common post catheter ablation [1-5]. AF recurrence is associated with symptomatic deterioration, thromboembolic events, hospital admissions and worse prognosis [6-9]. Therefore, definition of an accurate and easily obtainable predictor of AF recurrence is of crucial importance.

AF is associated with left atrial (LA) structural remodeling and functional deterioration due to a variable degree of myocardial hypertrophy, disarray, apoptosis and fibrosis [4,14,16]. In clinical practice, M mode and B mode echocardiography-derived indices of LA size are routinely used to assess left atrium (LA) [10]. However, these parameters have important limitations to describe complex myocardial changes associated with AF [11].

Speckle tracking is an echocardiographic technique which has gradually gained relevance in the last decade. Quantification of myocardial deformation based on SLE overcomes most of the limitations of classic echocardiography and provides an early detection of myocardial funticonal impairment. Today, its feasibility and usefulness to measure LA function are highly supported by literature and several studies demonstrated that STE could provide additional prognostic information beyond conventional echocardiographic parameters [12].

Recent advances in echocardiography equipment and image post-processing allow an assessment of LA strain and strain rate [12]. The speckle-tracking echocardiography (STE)-derived LA longitudinal strain has been shown to be an accurate and reproducible parameter to evaluate LA longitudinal shortening [13-16]. Furthermore, LA strain has significantly correlated with underlying LA fibrosis [16-19] (figure 1).

Figure 1A,1B: Example showed a model of LA myocardial fibrosis dervied from cardiac magnetic resonance image and curves of LA phasic strain and strain rate derived by SLE.

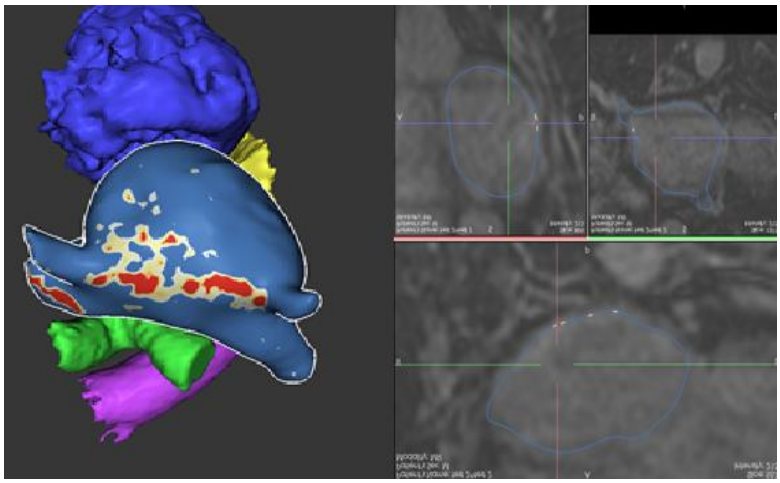

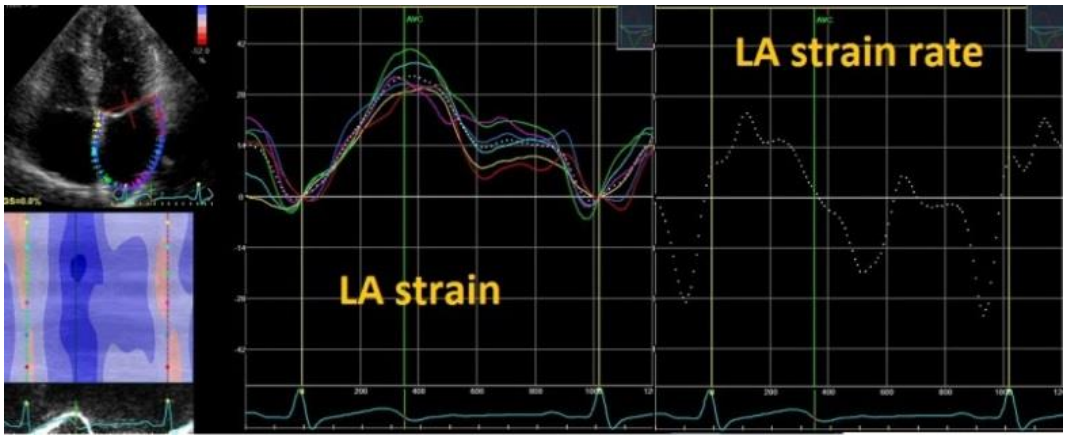

A recent standardization of speckle tracking analysis regarding all cardiac chambers supported the integration of STE in diagnostic and prognostic protocols in daily practice. This suggests that LA strain provides a comprehensive and quantitative assessment of LA structure and function. Hence, it is tempting to speculate that the analysis of LA strain will show high accuracy to predict AF recurrence post catheter ablation [20]. However, LA strain can be affected by several factors not related to LA structural damage such as loading conditions or arrhythmias [21,22]. Moreover, in the real-world setting, the value of LA strain to predict AF recurrence following catheter ablation is not known.

Therefore, the aim of the present study is fourfold:

(1. To evaluate feasibility of STE-derived strain assessment in patients undergoing catheter ablation for paroxysmal or persistent AF.

(2. To determine the acute effect of catheter ablation on LA structure and function.

(3. To define echocardiographic predictors of AF recurrence during long-term follow-up.

(4. To define the role of LA strain in the diagnosis of HFpEF in patients with history of AF.

Chapter 2

How to assess left atrial function in patients with paroxysmal atrial fibrillation undergoing first or redo catheter ablation

Background:

Both atrial fibrillation (AF) and catheter ablation (CA) may be associated with changes in left atrial (LA) structure and function. However, the data describing acute effects of CA on LA function are scarce.

Purpose:

To assess the potential value of different indices of LA morphology and function in patients with paroxysmal AF undergoing the first or the redo CA during sinus rhythm.

Methods:

We prospectively enrolled 114 consecutive patients (age 63±21 years, 32% females) with symptomatic paroxysmal AF and preserved left ventricular (LV) ejection fraction (≥ 50%) undergoing CA during sinus rhythm, and 23 age, sex matched healthy controls. Patients with valvular AF, reduced LV ejection fraction or in AF at the time of CA were excluded.

All patients underwent comprehensive echocardiography at one-day pre and at one-day post CA. The longitudinal component of LA reservoir, conduit and contractile strain (LAS) and strain rate (LASR) were assessed using the two-dimensional speckle tracking echocardiography as average of segmental values in apical views. Intra- and interobserver variability was assessed by two operators in 12 randomly selected patients.

Results:

A total of 88 (77%) patients underwent the first CA (First-CA) while the remaining 26 (23%) patients had the redo procedure (Redo-CA) after initially successful CA. Pre-ablation, both groups of patients with paroxysmal AF had significantly lower magnitude of all three components of LAS and LASR compared with controls (all $p < 0.01$). However, the Redo-CA versus the First-CA group showed significantly lower contractile LAS and LASR, reservoir LAS, and LA emptying fraction (all $p<0.05$). In contrast, all remaining indices of LA or LV size and function, including conduit LAS or LSR, were similar.

Catheter ablation was associated with significant decrease in contractile and reservoir LAS and LASR in both groups while no significant difference was observed for conduit LAS or

LASR. Out of the conventional parameters, LA emptying fraction significantly decreased while LA volume index and E/e' ratio significantly increased in both groups (all $p<0.05$).

Table 1: Comparison of physical characteristics and echocardiography parameters between group I (first time-ablation) and group II (redo-ablation) before ablation with control group.

Variables	Control group	AF group I (pre-ablation)	AF group II (pre-ablation)	P value
Age, y	55 ± 11	63 ± 9	59 ± 10	0.14
Males, n (%)	14 (60)	47 (63)	13 (59)	0.46
BMI	23.4 ± 4.2	26.9 ± 4	26.9 ± 3.9	0.02
HR	65 ± 7	64 ± 12	69 ± 10	0.85
LV end-diastolic diameter (cm)	4.8 ± 0.3	5.0 ± 0.6	5.0 ± 0.5	0.66
LV end-systolic diameter (cm)	3.2 ± 0.4	3.2 ± 0.5	3.3 ± 0.5	0.44
LV relative wall thickness	0.41 ± 0.05	0.45 ± 0.06	0.44 ± 0.05	0.06
LV mass index (g/m^2)	86 ± 18	93 ± 27	93 ± 20	0.16
LV end-diastolic volume index (mL/m^2)	52 ± 11	57 ± 13	56 ± 12	0.34
LV end-systolic volume index (mL/m^2)	20 ± 9	22 ± 8	21 ± 7	0.52
LV ejection fraction (%)	65.4 ± 6.7	63.05±6.1	62.69±7.8	0.47
LV global LS (%)	-21.3 ± 2.7	-19.2±2.6	-18.5±3.5	0.09
E/e' Ratio	6.9 ± 2.1	7.96±1.96	7.85±2.36	0.69
E/A Ratio	1.15±0.5	1.18±0.49	1.41±0.49	0.07
LA volume index (mL/m2)	26 ± 9	35 ± 8	34 ± 7	<0.01
LA reservoir LS (%)	37.02±7.23	27.01±6.94	23.14±8.46	<0.01
LA reservoir LSR (s^{-1})	1.66±0.37	1.28±0.28	1.17±0.37	<0.01
LA conduit LS (%)	19.45±6.02	14.32±4.49	13.88±5.30	<0.01
LA conduit LSR (s^{-1})	-1.73±0.61	-1.13±0.41	-1.10±0.42	<0.01
LA contractile LS (%)	16.25±0.63	13.58±5.08	10.09±4.10	<0.01
LA contractile LSR (s^{-1})	-2.1±0.35	-1.64±0.46	-1.31±0.49	<0.01

Table 2: Comparison of LA parameters in both group of catheters ablation (pre-ablation and post-ablation).

Variables	Group I (pre-ablation)	Group I (post-ablation)	P value	Group II (pre-ablation)	Group II (post-ablation)	P value
LA reservoir LS (%)	27.01±6.94	21.39±6.56	<0.001	23.14±8.46	19.75±7.47	0.006
LA reservoir LSR (s^{-1})	1.28±0.28	1.12±0.30	<0.001	1.17±0.37	0.96±0.23	0.001
LA conduit LS (%)	14.32±4.49	12.65±4.41	0.22	13.88±5.30	12.35±3.90	0.24
LA conduit LSR (s^{-1})	-1.13±0.41	-1.12±0.4	0.8	-1.10±0.42	-1.10±0.37	0.9
LA contractile LS (%)	13.58±5.08	9.26±3.63	<0.001	10.09±4.10	8.73±3.47	0.01
LA contractile LSR (s^{-1})	-1.64±0.46	-1.17±0.42	<0.001	-1.31±0.49	-1.09±0.42	0.008
LA volume index (mL/m^2)	35.49±7.2	38.71±7.84	0.001	34.32±8.11	37.54±8.69	0.015
LA emptying fraction (%)	53.7±10.74	48.41±11.51	<0.001	48.62±9.44	42.72±12.06	0.008
LA stiffness index	0.32±0.13	0.47±0.199	<0.001	0.39±0.22	0.46±0.26	0.13
LV ejection fraction (%)	63.05±6.11	63.02±5.12	0.29	62.69±7.88	62.54±7.12	0.91
LV global LS (%)	-19.2±2.61	-18.77±3.24	0.21	-18.59±3.49	-19.29±3.66	0.52
E/e' Ratio	7.96±1.96	9.13±2.22	0.01	7.85±2.36	8.57±2.22	0.16
E/A Ratio	1.18±0.49	1.42±0.52	0.01	1.41±0.49	1.45±0.47	0.14

Technical drawing and analysis of LA strain

The data on the accuracy of automated analysis of LA strain (LAS) are unavailable and despite standardization efforts, LAS is reported to be vendor specific. Furthermore, the level of agreement between 2D and 3D left atrial strain (LAS) and its correlates to 2D LVGLS has never been adequately studied. Therefore, we aimed to assess potential value of LA reservoir and contractile strain obtained with different vendors and to compare automated with manual LAS analysis in patients with atrial fibrillation (AF) undergoing CA during sinus rhythm. Secondly, to investigate the consistency between 3D and 2D LAS and to assess its relationship to 2D LVGLS.

A comparison of two vendors

We prospectively enrolled 60 consecutive patients (age:62±21 years, 66% male) with symptomatic AF and preserved left ventricular (LV) ejection fraction (≥ 50%) undergoing the first CA during sinus rhythm. All patients underwent comprehensive echocardiography at one day pre-CA and at one day post-CA (36 scanned by Philips and 24 scanned by GE). Reservoir and contractile LAS were assessed using the two-dimensional SLE as average of segmental values in four-chamber 4CH and 2CH apical views using the onset of QRS as a reference point. From 36 patients scanned by Philips, 14 subjects were scanned by GE in the

same time and LA strain was measured in LA data sets of different image quality using software packages from two companies (GE and TomTec).

CA was associated with significant decrease in magnitude of reservoir and contractile LAS in both groups of patients (all p<0.001) (figure 1A,1B), decrease of LA emptying fraction, and increase in LA volume index and LA stiffness index (table 1). Among all the indices of LA size and function, LA contractile strain showed the largest differences between the pre- and post-CA values in both groups of patients (p<0.001). Test-retest variability of reservoir and contractile LAS values showed no significant difference between the two vendors (figure 2).

Figure 1: Comparisons of the values of reservoir and contractile LA strain at pre-CA with values at post-CA in both groups.

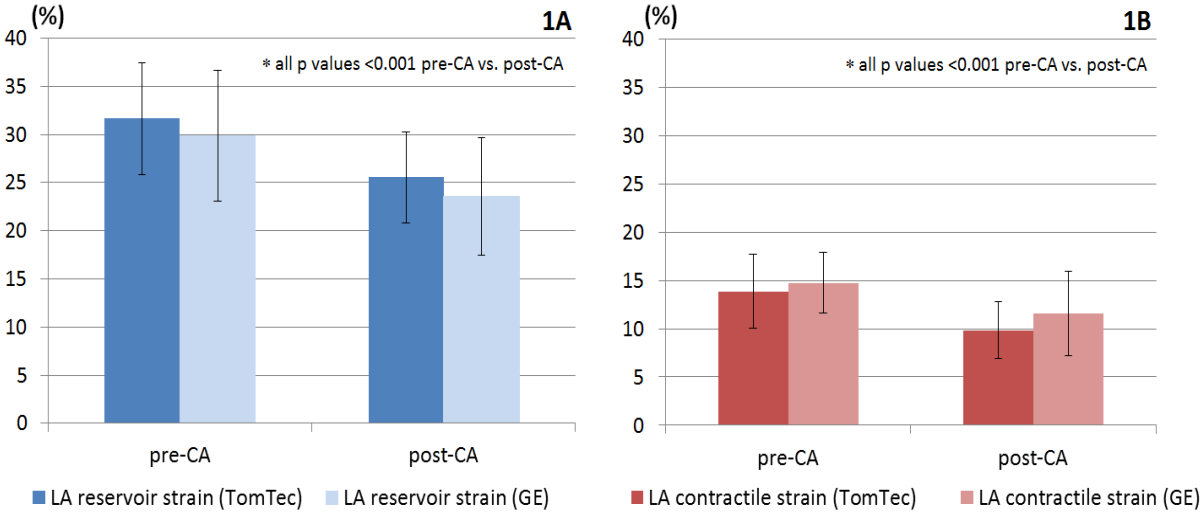

Figure 2: Correlation between values of LA reservoir strain (LASres) and contractile strain (LAScont) in 14 patients (13 at SR) scanned by the two vendors.

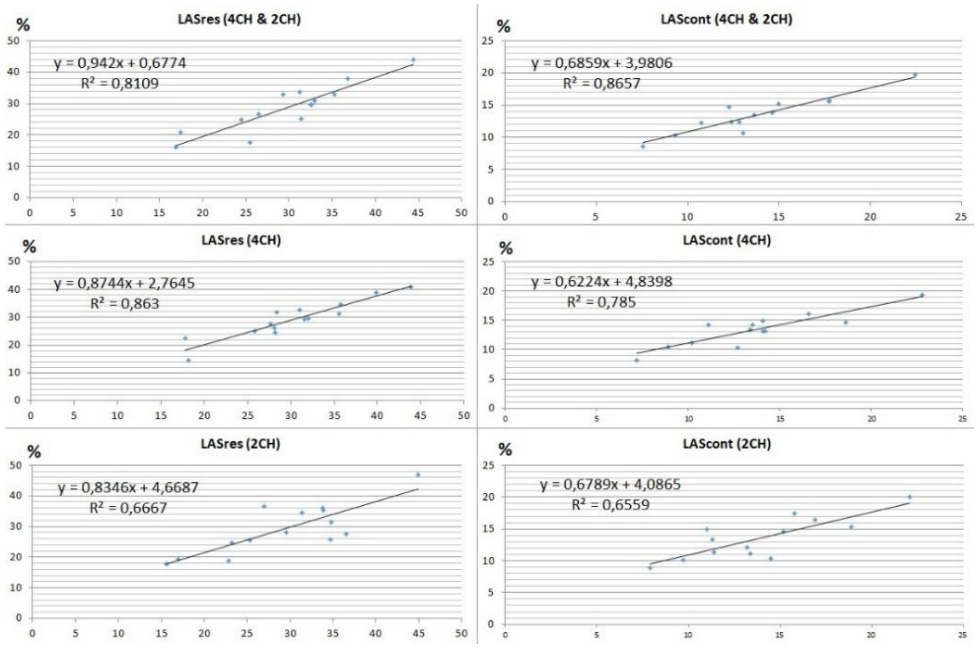

AutoStrain-derived LAS

We prospectively enrolled 36 consecutive patients (age:62±22 years, 33% female) with symptomatic AF and preserved left ventricular (LV) ejection fraction (≥ 50%) undergoing the CA during sinus rhythm. All patients underwent comprehensive echocardiography at 1-day pre-CA and at 1-day post-CA. Reservoir and contractile LAS were assessed using both the automated (AutoStrain LA; Philips, Andover, USA) and the manual technique as average of segmental values in apical 4CH view using the onset of QRS as a reference point.

Radio-frequency CA was associated with significant decrease in magnitude of reservoir and contractile LAS in all patients, and increase in LA end-systolic (max) and end-diastolic (min) volume index (all p<0.001) (figure 1). The correlation between (semi-) automated and manual LAS assessment was excellent (r ≥ 0.8) in all measurements (figure 2A,2B). The manual correction was needed in 7 out of 36 patients (19%). Despite this, the time needed to perform AutoStrain-derived analysis was significantly lower than the time needed for the manual LAS analysis (12±3 ms vs. 40±5 ms, p<0.01). Moreover, in 10 randomly selected patients, the AutoStrain showed significantly lower interobserver variability than the manual LAS analysis (3.1% vs. 6.7%, p<0.01).

Figure 1: Comparisons of the values of LA strain and volume indices at pre-CA with values at post-CA using automated software.

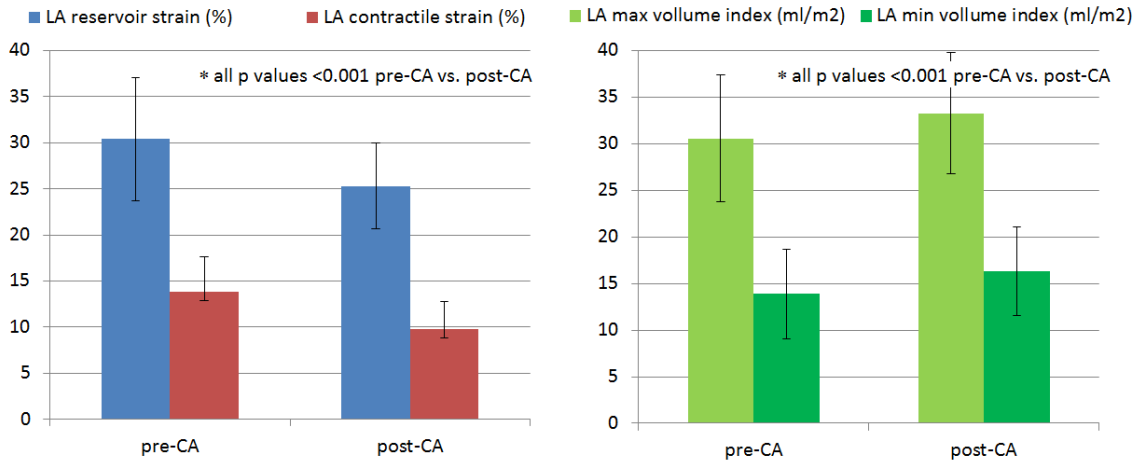

Figure 2A: The correlation between automated and manual analysis of reservoir and contractile LA strain (LAS) in 36 patients.

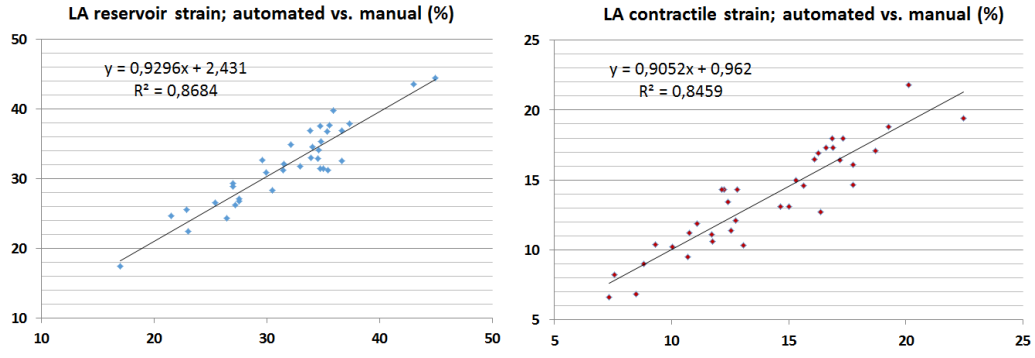

Figure 2B: Bland-Altman plots showing differences between inter- and intra-observer measurements of LA reservoir strain in 20 patients.

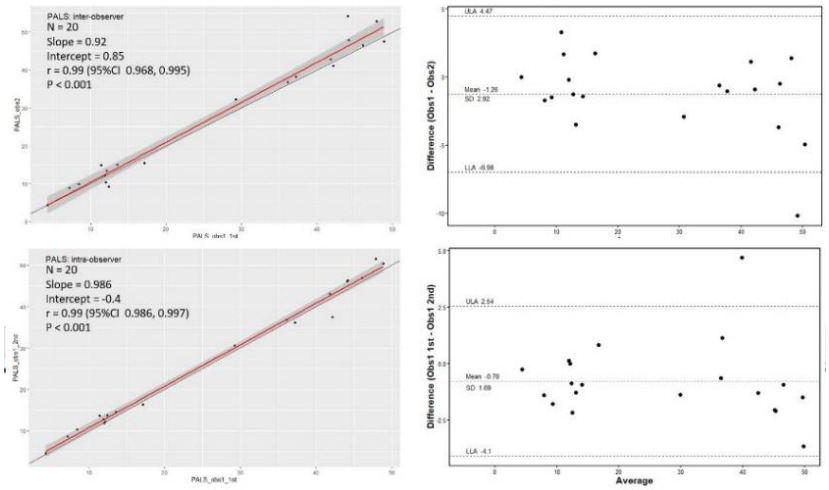

Comparison between 2D and 3D LA strain and its correlates to LV global longitudinal strain

We included 38 patients who have consecutively undergone 2D-and 3D-SLE. Reservoir, conduit and contractile LAS have been calculated from 2D acquisitions and 3D full volume data using semi-automatic quantification. 3D LAS analysis was feasible in 35 patients (92%) were appropriate for 3D tracking (Figure 1).

Figure 1: Image showing LAS reservoir (LASr), conduit (LAScd) and contractile (LASct) using semi-automatic 4DGE Left Atrial Quantification (LAQ).

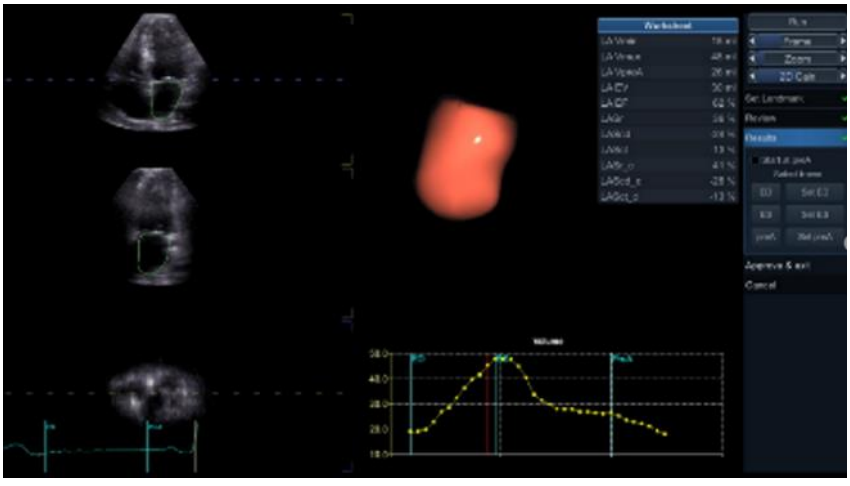

The correlation between 2D and 3D LA volume and strain in 35 patients. 2D and 3D LA strain (LAS) values present a moderate agreement which is related to technical considerations. Among the three LA phasic functional indices, LAS reservoir showed the best agreement.

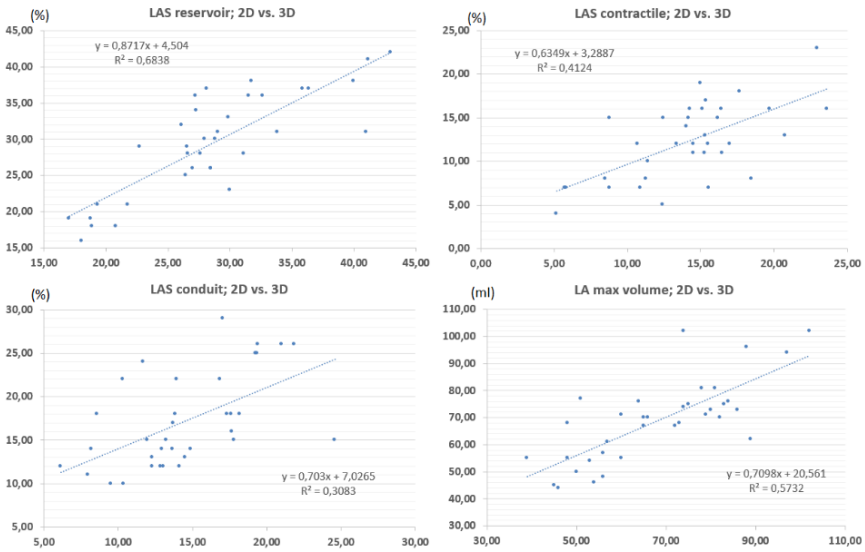

The correlation between 2D LV GLS, LA max volume and LA strain (LAS) reservoir, calculated from 2D acquisitions and 3D full volume data using semi-automatic quantification in 35 patients, was modest.

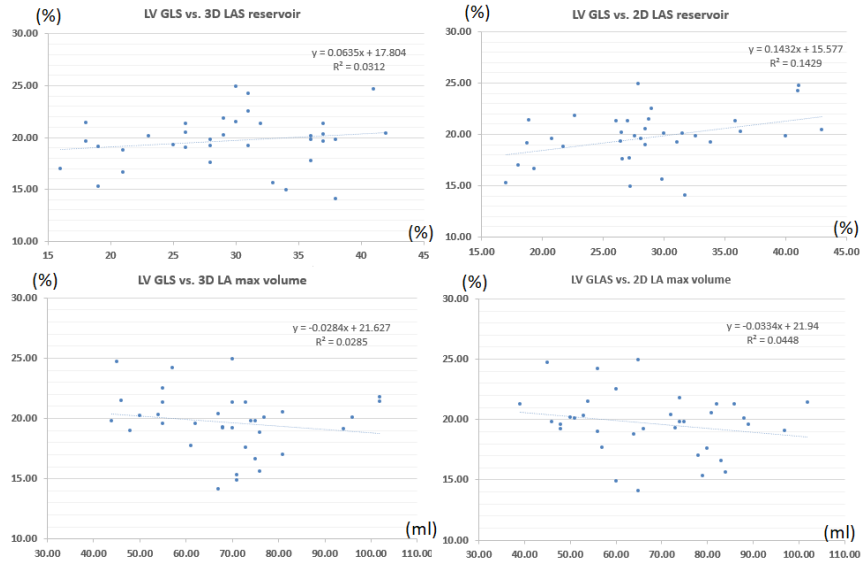

Conclusions:

Radio-frequency CA is associated with changes of LA structure and function. Reservoir LAS measured by 2D speckle tracking remains the most reproducible parameter to assess LA function. Although the variation among the two vendors was small, it should be considered in performing serial studies.

The AutoStrain-derived LAS analysis showed a high correlation with manual LAS analysis. Moreover, the AutoStrain technique was associated with significantly shorter analysis time and lower interobserver variability compared with the manual technique. Performance of 3D speckle tracking in the evaluation of LA reverse remodelling needs more invitagation.

Chapter 3

Catheter ablation during sinus rhythm is associated with acute loss of left atrial contractile function in paroxysmal atrial fibrillation

Background:

Catheter ablation is the recommended treatment in patients with paroxysmal atrial fibrillation (AF). However, the data on acute effects of catheter ablation on left atrial (LA) contractile function are scarce.

Purpose:

Firstly, to describe acute effects of catheter ablation on LA contractile function in patients with paroxysmal AF and in sinus rhythm at the time of ablation. Secondly, to assess potential value of different indices of LA morphology and function.

Methods:

We prospectively enrolled 50 consecutive patients (age:62±21 years, 56% female) with symptomatic paroxysmal AF and preserved left ventricular (LV) ejection fraction (≥ 50%) undergoing the first catheter ablation during sinus rhythm, and 23 healthy controls.

Patients with valvular AF, reduced LV ejection fraction or in AF at the time of ablation were excluded. All patients underwent comprehensive echocardiography at one day pre and at one day post ablation. The LA reservoir, conduit and contractile strain and strain rate (SR) were assessed using the two-dimensional speckle tracking echocardiography as average of segmental values in apical views.

Results:

Pre ablation, patients with paroxysmal AF had significantly lower magnitude of all three components of LA strain and SR compared with controls (all $p < 0.01$) (Figure 1A, 1B). Catheter ablation was associated with significant decrease in magnitude of all three components of LA strain and SR (all $p<0.05$) (Figure 1A,1B), decrease of LA emptying fraction (54±10% vs. 49±12%, $p<0.01$), and increase in LA stiffness index (0.32±0.12 vs. 0.45±0.14, $p<0.001$), LA volume index (36±8% vs. 38±8%, $p<0.01$), and E/e' ratio (8±2% vs. 9±2%, $p<0.01$). Among all the indices of LA size and contractile function, LA contractile strain and SR showed the largest differences between the pre- and post- ablation values ($p<0.01$).

Conclusion:

In paroxysmal AF, catheter ablation is associated with acute loss of LA contractile function in patients undergoing ablation during sinus rhythm. LA contractile strain and strain rate appear to be the most promising parameters to describe LA contractile function.

Figure 1: LA strain (1A) and strain rate (SR) (1B) in the control group and the AF (pre- and post-ablation).

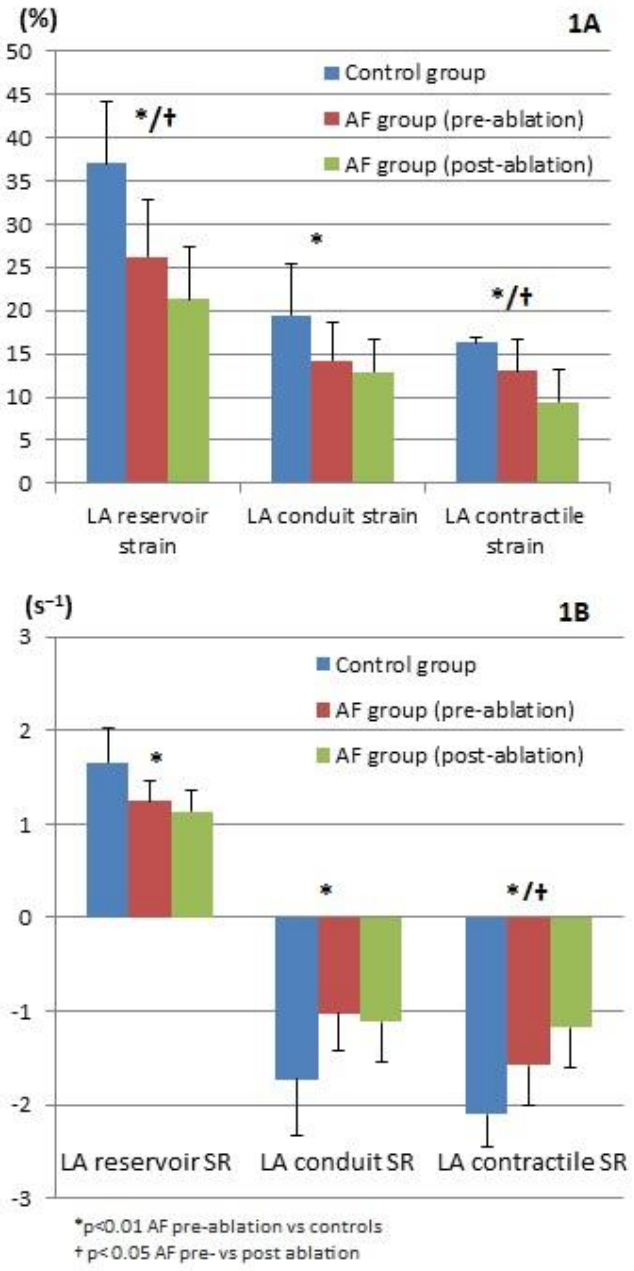

Chapter 4

Left atrial performance in patients with paroxysmal and long-standing persistent atrial fibrillation undergoing catheter ablation

Background:

Both atrial fibrillation (AF) and catheter ablation (CA) may be associated with changes in left atrial (LA) structure and function. However, the data describing acute and short-term effects of CA on LA contractile function in different types of AF are scarce. Therefore, the aim of the present study was to assess patterns of LA structural and functional remodeling in patients with paroxysmal or long-standing persistent AF undergoing first or redo CA.

Methods:

We prospectively enrolled 111 consecutive patients (age: 63±9 years, 35% females) with paroxysmal AF undergoing first (66%) CA (first-CA group) or redo (20%) CA (redo-CA group) during sinus rhythm, 15 individuals (14%) with long-standing persistent AF (PAP group) undergoing first CA during AF. All patients were symptomatic and had preserved (≥50%) left ventricular ejection fraction. Control group consisted of 23 healthy controls.

All patients underwent comprehensive transthoracic echocardiography one day pre-CA and one day post-CA, and at 3-month follow-up. The LA reservoir, conduit and contractile longitudinal strain (LAS) and strain rate (LASR) were assessed using two-dimensional speckle tracking echocardiography as average of segmental values in apical views.

Results:

Pre-CA, the largest LA volume index (44±15 ml/m²) was observed in the PAF group, followed by both groups of paroxysmal AF (35±8 ml/m²) and controls (24±10 ml/m²) ($p<0.001$). The lowest reservoir and contractile LAS were noted in the PAF group (13±5% and 0%), followed by the redo-CA group (22±6% and 9±4%), versus the first-CA group (27±8% and 13±4%) and controls (37±7% and 16±4%) ($p<0.001$). LASR followed similar trend. Post-CA, LA volume index showed acute small increase in all groups. Reservoir and contractile LAS and LASR decreased only in the first-CA group while they remained unchanged in the redo-CA group or even increased in the PAF group. At 3-month follow-up, LA volume index was reduced compared with baseline although significantly only in the PAF group. In contrast, LAS and LASR did not show uniform improvement in all AF groups and on average they remained significantly lower compared with controls ($p<0.01$).

Three distinct patterns of reservoir and contractile LAS were recognized. The concave (U) LAS pattern with an acute drop of LAS after CA and almost complete recovery during follow-up, which was observed mostly in the first-CA group. The flat LAS pattern without significant changes between examinations, which was characteristic mainly for the redo-CA group. The gradually improving LAS pattern, which was observed in the PAF group.

Conclusion:

LAS seems to be useful and powerful tool to monitor LA phasic function during CA. LAS shows distinct behavior in patients with different types of AF undergoing CA. The AF-type-specific LAS patterns reflect complex interaction between extent of LA remodeling and CA.

Introduction

Atrial fibrillation (AF) is a one of the major causes of cardiovascular morbidity in developed countries with steadily increasing prevalence (1). In selected patients, catheter ablation (CA) is recommended therapy to improve symptoms and to prevent AF recurrence (1). Both AF and CA are associated with left atrial (LA) structural and functional remodeling, which may determine the success of CA and AF recurrence (1-3). Thus, accurate assessment of LA structure and function is of crucial importance.

In clinical practice, Doppler echocardiography-derived indices of LA size, pulmonary vein or transmitral flow are routinely used for LA assessment. However, these parameters are not accurate to describe complex myocardial changes associated with AF and CA (4,5). Two-dimensional speckle tracking echocardiography-derived LA longitudinal strain (LAS) has emerged as an accurate and reproducible parameter to quantify LA longitudinal function (6,7). Low baseline LAS has been shown to predict AF reverse LA remodeling and AF recurrence after CA (8-12). Furthermore, LAS is inversely associated with LA fibrosis evaluated using magnetic resonance or electro-anatomical mapping (13-15). This suggests that LAS may provide a comprehensive and quantitative assessment of LA performance. However, data describing acute and short-term effects of CA on LA contractile function in different types of AF are scarce. Therefore, the aim of the present study was to assess patterns of LA structural and functional remodeling in patients with paroxysmal or long-standing persistent AF undergoing first or redo CA.

Methods

Design A prospective, observational and single-center study.

Patients All consecutive patients (n=212) with symptomatic AF undergoing elective CA between 10/2017 and 7/2018 were screened for eligibility according the following inclusion criteria: (1) paroxysmal or long-standing persistent AF; (2) preserved LV ejection fraction (≥ 50%). Patients with permanent or valvular AF, cardiomyopathy or congenital heart diseases, history of myocardial infarction or coronary revascularization, post cardiac surgery for any

cause, pacemaker, and reduced LV ejection fraction (< 50%) were excluded. The final study population consisted of 118 patients with paroxysmal AF undergoing first (81%) or redo (19%) CA during sinus rhythm, and 20 individuals with long-standing persistent AF undergoing first CA during AF. Control group consisted of 23 healthy controls. Study was approved by the Ethics Committee of our institution. Each patient signed informed consent before participating in the study.

Protocol All participants underwent extensive encircling pulmonary vein isolation guided by an electro-anatomical map using the Carto 3 mapping system (Biosense-Webster, CA, USA). History, physical examination and laboratory data were recorded during the admission for CA. Furthermore, all patients underwent comprehensive transthoracic echocardiography at 1-day pre-CA, at 1-day post-CA and at 3-month follow up. Patients were followed for 3 months. All hospitalizations, emergency room admissions or outpatients visit were recorded. Any suspicious symptoms or abnormal electrical activity recordings at Holter were adjudicated by an experienced interventional electrophysiologist. The AF recurrence was defined as any documented AF episode lasting ≥ 30 seconds that occurs after the first 3 months post-CA (1,16). In our study, a total of 13 patients (12%) had early AF recurrence after CA but we considered the period of the first 3 months after CA as a blanking period (16).

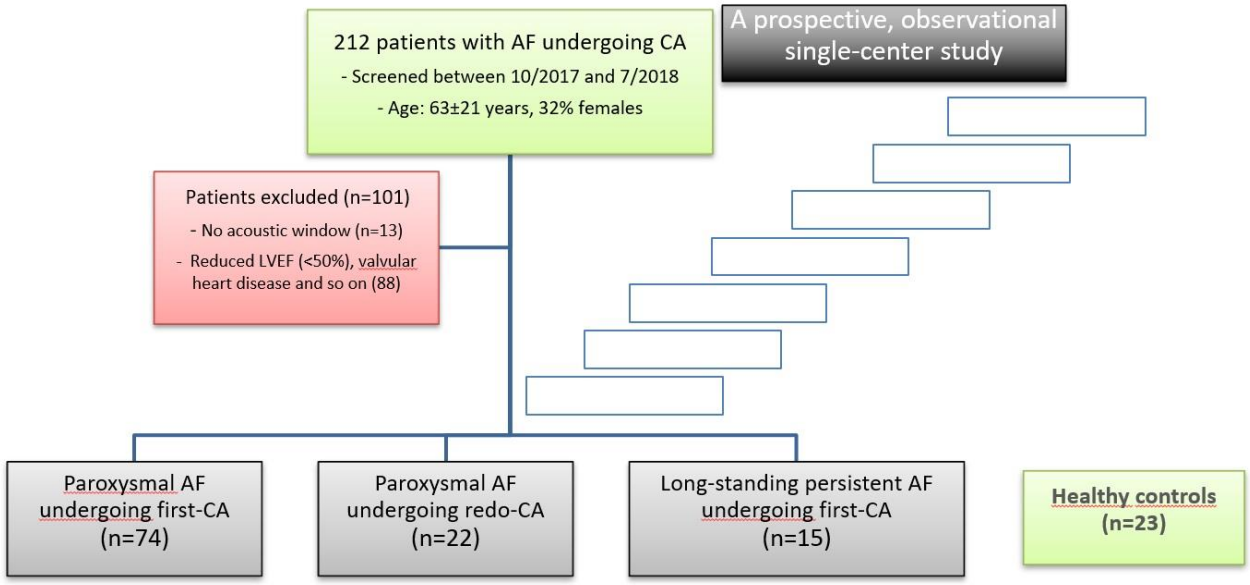

Doppler echocardiography A comprehensive 2D transthoracic echocardiographic examination was performed using Vivid E95 (GE HealthCare, Horten, Norway) ultrasound system. All acquired images were stored digitally for offline analysis using a commercially available software EchoPac (GE HealthCare). All examinations were recorded and analyzed by the same operator. Average of at least 3 beats (in sinus rhythm) or 5 beats (in AF) was

taken for each measurement. Blood pressure and heart rate was recorded during each examination. The biplane Simpson method was used to assess LV volumes and ejection fraction (4). LA antero-posterior diameter was measured at end-systole using the parasternal long-axis view (4). Maximum and minimum LA volume and LA emptying fraction were calculated from the apical 4- and 2-chamber views using the area-length method (4). Right atrial (RA) area and volume, and right ventricular (RV) end-diastolic basal and mid-cavity diameters were measured in the modified apical 4-chamber view (4). LV global longitudinal strain (GLS), RV GLS and free wall longitudinal strain, and RA reservoir strain (RASr) were assessed using speckle tracking technique in views optimized for each chamber and at frame rate of >60 FPS (4,17).

Assessment of longitudinal LAS and LASR was performed using speckle tracking echocardiography as recommended (17). In brief, optimized apical 4-, 3, and 2-chamber views were recorded during breath hold. LA endocardial borders were traced manually in all views. Region of interest was manually adjusted and tracking quality was previewed before generating LAS and LASR curves. The LA reservoir (LASr), conduit (LAScd) and contractile (LASct) longitudinal strain and strain rate (SR) were assessed as average of segmental values in apical 4- and 2-chamber views using the onset of QRS as a reference point (17). LA stiffness index was calculated as the E/e' divided by LASr. LA mechanical dispersion (MD) was derived as the standard deviation of time from the onset of QRS complex to peak positive LAS in 6 segments using the apical 4-chamber view (18). Furthermore, RA-LA MD was assessed as the standard deviation of time from the onset of P wave to peak negative LAS.

Intra- and inter-observer variability for indices of LA size and function was assessed by two operators in 12 randomly selected patients. The intra- and the inter-observer variability for LAS and LASR assessment were below 5%, which was lower than that of the conventional LA indices.

Statistical analysis

Data are expressed as mean ± SD for continuous variables and as counts or percentages for categorical variables. One-way or repeated measures ANOVA, unpaired or paired Student t-test, Pearson $\chi 2$ or Fisher exact tests were used as appropriate. Tukey-Kramer test was used for multiple comparisons. For all tests, values of $p<0.05$ were considered significant. Statistical analysis was performed using the SPSS version 23 (SPSS inc, Chicago, Illinois, USA) and the GraphPad Prism version 6.0 (GraphPad Software, San Diego, California, USA).

Results

The images quality for LAS analysis was suboptimal in 13 patients (feasibility 92%) and they were excluded. Additional 14 patients (10%) missed post-CA or follow-up echocardiography or withdrew informed consent. Final study population of 111 patients (63±9 years, 65% males) was divided into three groups. The first-CA group consisted of 74 patients (66%) with

paroxysmal AF undergoing the first CA. The redo-CA group consisted of 22 individuals (20%) with paroxysmal AF undergoing the redo CA. In both groups of patients with paroxysmal AF, both CA and all the echocardiographic recordings were performed during sinus rhythm. No clinical episode of AF was recorded within 4 weeks leading to CA. The PAF group consisted of 15 patients (14%) with long-standing persistent AF undergoing the first CA. In contrast to paroxysmal AF groups, PAF patients had both CA and pre-CA echocardiographic examination during AF while the post CA and follow-up echocardiography during sinus rhythm. The blood pressure did not show significant differences between groups or between different echocardiographic examinations.

Baseline clinical and echocardiographic characteristics are shown in Table 1. Compared with two groups of patients with paroxysmal AF, patients with PAF were significantly older, had higher NT Pro-BNP and lower MDRD (all $p < 0.05$). We observed significantly lower LV ejection fraction, LV GLS, TAPSE and RV GLS in the PAF versus the first-CA or the redo-CA group (all $p < 0.05$). RASr was highest in the first-CA group followed by the redo-CA and the PAF group (all $p < 0.01$). Table 2 shows indices of LA size and function in three groups. Patients with PAF had significantly larger LA volume and stiffness index, and lower LA emptying fraction compared with other two groups (both $p < 0.01$). The lowest LASr and LASct were observed in the PAF group (13±5% and 0%), followed by the redo-CA group (22±5% and 9±4%), the first-CA group (27±8% and 13±4%) and healthy controls (37±7% and 16±4%) ($p<0.001$). LASR followed similar trend. LA MD was significantly larger in the PAF versus the other two groups ($p<0.001$).

Acute effects of CA At 1-day post CA, all patients had sinus rhythm. We observed small acute increase of LA volume index in all groups (Figure 1A). LASr, LASct, LASRr and LASRct decreased only in the first-CA group. In contrast, they remained unchanged in the redo-CA group or increased in the PAF group (Figure 1B, 1C). LA MD increased in all groups (Figure 1D). In contrast, LV GLS did not show any significant differences compared with pre-CA (table 2).

At 3-month follow-up, LA volume index was slightly reduced compared with pre-CA in all groups but significantly only in the PAF group ($p<0.05$) (Figure 1A, Table 2). In contrast, LAS and LASR did not show uniform changes in all AF groups (Figure 1B, 1C, Table 2). In the first-CA group, LASr, LASct, LASRr and LASRct showed almost complete recovery to pre-CA values (all $p < 0.001$ versus post-CA). In the redo-CA group, no significant changes in LAS or LASR were observed between pre-CA, post-CA or 3-month follow up. In the PAF group, LAS and LASR showed gradual improvement with 3-month follow-up values approaching the ones observed in the redo-CA group. At follow up, patients in the first-CA group had significantly higher LAS and LASR compared with other two AF groups ($p<0.01$). Yet, LAS and LASR remained significantly lower than those observed in healthy controls ($p<0.001$). LA MD significantly decreased in the first-CA and PAF groups (both $p < 0.001$) while it slightly increased in the redo-CA group (NS).

Patterns of LAS

Figure 2 shows representative examples while figure 1B and 1C shows average values of LASr and LASct, respectively, in three groups of patients. Three distinct patterns of LAS were recognized. The concave (U) LAS pattern with an acute drop of LAS after CA and almost complete recovery during follow-up, which was observed mostly in the first-CA group. The flat LAS pattern without significant changes between examinations, which was characteristic for the redo-CA group. The gradually improving LAS pattern, which was observed in the PAF group.

Impact of age, gender, hypertension and metabolic risks factors on left atrial function

The effects of CA on LA function were analyzed in several subgroups of patients with paroxysmal AF undergoing the first CA. In the first sub-analysis, patients were divided into four groups according to the hypertension, dyslipidemia and diabetes mellitus. A total of 37 (50%) patients had hypertension with (n=18; 24%) or without (n=19, 26%) metabolic risks factors. The remaining 37 (50%) individuals had normal blood pressure with (n=11, 15%) or without (n=26, 35%) metabolic risks factors. All four groups of patients had concave LAS pattern characteristic for the first-CA group (Figure 3). Pre-CA, patients with hypertension and metabolic risks factors showed significantly lower LASr, LASct, LASRr and LASRct compared with other three groups (all $p < 0.05$). Post-CA, LAS and LASR significantly decreased in all groups (all $p<0.05$). At 3-month follow up, LAS and LASR showed almost complete recovery to pre-CA values in all groups. Yet, patients with metabolic risk factors had significantly lower LAS than metabolically healthy individuals ($p<0.05$). In different sub-analyses, at pre-CA, elderly (≥ 65 years old) patients and individuals with obesity (BMI ≥ 30kg/m²) or overweight (25 ≤ BMI < 30kg/m²) showed significantly lower LAS and LASR than younger ones with normal weight (all $p<0.05$). In obese patients, these differences remained significant also at follow-up. In contrast, elderly patients had similar follow-up LAS as younger ones (NS). No significant differences in LAS magnitude or pattern were noted between males and females.

Impact of LA size and function

A total of 34 (46%) patients had normal LA size (LAVI ≤ 34 mL/m²), while 18 (24%) had mild LA dilation (35 ≤ LAVI ≤ 41 mL/m²), and 22 (30%) had moderate LA dilation (LAVI ≥ 42 mL/m²). Similar LAS time course was observed in all three groups (Figure 4A). Although, patients with moderate LA dilation had significantly lower LASr throughout the study compared with subjects with less dilated LA. Patients with reduced (< 50%) versus preserved (≥ 50%) LA emptying fraction had lower LASr at each time point (all $p < 0.05$) while the LAS pattern was similar (Figure 4B).

Low versus high LASr at follow-up

In the first-CA group, a total of 25 (30%) patients had low follow-up LASr (< 22%), which was below the average pre-CA value in the redo-CA group. Out of these patients with low LASr at follow-up, 1 subject (1%) had flat LAS pattern with no CA-induced stunning suggesting insufficient CA, 8 patients (11%) had CA-induced stunning but no recovery of LASr between post-CA and follow-up despite absence of recurrent AF, and 16 patients (18%) had already low baseline LASr despite preserved concave pattern, which was typical for the first-CA group. Pre-CA, patients with lower versus higher LASr at follow-up had significantly higher BMI (29±6 kg/m² versus 26±3 kg/m², p = 0.005) and NT Pro-BNP (394±467 mg/ml versus 179±289 pg/ml, p = 0.034), lower MDRD (72±14 ml/min/1.73 m² versus 82±9 um/min/1.73 m², p = 0.003) and tended to have lower LV GLS (-18±3 % versus -20±3 %, p = 0.055). Pre-CA, LA volume index (34±6 versus 28±9 ml/m², p = 0.037) was larger while LA emptying fraction (52±11 % versus 59±9 %, p = 0.012) and LASr (23±7 % versus 31±6 %, p < 0.001) were lower in patients with low versus high LASr at follow-up. All other pre-CA characteristics were similar.

Discussion

In patients with paroxysmal or long-standing persistent AF undergoing the first- or the redo-CA we have found that: (1) Assessment of LAS was highly feasible and allowed for accurate quantification of LA phasic function in different subgroups of patients regardless of their clinical or imaging characteristics; (2) Both LASr and LASct appeared to be the most useful parameters to monitor (19) the three distinct patterns recognized in different types of AF, i.e. the concave pattern in the first-CA group, the flat pattern in the redo-CA group, and the improving pattern in the PAF group. Thus, each LAS pattern seems to reflect a specific stage of the LA remodeling process caused by complex interaction between AF and CA.

Assessment of LA phasic function AF is associated with LA structural remodeling and functional deterioration due to a variable degree of myocardial hypertrophy, disarray, apoptosis and fibrosis (2). Accurate assessment of extent of LA deterioration is important to guide therapeutic management. Several studies have shown high feasibility and reproducibility of LAS to detect early abnormalities of LA phasic function in patients with paroxysmal or persistent AF undergoing CA (7-12,17). Furthermore, low baseline LAS has been associated with AF recurrence and large extent of LA fibrosis detected using magnetic resonance or electro-anatomical mapping (13-15). Corroborating these results, we have shown high feasibility (91%) and reproducibility of LAS assessment using recommended speckle tracking technique (4,17). Pre-CA, LAS was significantly lower in patients with AF versus healthy controls. The lowest LAS was observed in persistent AF, followed by paroxysmal AF undergoing the redo CA and finally, the first CA. Moreover, in the present study, age, obesity, hypertension, metabolic risks factors and LA dilation were all associated with lower LAS. This suggests that LAS may accurately reflect the extent of LA structural damage induced by AF and CA (19-21). Out of all the indices of phasic LA function, LASr and LASct showed to be the most clinically useful to monitor LA function throughout the study.

Assessment of LASr may be superior to LASct because LASr can be measured also during AF rhythm, when LASct is negligible. Strain rate curve was noisy, which made the timing of phasic LA events challenging. In contrast, different components of phasic LA function were easily recognizable on LAS curve in the majority of patients. There is an ongoing debate whether LAS can provide incremental information over LV GLS. In patients with sinus rhythm and different LV disorders, LV end-diastolic pressure, LV end-systolic volume index and LV GLS have been shown to be independently associated with LAS (22,23). In contrast, we have not observed these relationships, i.e. LV GLS was similar in different types of AF or study time points while LAS showed significant changes. An explanation could be that, in contrast to previous reports, our study included patients with primary LA problem, i.e. non valvular AF, with preserved LV size and ejection fraction (22,23). This suggests that in AF undergoing CA, LASr may be a widely applicable tool to monitor LA function while providing incremental information over LV assessment.

Patterns of LA structural and functional remodeling

In all three groups of AF, LA volume index and mechanical dispersion showed acute increase, suggesting LA stunning, followed by decrease during follow up, reflecting LA reverse remodeling. LA MD has been recently introduced to measure intersegmental differences in shape of LAS curves reflecting the complex geometry and scarring of the LA (18,24). In paroxysmal AF, feature or speckle tracking – derived LA MD was associated with history of stroke or AF recurrence post CA, respectively (18,24). In contrast to LAVI and LA MD showing similar changes in all three groups, a AF-type specific time course of LASr and LASct was observed. Firstly, the concave LAS pattern, characterized by an acute decrease of LAS post CA followed by almost complete recovery to pre-CA values during follow up, was observed only in patients with paroxysmal AF undergoing the first CA. Exceptions to this pattern were noted in 14 (19%) patients, out of whom a total of 6 (8%) subject had no LA functional stunning and 8 (11%) individuals had no recovery during follow up. The remaining 60 (81%) showed the concave LAS pattern regardless of their clinical or imaging characteristics. LA stunning following electrical cardioversion of AF is a known phenomenon (25). However, we have demonstrated for the first time, that, CA during sinus rhythm leads to LA mechanical dysfunction. Secondly, the flat LAS pattern was observed in all subjects (100%) in the redo-CA group and in 6 (8%) patients in the first-CA group. The flat LAS pattern was characterized by only a minimal CA-induced decrease followed by a slight increase at follow-up. This pattern may reflect more extensive LA fibrosis associated with longer duration of AF and redo CA ablation. Finally, the improving LAS pattern with gradual increase of LAS at each time point from pre-CA to follow up was characteristic for patients with long-standing persistent AF. It is of note, that a small recovery of LASct was observed already at 1-day post CA despite combined effect of CA and electrical cardioversion followed by a large (225%) LASct increase during follow up. In fact, in the PAF group, follow-up LAS and LA MD approached values of these parameters observed in the redo-CA group despite persistently larger LA volume index. The first-CA group showed the highest LAS and the lowest LA MD at

follow up. This supports the hypothesis that both LAS and LA MD may reflect the extent of LA fibrosis induced by redo CA or by long-standing persistent AF (13-15,26).

Limitations

The analysis of LAS using speckle tracking may be vendor dependent, similarly to the LV GLS (4). However, inter-vendor variability affects absolute values of LAS rather than relative changes between serial examinations (4). In the present study, the same echo machine and analyzing software were used for all the analyses. This suggests that our findings may be extrapolated also to different vendors or software versions as long as the same equipment is used for serial assessment.

Conclusions

LAS seems to be useful and powerful tool to monitor LA phasic function during CA. LAS shows distinct behavior in patients with different types of AF undergoing CA. The AF-type-specific LAS patterns reflect complex interaction between extent of LA remodeling and CA. The potential role of these characteristic patterns to predict CA efficacy remains to be investigated in long-term study.

Figure 1. Time course of LA volume index (1A), reservoir LAS (1B), contractile LAS (1C) and LA mechanical dispersion (1D) in the First-CA, the Redo-CA and the PAF groups.

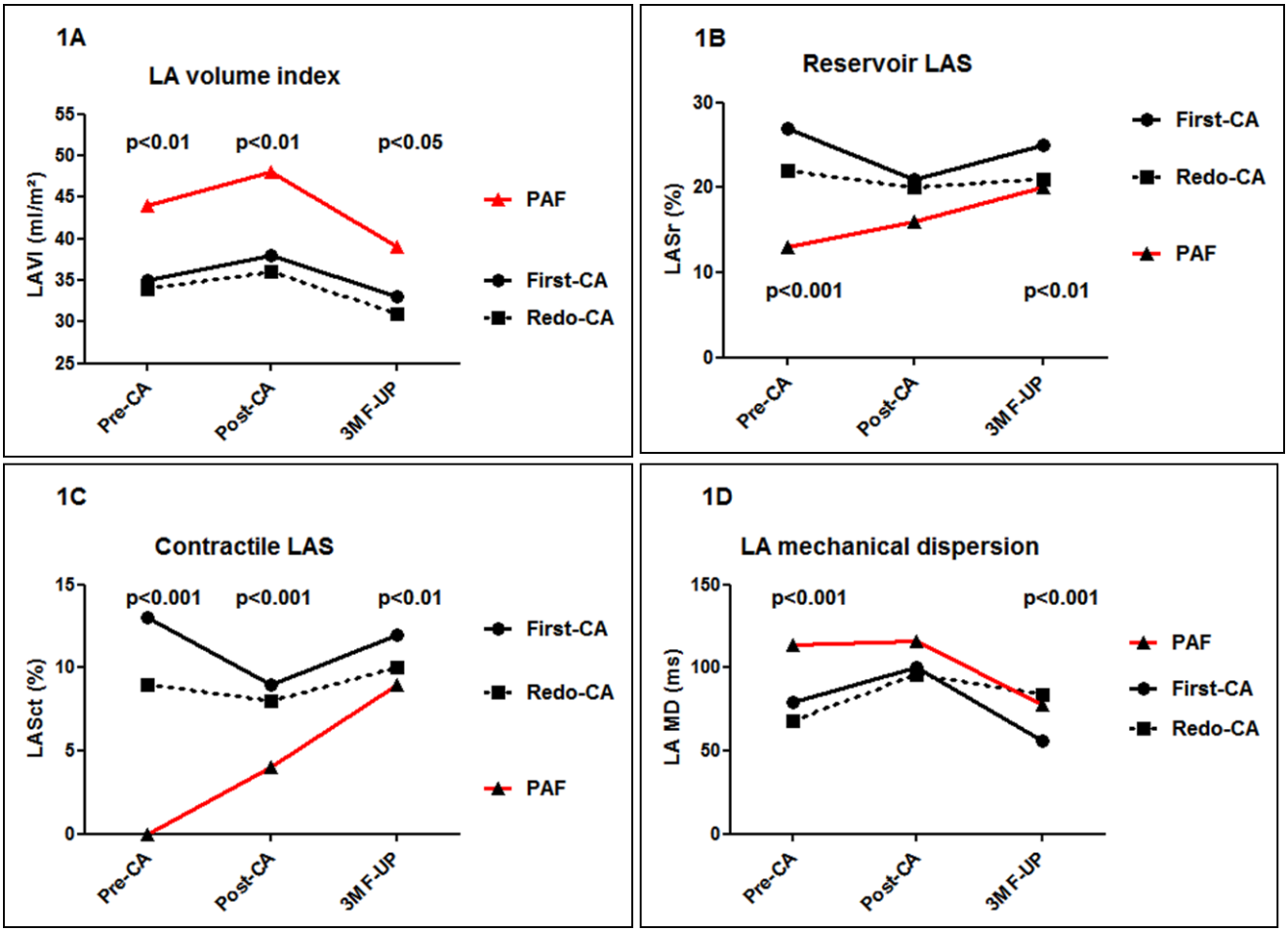

Figure 2. Individual examples of LAS from apical four chamber view at 1-day pre-CA (2A2D2G), at 1-day post-CA (2B2E2H) and at 3-month follow-up (2C2F2I) in the First-CA, (2ABC), the Redo-CA (2DEF) and the PAF (2GHI) groups. LASr = reservoir left atrial strain

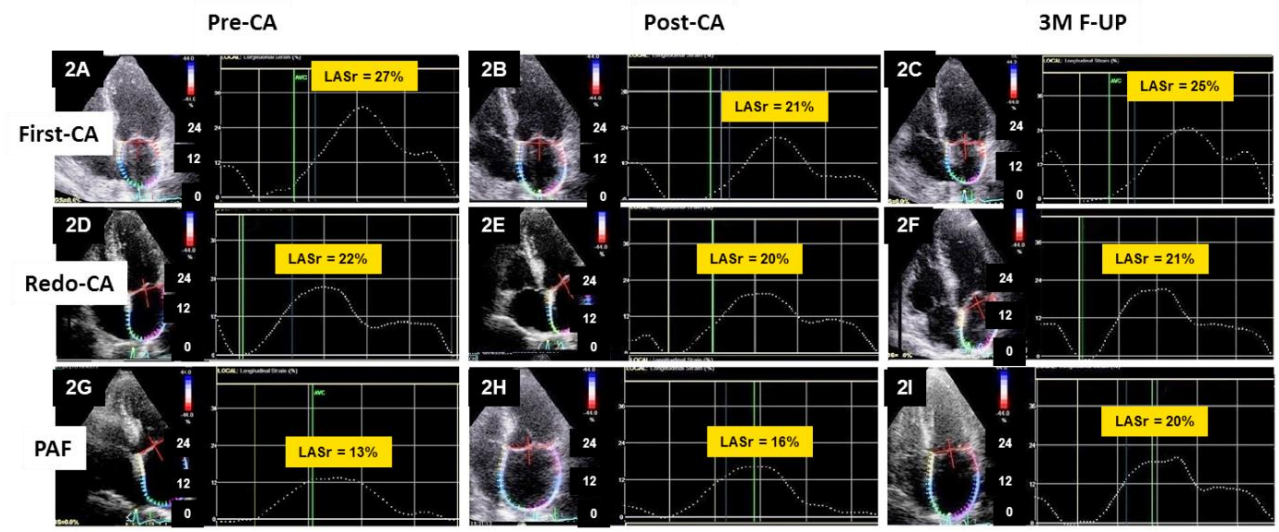

Figure 3. Reservoir (LASr) and contractile (LASct) strain in 4 subgroups of patients with paroxysmal AF undergoing the first CA ablation (First-CA group) according to the presence of hypertension and metabolic risk factors, i.e. dyslipidemia and or diabetes mellitus.

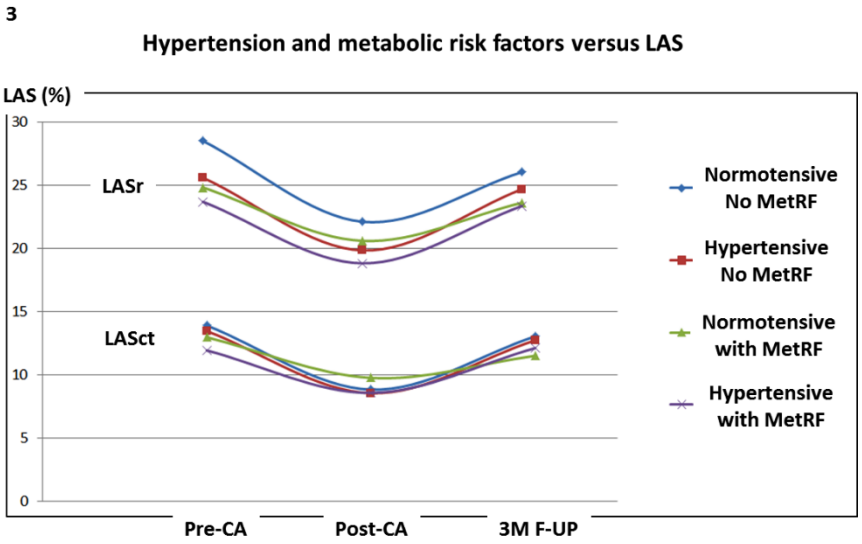

Figure 4. Reservoir (LASr) and contractile (LASct) strain in subgroups of patients with paroxysmal AF undergoing the first CA ablation (First-CA group) according to LA volume index (4A) and LA emptying fraction (4B).

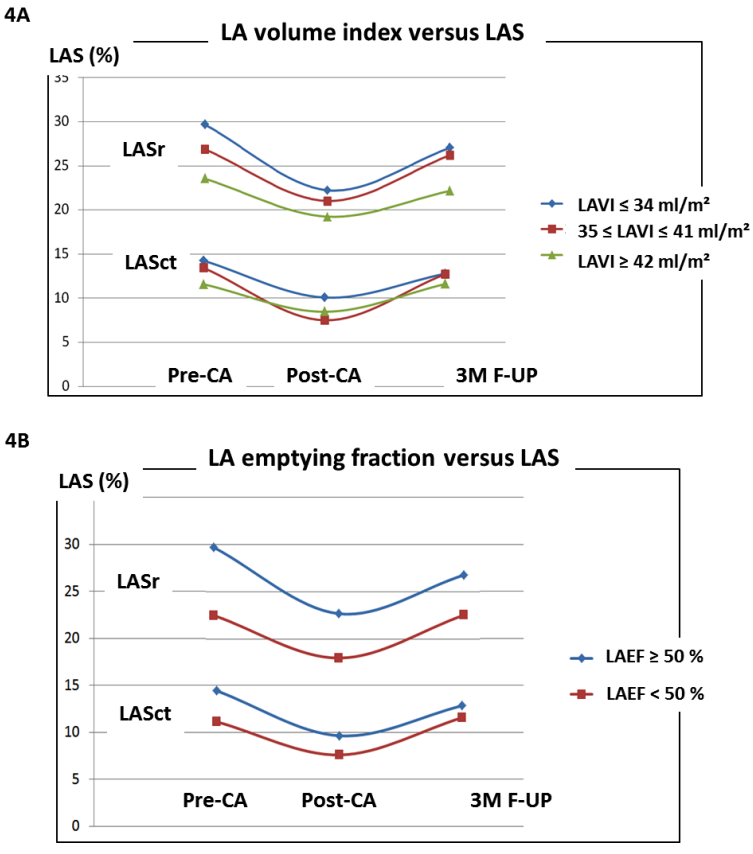

Table 1: Baseline clinical and echocardiographic characteristics in patients with paroxysmal AF undergoing the first or the redo CA, and with long-standing persistent AF.

	Paroxysmal AF (first-CA group) n=74	Paroxysmal AF (redo-CA group) n=22	Long-standing persistent AF (PAF group) n=15	P (ANOVA)
Age, y	63 ± 9	59 ± 10	67 ± 10	0.04
Males, n (%)	47 (63)	13 (59)	12 (80)	0.458
Obesity, n (%)	18 (24)	6 (27)	5 (33)	0.54
Hypertension, n (%)	37 (50)	6 (27)	10 (50)	0.14
Diabetes mellitus, n (%)	5 (7)	1 (5)	2 (13)	0.577
Cardiovascular disease, n (%)	4 (5)	2 (9)	1 (7)	0.394
Heart failure, n (%)	10 (14)	2 (9)	3 (20)	0.908
NT Pro-BNP (pg/mL)	274 ± 381	299 ± 319	904 ± 628	< 0.001
MDRD (mL/min/1.73m^2)	78 ± 12	73 ± 14	68 ± 17	0.01
LV end-diastolic diameter (cm)	5.0 ± 0.6	5.0 ± 0.5	4.9 ± 0.4	0.852
LV end-systolic diameter (cm)	3.2 ± 0.5	3.3 ± 0.5	3.2 ± 0.3	0.66
LV relative wall thickness	0.45 ± 0.06	0.44 ± 0.05	0.43 ± 0.05	0.443
LV mass index (g/m^2)	93 ± 27	93 ± 20	94 ± 19	0.962
LV end-diastolic volume index (mL/m^2)	57 ± 13	56 ± 12	51 ± 10	0.156
LV end-systolic volume index (mL/m^2)	22 ± 8	21 ± 7	21 ± 7	0.512
LV ejection fraction (%)	64 ± 6	62 ± 8	58 ± 14	0.021
LV global longitudinal strain (%)	-19 ± 3	-18 ± 3	-16 ± 2	< 0.001
Transmitral flow E wave (m/s)	0.85 ± 0.18	0.80 ± 0.19	0.94 ± 0.22	0.912
Transmitral flow A wave (m/s)	0.68±0.17	0.62±0.18	NA	NA
E/A	1.17 ± 0.49	1.35 ± 0.45	NA	NA
Deceleration time (ms)	206 ± 60	171 ± 47	161 ± 50	0.004
e' septal (m/s)	0.09 ± 0.07	0.08 ± 0.02	0.09 ± 0.03	0.764
e' lateral (m/s)	0.11 ± 0.03	0.11 ± 0.03	0.12 ± 0.04	0.103
E/e'	9 ± 2	8 ± 3	9 ± 3	0.223
Systolic PAP (mmHg)	28 ± 5	29 ± 7	31 ±76	0.251
RV end-diastolic diameter basal (cm)	3.7 ± 0.4	3.7 ± 0.5	3.9 ± 0.4	0.779
RV end-diastolic diameter mid (cm)	2.5 ± 0.4	2.6 ± 0.4	2.6 ± 0.3	0.628
TAPSE (mm)	24 ± 3	23 ± 4	22 ± 3	0.016
RV global longitudinal strain (%)	-21 ± 4	-20 ± 5	-16 ± 3	0.004
RV free-wall longitudinal strain (%)	-24 ± 5	-22 ± 6	-20 ± 3	0.04
RA volume index (ml/m^2)	27 ± 7	25 ± 6	28 ± 9	0.104
RA reservoir strain (%)	35 ± 11	29 ± 9	18 ± 6	< 0.001

Abbreviations LV = left ventricular, MDRD = modification of diet in renal disease, PAP = pulmonary artery pressure, RA = right atrial, RV = right ventricular, TAPSE = tricuspid annular plane systolic excursion

Table 2: Left atrial size and function 1-day pre-CA, 1-day post-CA and at 3-month follow-up in 3 groups of patients with AF.

	First-CA group n=74	**Redo-CA group n=22**	**PAF group n=15**	**P (ANOVA)**
Heart rhythm				
Pre-CA	Sinus	Sinus	AF	NA
Post-CA	Sinus	Sinus	Sinus	NA
3-month follow up	Sinus	Sinus	Sinus	NA
Heart rate (bpm)				
Pre-CA	64 ± 12	69 ± 10	85 ± 15	< 0.001
Post-CA	68 ± 12	68 ± 9	71 ± 12†	0.657
3-month follow up	66 ± 11	69 ± 10	69 ± 14†	0.436
LA volume index (mL/m^2)				
Pre-CA	35 ± 8	34 ± 7	44 ± 15	0.003
Post-CA	38 ± 8†	36 ± 8	48 ± 14	0.002
3-month follow up	33 ± 8 Ⅱ	31 ± 6§	39 ± 10∗	0.015
LA sphericity index				
Pre-CA	0.68 ± 0.08	0.68 ± 0.06	0.69 ± 0.08	0.766
Post-CA	0.67 ± 0.10	0.70 ± 0.08	0.66 ± 0.08	0.388

3-month follow up	0.67 ± 0.12	0.71 ± 0.05	0.64 ± 0.19	0.230
LA stiffness index				
Pre-CA	0.32 ± 0.14	0.43 ± 0.22	0.81 ± 0.47	< 0.001
Post-CA	0.47 ± 0.20‡	0.46 ± 0.27	0.87 ± 0.63	< 0.001
3-month follow up	0.33 ± 0.13 Ⅱ	0.43 ± 0.23	0.59 ± 0.28∗§	< 0.001
LA emptying fraction (%)				
Pre-CA	55 ± 11	48± 11	35 ± 11	< 0.001
Post-CA	50 ± 11†	45 ± 11	38 ± 7	< 0.001
3-month follow up	53 ± 10	50 ± 10	44 ± 9∗	< 0.003
Reservoir LAS (%)				
Pre-CA	27 ± 8	22 ± 6	13 ± 5	< 0.001
Post-CA	21 ± 7‡	20 ± 5	16 ± 7	0.056
3-month follow up	25 ± 6∗ Ⅱ	21 ± 7	20 ± 7∗	0.002
Reservoir LASR (s^{-1})				
Pre-CA	1.27 ± 0.30	1.10 ± 0.30	0.81 ± 0.22	< 0.001
Post-CA	1.09 ± 0.35‡	1.01 ± 0.31	0.83 ± 0.40	0.053
3-month follow up	1.25 ± 0.28 Ⅱ	1.10 ± 0.36	1.10 ± 0.27	0.031
Conduit LAS (%)				
Pre-CA	15 ± 5	13 ± 5	NA	0.235 (t test)
Post-CA	12 ± 5∗	12 ± 4	13 ± 6	0.934
3-month follow up	13 ± 4	12 ± 4	11 ± 4	0.073
Conduit LASR (s^{-1})				
Pre-CA	-1.14 ± 0.45	-1.18 ± 0.41	NA	0.695 (t test)
Post-CA	-1.08 ± 0.43∗	-1.14 ± 0.35	-1.11 ± 0.56	0.866
3-month follow up	-1.10 ± 0.36	-1.08 ± 0.36	-0.99 ± 0.42	0.584
Contractile LAS (%)				
Pre-CA	13 ± 4	9 ± 4	NA	< 0.001 (t test)
Post-CA	9 ± 4‡	8 ± 3	4 ± 2	< 0.001
3-month follow up	12 ± 4 Ⅱ	10 ± 4	9 ± 4 Ⅱ	0.002
Contractile LASR (s^{-1})				
Pre-CA	-1.62 ± 0.45	-1.18 ± 0.46	NA	< 0.001 (t test)
Post-CA	-1.10 ± 0.43‡	-1.13 ± 0.41	-0.49 ± 0.28	< 0.001
3-month follow up	-1.50 ± 0.46 Ⅱ	-1.24 ± 0.52	-0.90 ± 0.47 Ⅱ	< 0.001
LA mechanical dispersion (ms)				
Pre-CA	79 ± 27	68 ± 29	114 ± 22	< 0.001
Post-CA	100 ± 27‡	96 ± 25∗	116 ± 21	0.073
3-month follow up	56 ± 20‡ Ⅱ	84 ± 24	78 ± 28‡ Ⅱ	< 0.001
RA-LA mechanical dispersion (ms)	-21 ± 7	-18 ± 4	NA	0.039 (t test)
Pre-CA	-25 ± 10‡	-19 ± 4	-22 ± 3	0.048
Post-CA	-16 ± 5‡ Ⅱ	-18 ± 4	-19 ± 2	0.319
3-month follow up				
LV global longitudinal strain (%)	-19 ± 3	-18 ± 3	-16 ± 2	< 0.001
Pre-CA	-19 ± 3	-18 ± 3	-17 ± 3	0.166
Post-CA	-19 ± 2	-18 ± 4	-17 ± 3	0.196
3-month follow up				

∗ p<0.05, † p<0.01, ‡ p<0.001 Pre-CA versus Post-CA or pre-CA versus 3-month follow up, § p<0.05, Ⅱ p<0.001 Post-CA versus 3-month follow up

Abbreviations:

CA = catheter ablation, LA = left atrial, LAS = LA strain, LASR = LA strain rate, LV = left ventricular, NA = not applicable, RA = right atrial

Chapter 5

Impact of obesity and age on left atrial function in patients with paroxysmal atrial fibrillation undergoing catheter ablation

Background:

Obesity and older age are associated with increased risk of atrial fibrillation (AF) and heart failure (HF). Previous studies assessing the efficacy of catheter ablation (CA) in obese and elderly patients have shown conflicting data.

Purpose:

We thought to assess the impact of obesity and age on left atrial (LA) phasic function in patients with paroxysmal AF undergoing the first CA.

Methods:

We prospectively enrolled 112 consecutive patients (age:63±21 years; 32% female) with symptomatic paroxysmal AF and preserved left ventricular ejection fraction (≥ 50%) undergoing the first CA during sinus rhythm, and 23 healthy controls. Patients with valvular AF or in AF at the time of ablation were excluded.

All patients underwent comprehensive echocardiography at one day pre-CA and at one day post-CA, and after 3 months. The LA reservoir, conduit and contractile strain and strain rate (SR) were assessed using the 2D speckle tracking echocardiography as average of segmental values in apical views.

Results:

A total of 36 (32%) patients had normal weight (BMI < 25 kg/m²), while 50 (45%) overweight (25 ≤ BMI < 30 kg/m²), and 26 (23%) obesity (BMI ≥ 30 kg/m²). A total of 42 (38%) individuals were elderly (≥ 65 years old).

Pre-CA, all groups of patients with paroxysmal AF had significantly lower magnitude of all three components of LA strain and SR compared with controls (all $p<0.01$). Obese patients showed significantly lower magnitude of reservoir strain, contractile strain and SR compared with normal-weight patients (all $p<0.05$). Reservoir but not contractile strain was also significantly lower in over-weight versus normal-weight individuals.

Middle-age compared with elderly patients had significantly higher magnitude of reservoir strain, reservoir and contractile SR (all $p<0.05$). Post-CA, LA strain and SR significantly decreased in all groups of patients regardless of BMI or age (all $p<0.05$) (figure 1AB,2AB). At

3-month follow-up, LA strain and SR showed almost complete recovery to pre-CA values in all groups of patients. Yet, LA function remained significantly lower compared with controls (all p<0.01).

Moreover, individuals with obesity remained to have significantly lower LA function than patients with normal weight. Elderly patients with overweight tended to have lower follow-up LA function compared with middle-age patients with normal weight (p: 0.06). Out of the all indices of phasic LA function, reservoir strain showed to be the most clinically useful to monitor LA function throughout the study.

Conclusion:

Obese patients with paroxysmal AF had significantly lower LA function both pre- and post-CA than individuals with normal weight. This may imply a higher AF recurrent rate and risk for development of HF. Reservoir LA strain appears to be the most useful parameter to monitor LA function.

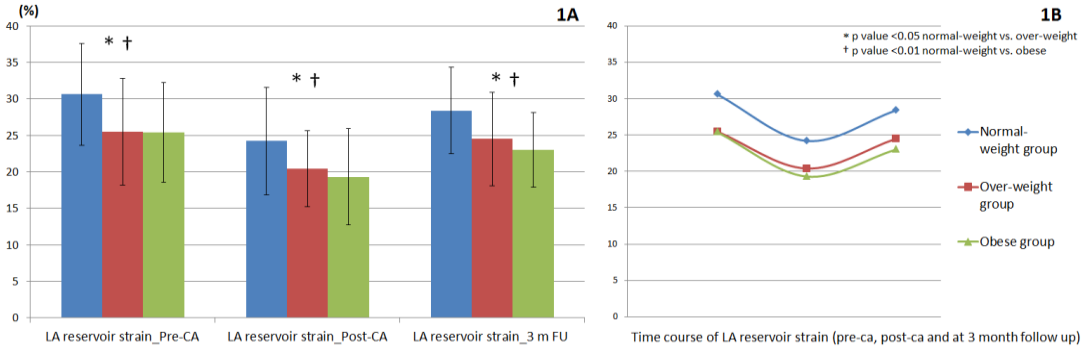

Figure 1: figures (1A,1B) showing the value and time course of LA reservoir strain (pre-ca, post-ca and at 3m FU) for 3 groups of patients

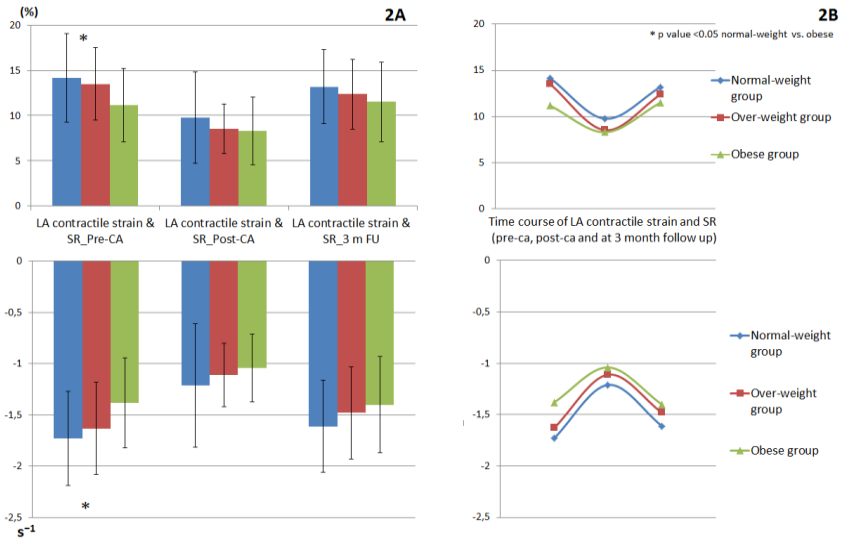

Figure 2: figures (2A,2B) showing the value and time course of LA contractile strain and strain rate (SR) (pre-ca, post-ca and at 3m FU) for 3 groups of patients

Chapter 6

Atrial mechanical dispersion in patients with atrial fibrillation undergoing catheter ablation: a strain study

Background:

Atrial mechanical dispersion (MD) might increase the risk of atrial fibrillation (AF). However, the data on atrial mechanical dispersion in patients with AF undergoing catheter ablation (CA) are scarce.

Purpose:

To describe effects of CA on inter- and left intra-atrial MD in patients with different sub-types of AF undergoing CA.

Methods:

We prospectively enrolled 138 symptomatic patients (age: 63±21 years, 32% females) with paroxysmal AF undergoing first (81%) or redo (19%) CA during sinus rhythm, and 20 individuals (age: 66±23 years, 20% females) with long-standing persistent AF undergoing first CA during AF. All patients had normal (≥50%) left ventricular ejection fraction. Control group consisted of 23 healthy controls.

The atrial strain and strain rate (SR) were assessed using the two-dimensional speckle tracking echocardiography as average of segmental values in all apical views for LA and in four chamber (4CH) apical view for RA. We quantified inter-atrial MD as the standard deviation of time from the onset of the P wave to peak negative strain curves (Image 1), and left intra-atrial MD as the standard deviation of time from the onset of QRS wave to peak positive strain curves (image 2) of all LA segmental components in 4CH apical view after setting adjusting the reference frame to coincide with the onset of the QRS.

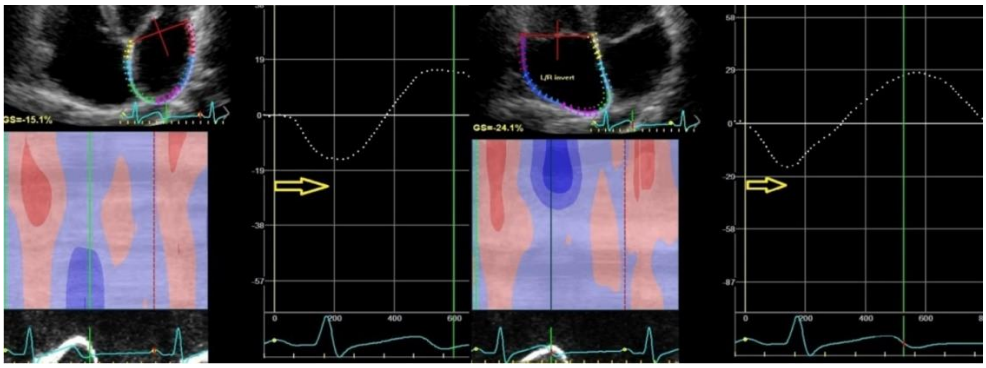

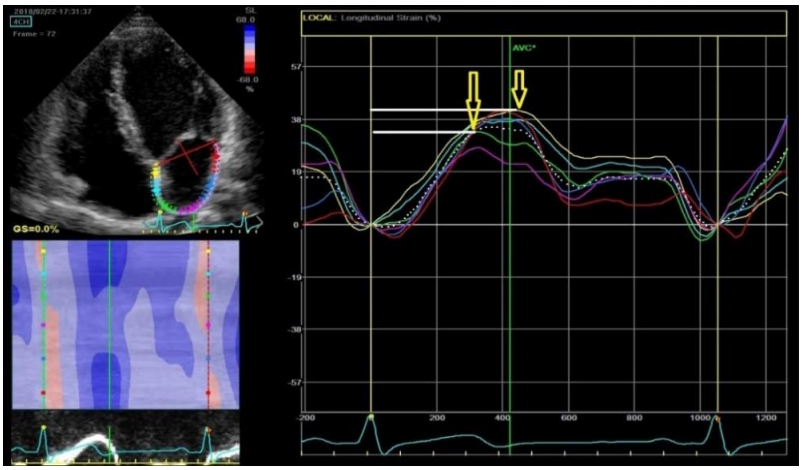

Results:

At 1-day pre-ablation, patients with long-standing persistent AF showed significantly lower reservoir strain of both atria and higher left intra-atrial MD as compared with both paroxysmal AF groups and controls (all $p<0.01$). The Redo-CA versus the First-CA group showed significantly lower LA reservoir strain ($p<0.01$) while left intra-atrial MD was similar. RA reservoir strain and inter-atrial MD was similar between groups with paroxysmal AF. At 1-day post-ablation, we observed a significant deterioration of reservoir LA strain and left intra-atrial MD only in the First-CA group.

After 3-month follow-up, left intra-atrial synchrony was significantly improved compared with pre-ablation in both groups of paroxysmal AF undergoing the first CA and long-standing persistent AF ($p<0.05$). The reservoir LA strain showed partial recovery to pre-ablation values in paroxysmal AF undergoing first-CA while it showed a continuous improvement in long-standing persistent AF. In contrast, patients with paroxysmal AF undergoing redo-CA did not show significant improvement in any of these indices. Inter-atrial MD and RA strain did not show significant improvement in either group.

Conclusion:

Atrial strain and MD shows distinct behavior in patients with different sub-types of AF post CA. Atrial MD may provide a complimentary information to strain when assessing LA function. This novel index might has a predictive value for AF recurrence after CA and could be used as a sensitive tool for the long-term follow-up of patients with AF.

Figures 1A,1B: showing the value and time course of LA reservoir strain (pre-ca, post-ca and at 3m FU) for 3 groups of patients.

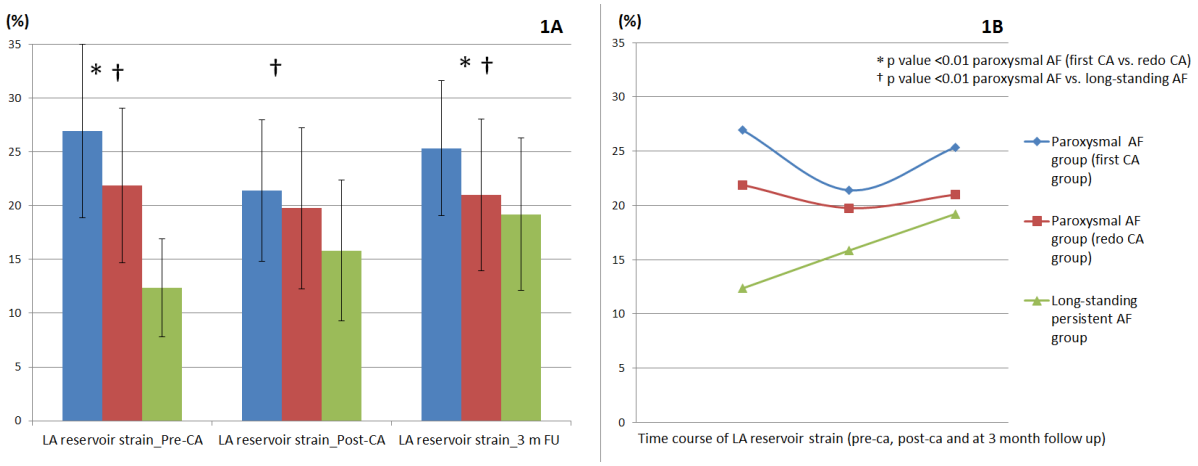

Figures 2A,2B: showing the value and time course of LA intra-atrial mechanical dispersion (pre-ca, post-ca and at 3m FU) for 3 groups of patients.

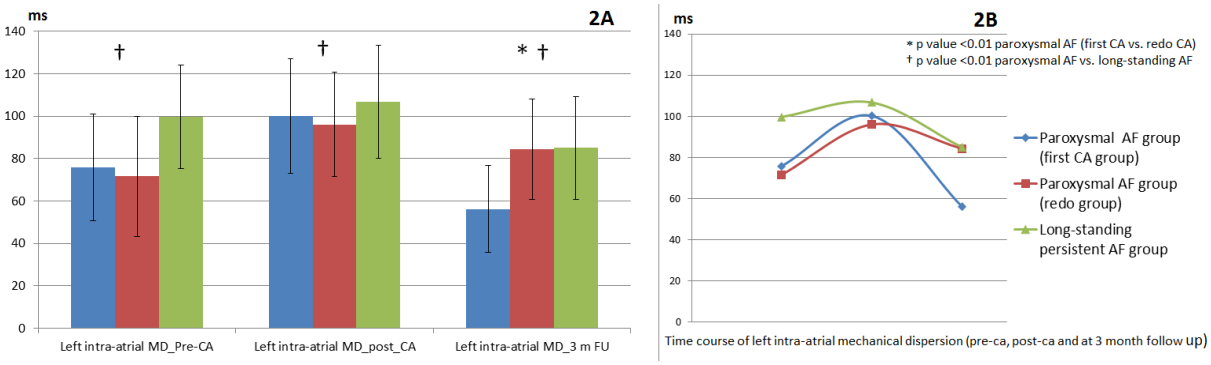

Figures 3A,3B,3C: showing the value and time course of LA reservoir strain and intra-atrial mechanical dispersion (pre-ca, post-ca and at 3m FU) for 3 groups of patients.

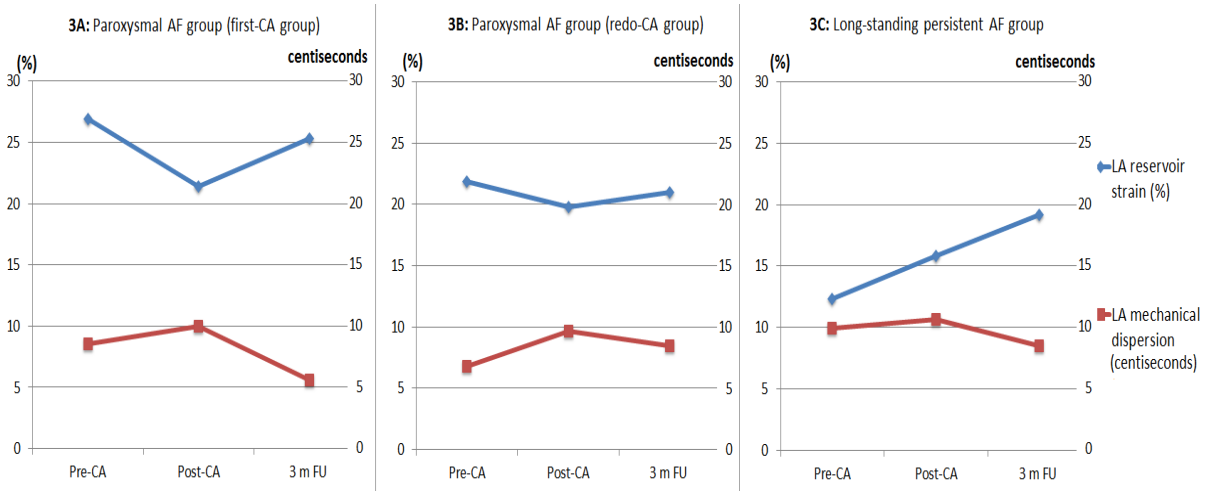

Chapter 7

Effects of catheter ablation on left atrial performance in different types of atrial fibrillation: a strain study

Background:

Atrial structural and functional changes may develop as a result of catheter ablation (CA) in patients with paroxysmal and persistent atrial fibrillation (AF). However, there is limited knowledge regarding the long-term impact of successful CA on atrial morphology and mechanics, and the relation between AF recurrence and atrial performance following CA is still under debate.

Aims:

Firstly, to describe the long-term effects of CA on LA remodeling and its correlates to the maintenance of sinus rhythm. Secondly, to compare the time course of LA and right atrial (RA) performance in patients with paroxysmal atrial fibrillation (AF) undergoing the first successful CA.

Methods:

We prospectively enrolled 178 consecutive patients (age: 63±9 years, 35% females) with paroxysmal AF undergoing first-CA (67%) or redo-CA (22%), and 20 individuals (11%) with long-standing persistent AF (PAF) undergoing first CA. All patients underwent comprehensive transthoracic echocardiography at baseline and at 12-month follow-up, including assessment of reservoir and contractile strain for both LA and RA using two-dimensional speckle tracking echocardiography in apical views.

Results:

During one-year follow-up, 144 (81%) patients maintained sinus rhythm whereas 34 (19%) patients had AF recurrence [first-CA group 16 (13%), redo-CA 8 (20%) and PAF 10 (50%)]. Significant improvement of LAS was observed only in patients with paroxysmal and long-standing persistent AF who underwent the first CA and who remained in sinus rhythm. In contrast, recurrent AF was associated with absence of LAS improvement. In the redo-CA group, LAS did not show significant increase from baseline regardless of long-term maintenance of sinus rhythm.

Moreover, at follow-up, no significant differences in LAS between redo-CA patients with sinus rhythm versus AF were observed. Of note, in patients with long-standing persistent AF and SR, follow-up LAS increased to values observed in the redo-CA group. Although the RA

motion was not affected in the early phase, both reservoir and contractile RAS showed a significant increase between 3-month and 12-month follow up.

Conclusion:

LA performance following CA is strongly affected by complex interplay between extent of atrial electro-structural remodeling and CA procedure.

Introduction

Radio-frequency catheter isolation (CA) is associated with changes of left atrial (LA) size and shape [1,2]. However, the impact of successful CA on LA and right atrial (RA) morphology and mechanics is still under debated [3]. Furthermore, while atrial fibrillation (AF) is considered more like a LA disease, the contribution of right atrium (RA) to the AF pathogenesis is not fully studied and its relationship to the CA outcome is still under investigation [4,5]. Recent advances in echocardiography equipment and image post-processing allow an assessment of atrial strain and strain rate (SR) [6]. The Speckle Tracking Echocardiography (STE)-derived LA longitudinal strain has been shown to be an accurate and reproducible parameter to evaluate LA longitudinal shortening [7,8]. Furthermore, LA strain (LAS) has significantly correlated with underlying LA fibrosis [9]. This suggests that the LAS provides a comprehensive and quantitative assessment of LA structure and function. Hence, it is tempting to speculate that the analysis of LAS will show high accuracy to predict AF recurrence post CA. However, LA strain can be affected by several factors not related to LA structural damage such as loading conditions or arrhythmias [6,10]. Therefore, we aimed to describe atrial performance in patients with a history of AF who underwent radio-frequency CA and its long-term impact on overall cardiac performance.

Methods

Design: Prospective, single-center, observational study.

Patients: All consecutive patients (n=212) with symptomatic AF undergoing elective CA between 10/2017 and 7/2018 were screened for eligibility according to the following inclusion criteria: (1) paroxysmal or long-standing persistent AF; (2) preserved left ventricular ejection fraction (LVEF) (≥ 50%). Patients with permanent or valvular AF, cardiomyopathy or congenital heart diseases, history of myocardial infarction or coronary revascularization, post cardiac surgery for any cause, pacemaker, and reduced LVEF (< 50%) were excluded. The final study population consisted of 178 patients with paroxysmal AF undergoing the first (67%) or the redo-CA (22%), and 20 individuals (11%) with long-standing persistent AF (PAF) undergoing first CA. Control group consisted of 23 healthy controls. Study was approved by the Ethics Committee of our institution. Each patient signed informed consent before participating in the study.

Protocol: All participants underwent extensive encircling pulmonary vein isolation guided by an electro-anatomical map using the Carto 3 mapping system (Biosense-Webster, CA, USA). History, physical examination and laboratory data were recorded during the admission for CA. Furthermore, all patients underwent comprehensive transthoracic echocardiography at baseline and after one-year follow-up. All hospitalizations, emergency room admissions or outpatients visit were recorded. Any suspicious symptoms or abnormal electrical activity recordings at Holter were adjudicated by an experienced electrophysiologist. The AF recurrence was defined as any documented AF episode lasting ≥ 30 seconds that occurs after CA [11].

Echocardiography: A comprehensive 2D transthoracic echocardiographic examination was performed using Vivid E95 (GE HealthCare, Horten, Norway) ultrasound system. All acquired images were stored digitally for offline analysis using a commercially available software (EchoPac, GE HealthCare). All examinations were recorded and analyzed by the same operator. Average of at least 3 beats (in sinus rhythm) or 5 beats (in AF) was taken for each measurement. Blood pressure and heart rate was recorded during each examination. The biplane Simpson method was used to assess LV volumes and ejection fraction [7]. LA antero-posterior diameter was measured at end-systole using the parasternal long-axis view [7]. Maximum and minimum LA volume, LA emptying fraction and LA expansion index were calculated from the apical 4- and 2-chamber views using the area-length method [7]. RA area and volume, and right ventricular (RV) end-diastolic basal and mid-cavity diameters were measured in the modified apical 4-chamber view [7]. LV global longitudinal strain (GLS), RV GLS and RV free wall longitudinal strain were assessed using speckle tracking technique in views optimized for each chamber and at frame rate of >60 FPS [7,12].

Assessment of longitudinal LAS, LASR, RAS and RASR were performed using SLE as recommended [12]. In brief, optimized apical 4-, 3, and 2-chamber views were recorded during breath hold. LA endocardial borders were traced manually in all views. Region of interest was manually adjusted and tracking quality was previewed before generating LAS and LASR curves. The LA reservoir (LASr), conduit (LAScd) and contractile (LASct) strain and SR were assessed as average of segmental values in apical views using the onset of QRS as a reference point [12]. The RA reservoir (RASr), conduit (RAScd) and contractile (RASct) strain and SR were assessed as average of segmental values in apical 4-chamber view [12]. Furthermore, LA stiffness index (LASI) was calculated as the E/e' divided by LASr and LA mechanical dispersion (LAMD) was derived as the standard deviation of time from the onset of QRS complex to peak positive LAS in 6 segments using the apical 4-chamber view. RA-LA MD was assessed as the standard deviation of time from the onset of P wave to peak negative RASr and LASr.

Statistical analysis

All analyses were performed using SPSS statistics software (Version 23; Chicago, IL, USA). Continuous variables were expressed as the means and standard deviations; categorical

variables were expressed as proportions. The paired t-test was used to test differences in normally distributed continuous variables in the same group, and unpaired t-test and ANOVA with post hoc test were used for exploration of differences among means of variables between different groups. A two-sided p value of less than 0.05 was considered to represent a statistically significant difference. The lack of inter- and intra-operator variability was assessed using Wilcoxon's non-parametric test for matched data.

Results

The baseline clinical and echocardiographic characteristics of the study population are summarized in table 1. At baseline, there were no differences between the three groups with regard to the use of cardiovascular medications, except for the use of anti-coagulants drugs (table 1). At mid-term follow-up, a total of 13 patients (12%) had early AF recurrence after CA but we considered the period of the first 3 months after CA as a blanking period [11]. At long-term follow-up, 144 (81%) patients maintained sinus rhythm whereas 34 (19%) patients had AF recurrence [first-CA group 16 (13%), redo-CA group 8 (20%) and PAF group 10 (50%)]. Importantly, it was noticed that there was a significant decrease in the use of beta-blockers, anti-arrhythmic and anti-coagulants drugs in patients who maintained sinus rhythm (at baseline: 72%, 16% and 67% versus at follow-up: 52%, 6% and 49% respectively, all $p<0.05$) whereas a significant increase in the use of anti-arrhythmic drugs in patients who develop AF recurrence (at baseline: 19% versus at follow-up: 35%, $p<0.05$). In addition, no difference in mean systolic or diastolic blood pressure was noted during clinical follow-up in all groups of patients.

Echocardiographic changes during follow-up

The study population was subsequently divided into 6 groups according to the success of CA procedure. A significant improvement of LAS was observed only in patients with paroxysmal and long-standing persistent AF who underwent the first CA and who remained in sinus rhythm. In contrast, recurrent AF was associated with absence of LAS improvement. In the redo-CA group, LAS did not show significant increase from baseline regardless of long-term maintenance of sinus rhythm. Moreover, at follow-up, no significant differences in LAS between redo-CA patients with sinus rhythm versus AF were observed. Of note, in patients with long-standing persistent AF and SR, follow-up LAS increased to values observed in the redo-CA group. In the same direction, patients in the First-CA group had a lower LASI than those in the redo-CA and PAF groups. In all three groups, the LASI was highest in patients with AF recurrence compared to patients who maintained sinus rhythm (table 2).

The mid- and long-term effects of CA on LA and RA function were analyzed in group of patients with paroxysmal AF undergoing the first CA who maintained sinus rhythm during follow-up. At baseline, all patients with paroxysmal AF showed a significant reduction of reservoir and contractile LAS and RAS compared with controls (all $p<0.01$). CA was associated with a significant decrease in reservoir and contractile LAS while no significant

difference was observed for RAS. At 3-month follow up, the LAS showed full recovery, whereas the RAS did not show any significant change from 1-day post CA values. At 12-month follow-up, both reservoir and contractile LAS showed further improvement compared to baseline and 3-month values. LAMD derived from the LA strain curve followed a similar trend (figure 1). Although the RA motion was not affected in the early phase, both reservoir and contractile RAS showed a significant increase between 3-month and 12-month follow-up (figure 2). In brief, successful first CA in patients with paroxysmal AF is associated with acute decrease in LAS, followed by recovery to baseline value within 3 months and further improvement of both LAS and RAS during one year, whereas no significant change was noticed in the LV and RV longitudinal strains over time. The time course of LA and RA echocardiographic characteristics in this group of patients are summarized in table 3.

Discussion

In this real word sample, we have focused on functional atrial response to the CA procedure by studying the deformation of atrial myocardium taking into account the hemodynamic state. We have described the long-term consequence of the CA on the LA reverse remodeling and the impact of sinus rhythm restoration on overall cardiac performance. Importantly, a significant improvement in the LA performance was observed in patients who maintained SR during follow-up. In contrast, in patients who had recurrence of AF, this performance remained unchanged or deteriorated specifically in group of patients under the repeated CA. Interestingly, while the CA leads to symptoms improvement by reducing AF burden, it has not convincingly shown to improve atrial performance, from our experience, in all AF phenotypes.

It is well-known that the LA compliance is not only related to structural changes of atrial myocardium, but also related to pressure overload [10,13]. The stiff LA syndrome, related to fibrosis induced by chronic AF or subsequent to CA, is associated with a worsening LA expansion and it might also affect LA contractile [14,15]. On the other hand, atrial stunning occurring during the procedure affects negatively LA function and could be responsible for early AF recurrence within 3 months after the procedure [14,15]. Therefore, the temporary change in LA functional indices around the procedure should be interpreted with caution during the assessment of LA dysfunction related to AF. Furthermore, many studies reported that atrial MD has been linked to changes in atrial synchronous and remodeling following CA and it might contribute to AF recurrence after CA [16,17]. Our findings suggested atrial dyssynchrony linked to paroxysmal AF is reverse if the AF is diagnosed early and treated optimally. Thus, LAMD present at initial stages of symptomatic AF is an important parameter might be considered when assessing LA performance.

In accordance to a recent study reported that earlier AF was also associated with reduced RA reservoir strain [18], our study demonstrated that the improvement in reservoir LAS after the long-term maintenance of sinus rhythm highlights the positive effect of the CA on RA function. However, it was unclear whether changes in the RA function were representative

of the LA dysfunction, so we could not determine precisely the mechanical relationship between the LA and RA and if the LA remodeling had any potential influence on the RA reverse remodeling and vice versa [19]. Although, the stretch forces related to LA scars affected negatively RA motion, the RA-LA MD did not show any significant change over time and the RA showed a homogenous improvement in work distribution in long-term follow-up. This suggests, that in contrast to LAS, the RAS is mainly affected by AF self while CA has no direct effect, thus successful CA might lead to right heart reverse remodelling in the long-term follow-up.

There is an ongoing debate whether LAS and derived indices can provide incremental information over LV GLS. An explanation could be that, in contrast to previous reports, our study included patients with primary LA problem, i.e. non valvular AF, and with preserved LV size and ejection fraction. LV GLS is still the most sensitive component of myocardial deformation indices to monitor ventricular dysfunction in patients with AF [20]. On the contrary to previous studies reported that the LV longitudinal strain and SR improve significantly in patients who maintain SR [21,26], no significant change was noticed in group of patients with paroxysmal AF who maintain sinus rhythm after CA procedure. These findings suggest that the positive effect of sinus rhythm maintenance on ventricular systolic function might be a little bit late, perhaps beyond the first year after SR restoration. Furthermore, RV GLS and free wall LS followed the same trend although the RV is more sensitive to load changes than the LV. Thus, our study emphasized that atrial strain curve is a non-plane mirror of the curve of ventricular strain and it could reflex earlier ventricular dysfunction than other ventricular strain indices in patients with asymptomatic AF [22]. That supports the hypothesis that atrial strain is more sensitive to pressure overload than ventricular strain, specifically in left heart side, so LASI should be considered when we assess LA function under different loading conditions [23]. However, repeated CA might be associated with increased LA stiffness which lead to further atrial structural alterations and functional impairment specially in patients with high-burden AF [24,25].

Conclusion

Although the radio-frequency CA affected negatively LA performance in the acute phase, it has a long-term positive impact on both left and right atrial function. The integration of morphological and functional characteristics of atrial myocardium, specifically in patients with high risk of AF recurrence, will add value to determine atrial myocardial injury related to the CA. Repeated wide CA might affect negatively LA compliance and contractility despite sinus rhythm restoration.

Figure 1: Time course of LA reservoir and contractile strain, LA max and min volume index, and LA mechanical dispersion (Baseline, 1-day FUP, 3- and 12-month FUP) in group of patients with paroxysmal AF undergoing the first CA who maintained sinus rhythm during follow-up.

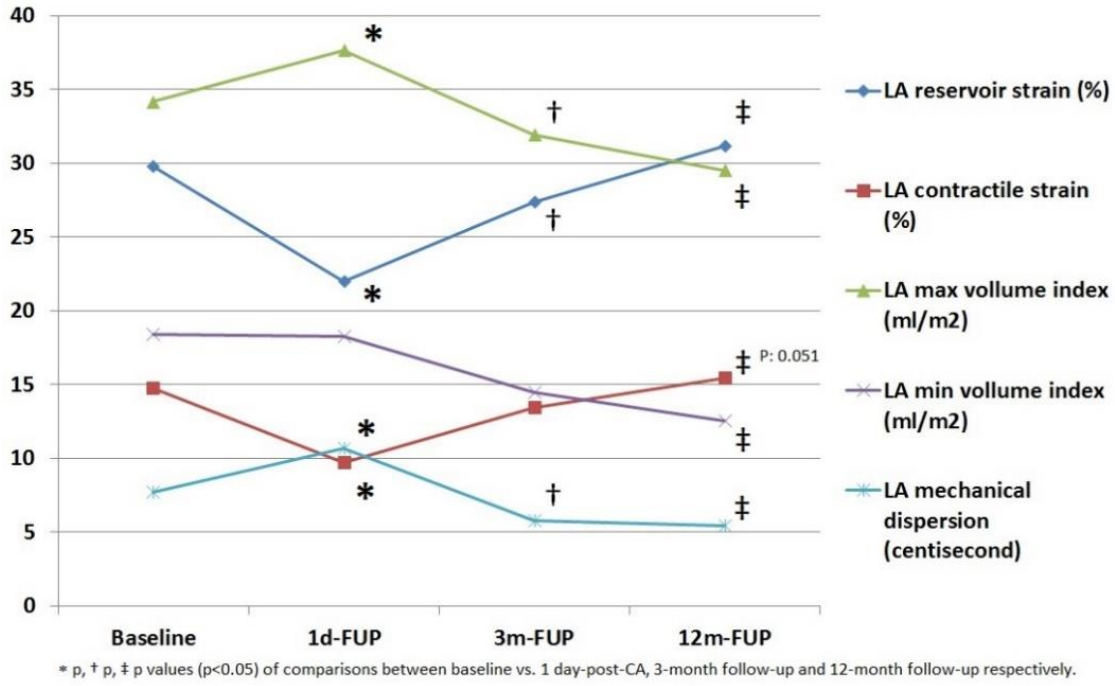

* p, † p, ‡ p values (p<0.05) of comparisons between baseline vs. 1 day-post-CA, 3-month follow-up and 12-month follow-up respectively.

Figure 2: Time course of reservoir and contractile LAS and RAS at Baseline, 1-day, 3-month and 12-month follow-up in group of patients with paroxysmal AF undergoing the first CA who maintained sinus rhythm during follow-up.

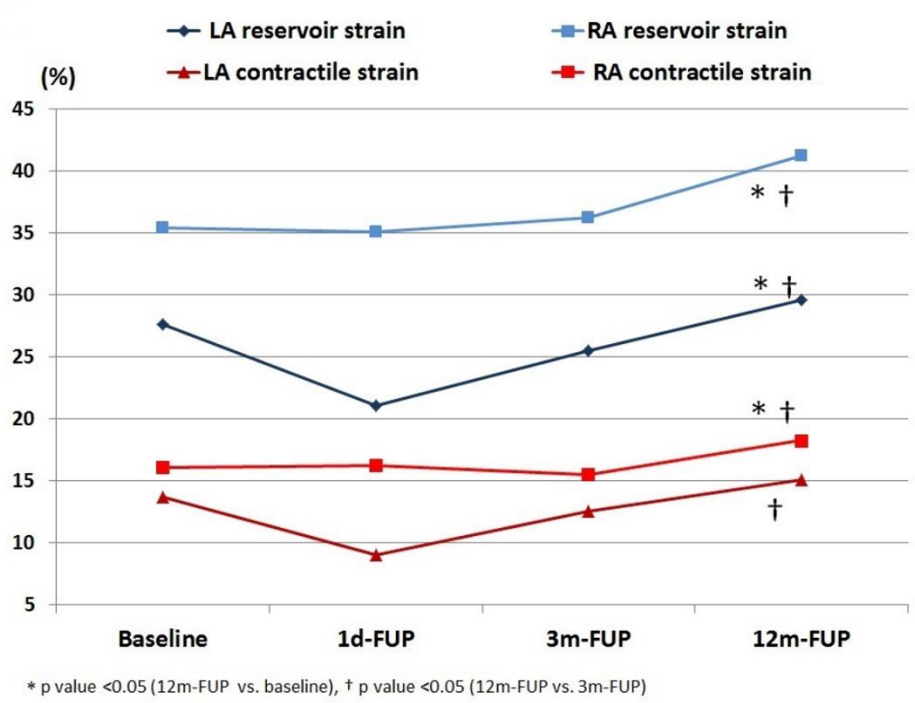

* p value <0.05 (12m-FUP vs. baseline), † p value <0.05 (12m-FUP vs. 3m-FUP)

Figure 3. Reservoir and contractile LAS at Baseline and 12-month follow-up in the First-CA (3A), the Redo-CA (3B) and the long-standing persistent AF (3C) group in patients who maintained sinus rhythm (SR) versus patients who had AF recurrence.

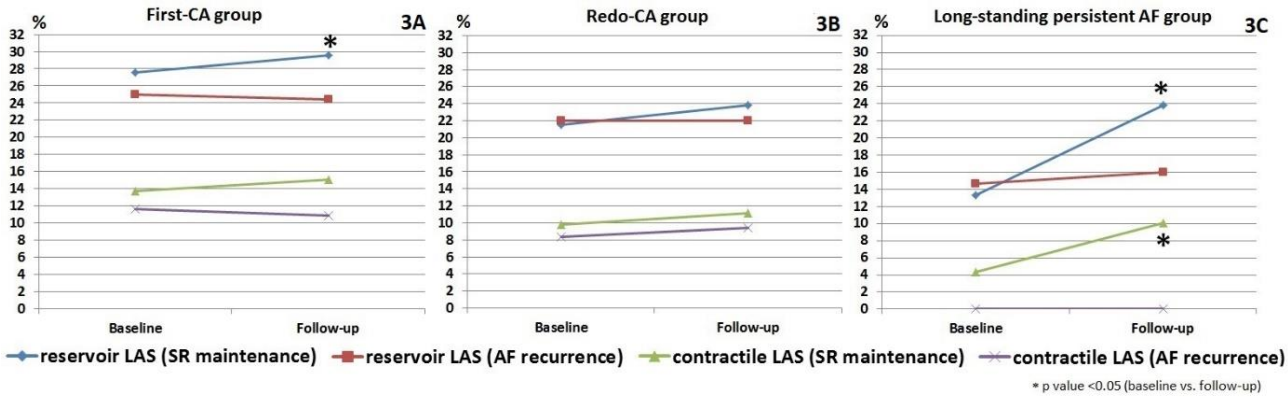

* p value <0.05 (baseline vs. follow-up)

Table 1: Baseline clinical and echocardiographic characteristics in patients with paroxysmal AF undergoing the first or the redo CA, and with long-standing persistent AF.

	Paroxysmal AF (first-CA group) n=112	Paroxysmal AF (redo-CA group) n=37	Long-standing persistent AF (PAF group) n=20	P (ANOVA)
Age, y	62 ± 9	61 ± 10	66 ± 10	0.239
Males, n (%)	75 (67)	24 (65)	16 (80)	0.458
Obesity, n (%)	25 (22)	12 (32)	8 (40)	0.173
Hypertension, n (%)	51 (45)	13 (35)	10 (50)	0.459
Diabetes mellitus, n (%)	6 (5)	1 (3)	2 (10)	0.508
Cardiovascular disease, n (%)	9 (8)	2 (5)	1 (5)	0.804
Heart failure, n (%)	15 (13)	3 (8)	3 (15)	0.657
NT Pro-BNP (pg/mL)	257 ± 345	311 ± 346	864 ± 577	< 0.001
MDRD (mL/min/1.73m^2)	78 ± 12	73 ± 14	70 ± 16	0.022
LV end-diastolic diameter (cm)	5.0 ± 0.6	5.0 ± 0.5	4.9 ± 0.4	0.646
LV end-systolic diameter (cm)	3.2 ± 0.5	3.3 ± 0.5	3.2 ± 0.4	0.577
LV relative wall thickness	0.45 ± 0.06	0.44 ± 0.05	0.44 ± 0.05	0.561
LV mass index (g/m^2)	88 ± 27	92 ± 20	91 ± 18	0.591
LV end-diastolic volume index (mL/m^2)	41 ± 14	43 ± 17	40 ± 15	0.837
LV end-systolic volume index (mL/m^2)	22 ± 8	21 ± 7	20 ± 7	0.564
LV ejection fraction (%)	63 ± 6	63 ± 8	60 ± 7	0.301
LV GLS (%)	-19 ± 3	-18 ± 3	-17 ± 3	0.013
E/A ratio	1.19 ± 0.46	1.47 ± 0.46	NA	NA
E/e' ratio	8 ± 2	8 ± 3	9 ± 2	0.239
Systolic PAP (mmHg)	28 ± 5	29 ± 7	31 ±6	0.027
LA max volume index (mL/m^2)	34.9±7.6	35.4±8.1	41.1±13.1	0.011
LA min volume index (mL/m^2)	18.1±4.1	19.4±8.4	26.7±13.1	< 0.001
LA emptying fraction (%)	53.7±10	45.6±10.9	37.2±11.5	< 0.001
LA expansion index	128.6±54	98.2±49	65.6±29.8	< 0.001
Reservoir LA strain (%)	27±7.2	21.6±7.1	13.9±5	< 0.001
Contractile LA strain (%)	13.1±4.3	9.5±4.2	4.4±2	< 0.001
LA stiffness index	0.32±0.13	0.45±0.24	0.75±0.44	< 0.001

Abbreviations: LV = left ventricular, MDRD = modification of diet in renal disease, PAP = pulmonary artery pressure.

Table 2: Left atrial size and function at baseline and after 12-month follow-up in 3 groups of patients.

	First-CA group (baseline)	First-CA group (follow-up)	P value (t test)	Redo-CA group (baseline)	Redo-CA group (follow-up)	P value (t-test)	PAF group (baseline)	PAF group (follow-up)	P value (t-test)
LA max VI (mL/m^2)									
SR maintenance	34.17±6.2	29.5±8.20	<0.001	36.3±8.7	30.38±8.5	0.002	44.1±13.4	33.8±11.5	0.008
AF recurrence	35.3±5.5	34.13±5.9	0.387	32.05±4.5	32.3±6.7	0.912	38.2±12.9	39.4±4.5	0.789
LA min VI (mL/m^2)									
SR maintenance	18.14±3.6	13.01±5.4	<0.001	20.5±9	14.4±6.4	<0.001	30±14.4	17.2±8.8	0.006
AF recurrence	18.1±4.1	17.5±4.9	0.626	15.3±3	18.9±6.4	0.095	23.3±11.3	24.02±5.4	0.867
LA EF (%)									
SR maintenance	53.9±10	57.06±6.9	0.087	44.4±11.8	53.07±8.1	0.001	34.1±13.2	50.7±9.8	0.004
AF recurrence	51.2±9.9	48.9±7.4	0.323	50.2±5.2	46.9±11.8	0.363	40.3±9.2	38.8±8.8	0.706
LA expansion index									
SR maintenance	132.2±56	140.7±38.4	0.350	94.3±52.4	123.2±42.7	0.002	58.9±32.6	112.2±42	0.003
AF recurrence	112.1±49	102.0±30	0.343	113.4±32.3	100.1±53.6	0.541	72.2±26	67.8±23.2	0.690
Reservoir LAS (%)									
SR maintenance	27.59±7.2	29.62±6.7	0.010	21.5±7.8	23.8±7.6	0.168	13.3±4.9	23.86±7.2	0.001
AF recurrence	24.9±6	24.4±4.3	0.723	22.02±3.3	22.04±7.2	0.988	14.62±5.3	16.04±4.89	0.433
Contractile LAS (%)									
SR maintenance	13.73±4.56	15.11±4.61	0.051	9.84±4.4	11.1±4.2	0.410	4.4±2	11.25±4.5	<0.001
AF recurrence	11.6±3.4	10.9±2.8	0.276	8.34±3.1	9.4±4.8	0.413	**(Post-CA) …….**	**……**	**NA**
LA stiffness index									
SR maintenance	0.30±0.12	0.30±0.13	0.414	0.46±0.26	0.44±0.28	0.616	0.73±0.31	0.44±0.19	0.022
AF recurrence	0.36±0.13	0.39±0.14	0.530	0.39±0.15	0.46±0.28	0.393	0.77±0.55	0.72±0.20	0.719
E/e' ratio									
SR maintenance	7.65±1.9	8.39±2.27	0.071	8.5±2.6	8.4±2.3	0.905	8.23±2	9.3±1.8	0.114
AF recurrence	8.9±2	9.05±2.3	0.830	8.17±2	9.3±3.5	0.383	9.6±2.4	10.5±2.2	0.312

Abbreviations: CA = catheter ablation, LA = left atrial, LAS = LA strain, LAVI = LA volume index, NA = not applicable, SR = sinus rhythm.

Table 3: Values of structural and functional indices of the LA and RA at Baseline, 1-day, 3-month and 12-month follow-up in the first-CA group underwent successful CA.

	First-CA group (baseline)	First-CA group (1-day post-CA)	P value∗ t-test	First-CA group (3-month follow-up)	P value† t-test	First-CA group (12-month follow-up)	P value‡ t-test
Reservoir strain (%)							
LA	27.59±7.2	21.05±6.62	<0.001	25.5±6.3	0.003	29.62±6.7	0.010
RA	35.41±11.5	35.05±8.39	0.832	36.25±10.7	0.126	41.22±9.41	0.001
Reservoir SR (s^{-1})							
LA	1.29±0.35	1.10±0.31	<0.001	1.28±0.31	0.364	1.41±0.30	0.033
RA	1.52±0.53	1.58±0.51	0. 929	1.54±0.45	0.721	1.79±0.48	0.005
Conduit strain (%)							
LA	14.59±4.79	12.38±4.29	<0.001	13.23±4.15	0.032	14.61±4.0	0.504
RA	19.02±8.2	18.8±6.18	0.924	17.47±8.20	0.350	23.08±0.61	0.005
Conduit SR (s^{-1})							
LA	-1.13±0.41	-1.07±0.4	0.249	-1.12±0.37	0.584	-1.18±0.33	0.715
RA	-1.28±0.55	-1.42±0.39	0.103	-1.11±0.33	0.131	-1.30±0.32	0.640
Contractile strain (%)							
LA	13.73±4.56	9.05±3.71	<0.001	12.55±4.12	0.053	15.11±4.61	0.051
RA	16.09±5.9	16.26±4.53	0.847	15.52±4.38	0.105	18.25±5.21	0.013
Contractile SR (s^{-1})							
LA	-1.66±0.46	-1.14±0.43	<0.001	-1.51±0.46	0.040	-1.77±0.51	0.154
RA	-1.86±0.62	-1.88±0.51	0.869	-1.74±0.49	0.058	-2.10±0.47	0.079
Volume indices (ml/m2)							
LA max VI	34.17±6.2	37.68±6.8	<0.001	32.76±8	0.016	29.5±8.20	<0.001
LA min VI	18.140±3.6	19.97±6.1	0.002	15.2±6.67	0.747	13.01±5.46	<0.001
RA max VI	26.96±6.27	24.96±7.75	0.087	23.11±4.91	<0.001	22.15±5.7	<0.001
Mechanical dispersion (ms)							
LA	77.26±26.9	106.58±34.8	<0.001	54.75±18.8	0.001	54.74±21.7	0.008
RA-LA	-20.9 ± 6.6	-24.7 ± 8.7	<0.001	-16.1 ± 4.9	0.001	-18.79±5.7	0.026
Derived functional indices							
LA emptying fraction (%)	53.9±10	49.2±10.57	<0.001	53.49±9.6	0.241	57.06±6.9	0.087
LA expansion index	132.2±56	106.3±48	<0.001	125.48±44.8	0.070	140.7±38.4	0.350
LA stiffness index	0.30±0.12	0.45±0.18	<0.001	0.32±0.12	0.642	0.30±0.13	0.414
Hemodynamics indices							
E/A ratio	1.11±0.36	1.40±0.51	<0.001	1.23±0.42	0.039	1.34±0.45	0.002
E/e' ratio	7.65±1.9	9.06±2.23	<0.001	7.99±1.93	0.935	8.39±2.27	0.071
SPAP	28.39±5.13	31.4±6.9	<0.001	26.9±4.3	0.045	28.11±5.2	0.902
Heart rate (bpm)	61.87±10.3	66.87±11.4	<0.001	65.96±11.4	0.213	65.37±10.7	0.065
Global longitudinal strain (%)							
LV	-19.06±2.99	-18.83±2.97	0.455	-18.60±2.51	0.440	-19.02±2.54	0.518
RV	-21.56±3.42	…….	NA	-21.13±3.16	0.789	-21.56±3.42	0.600
RV free wall	-25.45±4.17	…….	NA	-24.95±3.7	0.992	-24.95±3.70	0.607

∗ p, † p, ‡ p values of comparisons between baseline vs. 1 day-post-CA, 3-month follow-up and 12-month follow-up respectively. **Abbreviations:** CA = catheter ablation, LA = left atrial, LR = right atrium, SR= strain rate, VI = volume index, SPAP = systolic pulmonary artery pressure, NA = not applicable.

Chapter 8

Echocardiography markers of myocardial tissue deformation as independent predictors of sinus rhythm maintenance after catheter ablation for paroxysmal atrial fibrillation

Background:

Speckle Tracking Echocardiography (STE) provides a comprehensive and quantitative assessment of myocardial function. However, the accuracy of STE-derived indices to predict maintenance of sinus rhythm following radio-frequency catheter ablation is still under debate. Therefore, the aim of the present study is to define the accuracy of STE-derived parameters to predict long-term maintenance of sinus rhythm in patients with paroxysmal AF undergoing CA.

Methods:

We prospectively enrolled 218 consecutive patients (age: 62±10 years, 30% females) with paroxysmal AF undergoing first-CA. All patients with preserved ejection fraction (EF ≥ 50%) underwent comprehensive transthoracic echocardiography at baseline, including assessment of left ventricular (LV) global longitudinal strain (GLS), left atrial (LA) reservoir strain (LASr), LA conduit strain (LAScd) and LA contractile strain (LASct) using two-dimensional STE in apical views.

Results:

At 12 months follow up, a total of 39 (18%) patients had a documented recurrence of AF. Among imaging parameters, LASr > 23% showed the largest area under the curve (0.80) to predict long-term maintenance of sinus rhythm with sensitivity of 79% and specificity of 72%. Other parameters of LA function, LA diameter, maximum or minimum LA volume index, LV GLS or ejection fraction, and indices of LV diastolic function had lower area under the curve. Using multivariable logistic regression, LASr (OR 1.19, 95% CI 1.10-1.23, p<0.001) and LASct (OR 1.21, 95% CI 1.07-1.37, p=0.002) were independently associated with long-term sinus rhythm while maximum or minimum LA volume index was not.

Conclusion:

In patients with paroxysmal AF undergoing radio-frequency catheter ablation, preserved LA reservoir and contractile strain is independently associated with long-term maintenance of sinus rhythm, whereas LA diameter or volumes were not. LA strain may therefore be useful in management of patients with paroxysmal AF.

Introduction:

Atrial fibrillation (AF) recurrence is no uncommon post catheter ablation [1, 2]. AF recurrence is associated with symptomatic deterioration, thromboembolic events, hospital admissions and worse prognosis [3, 4]. Therefore, definition of an accurate and easily obtainable predictor of AF recurrence is of crucial importance. AF is associated with left atrial (LA) structural remodeling and functional deterioration due to a variable degree of myocardial hypertrophy, disarray, apoptosis and fibrosis [5, 6]. In clinical practice, two-dimensional echocardiography-derived indices of LA size are routinely used to assess left atrium (LA) [7]. However, these parameters have important limitations to describe complex myocardial changes associated with AF [8].

Recent advances in echocardiography equipment and image post-processing allow an assessment of LA strain and strain rate [9]. The speckle-tracking echocardiography (STE)-derived LA longitudinal strain has been shown to be an accurate and reproducible parameter to evaluate LA longitudinal shortening [10]. Furthermore, LA strain has significantly correlated with underlying LA fibrosis [11, 12]. This suggests that LA strain provides a comprehensive and quantitative assessment of LA structure and function. Hence, it is tempting to speculate that the analysis of LA strain will show high accuracy to predict AF recurrence post catheter ablation. However, LA strain can be affected by several factors not related to LA structural damage such as loading conditions or arrhythmias [13]. Moreover, in the real-world setting, the value of LA strain to predict rhythm outcome following catheter ablation is not known. Therefore, the aim of the present study is firstly to define echocardiographic predictors of SR maintenance in long-term follow-up, and secondly to determine the relation between LA and LV strains and to compare their predictive values in the risk stratification for AF recurrence following catheter ablation.

Methods:

Design: Prospective, single-center, observational study.

Patients: All consecutive patients with symptomatic AF undergoing elective catheter ablation between 10/2017 and 5/2019 were screened for eligibility according to the following inclusion criteria: (1) paroxysmal AF; (2) preserved left ventricular ejection fraction (LVEF) (≥ 50%). Patients with permanent or valvular AF, cardiomyopathy or congenital heart diseases, history of myocardial infarction or coronary revascularization, post cardiac surgery for any cause, pacemaker, and reduced LVEF (< 50%) were excluded. The final study population consisted of 218 patients with paroxysmal AF undergoing first catheter ablation. Control group consisted of 23 healthy controls. Study was approved by the Ethics Committee of our institution. Each patient signed informed consent before participating in the study.

Protocol: All participants underwent extensive encircling pulmonary vein isolation guided by an electro-anatomical map using the Carto 3 mapping system (Biosense-Webster, CA, USA). History, physical examination and laboratory data were recorded during the admission for

catheter ablation. Furthermore, all patients underwent comprehensive transthoracic echocardiography at baseline. Patients were discharged the day after ablation if the clinical status was stable. Following the procedure, all the patients were continuously monitored with ECG telemetry for at least 12 hours. All hospitalizations, emergency room admissions or outpatients visit were recorded. Any suspicious symptoms or abnormal electrical activity recordings at Holter were adjudicated by an experienced electrophysiologist. The AF recurrence was defined as any documented AF episode lasting ≥ 30 seconds that occurs after catheter ablation, after a blanking period of 3 months [14]. All the included patients underwent physical examination and a 24 h Holter recording at 3 months after the ablation. Additional Holter monitoring was performed if arrhythmic symptoms occurred. All documented AF episodes > 30 s were considered as a recurrence. Antiarrhythmic medication was continued for at least 3 months after catheter ablation and oral anticoagulation was continued for at least 6 months; and then stopped if no AF recurrences were detected or other indicators based on CHA2DS2-VASc cardioembolic risk score were reported.

Echocardiography: A comprehensive 2D transthoracic echocardiographic examination was performed using Vivid E95 (GE HealthCare, Horten, Norway) ultrasound system. All acquired images were stored digitally for offline analysis using a commercially available software (EchoPac, GE HealthCare). All examinations were recorded and analyzed by the same operator. Average of at least 3 beats (in sinus rhythm) or 5 beats (in AF) was taken for each measurement. Blood pressure and heart rate was recorded during each examination. The biplane Simpson method was used to assess LV volumes and ejection fraction [7]. LA antero-posterior diameter was measured at end-systole using the parasternal long-axis view [7]. Maximum and minimum LA volume, LA emptying fraction and LA expansion index were calculated from the apical 4- and 2-chamber views using the area-length method [7]. LV global longitudinal strain (GLS) was assessed using speckle tracking technique in views optimized for each chamber and at frame rate of >60 FPS. Assessment of longitudinal LA phasic strain was performed using SLE as recommended [10]. In brief, optimized apical 4- and 2-chamber views were recorded during breath hold. LA endocardial borders were traced manually in all views. Region of interest was manually adjusted and tracking quality was previewed before generating LAS and LASR curves. The LA reservoir (LASr), conduit (LAScd) and contractile (LASct) strain and SR were assessed as average of segmental values in apical views using the onset of QRS as a reference point [10].

Statistical analysis

All analyses were performed using SPSS statistics software (Version 23; Chicago, IL, USA). Continuous variables were expressed as the means and standard deviations; categorical variables were expressed as proportions. The paired t-test was used to test differences in normally distributed continuous variables in the same group, and unpaired t-test and ANOVA with post hoc test were used for exploration of differences among means of variables between different groups. A two-sided p value of less than 0.05 was considered to

represent a statistically significant difference. The lack of inter- and intra-operator variability was assessed using Wilcoxon's non-parametric test for matched data. Receiver operating characteristic (ROC) curves were generated to determine optimal cutoff values of continuous variable. The Cox proportional-hazards regression model was used to assess the clinical risk associated with increasing continuous increments of strain parameters.

Results

The baseline clinical and echocardiographic characteristics of the study population are summarized in table 1, 2. At baseline, there were no differences between the two groups with regard to the use of cardiovascular medications (table 1). Mean time from the first documented AF was present to the ablation procedure was 5.8±3.7 years. At mid-term follow-up, a total of 13 patients (12%) had early AF recurrence after catheter ablation but we considered the period of the first 3 months after catheter ablation as a blanking period [11]. At long-term follow-up, 179 (82%) patients maintained sinus rhythm whereas 39 (18%) patients had AF recurrence. Importantly, it was noticed that there was a significant decrease in the use of beta-blockers, anti-arrhythmic and anti-coagulants drugs in patients who maintained sinus rhythm (at baseline: 72%, 8% and 67% versus at follow-up: 52%, 6% and 49% respectively, all $p<0.05$) whereas a significant increase in the use of anti-arrhythmic drugs in patients who develop AF recurrence (at baseline: 19% versus at follow-up: 35%, $p<0.05$). In addition, no difference in mean systolic or diastolic blood pressure was noted during clinical follow-up in both groups of patients.

There was no difference in LV and RV dimensions, volumes or derived indices between the two groups and with no significant difference in LA diameter or maximum volume (tables 2). There was a significant difference was observed in LV GLS and E/é ratio between the two groups. However, patients with AF recurrence showed statistically significant reduced LASr and LASct at baseline compared to patients without recurrence (tables 2). Based on receiver operating characteristics, the higher AUC was obtained with LASr with a best cutoff value of 0.23 (sensitivity 79%, specificity 72%) than other LA functional or volume derived parameters (figure 1). Furthermore, the AUC for LASr was higher sensitive than LV GLS and other indices of LV diastolic function (figures 2, 3).

Discussion

The main findings of our study are: 1) In the global population of patients with non-significant LA dilation, both LASr and LASct were independent predictors of sinus rhythm maintenance after catheter ablation. 2) In the group of patients with AF recurrence, LA longitudinal dysfunction was also present in the absence of LA enlargement assessed by LA size. These results suggest that patients with higher LA strain values seem to have a greater likelihood for maintenance of sinus rhythm following ablation. In line with these observations, normal LA size does not exclude the risk of AF recurrence, but LA volume derived indices such as LAEF and LAEI, could discriminate patients with AF recurrence after

catheter ablation therapy compared with patients without recurrence. However, LA volume derived indices have many limitations during measurement based on 2D echocardiography images. Thus, LA strain represents a more subtle form of LA remodeling that was closely associated with AF freedom after catheter ablation.

It is well known that impaired LA strain increased risk of AF recurrence after catheter ablation and several studies have reported that LA strain is a predictor of AF recurrence after catheter ablation for paroxysmal AF, which is associated with worse outcome in the follow-up period [15-18]. Other studies also have reported that LA strain might be used as a predictor of sinus rhythm maintenance after ablation procedure, which is associated with better prognosis in long-term follow-up [19-21]. A recent meta-analysis reported that a dilated LA with diameter more than 50 mm and volume above 150 ml or LASr below 19% reflect an unstable LA that is unlikely to hold sinus rhythm after ablation [22]. In this context, our study demonstrated that non-impaired LASr is associates with sinus rhythm maintenance independent of LA size and potentially it can be used to guide the rhythm monitoring in this clinical setting. Furthermore, LASct also followed a similar trend which emphasized that the atrial booster function importantly contributes to LA functional preserve. Thus, it should be considered when we assess LA longitudinal function.

In contrast to a previous study reported that LA volume was the best predictor of AF recurrence following single ablation procedure in patients with paroxysmal AF, even in patients with a relatively small LA [23], our study demonstrated that LA volume was not an independent predictor of AF freedom in a multivariate logistic regression model and LA phasic strain showed more accuracy to predict the rhythm outcome in the patients with paroxysmal AF and non-significant LA enlargement. However, the interplay between LA dilatation and LA mechanical dysfunction and LV mechanics is critical, especially in patients with other risk factors associated with pressure overload, that makes the atrium susceptible to LA dilatation which in itself is an adaptive change related to LV high filling pressures [24]. Since LA pump function is less dependent on LV mechanics [25], this implies that the absolute value for LASr should be combined with LASct during the assessment of LA strain performance and LASct may be useful when the etiology of paroxysmal AF is suspected to be related to isolated atrial cardiomyopathy.

In agreement with previous studies reported that both LV GLS and LAS provided incremental predictive values over clinical and standard echocardiographic parameters in patients with AF, specifically LA strain was more useful than LV GLS in patients without LA enlargement [25, 26], our study also demonstrated that the prognostic value of LAS for maintenance of sinus rhythm was incremental over LV GLS in AF patients with preserved LVEF without LA enlargement. However, it is useful to combine both LA phasic strain and LV GLS to uncover LA and LV subtle longitudinal dysfunction in AF patients with preserved LVEF, especially in obese patients or patients with other risk factors, such as hypertension and diabetes. This

combination may be useful to override some limitation of myocardial strain assessment under different loading conditions, especially in patients with history of recurrent AF.

Limitation

First, patients cannot be monitored continuously throughout the follow-up period. Thus, asymptomatic episodes of AF may not have been detected during the follow-up. Secondly, there is no clear data on the exact AF burden before ablation procedures which may provide more information about the relation between LA functional remodeling and rhythm outcome. Thirdly, grading of diastolic dysfunction based on invasive measurements of filling pressures is missed in our study and since measurements were obtained at a single time point, strain measurements might be affected by pressure overload. Consequently, the serial assessment of LA phasic function should be considered when we assess the LAS under different loading conditions.

Conclusion

Both poor LA reservoir capacity and impaired contractile function are associated with an increased risk of paroxysmal AF recurrence following radio-frequency catheter ablation. LA reservoir strain is more accurate predictor of AF recurrence than other standard echocardiographic parameters and it might provide incremental predictive value for maintaining normal sinus rhythm over clinical features in patients with a history of paroxysmal AF. Further prospective studies are needed to determine the future implications of LA phasic strain in the process of selecting patients with history of AF to be referred to catheter ablation.

Table 1: Baseline clinical characteristics and medication in overall patients.

	Overall patients (n=218)	SR maintenance group (n=179)	AF recurrence group (n=39)	P value (SR maintenance vs. AF recurrence)
Age, y	62 ± 10	61 ± 9	66 ± 11	0.015
Males, n (%)	153 (62)	128 (70)	25 (64)	0.362
Body mass index (kg/m^2)	26.9 ± 4	26.9 ± 3.9	27 ± 4.2	0.907
Obesity, n (%)	58 (27)	40 (22)	18 (46)	0.466
CAD, n (%)	11 (5)	7 (4)	4 (10)	0.102
COPD, n (%)	14 (6)	11 (6)	3 (8)	0.723
Hyperlipidemia, n (%)	82 (38)	68 (38)	14 (36)	0.808
Hypertension, n (%)	88 (38)	71 (40)	17 (43)	0.653
Diabetes mellitus, n (%)	11 (5)	7 (4)	4 (10)	0.102
Current smoker, n (%)	21 (10)	18(10)	3 (7)	0.023
NT Pro-BNP (pg/mL)	266 ± 344	231 ± 282	518 ±574	< 0.001
Beta blockers	165 (76)	128 (72)	37 (95)	0.002
ACEi	44 (20)	30 (17)	14 (36)	0.025
ARBs	15 (6)	14 (8)	1 (2)	0.110
CCBs	14 (6)	12 (7)	2 (5)	0.275
Anti-platelets	26 (12)	19 (11)	7 (18)	0.697
Anti-coagulants	153 (70)	120 (67)	33 (84)	0.012
Anti-arrhythmic	28 (13)	14 (8)	14(36)	0.0101
Diuretics	25 (11)	15 (8)	10 (26)	0.060
Aldosterone antagonists	27 (12)	17 (9)	10 (26)	0.035
Digoxin	7 (3)	4 (2)	3 (8)	0.024

Abbreviations: ACEI = angiotensin converting enzyme inhibitors, AF = atrial fibrillation, ARBs = angiotensin II receptor blockers, BMI = body mass index, CCBs = calcium blockers, SR = sinus rhythm.

Table 2: Baseline echocardiographic characteristics in overall patients.

	Overall patients (n=218)	SR maintenance group (n=179)	AF recurrence group (n=39)	P value (SR maintenance vs. AF recurrence)
Heart rate (bpm)	65 ± 10	65 ± 10	69 ± 11	0.025
LV end-diastolic diameter (cm)	5.2 ± 0.3	5.2 ± 0.3	5.0 ± 0.5	0.740
LV end-systolic diameter (cm)	3.2 ± 0.5	3.2 ± 0.5	3.2 ± 0.6	0.138
LV relative wall thickness	0.43 ± 0.06	0.43 ± 0.06	0.42 ± 0.06	0.693
LV mass index (g/m^2)	94.3 ± 24	93.3 ± 23	99.3 ± 27.1	0.170
LV end-diastolic volume index (ml/m^2)	53.8 ± 12.9	55.3 ± 13.9	53.4 ±12.7	0.416
LV end-systolic volume index (ml/m^2)	21.5 ± 6.8	21 ± 6.7	22.4 ± 7.5	0.397
LV stroke volume index (mL/m^2)	32 ± 8.9	33 ± 9	33 ± 8.6	0.741
LV ejection fraction (%)	61 ± 6	61 ± 6	60 ± 7	0.472
LV global longitudinal strain (%)	-19.4 ± 2.8	-19.8 ± 2.7	-17.7 ± 2.4	< 0.001
E/A ratio	1.20 ± 0.45	1.18 ± 0.43	1.18 ± 0.43	0.197
e' lateral (m/sec)	0.09 ± 0.05	0.09 ± 0.3	0.1 ± 0.1	0.164
e' septal (m/sec)	0.10 ± 0.08	0.09 ± 0.03	0.11 ± 0.11	0.591
E/e' ratio	8.8 ± 3.6	8.1 ± 2.2	12.8 ± 6.7	< 0.001
Systolic PAP (mmHg)	29.8 ± 5.8	29.6 ± 5.9	30.6 ± 5.74	0.321
RV basal diameter (cm)	3.67 ± 0.38	3.7 ± 0.39	0.36 ± 0.27	0.210
RV mid diameter (cm)	2.49 ± 0.36	2.49 ± 0.36	2.60± 0.31	0.446
RV TAPSE	24.1 ± 3.5	24 ± 3.6	23.6 ± 3.1	0.616
RV global longitudinal strain (%)	-22.4 ± 4.8	-21.6 ± 6.8	-21.6± 6.8	0.717
RV free wall longitudinal strain (%)	-23.8± 5.2	-22.4 ± 4.8	-22.8± 6.5	0.790
LA diameter (cm)	3.9 ± 0.42	3.9 ± 0.41	4.1 ± 0.42	0.018
LA max volume index (ml/m^2)	33.54± 8.03	32.87 ± 7.59	36.59 ± 9.32	0.008
LA min volume index (ml/m^2)	16.73 ± 5.87	16.08 ± 5.05	19.71 ± 8.12	< 0.001
LA emptying fraction (%)	53.77 ± 9.51	54.89 ± 8.97	48.63 ± 10.28	< 0.001
LA expansion index	126.8 ± 48.3	132.7 ± 47.8	100.1 ± 41.2	< 0.001
Reservoir LA strain (%)	27.03 ± 7.30	28.4 ± 6.65	20.74 ± 6.92	< 0.001
Conduit LA strain (%)	14.21 ± 4.65	15.02 ± 4.3	10.5 ± 4.31	< 0.001
Contractile LA strain (%)	12.81 ± 3.77	13.4 ± 3.64	10.24 ± 3.26	< 0.001
LA stiffness index	0.36 ± 0.23	0.31 ± 0.14	0.65 ± 0.40	< 0.001
LA contractile strain index	47.69 ± 8.06	47.7 ± 8.03	50.12 ± 7.85	0.038

Abbreviations: AF = atrial fibrillation, LV = left ventricular, MDRD = modification of diet in renal disease, PAP = pulmonary artery pressure, RV = right ventricular, TAPSE = tricuspid annular plane systolic excursion, LA = left atrial, SR = sinus rhythm.

Table 3. Echocardiography predictors of high probability of long-term maintenance of sinus rhythm.

	Univariable Analysis		Multivariable Analysis	
	OR (95% CI)	p value	OR (95% CI)	p value
Reservoir LAS	1.20 (1.12 – 1.28)	<0.001	1.19 (1.10-1.23)	<0.001
LV GLS	1.35 (1.16 – 1.56)	<0.001		
LAVI	0.94 (0.91 – 0.98)	0.011		
Contractile LAS	1.28 (1.15- 1.43)	<0.001	1.21 (1.07-1.37)	0.002
LV GLS	1.35 (1.16 – 1.56)	<0.001		
LAVI	0.94 (0.91 – 0.98)	0.011		

CI = confidence interval, OR = odds ratio, LAS = left atrial strain, LV GLS = left ventricular global longitudinal strain, LAVI = left atrial volume index

Figure 1: Receiver-operating characteristic curves of left atrial reservoir strain (LASr), LA conduit strain (LAScd) and LA contractile strain (LASct), LA emptying fraction (LAEF), LA expansion index (LAEI), LA end-systolic (LAES) and end-diastolic (LAED) volume index (VI) to predict long-term maintenance of sinus rhythm.

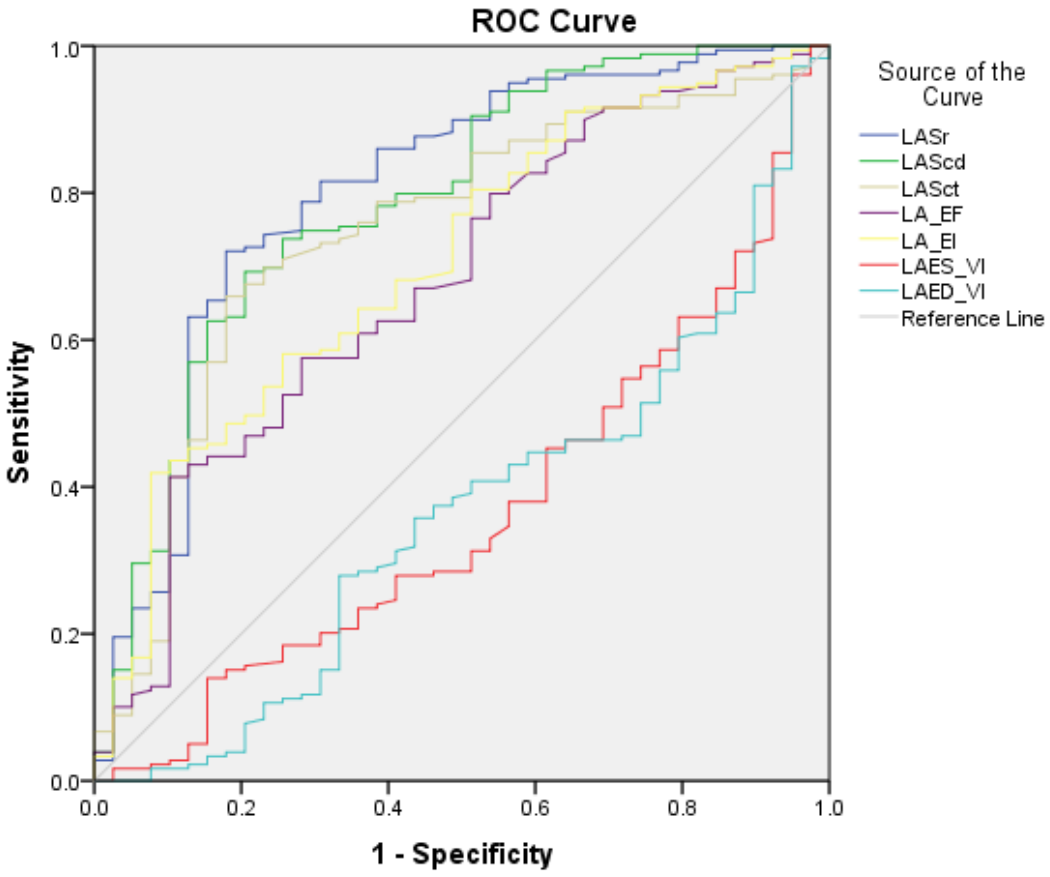

Diagonal segments are produced by ties.

Area Under the Curve

Test Result Variable(s)	Area	Std. Error[a]	Asymptotic Sig.[b]	Asymptotic 95% Confidence Interval	
				Lower Bound	Upper Bound
LASr	.802	.043	.000	.718	.886
LAScd	.788	.042	.000	.705	.871
LASct	.745	.044	.000	.658	.832
LA_EF	.680	.048	.000	.586	.773
LA_EI	.707	.045	.000	.619	.795
LAES_VI	.367	.048	.009	.274	.461
LAED_VI	.363	.048	.008	.269	.458

Figure 2: Receiver-operating characteristic curves of left atrial reservoir strain (LASr), left ventricular global longitudinal strain (LVGLS), LV ejection fraction (LVEF), LV mass index (LVMI), LV end- diastolic volume (LAEDV), LV end-systolic volume (LAESV) indices and LV stroke volume index (LVSVi) to predict long-term maintenance of sinus rhythm.

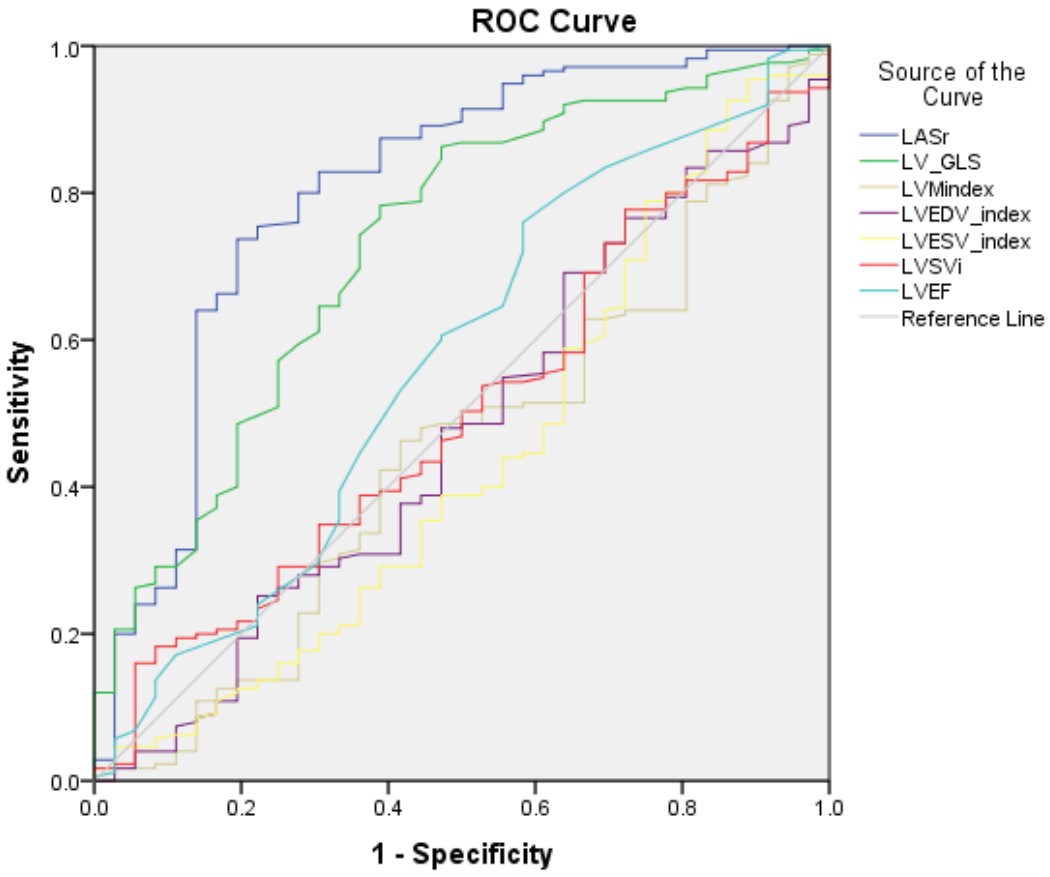

Diagonal segments are produced by ties.

Area Under the Curve

Test Result Variable(s)	Area	Std. Error[a]	Asymptotic Sig.[b]	Asymptotic 95% Confidence Interval	
				Lower Bound	Upper Bound
LASr	.803	.046	.000	.714	.892
LV_GLS	.728	.047	.000	.636	.821
LVM_index	.449	.053	.331	.344	.553
LVEDV_index	.473	.054	.617	.368	.579
LVESV_index	.439	.056	.247	.328	.549
LVSV_index	.500	.051	.994	.401	.600
LVEF	.570	.055	.189	.461	.678

Figure 3: Receiver-operating characteristic curves of left atrial reservoir strain (LASr), left ventricular global longitudinal strain (LVGLS) and deceleration time (DT) and other indices of LV diastolic function to predict long-term maintenance of sinus rhythm.

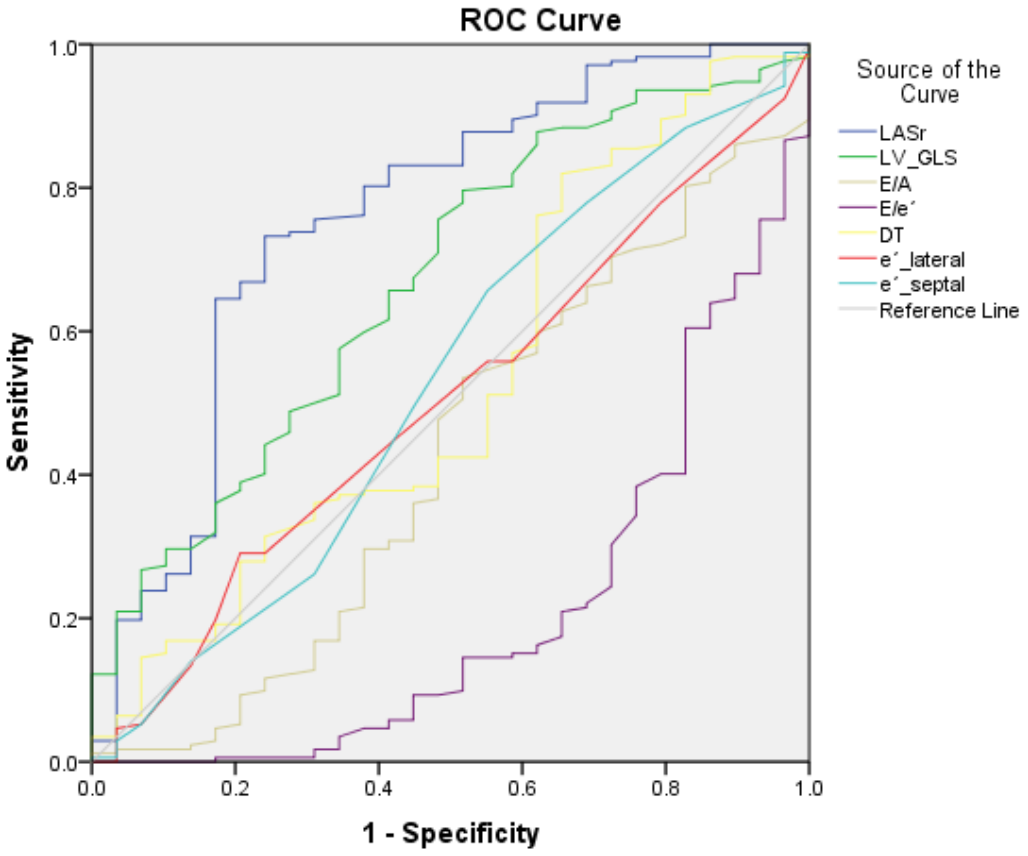

Diagonal segments are produced by ties.

Area Under the Curve

Test Result Variable(s)	Area	Std. Error[a]	Asymptotic Sig.[b]	Asymptotic 95% Confidence Interval	
				Lower Bound	Upper Bound
LASr	.760	.053	.000	.655	.864
LV_GLS	.669	.054	.004	.564	.774
E/A	.424	.061	.189	.305	.543
E/e´	.211	.050	.000	.113	.309
DT	.531	.062	.593	.410	.652
e´_lateral	.502	.056	.974	.393	.611
e´_septal	.528	.062	.628	.407	.650

Chapter 9

Impact of redo catheter ablation on left atrial geometry in patients with recurrent atrial fibrilation

Introduction:

Restoraion of sinus rhythm with radiofrequency catheter (RF) ablation in patients with paroxysmal and persistent atrial fibrillaion (Afib) results in left atrial (LA) remodeling. However, limited knowledge exists regarding the net effect of wide circumferenial RF pulmonary vein isolation (PVI) on the LA geometry.

Methods:

Over a 4 year period, all patients that underwent at least two point-by-point wide circumferenial PVI procedures for paroxysmal or persistent Afib in our center were included (n=82). In all patients a 3D rotational angiography of the left atrium was performed immediately before ablation, at index and repeat ablations. Left atrial geometry in terms of volume, sphericity, surface and anterior-posterior diameter were assessed in all patients between first-second and second-third PVI.

Results:

71 patients (31 paroxysmal Afib, 40 persistent Afib) underwent a rotational angiography before their first and second PVI, whereas 19 patients underwent a rotational angiography before their second and third PVI. There was a statistical significant reduction of the LA volume and the surface of the left atrium in all 71 patients.

Patients with paroxysmal atrial fibrillation also showed significant increase of the LA sphericity, whereas patients with persistent atrial fibrillation showed only a trend towards increased sphericity, without reaching statisitcal significance. The group of the 19 patients, who underwent a third PVI showed no differences of their LA geometry after electrical mapping of the gaps and focal RF re-isolation.

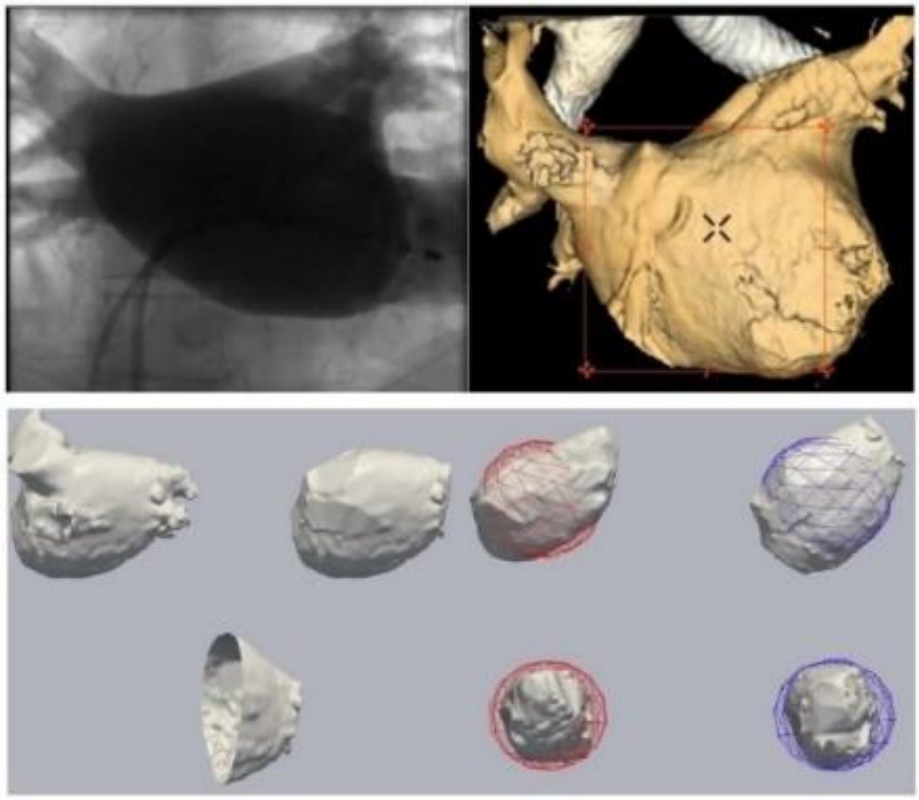

Conlusions:

Wide circumferential RF pulmonary vein isolation itself results in remodeling of the LA, irrespective of long-term maintenance of sinus rhythm, in both patients with paroxysmal and persistent Afib.

Chapter 10

Heart failure with preserved ejection fraction or non-cardiac dyspnea in paroxysmal atrial fibrillation: The role of left atrial strain

Background:

Diagnosis of heart failure with preserved ejection fraction (HFpEF) in patients with dyspnea and paroxysmal atrial fibrillation (AF) is challenging. Speckle tracking-derived left atrial strain (LAS) provides an accurate estimate of left ventricular (LV) filling pressures and left atrial (LA) phasic function. However, data on clinical utility of LAS in patients with dyspnea and AF are scarce.

Objective:

To assess relationship between the LAS and the probability of HFpEF in patients with dyspnea and paroxysmal AF.

Methods:

The study included 205 consecutive patients (62±10 years, 58% males) with dyspnea (NYHA≥II), paroxysmal AF and preserved LV ejection fraction (≥50%), who underwent speckle tracking echocardiography during sinus rhythm. Probability of HFpEF was estimated using H2FPEF and HFA-PEFF scores, which combine clinical characteristics, echocardiographic parameters and natriuretic peptides.

Results:

Patients with high probability of HFpEF were significantly older, had higher body mass index, NT-proBNP, E/e', pulmonary artery pressure and larger LA volume index than patients in low-to-intermediate probability groups (all $p<0.05$). All components of LAS and LA strain rate showed proportional impairment with increasing probability of HFpEF (all $p<0.05$). Out of the speckle tracking-derived parameters, reservoir LAS showed the largest area under the curve (AUC = 0.78, $p<0.001$) and the strongest independent predictive value (OR: 1.22, 95% CI 1.08-1.38) to identify patients with high probability of HFpEF.

Conclusions:

Reservoir LAS shows a high diagnostic performance to distinguish HFpEF from non-cardiac causes of dyspnea in symptomatic patients with paroxysmal AF.

Introduction

Diagnosis of heart failure with preserved ejection fraction (HFpEF) in elderly patients with dyspnea and paroxysmal atrial fibrillation (AF) is challenging. Both HFpEF and AF show high concomitant prevalence (1-4). Moreover, presence of HFpEF is associated with increased risk of future AF while AF triggers HFpEF (1, 2, 5). As non-cardiac causes of dyspnea are also common (1, 2, 6), there is a clinical need for simple parameters to distinguish HFpEF from non-cardiac dyspnea in daily practice.

HFpEF leads to left atrial (LA) pressure overload, fibrosis, remodeling and dysfunction (7-10). Speckle tracking-derived LA strain (LAS) has emerged as an accurate marker of elevated left ventricular (LV) filling pressures and LA functional impairment (3, 11). Several studies have shown high diagnostic accuracy of LAS to discriminate HFpEF from non-cardiac dyspnea in patients with sinus rhythm (12-14). However, the data on clinical utility of LAS to diagnose HFpEF in individuals with dyspnea and AF are limited. As both HFpEF and AF are associated with abnormalities of LA function, the accuracy of LAS to detect HFpEF may be impaired (1, 2, 6, 14). Therefore, the aim of the present study was to assess the relationship between LAS and the probability of HFpEF in patients with dyspnea and paroxysmal AF.

Methods

Design Prospective, single-center study.

Patients The study population consisted of 205 consecutive patients (62±10 years, 58% males) with limiting dyspnea (NYHA≥II), paroxysmal AF and preserved LV ejection fraction (≥50%) undergoing transthoracic echocardiography during sinus rhythm. Patients with suspected ischemic heart disease, more than mild heart valve disease, hypertrophic or restrictive cardiomyopathy, reduced LV ejection fraction (<50%), or post catheter ablation were excluded. Likelihood of HFpEF was assessed using H2FPEF and HFA-PEFF scores, which allow discriminating HFpEF from non-cardiac causes of dyspnea (1, 2). The H2FPEF score is a validated and robust algorithm relying on simple clinical and Doppler echocardiographic characteristics (age, body mass index, history of hypertension or atrial fibrillation, pulmonary artery systolic pressure and mitral E/e') (1). The HFA-PEFF diagnostic algorithm, combining Doppler echocardiography and natriuretic peptides, has been recently proposed in the consensus recommendation from the Heart Failure Association (HFA) of the European Society of Cardiology (ESC) (5). The H2FPEF or HFA-PEFF scores ≥5 suggest high probability of HFpEF (1, 2). All patients with paroxysmal AF were considered as patients with sinus rhythm in the HFA-PEFF and H2FPEF scores. Study was approved by the Ethics Committee of our institution. Each patient signed informed consent before participating in the study.

Echocardiography A comprehensive 2D transthoracic echocardiographic examination was performed using Vivid E95 (GE HealthCare, Horten, Norway) ultrasound system. All acquired images were stored digitally for offline analysis using a commercially available software (EchoPac, GE HealthCare). All examinations were recorded during sinus rhythm and analyzed

by the same operator. Average of at least 3 beats was taken for each measurement. Blood pressure and heart rate were recorded during each examination. The biplane Simpson method was used to assess LV volumes and ejection fraction (16). LA antero-posterior diameter was measured at end-systole using the parasternal long-axis view (16). Maximum and minimum LA volume, LA emptying fraction and LA expansion index were calculated from the apical 4- and 2-chamber views using the area-length method (16). Right ventricular (RV) end-diastolic basal and mid-cavity diameters were measured in the modified apical 4-chamber view (16). LV global longitudinal strain (GLS), RV GLS and RV free wall longitudinal strain (LS) were assessed using speckle tracking technique in views optimized for each chamber and at frame rate of >60 FPS (16, 17). Assessment of longitudinal LAS and strain rate (SR) were performed as recommended (17). In brief, optimized apical 4- and 2-chamber views were recorded during breath hold. LA endocardial borders were traced manually in all views. Region of interest was manually adjusted and tracking quality was previewed before generating LAS and LASR curves. The LA reservoir (LASr), conduit (LAScd) and contractile (LASct) strain and SR were assessed as average of segmental values in apical views using the onset of QRS as a reference point (17). The LA stiffness index was calculated as the E/e' divided by LASr. The contractile LAS index was calculated by the formula [(LASct/LASr) × 100].

Feasibility The echocardiographic images were suboptimal in 15 patients (feasibility 93%), who were excluded from the analysis.

Intra- and inter-observer variability for LAS was assessed by two operators in 10 randomly selected patients in each group. The intra- and the inter-observer variability for LAS and LASR assessment were below 5% and significantly lower ($p<0.05$) than that of the conventional LA indices.

Statistical analysis

Data are expressed as mean ± SD for continuous variables and as counts or percentages for categorical variables. One-way ANOVA or Fisher exact tests were used as appropriate. Receiver operating characteristic curves were constructed to assess diagnostic performance of LAS to identify patients with high probability of HFpEF. The association between LAS, LV GLS, RV GLS, RV free wall strain and probability of HFpEF was tested using univariable and multivariable logistic regression. For all tests, values of $p<0.05$ were considered significant. Statistical analysis was performed using the SPSS version 23 (SPSS inc, Chicago, Illinois, USA) and the GraphPad Prism version 6.0 (GraphPad Software, San Diego, California, USA).

Results

Clinical and echocardiography characteristics Table 1 and table 2 show baseline clinical and echocardiography characteristics, respectively, in three groups of patients according to their probability of HFpEF defined by each scoring system. A total of 29 patients (14%) showed high probability of HFpEF concordantly using both scores (figure 1).

Patients with high probability of HFpEF were significantly older, had higher prevalence of obesity and hypertension, higher percentage of diuretics use, higher NT-proBNP, E/e', pulmonary artery pressure, and larger LA volume index (LAVI) than patients in low-to-intermediate probability groups (all $p<0.05$).

Cardiac mechanics All components of LAS and LASR showed a proportional impairment with increasing probability of HFpEF defined by using both scores (table 2, figure 2, figure 3). Reservoir LAS had the most consistent changes across both scoring systems, which remained significant after normalization to E/e', LAVI and LV GLS (table 2). In contrast, LV or RV GLS were similar between groups.

Predicting high probability of HFpEF Out of the speckle-tracking derived parameters, reservoir LAS showed largest area under the curve (AUC = 0.78; $p<0.001$) to identify patients with high probability of HFpEF (figure 4). The cutoff value with high sensitivity (90%) was <28% while the cutoff with high specificity (80%) was <23%. In multivariable regression analysis, reservoir LAS emerged as the strongest independent predictors of HFpEF (table 3). Importantly, LA strain did not present a good correlation with E/e' but it demonstrated better agreement with LA max volume and derived indices than E/e' (figure 5).

Discussion

The findings of the present study can be summarized as follows: [1] Speckle tracking derived indices of LA phasic function appear to be proportionally impaired with increasing probability of HFpEF defined by using both HFA-PEFF and H2FPEF scores while LV and RV GLS did not; [2] Among speckle tracking-derived indices, reservoir LAS showed the highest accuracy and the strongest independent predictive value to identify HFpEF; [3] Assessment of reservoir LAS was highly feasible (93%) and reproducible. This suggests clinical potential of reservoir LAS to diagnose HFpEF in patients with history of AF.

LAS in diagnosis of HFpEF As causes of dyspnea in patients with AF history are not clear the identification of reliable parameter to distinguish HFpEF from non-cardiac causes of dyspnea in patients with a history of AF is clinically important. HFpEF is associated with diffuse abnormalities of both ventricular and atrial myocardium (1, 2). Speckle tracking-derived indices of LV and LA myocardial function have been recently proposed to be implemented in the diagnostic algorithm to identify elevated left atrial pressure or HFpEF (2, 3, 18). Out of these indices, LA phasic strain (3) and LAS have been demonstrated to be a sensitive marker of early diastolic dysfunction and elevated LA pressures, two hallmark features of HFpEF (1-3). LAS shows also significant correlation with progression of LV diastolic function, NT-proBNP and outcome (19-24). Likewise, reservoir LAS strain has been proposed as an additional parameter to grade LV diastolic dysfunction or to improve diagnostic performance of the HFA-PEFF score alone (6, 11, 25) or in a superior manner as compared with conventional echocardiographic indices to diagnose HFpEF (6, 13, 14). However, in these studies, the majority of patients had sinus rhythm and value of LA derived indices in patients

with AF is unclear. Extending these finding to patients with paroxysmal AF, our study demonstrates proportional reduction of phasic LAS and LASR with increasing probability of HFpEF. The earliest worsening in LAS performance was observed in LA reservoir function followed by contractile function, which deteriorated at later stages as LA afterload-work mismatch progresses. The relationship between LAS and probability of HFpEF remained significant after normalization to LV systolic function (GLS), LV filling pressures (E/e') and LA size (LAVI). As the accuracy to diagnose HFpEF was comparable to previous reports in patients with sinus rhythm (6) and our findings indicate the diagnostic value of reservoir LAS to identify HFpEF in wide spectrum of patients with dyspnea regardless of AF history.

LAS and prognostic perspective

The LA contractile phase is most dependent on atrial function as opposed to LV diastolic properties. In agreement to previous studies reported that patients with deteriorated clinical symptoms (NYHA>II) presented worse LA contractile function (26, 27), our study showed that the earliest changes in LAS performance was observed in LA reservoir function followed by contractile function; which deteriorated in later stages as work mismatch progresses. Therefore, in patients with a long history of diastolic dysfunction, there is an increased chance of loss of LA systole, thus more likely to develop AF since the LA myocardium have undergone an irreversible remodeling (28).

Similar to a previous study reported that LAS decreases with worsening diastolic dysfunction in a gradual manner (29), our study emphasized that the LAS curve is a non-plane mirror of the curve of LV strain and it could reflex earlier LV diastolic dysfunction than other LV strain indices. Changes in LA phasic function could be attributed to intrinsic LA myocardial dysfunction possibly in connection with altered LV function (28-30). This supports the hypothesis that the LAS is more sensitive to pressure overload than LV strain. Consequently, the serial assessment of LA phasic function should be considered when we assess the LAS under different loading conditions, especially in patients at risk of developing HF (29, 31]. The serial assessment of LAS may be used to unmask subclinical diastolic dysfunction, thus optimizing the time of referral patients to the HF clinic.

A prognostic importance of LA function in HFpEF was reported in many studies (29, 32, 33). Abnormal reservoir LAS (<23%) was significantly associated with worse NYHA class and with the risk of HF hospitalization at 2 years independently from age and sex (32). In a study of more than 350 patients, LA dysfunction in HFpEF was associated with a higher risk of HF hospitalization independent of potential clinical confounders, but not independent of LV strain and filling pressure (29).

The BNP and NT-proBNP levels were considered among the diagnostic criteria of HFA-PEFF risk scoring system. According to many studies demonstrated that reservoir LAS was a predictor of elevated serum BNP levels (25, 30, 34), it was observed in our study that impaired reservoir LAS was associated with an increase in NT-proBNP level independent of

changes in ventricular function. Our results supported the current studies that showed that reservoir LAS is more powerful prognostic factor in HFpEF than LV GLS and other dimensional and functional parameters.

Study limitations

The analysis of LAS using speckle tracking may be vendor dependent, similarly to the LV GLS. However, inter-vendor variability affects absolute values of LAS rather than relative changes between serial examinations. In the present study, the same echo machine and analyzing software were used for all the analyses. This suggests that our findings may be extrapolated also to different vendors or software versions as long as the same equipment is used for serial assessment. The pulmonary capillary wedge pressure (PCWP) was not measured. The PCWP measurement would create more understanding about changes in LA phasic function under diferent hemodynamic conditions, volume statue and heart rate variability.

Conclusions

In this cohort of patients with symptomatic paroxysmal AF and dyspnea, reservoir LAS showed to be clinically useful index to detect patients with high probability of HFpEF. This advocates for more liberal use of LAS in elderly patients with dyspnea.

Scale of H_2FPEF risk score [1].

	Clinical Variable	Values	Points
H_2	Heavy	Body mass index > 30 kg/m^2	2
	Hypertensive	2 or more antihypertensive medicines	1
F	Atrial Fibrillation	Paroxysmal or persistent	3
P	Pulmonary Hypertension	Doppler echocardiographic estimated right ventricular systolic pressure > 35 mmHg	1
E	Elder	Age > 60 years	1
F	Filling Pressure	Doppler echocardiographic E/e' > 9	1
H_2FPEF score			Sum (0-9)

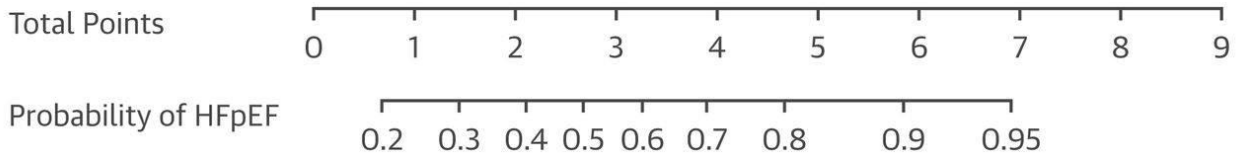

Scale of ESC HFA-PEFF risk score [2].

	Functional	Morphological	Biomarker (SR)	Biomarker (AF)
Major	septal e' < 7 cm/s or lateral e' < 10 cm/s or Average E/e' ≥ 15 or TR velocity > 2.8 m/s (PASP > 35 mmHg)	LAVI > 34 ml/m^2 or LVMI ≥ 149/122 g/m^2 (m/w) and RWT > 0,42 #	NT-proBNP > 220 pg/ml or BNP > 80 pg/ml	NT-proBNP > 660 pg/ml or BNP > 240 pg/ml
Minor	Average E/e' 9 -14 or GLS < 16 %	LAVI 29-34 ml/m^2 or LVMI > 115/95 g/m^2 (m/w) or RWT > 0,42 or LV wall thickness ≥ 12 mm	NT-proBNP 125-220 pg/ml or BNP 35-80 pg/ml	NT-proBNP 365-660 pg/ml or BNP 105-240 pg/ml

Major Criteria: 2 points	> 5 points; HFpEF
Minor Criteria: 1 point	2-4 points: Diastolic Stress Test or Invasive Haemodynamic Measurements

Figure 1. Classification of patients according to the probability of HFpEF using the H2FPEF and the HFA-PEFF scores.

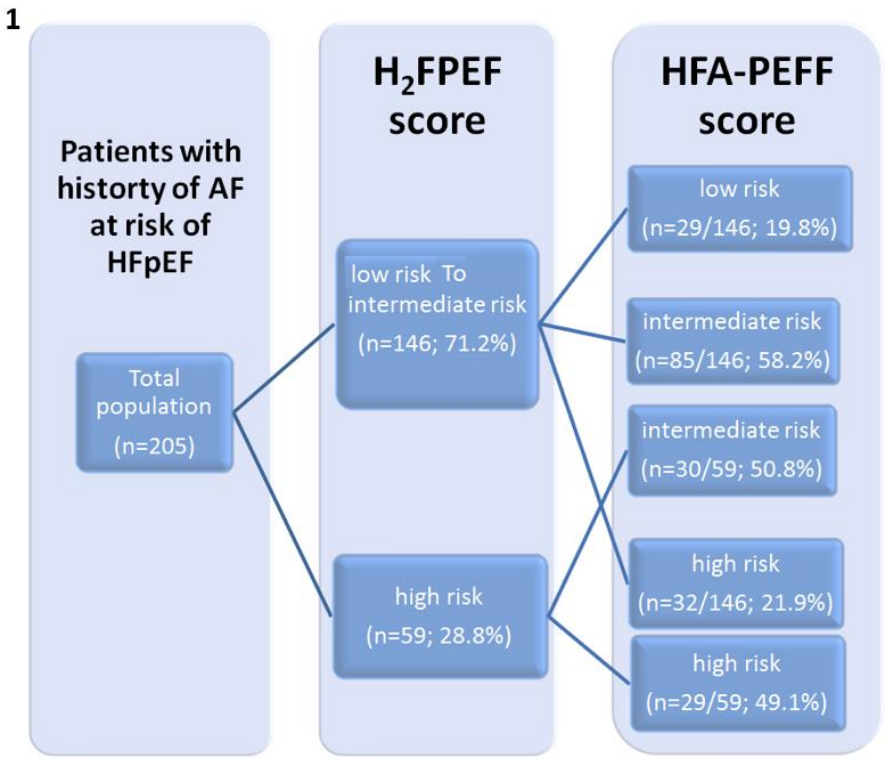

Figure 2. RV, LV and LA phasic strain in patients with low, intermediate and high probablity of HFpEF defined by the H2FPEF (2A) and the HFA-PEFF (2B) scores.

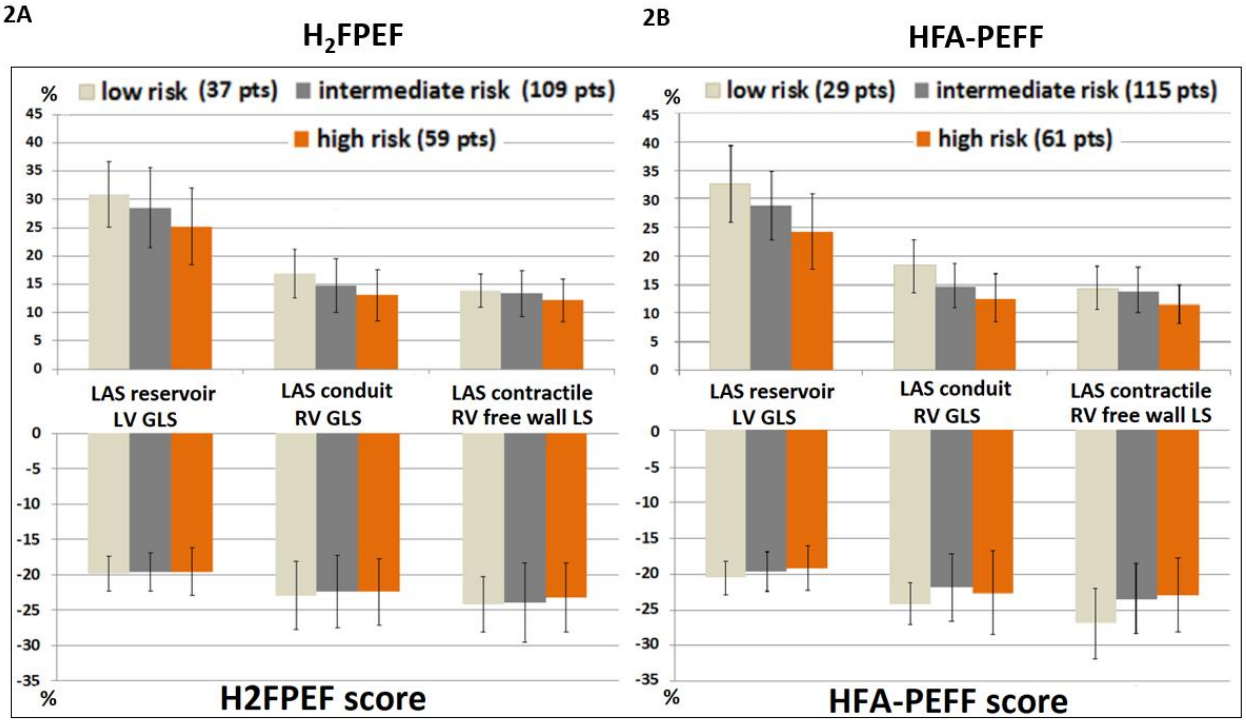

Figure 3. LA phasic strain per score using the H2FPEF (3A) or the HFA-PEFF (3B) score.

3A

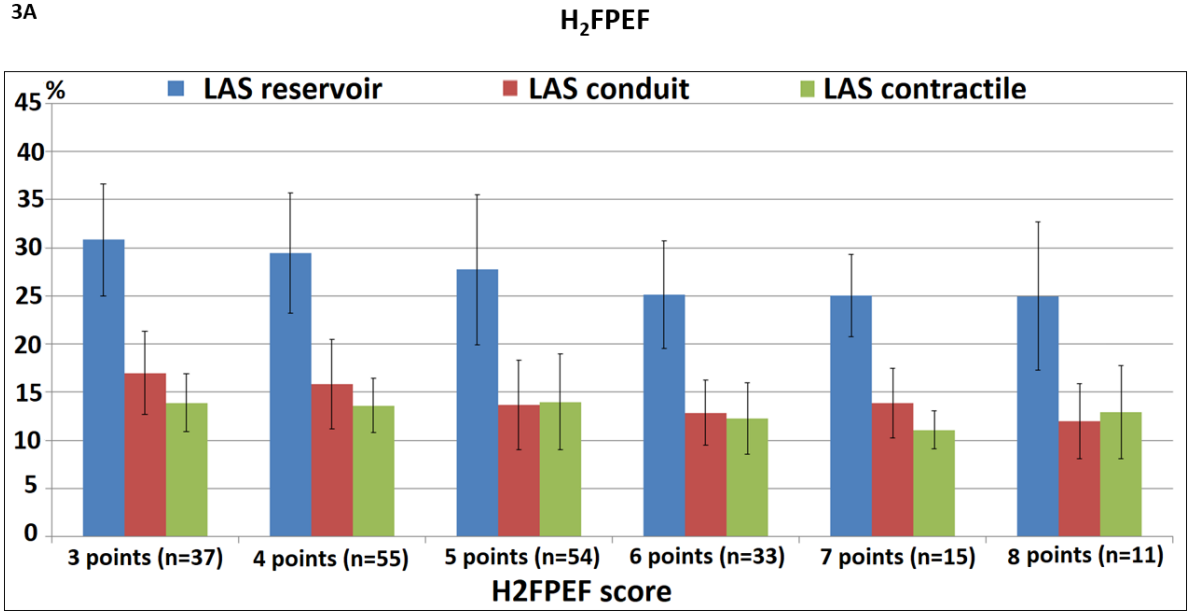

3B

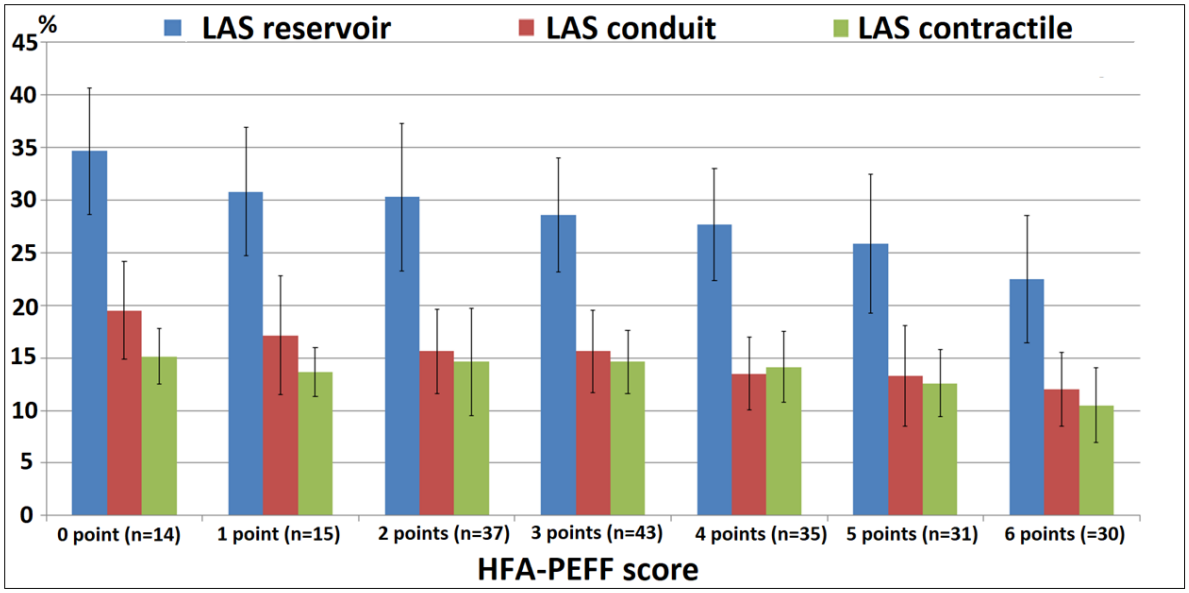

Figure 4. Receiver-operating characteristic curves of LAS, LV GLS, RV GLS and RV FWLS to predict high probability of HFpEF defined by H2FPEF (4A) or HFA-PEFF (4B) alone or by their agreement (4C).

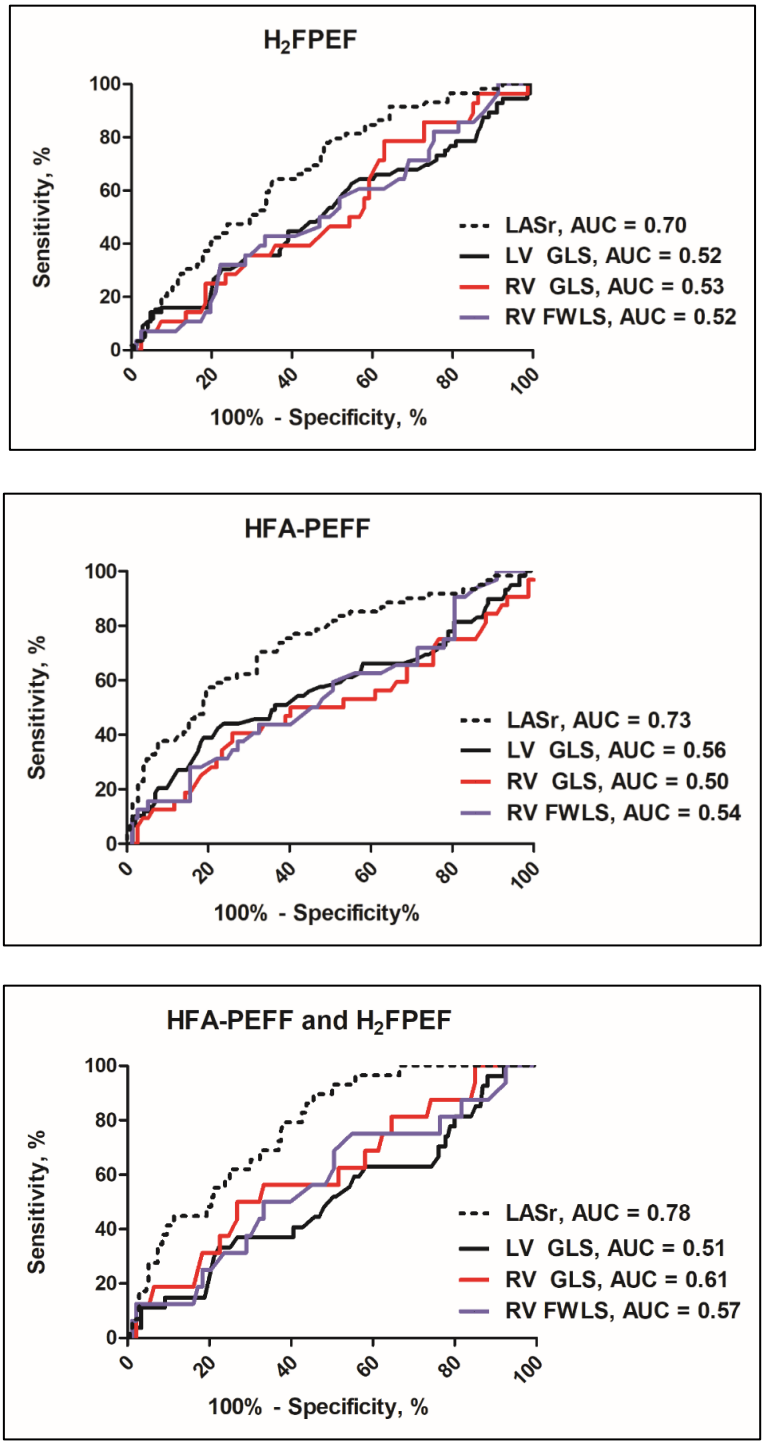

Figure 5A: The correlation between LA reservoir, conduit and contractile LA strain and LA contractile strain index with LV filling pressure index (E/e' ratio).

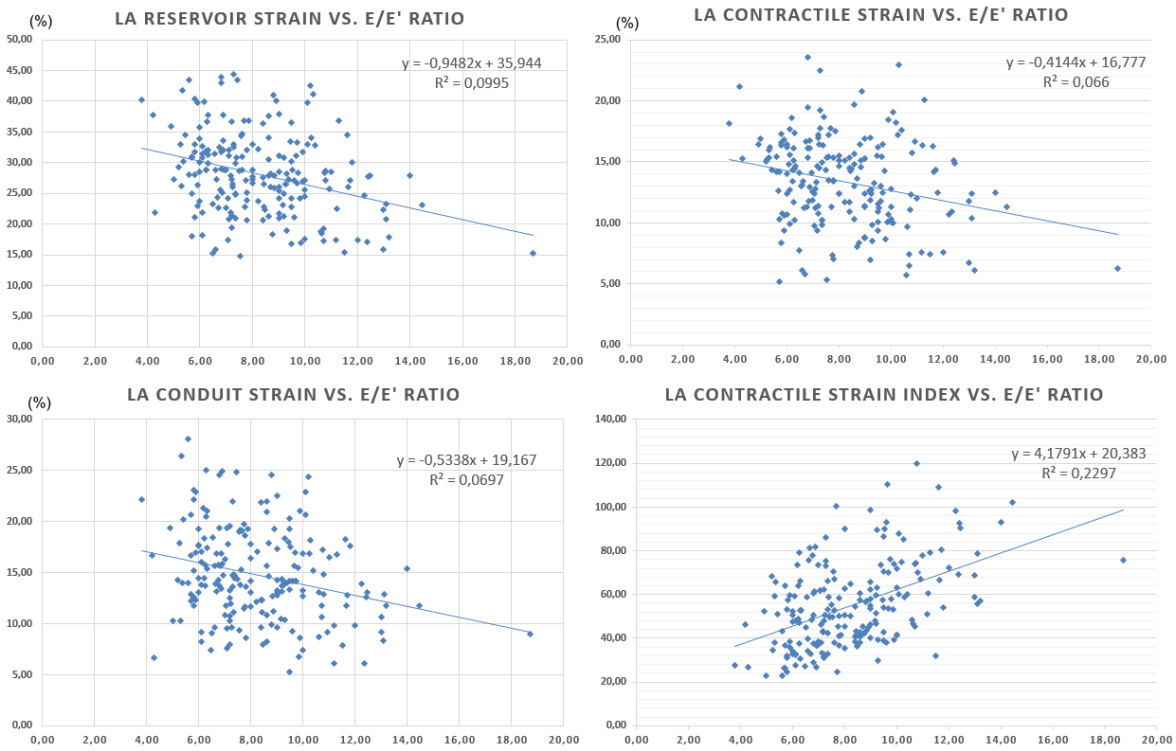

Figure 5B: The correlation between LA reservoir strain and derived LA stiffness index with LA max volume and derived volume indices (LA emapting fraction and LA expanstion index).

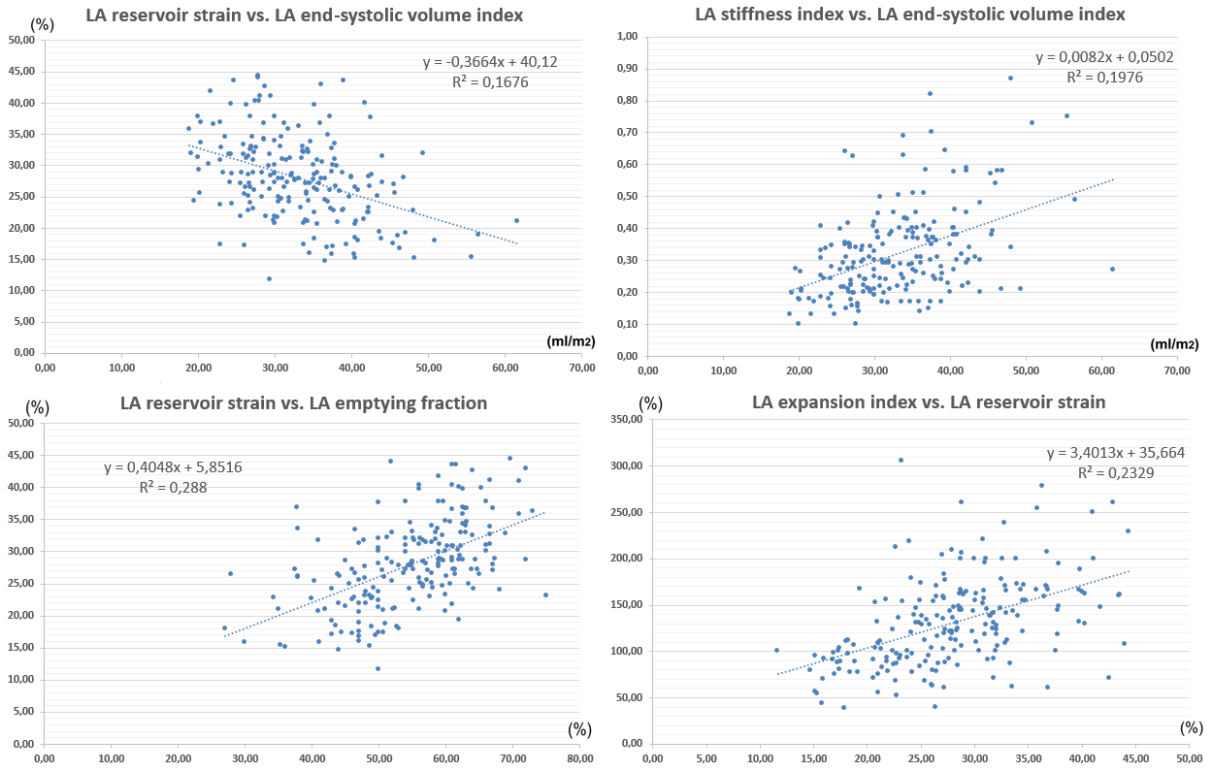

Table 1: Baseline clinical characteristics in patients with low, intermediate and high probability of HFpEF using the HFA-PEFF and the H_2FPEF scoring systems.

	HFA-PEFF score				H_2FPEF score			
	Low (0-1 points) (n=29)	Intermediate (2-4 points) (n=115)	High (≥5 points) (n=61)	P (ANOVA)	Low (3 points) (n=37)	Intermediate (4-5 points) (n=109)	High risk (6-9 points) (n=59)	P (ANOVA)
Age, y	57 ± 10	60 ± 10	66 ± 10	< 0.001	50 ± 8	62 ± 8	68 ± 9	< 0.001
Males, n (%)	18 (62)	81 (70)	45 (74)	0.528	29 (78)	77 (71)	38 (64)	0.346
BMI, kg/m^2	25.6 ± 4	27.3 ± 4	26.9 ± 3.1	0.107	25.6 ± 2.7	26 ± 3.3	29.7 ± 4.4	< 0.001
Obesity, n (%)	5 (17)	30 (26)	12 (20)	0.466	2 (5)	11 (10)	34 (58)	< 0.001
Hyperlipidemia, n (%)	6 (21)	44 (38)	24 (39)	0.176	8 (22)	34 (31)	32 (54)	0.001
Hypertension, n (%)	4 (14)	45 (39)	35 (57)	0.001	4 (14)	44 (40)	40 (68)	< 0.001
Diabetes, n (%)	0 (0)	5 (4)	4 (7)	0.369	0 (0)	5 (5)	4 (7)	0.288
Smoker, n (%)	3 (10)	14 (12)	6 (10)	0.886	1 (3)	14 (13)	8 (14)	0.498
NT Pro-BNP, pg/mL	78 ± 50	126 ± 124	526 ± 338	< 0.001	126 ± 151	224 ± 264	358 ± 343	< 0.001
Beta blockers, n (%)	18 (62)	83 (72)	55 (82)	0.117	21 (57)	77 (71)	53 (90)	0.001
ACEI, n (%)	1 (3)	17 (15)	16 (26)	0.018	1 (3)	18 (16)	15 (25)	0.014
ARBs, n (%)	0 (0)	11 (10)	8 (13)	0.133	1 (3)	7 (6)	11 (19)	0.010
CCBs, n (%)	1 (3)	3 (3)	12 (20)	0.526	0 (0)	8 (7)	8 (14)	0.053
Antiplatelets, n (%)	4 (14)	13 (11)	5 (8)	0.697	0 (0)	13 (12)	9 (15)	0.053
Anticoagulants, n (%)	15 (52)	73 (63)	50 (82)	0.007	15 (41)	75 (69)	48 (81)	< 0.001
Antiarrhythmics, n (%)	0 (0)	10 (9)	8 (13)	0.122	2 (5)	8 (7)	8 (14)	0.291
Diuretics, n (%)	1 (3)	19 (17)	19 (31)	0.060	1 (3)	17 (15)	21(36)	< 0.001
Digoxin, n (%)	0 (0)	2 (2)	2 (10)	0.284	1 (3)	2 (2)	1 (2)	0.909

Abbreviations: ACEI = angiotensin converting enzyme inhibitors, ARBs = angiotensin II receptor blockers, BMI = body mass index, CCBs = calcium blockers.

Table 2: Baseline echocardiography characteristics in patients with low, intermediate and high probability of HFpEF using the HFA-PEFF and the H_2FPEF scoring systems.

	HFA-PEFF score				H_2FPEF score			
	Low (0-1 points) (n=29)	Intermediate (2-4 points) (n=115)	High (≥5 points) (n=61)	P (ANOVA)	Low (3 points) (n=37)	Intermediate (4-5 points) (n=109)	High risk (6-9 points) (n=59)	P (ANOVA)
Heart rate, bpm	69 ± 10	64 ± 9	64 ± 11	0.065	65 ± 10	65 ± 10	65 ± 11	0.990
LVEDD, cm	5.0 ± 0.5	5.3 ± 0.4	4.8 ± 0.3	0.664	5.0 ± 0.4	5.4 ± 0.4	4.9 ± 0.5	0.574
LVESD, cm	3.2 ± 0.5	3.3 ± 0.5	3.1 ± 0.4	0.328	3.2 ± 0.4	3.2 ± 0.5	3.2 ± 0.5	0.742
LVRWT	0.42 ± 0.06	0.43 ± 0.05	0.44 ± 0.06	0.640	0.41 ± 0.07	0.43 ± 0.06	0.45 ± 0.06	0.008
LVMI, g/m^2	84 ± 27	92 ± 21	98 ± 23	0.019	93 ± 22	92 ± 22	93 ± 25	0.933
LVEDVI, mL/m^2	49 ± 10	54 ± 13	53 ± 13	0.107	56 ± 13	54 ± 12	51 ± 13	0.074
LVESVI, mL/m^2	19 ± 7	22 ± 7	22 ± 6	0.024	23 ± 8	22 ± 7	20 ± 6	0.065
LV SVI, mL/m^2	32 ± 9	33 ± 9	32 ± 9	0.633	35 ± 9	33 ± 9	31 ± 9	0.054
LVEF, %	64 ± 6	60 ± 6	59 ± 8	0.009	62 ± 7	60 ± 7	60 ± 7	0.588
LV GLS, %	-21 ± 2	-20 ± 3	-19 ± 3	0.101	-20 ± 2	-20 ± 3	-20 ± 3	0.915
E/A ratio	1.27 ± 0.4	1.14 ± 0.36	1.31 ± 0.56	0.038	1.30 ± 0.4	1.16 ± 0.47	1.23 ± 0.42	0.217
e' lateral, m/s	0.11 ± 0.02	0.09 ± 0.06	0.09 ± 0.03	0.011	0.11 ± 0.02	0.09 ± 0.03	0.09 ± 0.09	0.301
e' septal, m/s	0.1 ± 0.02	0.1 ± 0.09	0.09 ± 0.08	0.850	0.1 ± 0.02	0.1 ± 0.09	0.1 ± 0.08	0.825
E/e' ratio	6.4 ± 1.3	8.1 ± 1.8	9.6 ± 2.5	< 0.001	6.4 ± 1.3	8.1 ± 1.8	9.6 ± 2.5	< 0.001
sPAP, mmHg	26.9 ± 3.3	28.2 ± 4.6	33.9 ± 6.7	< 0.001	27.8 ± 3.7	28.5 ± 5.1	33.1 ± 6.9	< 0.001
RVD basal, cm	3.5 ± 0.34	3.7 ± 0.39	3.71 ± 0.39	0.206	3.7 ± 0.41	3.6 ± 0.38	3.8 ± 0.40	0.363
RVD mid, cm	2.45 ± 0.26	2.49 ± 0.39	2.52 ± 0.35	0.789	2.55 ± 0.31	2.45 ± 0.33	2.55 ± 0.42	0.399
RV TAPSE, mm	23.8 ± 2.8	24 ± 3.8	24.8 ± 3.7	0.635	23 ± 3.5	24 ± 3.8	24 ± 3.3	0.551
RV GLS, %	-24.1 ± 2.9	-21.9 ± 4.7	-22.6 ± 5.2	0.265	-22.9 ± 4.7	-22.4 ± 5.1	-22.1 ± 4.7	0.853
RV free wall LS, %	-26.8 ± 4.9	-21.8 ± 4.7	-22.5 ± 5.8	0.035	-24.2 ± 3.9	-23.9 ± 5.6	-23.2 ± 4.8	0.743
LA diameter, cm	3.6 ± 0.29	3.9 ± 0.4	4.1 ± 0.44	< 0.001	3.8 ± 0.32	3.9 ± 0.44	4.1 ± 0.42	0.006
LAVI max, mL/m^2	26.7 ± 4.1	31.9 ± 7.2	38.2 ± 6	< 0.001	30.1 ± 6.9	32.9 ± 6.7	35.3 ± 8.7	0.003
LAVI min, mL/m^2	13.1 ± 3.5	15.51 ± 4.8	19.2 ± 4.5	< 0.001	14.1 ± 4.5	16.3 ± 4.8	17.5 ± 5.4	0.005
LAEF, %	58.9 ± 8.1	55.3 ± 9.2	51.4 ± 7.6	< 0.001	56.3 ± 7.6	55.8 ± 9.1	51.5 ± 8.8	0.005
LA expansion index	159.3 ± 56	133.8 ± 47	111.5 ± 32.9	< 0.001	136.5 ± 38.5	137.9 ± 52.4	114.2 ± 39.4	0.006
Reservoir LAS, %	32.6 ± 6.2	28.8 ± 5.9	24.2 ± 6.5	< 0.001	30.8 ± 5.8	28.5 ± 7	25.2 ± 5.8	< 0.001
LASr/E/e', %	5.3 ± 1.7	3.8 ± 1.2	2.8 ± 1.2	< 0.001	4.8 ± 1.8	3.9 ± 1.3	2.8 ± 1.0	< 0.001
LASr/LAVI, %/ml	1.3 ± 0.3	1.0 ± 0.3	0.7 ± 0.2	< 0.001	1.1 ± 0.4	0.9 ± 0.4	0.8 ± 0.3	< 0.001
LASr/LV GLS	1.6 ± 0.3	1.5 ± 0.3	1.3 ± 0.3	< 0.001	1.6 ± 0.3	1.5 ± 0.3	1.3 ± 0.4	0.004
Reservoir LASR, s^{-1}	1.51 ± 0.29	1.33 ± 0.31	1.06 ± 0.22	< 0.001	1.48 ± 0.39	1.32 ± 0.30	1.15 ± 0.27	0.003
Conduit LAS, %	18.2 ± 5.2	14.8 ± 3.8	12.6 ± 4.2	< 0.001	16.9 ± 4.3	14.8 ± 4.6	13.1 ± 3.6	< 0.001
Conduit LASR, s^{-1}	-1.4 ± 0.34	-1.18 ± 0.41	-0.92 ± 0.31	< 0.001	-1.39 ± 0.41	-1.21 ± 0.39	-0.94 ± 0.33	< 0.001
Contractile LAS, %	14.3 ± 2.5	13.9 ± 3.6	11.5 ± 3.5	< 0.001	13.9 ± 2.9	13.7 ± 3.7	12.1 ± 3.6	0.016
Contractile LASR, s^{-1}	-1.87 ± 0.3	-1.68 ± 0.42	-1.33 ± 0.48	< 0.001	-1.76 ± 0.36	-1.7 ± 0.46	-1.43 ± 0.43	0.019
Contractile LAS index	44.8 ± 8.4	48.3 ± 8.1	47.8 ± 8.9	0.128	45.3 ± 7.4	48.3 ± 8.3	48.1 ± 9.1	0.180

Abbreviations: GLS = global longitudinal strain, LA = left atrial, LAEF = LA emptying fraction, LAS = LA strain, LASr = reservoir LAS, LASR = LA strain rate, LAVI = LA volume index, LV = left ventricular, LVEDD = LV end-diastolic diameter, LVEDVI = LV end-diastolic volume index, LVEF = LV ejection fraction, LVESD = LV end-systolic diameter, LVESVI = LV end-systolic volume index, LVMI = LV mass index, RV = right ventricular, RVD = RV end-diastolic diameter, sPAP = systolic pulmonary artery pressure, TAPSE = tricuspid annular plane systolic excursion.

Table 3. Predictors of high probability of HFpEF using HFA-PEFF (≥ 5), H_2FPEF (>5) and their combination.

	Univariable Analysis		Multivariable Analysis	
	OR (95% CI)	p value	OR (95% CI)	p value
HFA-PEFF				
Reservoir LAS	1.15 (1.09-1.22)	< 0.001	1.13 (1.04-1.22)	0.003
LV GLS	1.09 (0.97-1.21)	0.142		
RV GLS	3.04 (0.44-20.96)	0.259		
RV FWLS	1.05 (0.96-1.14)	0.271		
H_2FPEF				
Reservoir LAS	1.11 (1.05-1.16)	< 0.001	1.09 (1.01-1.18)	0.022
LV GLS	1.03 (0.92-1.15)	0.610		
RV GLS	1.02 (0.94-1.12)	0.609		
RV FWLS	1.02 (0.94-1.11)	0.605		
HFA-PEFF and H_2FPEF				
Reservoir LAS	1.19 (1.10-1.28)	< 0.001	1.22 (1.08-1.38)	0.001
LV GLS	1.03 (0.89-1.19)	0.666		
RV GLS	1.09 (0.97-1.23)	0.139		
RV FWLS	1.05 (0.94-1.17)	0.353		

CI = confidence interval, OR = odds ratio, LAS = left atrial strain, LV GLS = left ventricular global longitudinal strain, RV GLS = right ventricular global longitudinal strain, RV FWLS = right ventricular free wall longitudinal strain.

Chapter 11

Left atrial mechanics and functional capacity in HFpEF patients with paroxysmal atrial fibrillation

Background:

Exercise capacity and ventilatory efficiency are often impaired in heart failure patients with preserved ejection fraction (HFpEF). Since left atrial (LA) pressure, particularly during exercise plays a major role in the exercise intolerance observed in these patients, we aimed to characterize the contribution of resting LA mechanical properties, assessed by two-dimensional speckle tracking echocardiography upon exercise capacity.

Objective:

To evaluate relationship between LA mechanics, measured by LA strain (LAS) and parameters of exercise capacity, assessed by cardiopulmonary exercise testing (CPET) in HFpEF patients with dyspnea and paroxysmal atrial fibrillation (AF).

Methods:

The study included 23 consecutive patients (63 ± 8 years, 83 % males) with dyspnea (NYHA≥II), paroxysmal AF and preserved LV ejection fraction (≥50%), referred for elective pulmonary vein ablation. The probability of HFpEF was estimated using H2FPEF score. During sinus rhythm, all patients underwent speckle tracking echocardiography and cardiopulmonary exercise testing by treadmill. Peak oxygen uptake (VO2max) served as measure of functional capacity and ventilation/carbon dioxide output (VE/VCO2) slope as surrogate of ventilation/perfusion mismatch.

Results:

Out of all the echocardiographic indices, only LA contractile strain and strain rate showed significant correlation with peak VO2 (both $p < 0.05$). All three strain components of LA phasic function, i.e. reservoir, conduit and contractile LAS, had significant relationship with VE/VCO2 slope (all $p<0.050$). Patients with LA strain rate above the median had significantly higher VE/VCO2 slope ($p=0.025$) and lower peak VO2 ($p=0.010$). In contrast, no correlations were observed between exercise parameters and LA volumes or LA emptying fraction or any other echocardiographic indices.

Conclusions:

In HFpEF patients, VO2 max and VE/VCO2 slope are closely related to LA contractile strain, suggesting that abnormalities in LA mechanics may contribute to the blunted exercise capacity observed. Therefore, these markers can be used as an echocardiographic surrogate of functional capacity in HFpEF patients with paroxysmal AF.

Introduction

The prevalence of HFpEF, which accounts for approximately half of the patients with heart failure [1], is increasing steadily over the last years, thereby making it a global health problem [2]. Whereas initially its pathophysiology has been attributed to increased left ventricular (LV) and vascular stiffness, it became evident that not only abnormalities in LV function but also left atrial (LA) dysfunction is one of the components of the multifactorial mechanisms contributing to the disease [3]. Indeed, the left atrium modulates LV filling and alterations in atrial functional parameters have been detected at the earliest stage of HFpEF [4,5]. Apart from LA endocrine failure with deficient ANP production and ANP resistance, LA remodelling and LA regulatory failure with OS overload and excessive vasopressine, the mechanical failure of the left atrium itself contributes directly to the complex pathophysiological mechanism of HFpEF [3,6].

Whereas nowadays 2D-echocardiography is the recommended tool to evaluate LA function, speckle tracking echocardiography has emerged as a more sensitive and specific method for LA functional assessment[7,8]. It enables to dissect LA function in three phases of reservoir, conduit and contractile function, and provides deeper insight in the different components of LA mechanics. In HFpEF patients, studies have demonstrated that compared to healthy controls, LA reservoir as well as conduit and pump function are impaired [3,9].

HFpEF patients are characterized by exertional dyspnoea and impaired exercise capacity which can be objectivated by cardiopulmonary exercise testing (CPET) [10]. It offers the most objective and comprehensive assessment of functional capacity and provides important information about the individual functional capacity [10] by measuring not only peak oxygen uptake (VO2max) but also the ventilatory/carbondioxide output (VE/VCO2) slope reflecting ventilatory efficiency [10].

As we hypothesise that LA mechanics may interfere with functional capacity in HFpEF patients, the present study was set up to assess the interrelationship between 2D and strain echocardiographic parameters of LA function and exercise capacity, determined by CPET.

Methods

Study population: The study population consisted of 23 consecutive patients with limiting exertional dyspnoea (NYHA≥II) and paroxysmal atrial fibrillation undergoing maximal cardiopulmonary exercise test prior to pulmonary vein isolation. Patients with ischemic heart disease, moderate valvular heart disease, hypertrophic or restrictive cardiomyopathy or reduced LV ejection fraction (<50%), were excluded.

Likelihood of HFpEF was assessed using H2FPEF score, which allow discriminating HFpEF from non-cardiac causes of dyspnea [11]. All patients had a H2FPEF score ≥5 suggesting high probability of HFpEF [11]. Nt-proBNP (Roche Diagnostics) levels were measured in venous blood at rest. The study was approved by the local Ethical Committee and all pts gave written informed consent before participating in the study.

Exercise testing: All patients underwent maximal cardiopulmonary exercise test before enrolment in the cardiac rehabilitation program and were free of exercise-limiting co-morbidities, such as cerebrovascular disease, musculoskeletal impairment or vascular disease of the lower extremities. Patients could only be included if they performed a maximal exercise test with a RER >1.10. The protocol used for the exercise testing has been reported previously. Subjects were exercised on a computer-driven cyclo-ergometer (Marquette Case 8000, Marquette Electronics, Milwaukee, Wisc., USA) using a ramp protocol starting at 20 watts with gradual increase of 10 watts every minute. The 12 lead ECG and heart rate were recorded continuously during the test. Cuff blood pressure was measured every two minutes of the exercise test with a manual manometer. Subjects were exercised to their self-determined maximal capacity or until the physician stopped the test because of significant symptoms, such as chest pain or dizziness, potentially dangerous arrhythmias, ST-segment deviations, marked systolic hypotension or hypertension.

Respiratory gas measurements: Continuous respiratory gas measurements were obtained by using a Medical Graphics Cardiopulmonary Exercise System (Medical Graphics, Minneapolis, Minn., USA). The oxygen consumption (VO2), carbon dioxide production (VCO2), minute ventilation (VE), tidal volume, respiratory rate and mixed expiratory carbon dioxide concentration were continuously measured on a breath-by-breath basis. In addition, several derived variables such as the respiratory exchange ratio(RER) and the ventilatory equivalent for oxygen (VE/VO2) and CO2 (VE/VCO2) were calculated. Peak VO2 was expressed as the highest attained VO2 during the final 30 seconds of exercise. VE/VCO2-ratio was determined by linear regression analysis of the relation between VE and VCO2 during exercise, with data obtained over the complete duration of the exercise test (including respiratory compensation). Flow meters and gas analysers were calibrated for accuracy and linearity with a syringe of known volume and with precisely analysed gas mixtures on a daily basis.

Echocardiography: A comprehensive 2D transthoracic echocardiographic examination was performed using Vivid E95 (GE HealthCare, Horten, Norway) ultrasound system. All acquired images were stored digitally for offline analysis using a commercially available software (EchoPac, GE HealthCare). All examinations were recorded during sinus rhythm and analyzed by the same operator. Average of at least 3 beats was taken for each measurement. Blood pressure and heart rate were recorded during each examination. The biplane Simpson method was used to assess LV volumes and ejection fraction [12]. Maximum LA volume and LA emptying fraction were calculated from the apical 4- and 2-chamber views using the area-

length method [12]. LV and RV global longitudinal strain (GLS) were assessed using speckle tracking technique in views optimized for each chamber and at frame rate of >60 Herz [12,13]. Assessment of longitudinal LAS and strain rate (SR) were performed as recommended [14]. In brief, optimized apical 4- and 2-chamber views were recorded during breath hold. LA endocardial borders were traced manually in all views. Region of interest was manually adjusted and tracking quality was previewed before generating LAS and LASR curves. The LA reservoir (LASr), conduit (LAScd) and contractile (LASct) strain and SR were assessed as average of segmental values in apical views using the onset of QRS as a reference point [14,15].

Statistics

All results are expressed as mean ± SD. Student T-test and a Spearman correlation coefficient were used for appropriate comparisons. Statistical significance was set at a two-tailed probability level of less than 0.05.

Results

Clinical and echocardiographic characteristics of the study population are summarized in table 1. Demographic characteristics demonstrate a high incidence of hypertension whereas diabetes patients (3%) and patients with morbid obesity (BMI: 27,8 ± 5,0 kg/m2) were relatively rare. By definition H2FPEF score was elevated, ranging between 5 and 9 points suggestive for HFpEF. Also, the Nt-proBNP levels were elevated (325 ± 365 pg/ml). All patients showed a non-dilated left ventricle with preserved contractile function as evidenced by LV-EF and GLS. Pulmonary pressures were within normal limits (table 1). Table 2 summarizes the CPET characteristics. All individuals performed a maximal exercise test as evidenced by a RER >1.10 with a peak VO2 of 24.7 ±7 ml/kg/min and a VE/VCO2 slope of 28.4 ± 5,2.

Left atrial mechanical function and exercise capacity

Indices of LA size and function are depicted in table 3. Left atrial volume index was increased while LA emptying fraction was within normal limits. In contrast, LAS showed a significant reduction in all components of LA phasic function. Out of all the echocardiographic parameters, contractile LAS (Figure 1E) showed significant correlation with VO2max whereas the VE/VCO2 slope was inversely related to reservoir, conduit and contractile LAS (Figure 1). A significant correlation was observed between LASR and VO2max (r=-0,562, p=0.012) and VE/VCO2 slope (r=0,598, p=0.009). Pts with LASR above the median were characterized by a significantly higher VE/VCO2 slope (31,33± 4,54 vs 25,68 ± 3,46; p=0.025) and lower peak VO2 (18,59 ± 7,97 vs 25,48 ± 6,99 ml.min-1.kg-1.; p=0.010) (Figure 2). Finally, no correlations were observed between exercise parameters and LA volumes, LA emptying fraction or Doppler parameters of diastolic function.

Discussion

The findings of the present study can be summarized as follows: [1] Left atrial mechanical function is impaired in HFpEF. [2] The close relationship between exercise parameters and indices of left atrial strain suggest that in HFpEF patients with paroxysmal atrial fibrillation left atrial mechanical dysfunction plays a key role in the pathophysiology, thereby contributing to the blunted exercise capacity observed in these patients. [3] Based upon these observations we speculate that these left atrial strain markers can be used as an echocardiographic surrogate for the assessment of functional capacity in HFpEF patients with paroxysmal atrial fibrillation.

The left atrium plays a key role in maintaining optimal cardiac performance. Through its reservoir, conduit and pump function it modulates LV filling, maintains LV preload and cardiac output [16,17]. In addition, the compliance characteristics of the left atrium assures that the lungs remain free of congestion [3].

Recent studies have demonstrated that an impaired left atrial function more than left atrial remodeling bears diagnostic and prognostic value in HFpEF [18]. Left atrial mechanics correlate with left heart filling pressures, PA pressures, PA elastance and cardiac index at rest as well as during exercise [4,9] and a reduced atrial functional reserve during handgrip exercise is able to predict a blunted exercise capacity in HFpEF [19].

Our study is in line with these observations. The reported correlation between LA reservoir strain and maximal oxygen uptake and ventilatory efficiency suggest that abnormalities in left atrium mechanics might impede the augmentation of cardiac output during exercise and contribute to the exercise intolerance, observed in this study population.

In addition, it shows that abnormalities in LA function, measured at rest can decipher and identify the dynamic responses to exercise. The interplay between LA dilatation, LA mechanical dysfunction and atrial fibrillation is critical. Atrial fibrillation makes the atrium susceptible to LA dilatation which in itself is an adaptive change in HFpEF due to heightened LV filling pressures. On the other hand, LA dysfunction as well as heart failure and death have all been associated in previously asymptomatic elderly HFpEF subjects with enlarged LA volume [3]. We were unable to decipher any correlation between LA volume or emptying fraction and exercise capacity which similarly to previous observations indicates that LA mechanical function more than LA structure is the predominant correlate of abnormal hemodynamics in HFpEF [16]. Moreover, the highest correlation was observed between LA contractile strain and exercise parameters which emphasizes that the atrial booster function importantly contributes to exercise capacity [9].

Limitations

The assessment of LA strain is vendor dependent, a pitfall which has partly been overcome by using vendor independent software. Nevertheless, the cut-off value for abnormal LA strain is often not well defined. This implies that the absolute values for LA strain should be interpreted with caution [20].

Since measurements were obtained at a single time point, before pulmonary vein isolation and a control group was not included, further longitudinal studies are required to investigate the impact of pulmonary vein isolation upon LA mechanics and its relation to exercise capacity.

Clinical implications and Conclusion

Effective therapy for HFpEF patients remains elusive due in part to the myriad of pathophysiology's that cause this syndrome. We demonstrated that impairments in LA mechanics measured by LA strain play a key role in the pathophysiology and are associated with decreased peak oxygen consumption and ventilatory efficiency.

Although speculative, unloading the left atrium and/or augmentation of LA function may be an important future therapeutic strategy in HFpEF [3,3,21]. Furthermore, speckle tracking LA strain measurements may be helpful in guiding therapy in this subgroup of HFpEF patients. Future studies deciphering left atrial mechanics in HFpEF and evaluating novel therapies upon LA function are warranted [18].

Table 1: Study Population: Baseline demographics and echocardiography characteristics. LV = left ventricular, LVEDV = LV end-diastolic volume, LVESV = LV end-systolic volume, LV GLS = LV global longitudinal strain, IHD = ischemic heart disease, COPD = chronic obstructive pulmonary disease, LVESVI = indexed LVESV, LVEDVI = indexed LVEDV, LVEF = LV ejection fraction, LVEDD = LV end-diastolic diameter, LVMI = LV mass index, sPAP = systolic pulmonary artery pressure, RV GLS = right ventricular global longitudinal strain, BMI = body mass index.

Variable	All patients
Clinical Characteristics	
Age (years)	63 ± 9
BMI (kg/m2)	27,8 ± 5,0
Male sex (%)	83,00
Hypertension (%)	47
Smoker (%)	3
Diabetes (%)	3
IHD (%)	3
COPD (%)	10
Standard Echocardiogram	
LVEDVI (mL/m2)	53,9 ± 11,2
LVEDV (mL)	109,5 ± 23,5
LVESVI (mL/m2)	21,9 ± 7,0
LVESV (mL)	44,4 ± 14,2
LVEDD (mm)	50,4 ± 0,7
LVMI (g/m2)	90,5 ± 25,9
LVEF (%)	61,56,2
LV GLS (%)	-19,8 ± 2,3
RV GLS (%)	- 22,4 ± 4,0
E/A	1,3 ± 0,4
Mean E/e´	8,5 ± 2,4
PASP (mm Hg)	31,9 ± 7,1
RV TAPSE (mm)	24,7 ± 3,9
Biomarkers	
Nt-proBNP (pg/ml)	325,1 ± 365,7

Table 2: Study Population: Cardiopulmonary Characteristics. Data are expressed as mean ± standard deviation. Peak RER indicates peak respiratory exchange ratio, HRR heart rate reserve.

Variable	All patients
VO2 (mL/min)	2168 ± 532
VO2/Kg (mL/min/kg)	24,7 ± 7,0
Peak RER	1,1 ± 0,1
Peak Heart rate (bpm)	126 ± 27
HRR	19,1 ± 19,7
VE/VCO2 slope	28,4 ± 5,2

Table 3: Study Population: Echocardiographic characteristics of left atrium. Data are expressed as mean ± standard deviation or %. LA = left atrial, LAVI = LA volume index, LAS = left atrial strain, LASR = left atrial strain rate

Variable	All patients
LA volume (mL)	72,8 ± 20,8
LAVI (mL/m2)	35,8 ± 7,9
LA ejection fraction (%)	54,3 ± 8,3
LA Reservoir Phase	
Global strain-LASr (%)	26,5 ± 8,0
Global strain rate (/s)	-1,3 ± 0,3
LA Conduit Phase	
Global strain-LAScd (%)	13,7 ± 4,6
Global strain rate (/s)	-1,1 ± 0,4
LA Contractile Phase	
Global strain-LASct (%)	12,8 ± 4,2
Global strain rate (/s)	-1,6 ± 0,5

Figure 1: Relationship between left atrial reservoir (LASr) and contractile (LASct) strain and peak oxygen consumption (VO2max) and ventilatory efficiency (VE/VCO2 slope).

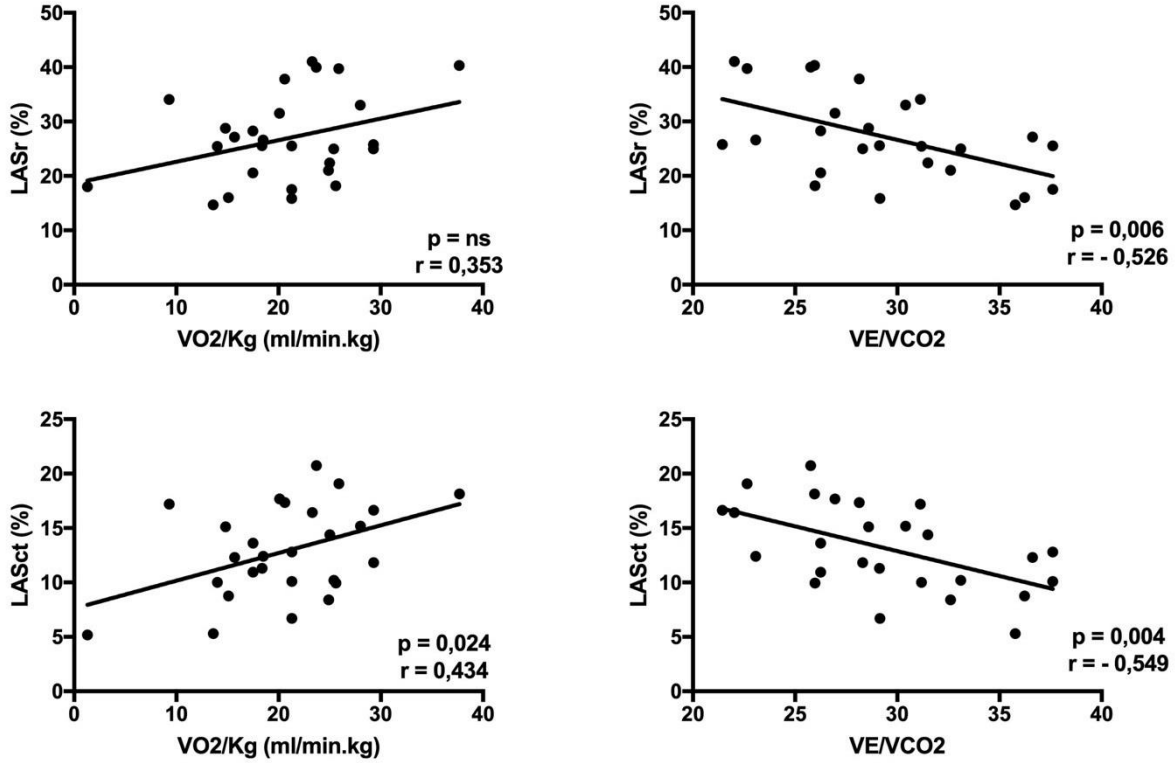

Figure 2: Peak oxygen consumption (VO2max) (upper panel) and ventilatory efficiency (VE/VCO2slope) (lower panel) in patients with and without left atrial strain rate above the median.

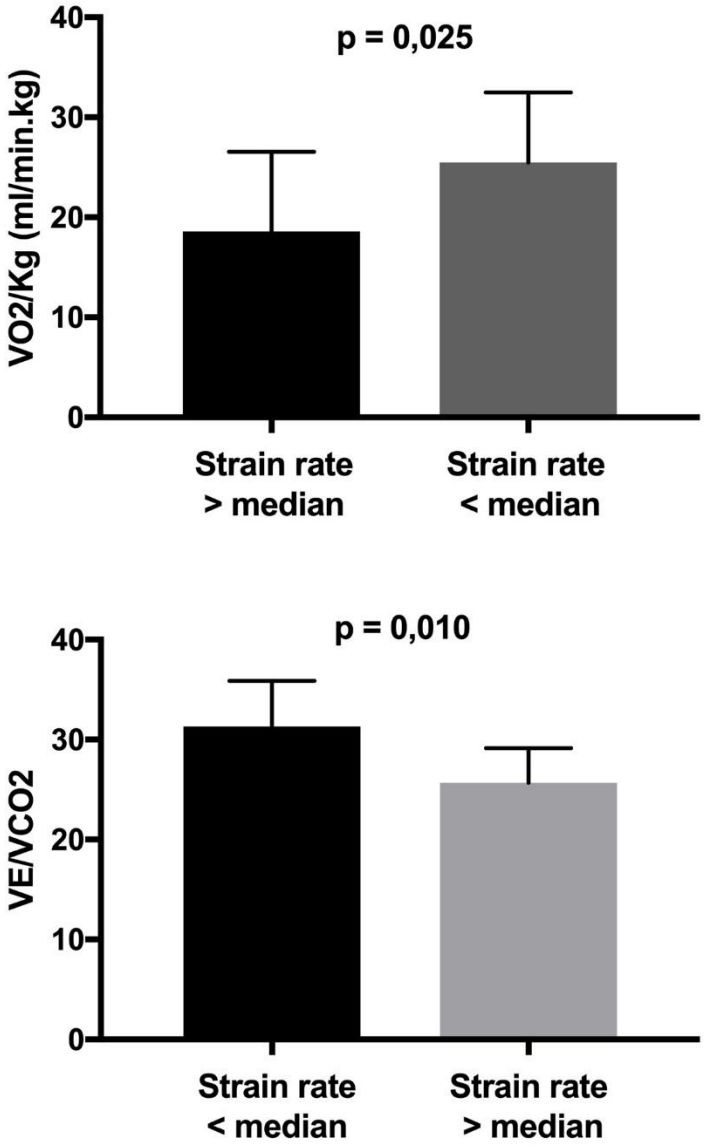

Chapter 12

Final conclusion of MODI-AF study

Atrial functional changes definitely precede atrial volume changes in patients with atrial fibrillation. Left atrial performance following catheter ablation is strongly affected by complex interplay between extent of atrial electro-structural remodeling and ablation procedure. However, left atrial electrical and structural remodeling are not always following each other in patients with atrial fibrillation following catheter ablation and atrial strain shows distinct behavior in patients with different types of atrial fibrillation.

Catheter ablation is associated with left atrial stunning in the acute phase followed by long-term improvement of both left and right atrial function. Repeat catheter ablation might affect negatively atrial compliance and contractility despite sinus rhythm restoration and symptomatic improvement. The atrial fibrillation-type-specific time course of left atrial strain reflects complex interaction between the extent of left atrial remodeling and ablation-induced myocardial injury.

Left atrial strain seems to be the most reproducible tool to monitor atrial phasic function during and after ablation procedures, and it might provide incremental predictive value for maintaining normal sinus rhythm over clinical features in patients with a history of paroxysmal atrial fibrillation. Furthermore, at early stage of atrial fibrillation, atrial dyssynchrony is reversible following the procedures regardless of the ablation strategies. Therefore, atrial mechanical dispersion could be a cofounder factor of great usefulness to identify patients with high risk of atrial fibrillation recurrence, specifically in patients who are candidates for repeat catheter ablation.

The integration of atria-ventricular strain images with clinical data, specifically in patients with diastolic dysfunction, could help to describe new phenotypes of co-morbidity of atrial fibrillation and heart failure in patients with left ventricular preserved ejection fraction. Indeed, left atrial phasic strain may be considered in the heart failure risk scoring system to have a better diagnosis in this clinical setting and it may be used as an echocardiographic surrogate of functional capacity in heart failure patients with atrial fibrillation, thus improving clinical outcome.

The assessment of left atrial strain is vendor dependent and the cut-off value for abnormal left atrial strain is not well defined. Many factors sucha as age, gender, metabolic disease or obesity are likely to influence left atrial strain and these factors should be considered during left atrial functional assessment. This implies that the absolute values for atrial strain should be interpreted with caution.

Future directions

The optimal selection of patients with history of atrial fibrillation for catheter ablation, through precise serial assessment of atrial anatomy and mechanics by using non-invasive substrate determination such as Speckle Tracking Echocardiography, will be the main key for successful procedures and best clinical outcome.

In the next decades, working on Speckle Tracking derived myocardial strain in this direction might help to build a new algorithm for automated diagnosis of imaging-based pathologies, thus monitoring myocardial function recovery in atrial fibrillation and heart failure patients who undergo treatment and rehabilitation.

Machine (full) semi-automatic assessment and neural networks-based algorithms will probably help clinicians to predict the rhythm outcome in these clinical settings.

Part 2

European association of cardiovascular imaging (EACVI) projects

Chapter 13

Multicentric Atrial Strain COmparison between Two different modalities: MASCOT HIT study

Cameli M.[1], Miglioranza MH.[2], Magne J.[3], Mandoli GE.[1], Benfari G.[4], Ancona R.[5], Sibilio G.[5], Reskovic Luksic V.[6], Dosen D.[6], Griseli L.[2], Van De Heyning CM.[7], Mortelmans P.[7], Michalski B.[8], Kupczynska K.[8], Di Giannuario G.[9], Devito F.[10], Dulgheru R.[11], Marchetta S.[11], Salustri A.[12], Abushahba G.[12], Morrone D.[13], Fabiani I.[13], Penicka M.[14], Katbeh A.[14], Sammarco G.[15], Esposito R.[16], Santoro C.[16], Pastore MC.[1], Comenale Pinto S.[5], Kalinin A.[17], Pičkure Ž.[17] Ažman Juvan K.[18], Zupan Mežnar A.[19], Coisne A.[20], Coppin A.[20], Opris MM.[21], Nistor DO.[21], Biering-Sørensen T.[22], Olson FJ.[22], Vaškelyté JJ.[23], Lapinskas T.[23], Gonzàlez Alujas T.[24], Galian-Gay L.[24], Motoc AI.[25], Papadopoulos CH.[26], Loizos S.[26], Ágoston G.[27], Szabó I.[27], Hristova K.[28], Tsonev SN.[28], Galli E.[29], Mihaila Baldea S.[30], Muraru D.[15], Mondillo S.[1], Donal E.[29], Galderisi M.[16], Cosyns B.[25], Edvardsen T.[31,32], Popescu BA[33].

1 Department of Medical Biotechnologies, Section of Cardiology, University of Siena, Siena, Italy
2 Cardiology Institute of Rio Grande do Sul, Porto Alegre, Brazil
3 CHU Limoges, Hôpital Dupuytren, Service Cardiologie, Limoges, France
4 Division of Cardiology, Department of Medicine, University of Verona, Verona, Italy
5 UOC Cardiologia/UTIC - "Santa Maria della Grazie" Hospital Pozzuoli, Pozzuoli, Italy
6 Department of Cardiovascular Diseases, University Hospital Centre Zagreb, Zagreb, Croatia
7 Department of Cardiology, Antwerp University Hospital, Edegem, Belgium
8 Department of Cardiology, Medical University of Lodz, Lodz, Poland
9 UO Cardiologia Ospedale Infermi di Rimini, Rimini, Italy
10 Ramazzini Hospital, Carpi, Italy
11 Cardiology Department - Heart Valve Clinic - University Hospital Liege, Liege, Belgium
12 Non-Invasive Department, Heart Hospital - Hamad Medical Corporation, Doha, Qatar
13 Cardiothoracic and Vascular Department, Pisa University, Pisa, Italy
14 Cardiovascular Research Center Aalst, Aalst, Belgium
15 Department of Cardiac, Thoracic and Vascular Sciences, University of Padua, Padua, Italy
16 Department of Advanced Biomedical Sciences, Federico II, University Hospital, Naples, Italy
17 Riga East Clinical University hospital, Department "Gailezers", Riga, Latvia
18 Department of Cardiovascular Surgery, University Medical Centre Ljubljana, Ljubljana, Slovenia
19 Cardiology Department, University Medical Centre Ljubljana, Ljubljana, Slovenia
20 Department of Clinical Physiology and Echocardiography – Heart Valve Clinic, Lille University Hospital, France
21 Institute of Emergency Cardiovascular Diseases and Transplant of Targu Mures, Targu Mures, Romenia
22 Department of Cardiology, Herlev and Gentofte Hospital, University of Copenhagen, Copenhagen, Denmark
23 Department of Cardiology, Lithuanian University of Health Sciences, Kaunas, Lithuania
24 Hospital Vall d'Hebron, Barcelona, Spain
25 Centre for Cardiovascular Diseases, University Hospital of Brussels, Brussels, Belgium
26 Korgialenio Benakio - Red Cross Hospital, Athens, Greece
27 University of Szeged, Department of Family Medicine, Szeged, Hungary
28 Medical Center for Cardio-vascular Diseases, Sofia, Bulgaria
29 University of Rennes, CHU Rennes, Inserm, LTSI – UMR 1099, F-35000 Rennes, France
30 University of Medicine and Pharmacy Carol Davila - Emergency and University Hospital, Bucharest, Romania
31 Center for Cardiological Innovation, Department of Cardiology, Oslo University Hospital, Rikshospitalet, Oslo, Norway.
32 University of Oslo, Norway
33 Department of Cardiology, University of Medicine and Pharmacy “Carol Davila” – Euroecolab, Emergency Institute for Cardiovascular Diseases “Prof. Dr. C. C. Iliescu”, Sos. Fundeni 258, 022328 Bucharest, Romania

Abstract:

Background:

Two methods are currently available for the measurement of left atrium (LA) strain by speckle tracking echocardiography (STE), which use different reference timing for starting the analysis: QRS (QRS-LASr) and P wave (P-LASr). The aim of the MASCOT HIT study was to define which of the two is more reproducible, more feasible, and less time consuming and to provide a common standard method.

Methods:

26 expert centres enrolled patients with a complete 2D echocardiography study. LA strain was analyzed by two different independent imagers (young vs senior, defined by a proved experience in echocardiography) in a blinded fashion. The study population included: healthy subjects, patients with LA pressure overload and patients with LA volume-pressure overload. The difference between the inter-correlation coefficient (ICC) obtained by the two observers using the two techniques was analyzed. The feasibility and time for the analysis of the two methods were also compared.

Results:

The study included 938 subjects: 309 controls, 333 patients with LA pressure overload, and 296 with LA volume-pressure overload. The ICC was slightly superior for QRS-LASr: 0.93 (95%CI 0.92-0.94) vs 0.90 for P-LASr (95%CI 0.89-0.92). Regarding feasibility, the young operators calculated QRS-LASr in 90% of cases, the experts in 95%. Substantial agreement between the young and senior operators was found for QRS-LASr analysis (Cohen's Kappa 0.63). The feasibility of P-LASr was 85% when measured by young operators and 88% by seniors, and only a moderate agreement between the young and senior operators was found (Kappa coefficient 0.48). Median time for measuring QRS-LASr was 110 seconds (IR 78-149) for the young and 110 seconds (IR 78-155) for senior echocardiographers. Conversely, median time for measuring of P-LASr was 120 seconds (IR 80-165) and 120 seconds (IR 90-161), respectively.

Conclusions:

STE-derived LA strain is feasible in most patients. Using the QRS complex as the reference point for analysis results is a more reproducible, more feasible and less time-consuming method compared to the use of the P wave as a reference.

Background

The left atrium (LA) acts as a reservoir receiving blood from the pulmonary veins during ventricular systole and isovolumic relaxation, as a passive conduit during early filling and diastasis, and as a booster pump during late diastole, at atrial contraction.(1) The study of LA function gained attention in recent years, mostly due to deformation imaging and to the growing evidence of prognostic value of the method. Speckle tracking echocardiography (STE), which assesses the LA longitudinal deformation, is the most promising technique for direct evaluation of LA function. (2) It offers opportunities to measure quantitative parameters of LA function but still lacks clear standardization in this setting. There are two methods available for the measurement of LA strain by STE, using different ECG reference points for the analysis: QRS (left atrial strain during reservoir phase, QRS-LASr) and P wave (P-LASr).(3,4) The recent European Association of CardioVascular Imaging/American Society of Echocardiography (EACVI/ASE) standardization paper(5) on LA imaging using 2D STE, describes both methods and recommends the use of QRS onset as reference point. A multi-centric study with a head-to-head comparison of LA strain methods in terms of reproducibility, feasibility and time needed for analysis is, however, not currently available. This is the main rational of the Multicentric Atrial Strain COmparison between Two different modalities (MASCOT), the study initiated by the Heart Imagers of Tomorrow (HIT), the young group of the EACVI. MASCOT sought to compare the agreement between 2 operators. The superiority of QRS-LASr over P-LASr was tested as the primary objective. Secondary objectives included: assessment of feasibility and time needed for the analysis with the two modalities; comparison of results between groups; comparison of performance between less experienced and more experienced readers (young vs expert).

Methods

Population of the study

From July 1 to October 31, 2018, HIT Members and/or Ambassadors were asked to prospectively collect echocardiographic images of three groups of patients referred to echo-laboratories for clinically indicated echocardiograms: healthy subjects, patients with aortic stenosis (AS) and arterial hypertension (AH), included in the LA pressure overload group, and patients with mitral regurgitation (MR) and heart failure (HF), included in LA pressure-volume overload group. Inclusion criteria were: age over 18 years; informed consent. Inclusion criteria for the single groups are described in the Appendix. Exclusion criteria were: valvular prosthesis; permanent or persistent atrial fibrillation; cardiac transplantation; poor acoustic window. Each center obtained approval from its own Ethics committee. All subjects signed an informed consent for inclusion in the study. All procedures were conducted in accordance with the Declaration of Helsinki.

Standard Echocardiography

Each echocardiogram was performed by an expert imager using a commercially available system (GE Medical Systems, Northen) equipped with a 1.5-3.6-MHz transducer. All the subjects were studied in the left lateral recumbent position. Standard left ventricular (LV) diameters were measured in long-axis parasternal view. LV and LA volumes were assessed from apical four-chambers and two-chambers views using the biplane modified Simpson's method, according to current ASE/EACVI recommendations (7). Maximal and minimal LA volumes were measured at end-systole, just before the mitral (MV) valve opening (at the beginning of the P wave) and at the mitral valve closure, respectively, both in apical four- and two-chambers view. All LA volumes were then indexed to body surface area (BSA). Left ventricular mass was calculated from 2D images and subsequently indexed to BSA. LV diastolic function was assessed according to current recommendations (8). The E/e' ratio was calculated as an estimate of LV filling pressures (8). Measurements of dimensions and longitudinal function of the right ventricle (RV) were made according to the ASE/EACVI recommendations (9). MV and tricuspid valve assessment and evaluation of valve regurgitation and stenosis severity was assessed according to ESC guidelines (10).

Speckle Tracking Echocardiography

A 2D grey-scale apical four- and two-chambers views were acquired, during three consecutive cardiac cycles, with a frame rate of 40-80 fps in each patient. Each exam was performed or verified by a senior imaging expert for quality assurance purposes.

For LA strain analysis, a complete tutorial was provided to each imager to reduce the risk of bias. The EACVI/ASE document for the standardization of LA deformation imaging by STE was used as a reference (5).

Each Center analyzed LA strain using off-line semi-automatic 2D strain software (EchoPAC, GE, USA) by two independent echocardiographers, one young and one senior, blinded to each other.

Young and senior operators were defined according to their echocardiographic experience, that is <10 and ≥10 years respectively.

Each operator calculated LA parameters of longitudinal deformation with both techniques. For QRS method, LA endocardial border was manually traced at LV end-systole in both apical views. The software automatically generated a region of interest (ROI) including six segments with different colors per view. Then, the ROI was manually adjusted to include the thickness of the LA myocardium and optimize tracking quality analysis. A curve was then generated for each of the 12 atrial segments during the QRS-to-QRS cardiac cycle analysis. The analyzed parameters are shown in Figure 1, left. The ECG reference was then changed on the software to the P wave, leading to a P wave-to-P wave cardiac cycle analysis. The ROI was again traced and adjusted in both apical views and LA strain curves were generated (Figure 1, right).

The image quality, feasibility and the time needed for LA strain analysis by both methods were also analyzed.

LV strain was measured using the QRS complex as a reference time-point and the ROI was manually traced by an endocardial point-and-click approach. The ROI was manually corrected, if needed, in each apical view (four-, two- and three-chambers). The 18 segments model was used and global longitudinal strain (GLS) was reported (11).

Data collection

The participating centers were chosen among cardiac imaging laboratories with long-time experience in advanced echocardiography and strain analysis, and publications in the field.

Each study investigator was given access to an online platform (REDcap™) with private credentials to MASCOT archive. Data reporting was blinded to the results of the second operator. Patient data were anonymized, giving a unique code to each patient included in the study, to guarantee privacy accordingly to national and international laws.

Statistical analysis

Data are presented as means ± SD, median and interquartile range (for continuous variables), or percentages (for binary variables), as appropriate. Normality was assessed using Kolmogorov-Smirnov test. Comparisons across patient groups were performed using analysis of variance (ANOVA), χ^2 test, with or without continuity correction. Absolute agreement between young and senior operators was tested using a two-way mixed model considering average measurements. Interrater reliability was tested by Cohen's Kappa coefficient. Pearson's correlation coefficients were calculated to assess the relationships between continuous variables in data with normal distribution. ICC was computed by a single-rating, absolute-agreement, and 2-way random-effects model with 3 raters per Centre.

All analyses were performed using SPSS (Statistical Package for the Social Sciences, Version 20.0, SPSS Inc., Chicago, IL, USA). The significance level was set at 0.05 for all analyses.

Results

General characteristics of the population

The MASCOT HIT study enrolled 1037 subjects, of which 99 were excluded due to incomplete data provided. The final population was thus composed of 938 subjects: 309 healthy controls; 139 patients with AH, 194 patients with AS (total of 333 in the LA pressure overload condition group); 128 patients with MR and 168 patients with HF (total of 296 included in LA volume-pressure overload group). Mean population age was 59±14 years, 55.7% males. Table 1 describes the clinical characteristics of the study population, while Table 2 presents the standard echocardiographic parameters.

Assessment of left atrial function

The values of global QRS-LASr, QRS-LASct and P-LASr in the different groups are showed in Table 3. Figure 2 presents box and whisker plots for global QRS-LASr, P-LASr and GLS.

The inter-operator reproducibility by ICC was excellent for both measures of LA strain, but was slightly superior for global QRS-LASr compared to global P-LASr (0.93 vs 0.90 respectively). The reproducibility for LA strain was close to the ICC value for LV GLS. When analyzing the study groups separately, we found that the reproducibility was better in the pathological left atria compared to healthy individuals, with the best results in the pressure-volume overload model. All the ICC values are summarized in Table 4.

Variability of QRS-LASr and P-LASr values was not affected by LA volume or E/e' ratio. Even if a trend of higher reproducibility can be found in MASCOT data both for QRS and P measurements in patients with dilated LA or elevated filling pressures, this did not reach statistical significance.

Young operators were able to analyze QRS-LASr in both apical views in 90% of subjects, in only one apical view (4 or 2 chambers) in 9%, and the analyses were not obtainable in only 1% of cases. Senior operators reported a QRS-LASr feasibility of 95%. Substantial feasibility agreement was found between young and senior operators (Cohen's Kappa 0.63). These values were similar to those for LA volume and LVEF feasibility (97% and 95% respectively). The feasibility of P-LASr method in young imagers was 85% in both views, 12% in only one apical view, while 3% of cases were not feasible. The feasibility of the P-LASr method in senior operators was 88%, with a Kappa coefficient of 0.48. Experience with strain analysis was not associated with the time needed for analysis. QRS-LASr required less time to be obtained than the P-LASr. The median time to perform the measurements for global PALS was 110 seconds (IR 78-149) and 110 seconds (IR 78-155) in young and senior echocardiographers respectively. The median time to measure global P-LASr was 120 seconds (IR 80-165) and 120 seconds (IR 90-161) for young and senior echocardiographers, respectively.

Both QRS-LASct and P-LASct methods evaluate the contractile function of the LA. From our data, Pearson's correlation analysis revealed a good correlation between the two methods, both when assessed by young and by senior operators (Table 5). A strong correlation was also found between the two indices of reservoir function.

Discussion

The main findings of the MASCOT HIT study are: 1) LA strain analyses by using the QRS as reference point provides excellent inter-operator variabilities, but slightly lower compared to LV GLS; 2) the measurement of global QRS-LASr is more feasible than global P-LASr with a substantial agreement between the senior expert and young imagers; 3) assessment of LA strain by QRS method is faster; 4) there is an overall good correlation between the values of

QRS-LASr and P-LASr (indices of LA compliance and reservoir function), better in patients with LA pressure and volume-pressure overload than in healthy controls.

The importance of the assessment of LA function over LA size is becoming more and more appropriate, not only for research purposes but also for everyday practice.(12-14) Since the application of STE to other chambers than the LV, the additional role of LA deformation imaging has been explored in several clinical settings, mostly including conditions of atrial volume or pressure-volume overload e.g. heart valve diseases (15-18), arterial hypertension (19-20), heart failure (21-24). This led to the conclusion that a reduced LA longitudinal strain could be useful for the diagnosis, management and prognostic stratification in several conditions.

Some authors argued that analyzing LA phases based on R-wave might differ among patients, due to the fact that R-wave is related to the LV depolarization, and not to the LA (25). Previous studies demonstrated a close correlation between atrial and ventricular dynamics, underlining the concordance between the mitral annulus motion with LV mechanics during the entire cardiac cycle. Wakami et al. (26) confirmed this hypothesis by finding a significant correlation between peak LA strain and LV systolic longitudinal strain. Moreover, the strong correlation between QRS-LASr and invasively measured LV end-diastolic pressure shows the close interdependence between LA and LV function during the entire cardiac cycle, suggesting QRS-LASr may have ae role as marker of atrial-ventricular interplay.

In the three groups of patients evaluated in MASCOT HIT Study, a superiority of QRS method, in terms of inter-operator reproducibility (evaluated by ICC), feasibility and time needed for the analysis, emerged from the study's results. Strain analysis showed a trend to a better reproducibility in patients with higher LA volume, however statistical significance was not reached. This could be explained by the fact that tracing the endocardial border is generally easier in dilated atria and the software is more capable to follow the displacement of speckles. The reproducibility of QRS-LASr was slightly superior to P-LASr in MASCOT HIT study population and in the three groups separately.

Current analytical software for calculating strain values are customized for R-wave zero-reference point so they automatically generate the frame where the endocardial tracing must be started. On the contrary, additional manipulations are needed to set the onset of P wave as the trigger and this procedure is done on the ECG trace acquired with the echocardiographic image. This aspect leads to important consequences: first, the arbitrariness of choosing the starting frame on the ECG is responsible for a higher operator-dependence and for lower inter-operator reproducibility and agreement according to operator experience. Second, the difficulty to obtain a good ECG trace where the P wave can be clearly defined reduces the feasibility of the method. Third, the search for a readable ECG where the operator can work during pre-analysis manipulation extends the time both during the echocardiographic study itself and during the off-line analysis. We decided to exclude

patients with persistent or permanent AF but the impossibility to perform LA strain using the P-wave method in this clinical setting is not negligible. These are important aspects from both clinical and research perspectives.

QRS-LASr and P-LASr demonstrated a good correlation in evaluating LA reservoir function in MASCOT HIT results, higher in patients than in control group. However, using a sum of parameters instead of a single index might decrease measurement accuracy, with possible mathematical errors and longer time needed for the analysis. Moreover, the strain curve measured by the QRS method seems to follow more closely the LA physiology.

Study limitations

Intra-operator reproducibility for strain parameters in each Centre was not tested. However, MASCOT HIT involved international imaging Centres with high experience in advanced echocardiography and STE. The deformation analysis was performed on single-vendor machine. This software was designed for the analysis of LV strain and then applied to the other cardiac chambers without being specifically designed for LA function analysis. However, at present, the application of this software for LA strain measurements is widely used in practice and is the most commonly used one in the published studies.

Clinical perspectives

LA strain assessment in different clinical settings has provided clear pathophysiological insights in addition to its diagnostic and prognostic relevance as demonstrated in several studies. However, there are some factors that still limit its wider use, mainly technical issues related to measurement standardization, choice of parameter to use and/or specific values to be used as cut-off in different settings. On the contrary, LV GLS has already overcome some of these practical aspects, being recommended on top of standard echocardiographic parameters in several clinical settings (e.g. early detection of cardiotoxicity in oncologic patients). This study provides relevant practical information about measuring LA strain and may represent a step forward for its better use in clinical practice.

Conclusions

The increasing clinical use of LA strain as an index of LA function requires proper standardization for its analysis. The QRS-LASr method has a better reproducibility compared to the P-LASr method. It also has a greater feasibility and shorter analysis time, both for senior and for younger imagers. Considering the several limitations of the P wave approach, including the impossibility to perform the analysis in AF patients, QRS-LASr should be considered the preferred parameter to use for LA strain analysis.

Table 1. Demographic and clinical characteristics

	Controls (n=309)	AH and AS (n=333)	MR and HF (n=296)	P value
Age, years	47.1±15.6	65.3±12.9	66.2±13.8	<0.0001
Female, %	47.7	47.4	38.4	0.029
Weight, kg	71.9±13.3	77.8±15.8	75±15.2	<0.0001
Height, cm	170±9.6	167.6±9.4	168.4±9.3	0.0013
BMI, kg/m²	24.8±3.9	27.7±4.8	26.4±4.7	<0.0001
BSA, m²	1.82±0.2	1.86±0.2	1.84±0.2	0.044
Heart rate, bpm	68.9±11.2	68.9±10.5	70.2±13	0.273
SBP, mmHg	123.4±14	135.7±18.4	127.4±20.7	<0.0001
DBP, mmHg	76±8.5	79.6±11.4	76.2±12.7	<0.0001

AH = Arterial hypertension; AS = Aortic stenosis; BMI = Body Mass Index; BSA = Body Surface Area; DBP = Diastolic blood pressure; HF = Heart Failure; MR = Mitral Regurgitation; SBP = Systolic blood pressure.

Table 2. Standard echocardiographic parameters

	Controls (n=309)	AH and AS (n=333)	MR and HF (n=296)	P value
IVS, mm	9.0±1.6	12±2.4	10.8±2.2	<0.0001
LV PW, mm	8.6±1.6	10.9±1.9	10.1±2.0	<0.0001
LV mass index, g/m²	75.6±19.1	107.6±31.9	120.4±35	<0.0001
LV EDD, mm	47.3±5.7	47.4±6.2	55.0±8.6	<0.0001
LV ESD, mm	30.6±5.7	31.0±6.6	39.8±11.0	<0.0001
LV EDV index, ml/m²	51.2±12.5	51.9±14.4	75.2±30.2	<0.0001
LV ESV index, ml/m²	20.4±6.5	21.9±9.2	41.7±28.9	<0.0001
LV EF, %	60.4±6.7	58.5±9.2	47.0±14.6	<0.0001
LA max volume index, ml/m²	26.0±6.7	35.1±13.4	45.9±19.0	<0.0001
LA preA volume index, ml/m²	16.7±5.8	25.1±12.5	33.3±15.7	<0.0001
LA min volume index, ml/m²	10.3±4.3	16.3±10.4	24.2±14.4	<0.0001
E/A ratio	1.3±0.5	1.0±0.5	1.48±1.0	<0.0001
Mitral E DT, ms	196.8±53.4	223.5±76.8	199.4±76.7	<0.0001
E/e' ratio	7.0±2.8	11.8±6.3	13.4±7.9	<0.0001

AH = Arterial hypertension; AS = Aortic stenosis; DT= Deceleration time; EDD = End-diastolic diameter; EDV = End-diastolic volume; EF = Ejection fraction; ESD = End-systolic diameter; ESV = End-systolic volume; HF = Heart Failure; IVS = Interventricular septum; LA = Left atrial; LV = Left ventricular; MR = Mitral Regurgitation; PW = Pulsed wave.

Table 3. Speckle tracking echocardiography parameters

	Controls (n=309)	AH and AS (n=333)	MR and HF (n=296)	P value
Global QRS-LASr *y*, %	35.4±11.7	22.9±8.4	19.1±8.9	<0.0001
Global QRS-LASr *s*, %	33.5±10.9	23.0±8.5	18.9±9.2	<0.0001
Global QRS-LASct *y*, %	15.5±5.4	13.3±5.5	10.1±5.7	<0.0001
Global QRS-LASct *s*, %	15±5.3	13.4±5.7	10±5.7	<0.0001
Global P-LASr *y*, %	31.2±8.5	21.8±6.9	19.2±7.6	<0.0001
Global P-LASr *s*, %	30.5±8	21.9±6.8	19.2±7.4	<0.0001
LV GLS *y*, %	-19.9±3.1	-17.6±3.3	-15.5±5.7	<0.0001
LV GLS *s*, %	-19.7±3.0	-17.4±3.3	-15.3±5.4	<0.0001

AH = Arterial hypertension; AS = Aortic stenosis; GLS = Global longitudinal strain; HF = Heart Failure; LV = Left Ventricular; MR = Mitral Regurgitation; LASct = Left atrial strain during contraction phase with P as starting point; P-LASr = Left atrial strain during reservoir phase with P as starting point; QRS-LASct = Left atrial strain during contraction phase with QRS as starting point; QRS-LASr = Left atrial strain during reservoir phase with QRS as starting point; P; y = young; s = senior

Table 4. Intraclass Correlation Coefficient (ICC)

	ICC	95%CI lower bound	95% CI upper bound
Study population			
Global QRS-LASr			
Average measures	**0.93**	0.92	0.94
Global P-LASr			
Average measures	**0.90**	0.89	0.92
GLS			
Average measures	**0.96**	0.95	0.96
Controls			
Global QRS-LASr			
Average measures	**0.84**	0.80	0.88
Global P-LASr			
Average measures	**0.80**	0.75	0.85
LA pressure overload			
Global QRS-LASr			
Average measures	**0.92**	0.90	0.94
Global P-LASr			
Average measures	**0.90**	0.87	0.92
LA volume-pressure overload			
Global QRS-LASr			
Average measures	**0.95**	0.93	0.96
Global P-LASr			
Average measures	**0.94**	0.92	0.95

P-LASr = Left atrial strain during reservoir phase with P as starting point; QRS-LASr = Left atrial strain during reservoir phase with QRS as starting point.

Table 5. Values of r coefficients for the correlation between indices of LA reservoir function (QRS-LASr and P-LASr) and of LA contraction (QRS-LASct and P-LASct)

	P-LASr	P-LASct	p
CONTROLS measured by young operators			
QRS-LASr	0.76		<0.001
QRS-LASct		-0.47	<0.001
CONTROLS measured by senior operators			
QRS-LASr	0.71		<0.001
QRS-LASct		-0.52	<0.001
LA PRESSURE OVERLOAD measured by young operators			
QRS-LASr	0.82		<0.001
QRS-LASct		-0.71	<0.001
LA PRESSURE OVERLOAD measured by senior operators			
QRS-LASr	0.80		<0.001
QRS-LASct		-0.67	<0.001
LA PRESSURE-VOLUME OVERLOAD measured by young operators			
QRS-LASr	0.87		<0.001
QRS-LASct		-0.69	<0.001
LA PRESSURE-VOLUME OVERLOAD measured by senior operators			
QRS-LASr	0.88		<0.001
QRS-LASct		-0.82	<0.001

P-LASct = Left atrial strain during contraction phase phase with P as starting point; P-LASr = Left atrial strain during reservoir phase with P as starting point; QRS-LASr = Left atrial strain during reservoir phase with QRS as starting point; QRS-LASct = Left atrial strain during contraction phase with QRS as starting point.

Figure 1. Left atrial strain parameters by both modalities

Left (QRS strain). Two positive deformation curves can be identified: the earlier and taller, QRS-LASr, is measured from LV end-diastole (QRS onset) to peak LA strain and corresponds to the LA reservoir phase. The second and shorted curve, during LA contraction phase, is called QRS-LASct. QRS-LASr and its corresponding time to peak (TTP) were measured at the end of this reservoir phase; QRS-LASct and its TTP were calculated just before atrial contraction.

Right (P strain). P-LASct was defined as the first obtained curve below the baseline, evaluating LA contraction phase; P-LAScd, assessing the LA strain during conduit phase, as the second positive curve. P-LASct and P-LAScd sum was calculated to achieve P-LASr.

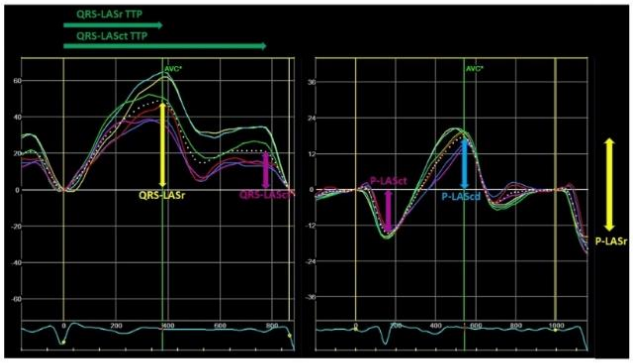

Figure 2. Global QRS-LASr, global P-LASr and GLS in the different study groups.

Comparison of strain parameters measurements between senior (blue) and young (red) operators. From the left: global QRS-LASr, global P-LASr and left ventricular GLS. LASr = left atrial strain during reservoir phase; GLS = global longitudinal strain.

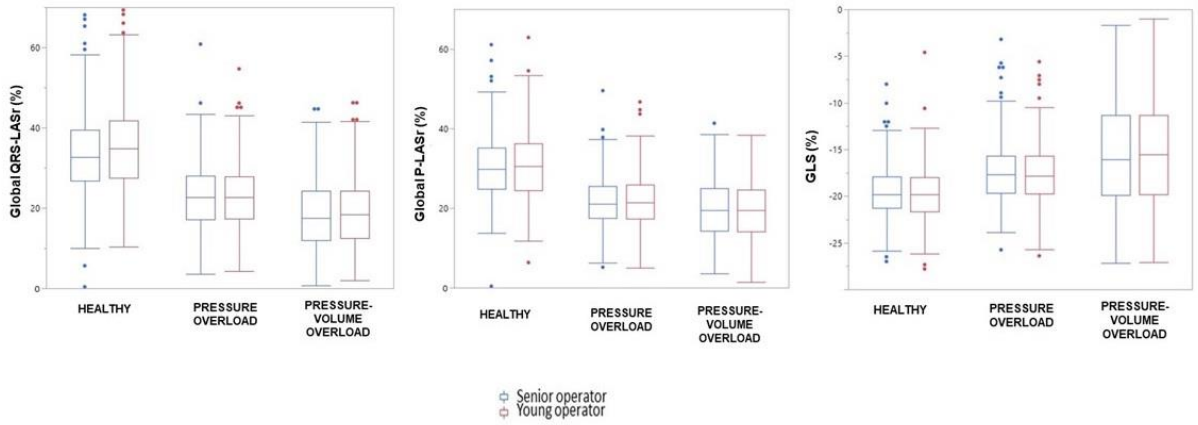

Chapter 14

Inter-center reproducibility of standard and advanced echocardiographic parameters in the EACVI AFib Echocardiographic Registry

[1]Maurizio Galderisi, [2]Erwan Donal, [3]Julien Magne, [1]Ciro Santoro,[4]Leyla Elif Sade, [5]Martin Penicka, [5]Asim Katbeh, [6]Bernard Cosyns,[7]Matteo Cameli, [8]Jadranka Separovic, [9]Vlatka Reskovic, [1]Francesco Lo Iudice, [10]Eustachio Agricola, [11]Rodolfo Citro, [12]Andreas Hagendorff,[13,14] Patrizio Lancellotti, [15,16]Gilbert Habib,[17]Antonella Moreo, [18]Nuno Cardim, [19]Vito Maurizio Parato, [20]Alexsandar Neskovic,[21]Monica Rosca,[3]Elena Galli, [6]Andreaa Motoc,[7]Giulia Mandoli, [10]Giacomo Ingallina, [11]Costantina Prota,[12]Stephen Stoebe, [13]Federica Ilardi, [15]Andreina Carbone, [17]Benedetta De Chiara, [19]Michele Scarano, [22]Jose Luis Zamorano,[21]Bogdan Alexandru Popescu, and [23]Thor Edvardsen.

[1]Department of Advanced Biomedical Sciences, Federico II University Hospital, Naples, Italy
[2]Department of Cardiovascular Disease, Pontchaillou University Hospital, Rennes, France
[3]Service Cardiologie, CHU Limoges, Hopital Dupuytren, Limoges, France[4]
Cardiology Department, University of Baskent, Ankara, Turkey
[5]Cardiovascular Center Aalst, OLV Clinic, Aaalst, Belgium
[6]Department of Cardiology, Centrum voor hart –en Vaatziekten, UZ Brussel, Brussel, Belgium
[7]Department of Cardiovascular Disease, University of Siena, Siena
[8]School of Medicine, University of Zagreb and University Hospital Center Zagreb,Croatia
[9]University Hospital Center Zagreb, Croatia
[10]San Raffaele Scientific Institute, Milan, Italy
[11]Cardiovascular Department, University Hospital San Giovanni di Dio e Ruggi d'Aragona, Salerno, Italy
[12]Department of Cardiology, University Hospital of Leipzig, Leipzig, Germany
[13]GIGA Cardiovascular Sciences, University of Liege Hospital, Liege, Belgium
[14]Gruppo Villa Maria Care and Research, Anthea Hospital, Bari, Italy
[15]APHM, La Timone Hospital, Cardiology Department, Marseille, France
[16]Aix Marseille University, APHM, MEPHI , IHIJ-Mediterranee Infection, Marseille, France
[17]Dipartimento Cardiotoracovascolare De Gasperis, Bicocca University and Niguarda Ca' Granda Hospital[18]Cardiology Department, Hospital Da Luz, Lisbon, Portugal
[19]Cardiology Unit of Emergency Dept, Madonna del Soccorso Hospital, San Benedetto del Tronto, Italy
[20]Department of Cardiology, Clinical Hospital Center Zemun, University of Belgrade, Serbia
[21]University of Medicine and Pharmacy "Carol Davila", Euroecholab; Emergency Institute of Cardiovascular Diseases "Prof. Dr. CC. Iliescu, Bucharest, Romania
[22]Cardiology Department, Hospital Universitario Ramon y Cajal, Madrid, Spain
[23]Department of Cardiology, Oslo University Hospital, Oslo, Norway

Abstract

Our study aimed to assess the inter-center reproducibility of 16 echo laboratories involved in the EACVI AFib Echo Europe. This was done on a dedicated setting of 10 patients with sinus rhythm (SR) and 10 with persistent atrial fibrillation (AF), collected by the Principal Investigator. Images and loops of echo-exams were stored and made available for labs. The measurements tested included primary echo-Doppler parameters, global longitudinal strain (GLS) and peak atrial longitudinal strain (PALS). Single measures interclass correlation coefficients (ICC) of left ventricular mass and ejection fraction were suboptimal in both patients with SR and AF. Among diastolic parameters, ICCs of deceleration time were poor, in particular in AF (=0.50). Single measures ICCs of left atrial size and function, besides optimal in AF, showed an acceptable despite moderate concordance in SR. ICC of GLS was 0.81 and 0.78 in SR and AF respectively. Single measures ICCs of PALS were suitable but lower in 4-chamber than in 2-chamber view. GLS distribution was completely homogeneous in SR, whereas GLS of AF and PALS of both SR and AF presented a limited number of outliers. GLS mean±SE of the 16 labs was 19.7±0.36 (95% CI 18.8-20.4) in SR and 16.5±0.29 (95% CI 15.9-17.1) in AF, whereas PALS mean±SD was 43.8±0.70 (95% CI 42.3-45.3) and 10.2±0.32 (95% CI 9.5-10.9) respectively. In conclusion, while the utilization of some standard-echo variables should be discouraged in registries, the application of GLS and PALS could be largely promoted because their superior reproducibility, even in AF.

Introduction

The European Association of Cardiovascular Imaging (EACVI)AFib Echo Europe Registry is a multi-center European observational, cross-sectional registry which has been designed with the aim of evaluating relationships of structural and functional parameters obtainable by transthoracic echocardiography with thromboembolic and bleeding risk profile in patients with any kind (paroxysmal, persistent and permanent) of non-valvular atrial fibrillation (AF) [1]. By this registry, it is expectable to collect data on echocardiographic phenotype of patients with AF and to test the level of agreement of different echocardiographic measurements with the available risk scores. Currently, twenty European centers decided to participate and are active in patient's enrollment.

When designing an echocardiographic registry involving several echocardiographic laboratories, quality control is fundamental to reduce variability measurement among laboratories. Accordingly, operators should have a certified expertise by applying appropriate procedures for data acquisition, storage and interpretation. Standardized approaches involving operator, equipment and training should be well established. The EACVI takes particular attention to these aspects encouraging training programs and standardized procedures of centers devoted to research [2]. In this view, the control of the inter-center reader reproducibility of different laboratories involved in a registry is of

paramount importance. A low variability measurement is strongly warranted to increase the consistency of studied parameters among the participating centers.

The objective of this study was to inter-center reproducibility of main standard and advanced echo-Doppler variables among the echocardiographic laboratories involved in EACVI Afib Echo Europe. This was done on a dedicated setting of patients with both sinus rhythm (SR) and history of paroxysmal AF and persistent AF or made available in the data-storing system of the echo lab of the Principal Investigator (PI).

Methods

EACVI AFib Echo Europe Registry has been designed with the aim of assessing the relationship of echocardiographic measurements of left atrial (LA) size and function, left ventricular (LV) geometry, systolic and diastolic function with clinical scores of thromboembolic and bleeding risks as evaluated by using CHA2DS2VASc and HASBLED scores. This is a multicenter registry involving 20 reference European echocardiographic laboratories, chosen among the accredited echo labs under the guidance of European National Societies and Working Groups, along a period initially establish to be of 6 months and subsequently prolonged for additional 6 months. The Registry was initially approved by the Ethical Committee of the PI (Federico II University Hospital of Naples, Italy, protocol 8/18) and then after by the other participating centers. After obtaining their informed consent, all consecutive patients with non-valvular permanent, persistent or paroxysmal AF (with heart rate ranging between 60 and 100 bpm) and undergoing a transthoracic echocardiography exam will be enrolled in the echocardiographic labs. Exclusion criteria were as follow: previous catheter or surgical ablation, LA appendage occlusion, cardiac surgery or percutaneous non-coronary interventional procedures, moderate-to-severe aortic and mitral valve stenosis, severe aortic and mitral valve regurgitation, aortic and mitral prosthesis, sepsis and inadequate quality echo images.

Before beginning the enrollment, the PI supplied a brief illustrative echocardiographic tutorial explaining how to perform all the measurements required to registry (in agreement with the most recent EACVI recommendations) [3,4] to all participating centers in order to standardize and homogenize all the measurements obtained.

This training was preliminary to the acquisition by the same PI of echocardiographic images and raw-DICOM loops of 10 cases with SR and history of paroxysmal AF and 10 with permanent AF, randomly selected from a preliminary list of the 50 cases of patients with permanent AF or paroxysmal AF history. These acquisitions were performed according to the ASE/EACVI Chamber quantification recommendations and the ASE/EEA Expert consensus on myocardial mechanics [3,4]. These cases were transferred on a cloud secured storage platform (drop box) in order to make these available for the reading of all the participating centers. Parasternal long-axis M-mode screen of the left ventricle and left atrium, imaging of

Doppler mitral inflow and pulsed Tissue Doppler of septal and lateral mitral annulus, as well as video-clips of apical long-axis, 4- and 2-chamber views were all stored in the drop box.

The readers of the echocardiographic labs were all expert on both standard and advanced echocardiographic techniques. The measurements tested for the inter-center reproducibility included:

1. standard primary echo parameters (according to the American Society of Echocardiography (ASE) /EACVI recommendations on chamber quantification [3] such as:

- measurements of LV mass (septal and posterior wall thickness and LV internal end-diastolic diameter), and of LV ejection fraction (EF) (end-diastolic and end-systolic volume by Simpson biplane)

- measurements of LA size: LA antero-posterior diameter, LA maximal and minimal volumes,

- Doppler measurements of LV diastolic function: transmitral E/A ratio and E velocity deceleration time, pulsed tissue Doppler derived e' velocity of lateral and septal mitral annulus, and E/e' average ratio, according to the 2016 ASE/EACVI recommendations on diastolic function [5];

2. advanced echo parameters by using speckle tracking echocardiography such as LV global longitudinal strain (GLS) - as the average of 17-model regional strain recorded in apical long-axis, 4- and 2-chamber views - and peak atrial longitudinal strain (PALS), as the average of apical 4- and 2-chamber views. Regional LV longitudinal strain and GLS as well as LA regional strain and PALS measurements were performed according to the majority of EACVI/ASE/Industry Task Force standard criteria [6,7]. LA regional strain and PALS were measured at end-diastole (ECG trigger at the upslope of the R-wave), and the narrowest ROI was chosen in order to adequately track thin LA walls. Measurements of GLS and PALS were performed automatically, with the possible adjustment of border traces when judged to be needed by the reader. All the reported echocardiographic measurements were averaged from three cardiac cycles in patients in sinus rhythm and from five cardiac cycles during AF. Of note, the reproducibility of PALS was also tested separately in apical 4- and 2-chamber views.

Statistical analyses

Continuous data were expressed as mean ± standard deviation (SD). The reproducibility among the laboratories involved was tested by calculating single measures intra-class correlation coefficients (ICC) and 95% confidence intervals (CI), separately on the data set of patients in SR and in those with AF. In fact, in the present study in which several echo labs were involved in the measurement reproducibility processes, the "single measures ICC" appear to be more appropriate than the "average measures" to verify the reliability of a scale that is scored by just several raters at one occasion. When using this kind of analysis,

since ICC ranges from 0 to 1, an ICC close to 1 indicates high agreement of measurements whereas a low ICC close to zero means that measurements are not concordant. Accordingly, values <0.5 are indicative of poor reliability, values between 0.5 and 0.75 indicate moderate reliability, values between 0.75 and 0.90 indicate good reliability, and values >0.90 indicate excellent reliability. In addition, the distribution of specific variables in the individual echo labs was assessed by boxplot models. The standard error (SE) of the mean and the upper and lower 95% confidence interval (CI) among the echo laboratories involved were also used to calculate the range of variance for specific variables.

All statistical analyses were performed by the SPSS software, release 12 (SPSS Inc, Chicago, IL, USA).

Results

Sixteen echocardiographic laboratories participated to the reproducibility tests. The demographic characteristics of the two study groups (SR and AF) are summarized in Table 1.

Table 2 reports the reproducibility analysis of parameters of LV geometry and function. The single measures ICC of LV mass (=0.67) and LV EF (=0.49) were suboptimal in both patients with SR and AF. Among diastolic parameters, the ICCs of E velocity DT were poor, in particular in patients with AF (=0.50). The ICC of GLS was 0.81 and 0.78 in patients with sinus rhythm and AF respectively.

Table 3 lists the single measures ICC of LA size and function. The single measures ICCs, besides optimal in patients with AF, showed an acceptable despite moderate concordance in patients with SR. Notably, the single measures ICCs of PALS were lower in 4-chamber than in 2-chamber view in the SR and in AF setting as well.

Figure 1 and Figure 2 depict the boxplot distribution of GLS and PALS respectively in the 16 echo laboratories involved in the reproducibility tests. GLS distribution was completely homogeneous in SR patients, with a limited number of outliers in patients with AF. PALS presented a limited number of outliers in both patients with SR and AF. In addition, GLS mean ± SE of the 16 labs was 19.7±0.36% (95% CI 18.8-20.4) in patients in SR and 16.5±0.29% (95% CI 15.9-17.1) in patients with AF, whereas PALS mean ± SD was 43.8±0.70% (95% CI 42.3-45.3) and 10.2±0.32% (95% CI 9.5-10.9) respectively (data not in Figures). These findings show the very narrow range of variability of GLS and PALS, in both patients with SR and AF.

Discussion

The analysis of inter-center reproducibility is a preliminary, fundamental condition for the startup and the development of echocardiographic registries in which the measurements taken in different laboratories are collected and combined together for statistical end-points. To the best of our knowledge, we are the first to present this kind of reproducibility

in separate settings of patients with SR and AF, before starting the recruitment of the EACVI AFibEcho Registry. Noteworthy, the reproducibility tests were performed by accredited, highly selected echocardiographic labs with consolidated expertise in both standard and advanced echocardiography. The tests were preceded by the supply of a tutorial provided by the PI to all the participating centers in order to homogenize both the acquisition and the reading procedures. Last but not least, a single vendor was chosen for both the imaging acquisition on the echocardiographic machines and the measurement reading by a dedicated work-station with the same updated release. This strict methodology and harmonization between co-investigators obviously limit the extension of the results to the overall panorama of the echocardiographic machines but also strengths the amount of the data collected in different echocardiographic laboratories.

The findings of the present study demonstrate that the inter-center reading reproducibility of echocardiographic Doppler parameters chosen is consistent with the aims of the EACVI AFib Echo Registry [1]. In this context, the single measures ICCs were optimal for the majority of parameters whereas others showed a moderate concordance and only one (transmitral E velocity DT) a poor concordance.

Our data confirmed the suboptimal, large variability of some parameters such as LV mass and LV EF obtainable by standard echocardiography. The calculation of LV mass implies a geometric assumption and the use of 2D guided M-mode or direct 2D echocardiographic linear primary measurements, each on one with own intrinsic variability [8]. Accordingly, LV mass has a recognized large inter-observer variability (SE = 30.2 g, 95% CI width = 59 g) and a poor inter-study (test–retest) reproducibility, with SDs of the difference between successive measurements ranging from 22 to 40 g (95% CI, 45–78 g) [9]. These findings are worse compared to previous results obtained by echo labs particularly devoted in this kind of measurement [10]. In the present study, the single measures ICCs of LV mass showed moderate variability in the SR setting (0.67), which became poor in patients with AF (0.42).The large RR variability caused by AF can obviously provoke a detrimental impact on the primary linear measurements needed to determine LV mass. The poor reproducibility of 2D-echocardiographic derived LV EF is also well known and now confirmed in the present study, single measures ICC being 0.49 in patients with SR and 0.40 in those with AF respectively. LV EF reproducibility was previously tested and both +7% of inter-observer reading variability [11] and +10% of test-retest variability [12] were observed. The suboptimal reproducibility of E velocity DT (single measures ICC = 0.61 and 0.50 in patients with sinus rhythm and AF respectively) could also have been expected. Diastolic time intervals such as isovolumic relaxation and DT have shown a larger variability than Doppler-derived diastolic velocities in both multicenter and inter-study experiences [13,14].This variability was obviously amplified in the setting of AF, due the RR variability own of this arrhythmia [15]. Conversely, the reproducibility of the other diastolic parameters chosen for the Registry was moderate (transmitral E/A ratio) to good (septal and lateral e' velocity, E/e' ratio). The reproducibility of GLS was good in patients with SR (single measures ICC = 0.81)

and remained stable even in the AF setting (0.78). In relation with its relative operator independency, GLS had previously shown a substantial good variability [16,17], which is lower when compared with LV EF also in test-retest evaluations [12,18]. Of interest, the precision in GLS measurements has been recently shown to be improved after training, regardless the experience, in a multi-center study on an oncologic population [19]. Besides LV EF, the use of GLS has been recently promoted as a key parameter of LV systolic function in the EACVI standardization of the adult echocardiography report [20].

The reproducibility tests of LA size and function provided further information. According to analysis of single measure ICCs, the variability of all the chosen parameters, including PALS, was lower in patients with AF than in those with SR. Notably, the single measures ICCs of minimal LA volume, in particular in the SR setting (0.71), were lower than those of maximal LA volume. It is conceivable that the absence of an ECG reference point when measuring minimal LA volume, might have reduced the consistency of this measurement in comparison with the determination of maximal LA volume, which is addressed by the R wave onset at the ECG trace. The lower variability of PALS in permanent AF can be considered only partially unexpected. AF is a condition associated to larger LA cavity and easier cavity border detection and also to an intrinsically smaller deformation of LA walls than SR. It is also of interest that single measures ICCs of PALS were lower in apical 4- than in 2-chamber view. The tracing of LA cavity borders and the consequent regional strain of the 4-chamber view can be difficult to obtain accurately in correspondence of the atrial septum drop-out [5], a characteristic which could induce a lower grade of accuracy of apical 4-chamber derived PALS we found. An ASE/EACVI consensus document of the EACVI/ASE Industry Task Force to standardize deformation imaging has recently promoted the possible use of the single 4-chamber view for calculating PALS [7], a choice which does not seem to be supported from our findings. However, the reproducibility of average PALS based on single measures was good in both patients with SR (ICC=0.75) and AF (ICC=0.81). These results confirm the data previously found in single center studies [21-23], extending the information to a multicenter investigation.

Noteworthy, the suitable reproducibility of GLS and PALS was further strengthened by the boxplot models showed in Figures 1 and 2 - which showed a substantially homogeneous distribution of both speckle tracking derived parameters - and by the low SE and the very narrow range of 95% CI, independently on the rhythm condition.

In conclusion, the present study provides important information on the parameters which will be of a great importance in the analyses of EACVI Afib Echo Registry and also adds interesting insights on the general use of echo-Doppler measurements in multicenter registries. While the utilization of some traditional standard echocardiographic variables, currently applied in large epidemiologic and interventional trials – in particular LV mass and LV EF – should be discouraged in registries not provided of a central reading by a dedicated echocardiographic core lab, the application of advanced echocardiographic parameters

obtainable by speckle tracking echocardiography (GLS and PALS) could be largely preferred because their relatively operator independence which facilitates the achievement of a suitable reproducibility even in patients with AF, a critical clinical setting in which the accuracy of measurements is mandatory.

Table 1. Characteristics of the study population.

Sinus rhythm = 10

Variable	Mean ± SD	Range
Sex (F/M)	5/5	
BMI (Kg/m2)	23.5 ± 3.4	18.2 - 27.7
Systolic BP (mm Hg)	116.7 ± 8.7	110.0 - 130.0
Diastolic BP (mm Hg)	70.0 ± 5.0	60.0 - 80.0
Mean BP (mm Hg)	85.6 ± 5.0	76.7 - 93.3
Heart rate (bpm)	68.0 ± 7.8	55.1 - 80.2

Atrial fibrillation = 10

Variable	Mean ± SD	Range
Sex (F/M)	5/5	
BMI (Kg/m2)	28.5 ± 4.8	22.1 - 36.4
Systolic BP (mm Hg)	125.0 ± 10.8	110.0 - 140.0
Diastolic BP (mm Hg)	79.5 ± 7.6	65.0 - 90.0
Mean BP (mm Hg)	94.7 ± 8.5	80 - 106.7
Heart rate (bpm)	76.2 ± 13.8	80.2 - 99.3

BMI = Body mass index, BP = Blood pressure

Table 2. Inter-class correlation coefficients of echo measures of LV geometry and function

Patients in sinus rhythm

Parameter	**Single measures**		
	ICC	*95% CI*	*P*
LV Mass	0.67	0.47 – 0.88	<0.0001
LV EF	0.49	0.29 - 0.77	<0.0001
LV GLS	0.81	0.65 - 0.93	<0.0001
E/A ratio	0.72	0.53 – 0.90	<0.0001
DT	0.61	0.40 – 0.85	<0.0001
e' septal	0.73	0.55 – 0.90	<0.0001
e' lateral	0.85	0.71 – 0.95	<0.0001
E/e' ratio	0.87	0.73 – 0.97	<0.0001

Patients in atrial fibrillation

Parameter	**Single measures**		
	ICC	*95% CI*	*P*
LV Mass	0.42	0.23 – 0-72	<0.0001
LV EF	0.40	0.20 - 0.75	<0.0001
LV GLS	0.78	0.61 - 0.93	<0.0001
E/A ratio	0.72	0.53 – 0.90	<0.0001
DT	0.50	0.29 – 0.78	<0.0001
e' septal	0.77	0.59 – 0.92	<0.0001
e' lateral	0.71	0.52 – 0.89	<0.0001
E/e' ratio	0.75	0.57 – 0.91	<0.0001

DT= Deceleration time; CI: Confidence interval, EF = Ejection fraction, GLS = Global longitudinal strain, ICC= Inter-class correlation coefficient, LV =Left ventricular

Table 3. Inter-class correlation coefficients of measures of LA size and function.

Patients in sinus rhythm

Parameter	**Single measures**		
	ICC	*95% CI*	*P*
LAD	0.72	0.53 - 0.89	<0.0001
LAV max	0.73	0.54 - 0.90	<0.0001
LAV min	0.71	0.52 - 0.89	<0.0001
PALS 4CH	0.71	0.51 - 0.89	<0.0001
PALS 2CH	0.75	0.57 – 0.91	<0.0001
PALS AVG	0.75	0.57 – 0.91	<0.0001

Patients in atrial fibrillation

Parameter	**Single measures**		
	ICC	*95% CI*	*P*
LAD	0.75	0.57 - 0.91	<0.0001
LAV max	0.89	0.78 - 0.97	<0.0001
LAV min	0.87	0.74 - 0.96	<0.0001
PALS 4CH	0.71	0.51 - 0.91	<0.0001
PALS 2CH	0.81	0.64 – 0.94	<0.0001
PALS AVG	0.81	0.66 – 0.94	<0.0001

CI: confidence interval, ICC: inter-class correlation coefficient, LAD: left atrial antero-posterior diameter; LAV max: maximum left atrial volume; LAV min: minimum left atrial volume; PALS 4CH: peak systolic atrial longitudinal strain in 4 apical chambers view; PALS 2 CH: peak atrial longitudinal strain in 2 chambers apical view; PALS AVG: average peak atrial systolic longitudinal strain (between 4CH and 2 CH)

Figure 1. Distribution of left ventricular GLS in the 16 echo labs.
Boxplot of GLS in 10 patients in sinus rhythm (a) and in 10 patients AF (b) measured by the different 16 echocardiographic laboratories. For each echo lab, black horizontal bar (= median), white boxes (= 95% CI) and vertical bars (minimal and maximal value) are reported. Black dots are outliers of individual echo labs. E= Echo lab

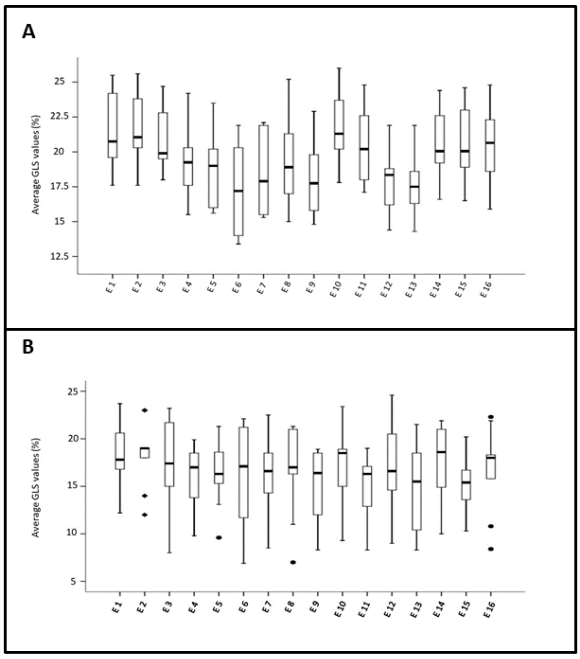

Figure 2. Distribution of PALS in the 16 echo labs. Boxplot of GLS in 10 patients in sinus rhythm (a) and in 10 patients AF (b) measured by the different 16 echocardiographic laboratories. For each echo lab, black horizontal bar (= median), white boxes (= 95% CI) and vertical bars (minimal and maximal value) are reported. Black dots are outliers of individual echo labs. E=Echo lab

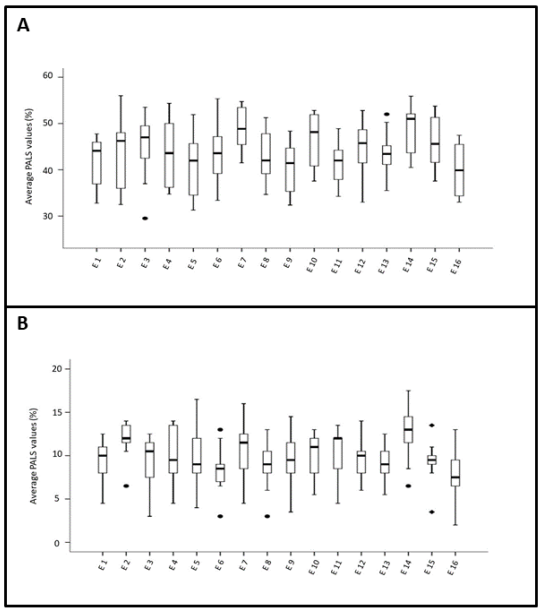

Part 3

Other studies

Chapter 15

Left atrial function in breast cancer patients undergoing chemotherapy

Left atrial contractile function in breast cancer patients undergoing trastuzumab therapy

Background:

Trastuzumab (TZ) therapy is associated with left ventricular (LV) dysfunction due to cardiotoxicity. However, data on left atrial (LA) function in patients receiving TZ are scarce.

Purpose:

To compare effects of TZ therapy on LA contractile strain (LASCT) versus on left ventricular global longitudinal strain (LV GLS) and ejection fraction (LVEF) in breast cancer patients treated with TZ.

Methods:

We have prospectively enrolled 23 consecutive breast cancer patients (age 53±10 years, 100% females) with normal LVEF (> 50%) scheduled for TZ therapy. No patient had history of heart or internal disease. Comprehensive transthoracic echocardiography was performed pre TZ therapy and then at 3-month intervals. LV GLS and LASCT were assessed using the two-dimensional speckle tracking echocardiography as average of segmental values in apical views. Cardiotoxicity was defined by a symptomatic reduction of LV GLS =12%.

Results:

A total of 9 (39%) patients showed cardiotoxicity at median of 189 days (IQR 167-203) from baseline. Both groups had similar baseline characteristics (NS). At follow-up, patients with versus without cardiotoxicity showed significant decrease in magnitude of LV GLS (-17±3.6% vs. 1±8.3%, p<0.001), LVEF (-9±9.3% vs. 3±9.1%, p=0.015) and LASCT (-19±9.9% vs. -3±21.2%, p=0.0025). In contrast, the conventional parameters of LA morphology and function did not change significantly (NS).

All patients with diagnosis of cardiotoxicity received ACE inhibitors and/or betablockers, and continued with TZ therapy. Control echocardiography after 3 months showed a significant improvement of LV GLS, LVEF and LASCT in 4 (44%) patients while no favorable changes or even deterioration were observed in the remaining individuals (Figure, red color).

In patients without LV GLS-derived cardiotoxicity, only LASCT showed mild reduction between baseline and last available echocardiogram. In contrast all the remaining parameters did not change during the entire follow-up.

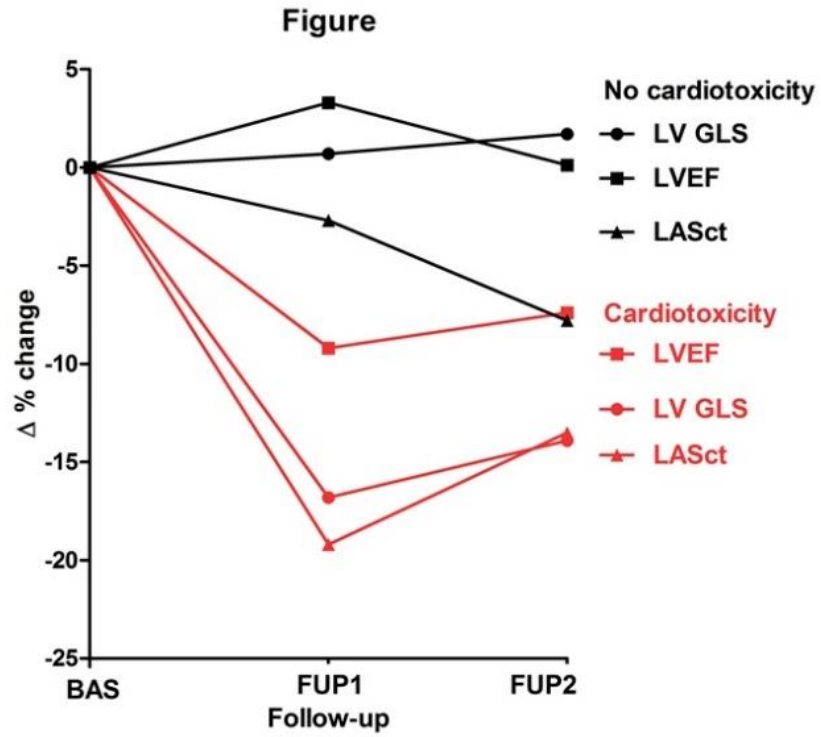

Image: LVGLS pre (Avg -20. 1%) and post Cardiotoxicity (Avg -16. 1%).

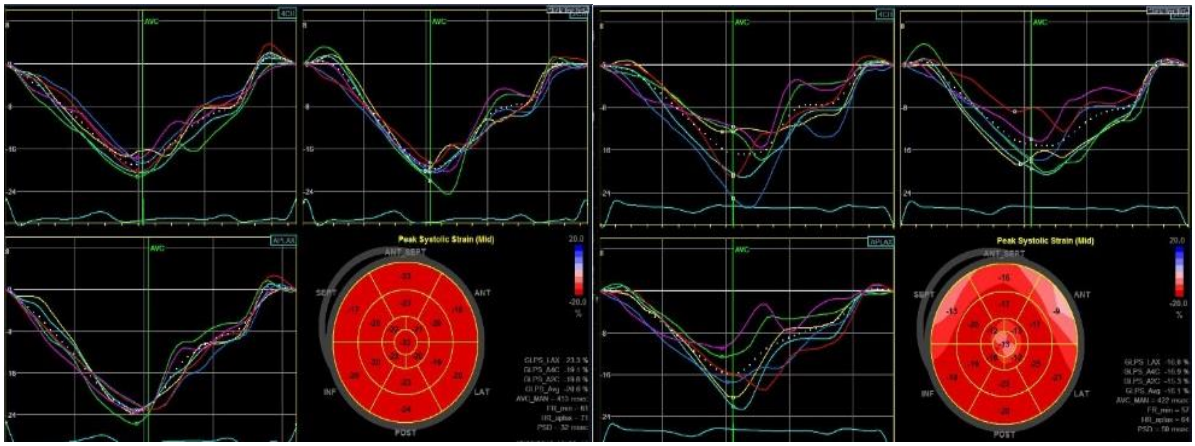

Conclusion:

LASCT appears to be a sensitive parameter to assess effects of TZ therapy on LA. Its incremental value over LV functional parameters needs to be demonstrated in a large study.

Left atrial contractile strain, left ventricular strain or ejection fraction to assess cardiotoxicity in breast cancer patients receiving trastuzumab therapy?

Background:

In breast cancer patients undergoing Trastuzumab (TZ) therapy, early detection of cardiac dysfunction is of critical importance.

Purpose:

To compare potential value of left ventricular ejection fraction (LVEF), global longitudinal strain (LV GLS) and left atrial contractile strain (LAS) in HER2-positive breast cancer patients undergoing TZ therapy.

Methods:

The study population consisted of 23 HER2-positive breast cancer patients (age 53±10 years, 100% females), with normal LVEF (> 50%) receiving TZ. Patients with previous heart disease, hypertension or diabetes mellitus were excluded. All patients underwent transthoracic echocardiography before and at 3-month intervals during TZ therapy.

Several different loops for each apical plane have been recorded to assess LV GLS and LAS using speckle tracking. Cardiotoxicity was defined in three different ways according to each parameter as a 5% symptomatic or 10% asymptomatic fall of LVEF to < 50% (LVEFctox), by a reduction of LV GLS =12% (GLSctox) or of contractile LAS by =15% (LASctox), from baseline.

The interobserver variability for LVEF, LV GLS and LAS was assessed in 10 patients by two experienced operators, using both the same 3 apical views and different apical views of their choice.

Results:

A total of six (26%), 9 (39%) and 9 (39%) patients developed LVEFctox, GLSctox and LASctox, respectively. All patients with the LVEFctox showed also the LV GLSctox. In contrast, the LASctox was observed only in 67% and 56%, respectively, of patients with the LVEFctox and GLSctox.

The interobserver variability using the same apical loops was the lowest for LV GLS (2±4%), followed by LAS (4±14%) and LVEF (8±12%). Free choice of apical loops was associated with an increase of variability for both LV GLS (6±6%) and LAS (9±26%), but less for LVEF (10±12%).

Figure: left atrial cardiotoxicity in breast cancer patients undergoing chemotherapy.

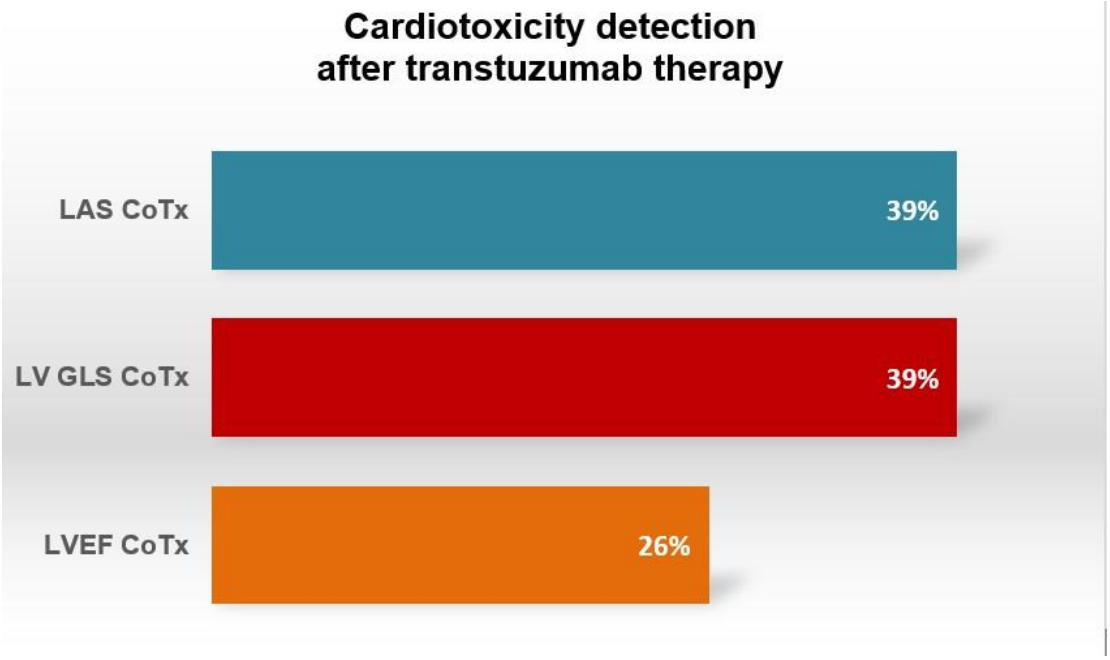

Conclusions:

To assess cardiotoxicity, LV GLS seems to represent an optimal balance between sensitivity and reproducibility. LVEF is less sensitive and reproducible, however, also less affected by selection of apical views. Contractile LAS is sensitive but shows higher coefficient of variations and is discordant with LV functional indices.

Chapter 16

Comparison between echocardiography and three-dimensional rotational angiography: the implication for successful percutaneous left atrial appendage closure

Background:

In patients undergoing percutaneous left atrial appendage (LAA) closure, the assessment of LAA ostium is critical for sizing of LAA closure device. Three dimensional rotational angiography (3DRA) has recently emerged as an alternative to TEE for LAA ostium assessment. However, the data on comparison between both methods are scarce.

Purpose:

Firstly, to compare LAA ostium measurements obtained by TEE versus those obtained by 3DRA. Secondly, to assess procedural outcome of the TEE- versus the 3DRA-guided sizing of LAA closure device.

Methods:

We prospectively studied 67 consecutive patients who underwent LAA closure (age 76±19 years; 42% Female, CHA2DS2-VASc score 4.73, HASBLED score 3.66). Patients were divided into two groups.

The 3DRA-guided group consisted of 29 (43%) patients who underwent both 2D/3D TEE and 3DRA during the LAA closure procedure.

The 3DRA dataset containing the whole LAA was analyzed to assess LAA ostium size in end systole by an operator blinded to the TEE-derived measurements. In the 3DRA-guided group, the LAA closure device sizing was guided by the 3DRA assessment. In the remaining 38 (57%) patients, the LAA closure device sizing was guided by TEE (the TEE-guided group). In all patients, TEE was repeated at 3-6 months.

Results:

The 3DRA-derived maximal diameter of LAA ostium was by 6.7±3.3 mm and 5.3±3.4 mm larger than those derived by 2D and 3D TEE, respectively (both $p<0.05$). Similar trend was observed for LAA minor diameter, 3D area-derived diameter or LAA length.

The concordance in LAA closure device sizing between the 3DRA- and the TEE-derived assessment was observed only in 42% of patients. The compressed diameter of the

implanted closure device showed a significantly higher correlation with LAA maximal diameter assessed by 3D TEE (r=0.74) versus by 3DRA (r=0.61) ($p<0.05$).

Both the 3DRA-guided and the TEE-guided groups had similar occurrence of periprocedural complications or mild pericardial effusion. At follow-up, the 3DRA versus the TEE-guided group did not show any higher prevalence of significant para device leak (NS) or device-attached thrombus (7.9% vs. 3.4%, p=0.4).

Conclusion:

The 3DRA-derived indices of LAA ostium are consistently larger than the TEE-derived ones because of TEE under-sizing or because of 3DRA contrast induced overload. However, neither TEE nor 3DRA appears clinically superior to the other in guiding LAA closure and both modalities show a similar outcome.

Figure 1: Bland-Altman analysis of difference between maximal diameter of LAA ostium measured by 3D angiography and 3D echocardiography in 29 patients received LAA closure.

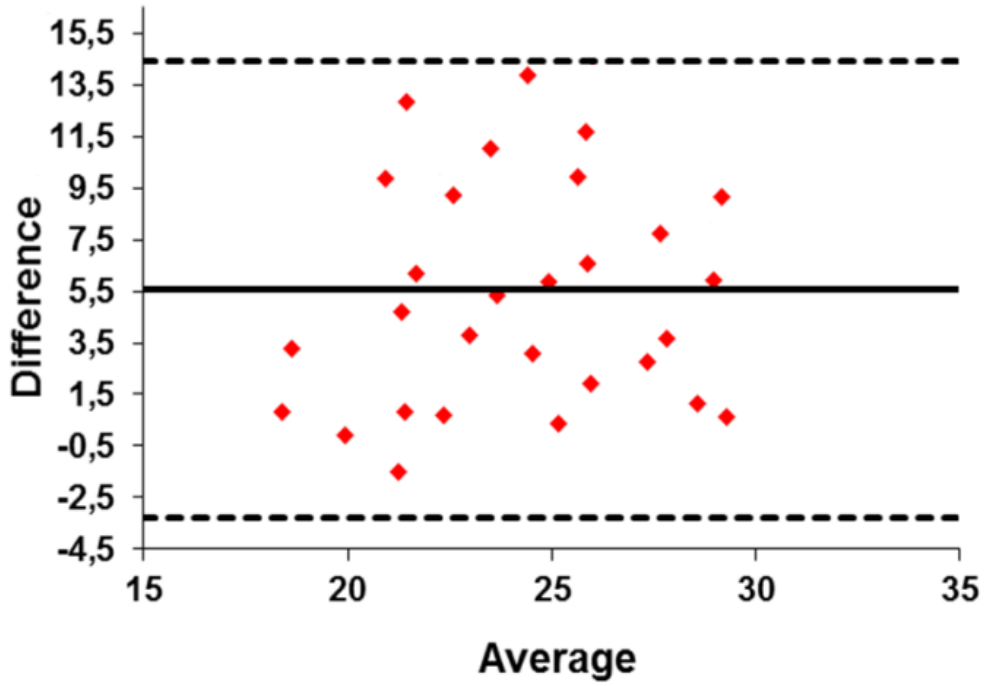

Figure 2: Correlation analysis between the LAA dimensions measured by 3D angiography to 3D echocardiography in 29 patients received LAA closure.

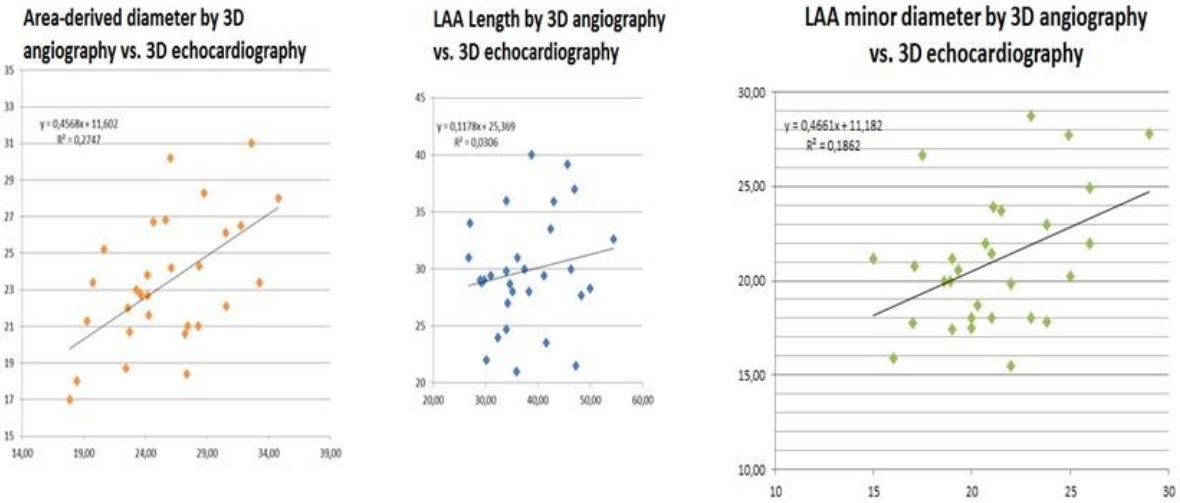

Figure 3: Exmaple of 3D rational angiography and 3D echocardiography images shown an elliptical shape of LAA ostium before and after the deployed device in the appendage. 3D echocardiography and biplane view of the deployed device in the appendage showing stability.

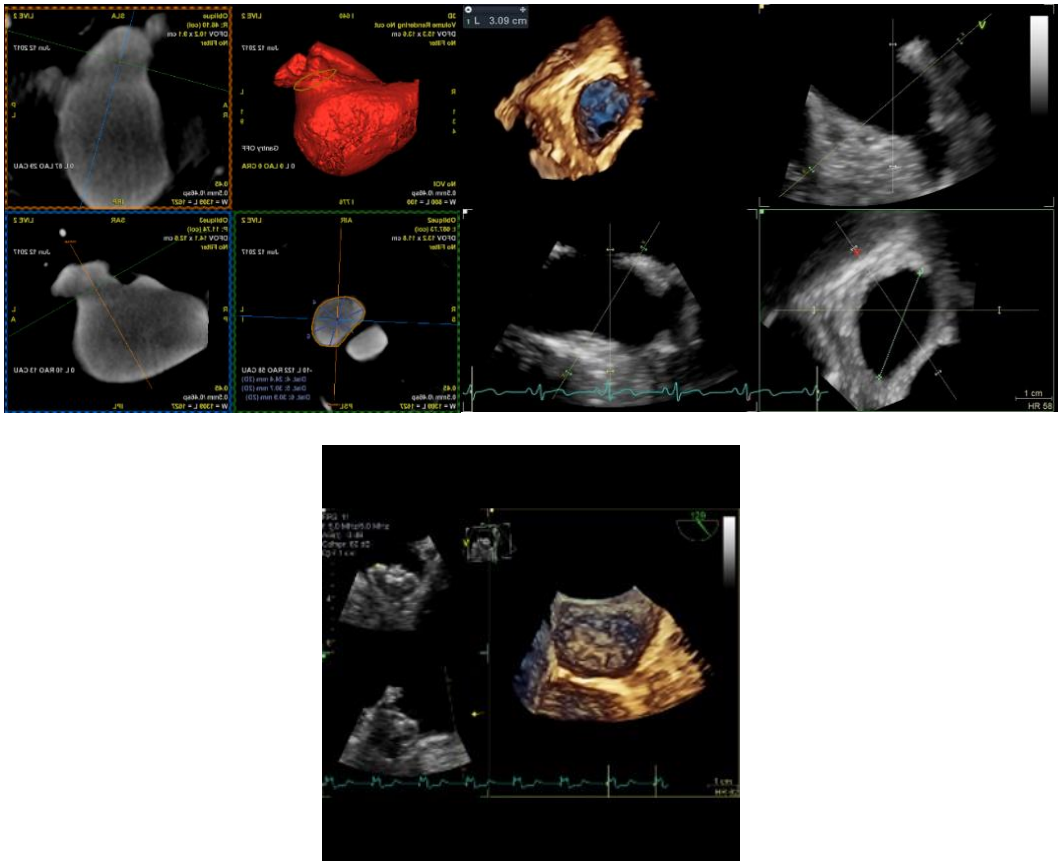

Figure 4. 3D rotational angiography and 3D echocardiography images from the single non-implantable patient. There was no stability of the device in the appendage. (A) 3D appendage segmentation. Multiplanar reconstruction at the neck of the appendage. Maximum diameter is 30.5 mm. (B) transesophageal echocardiography at 47° plane. Maximum diameter is 27 mm. (C) the view of device in the left atrial appendage after deployment, showing lack of compression. (D) Biplane view of the deployed device in the appendage, showing lack of stability.

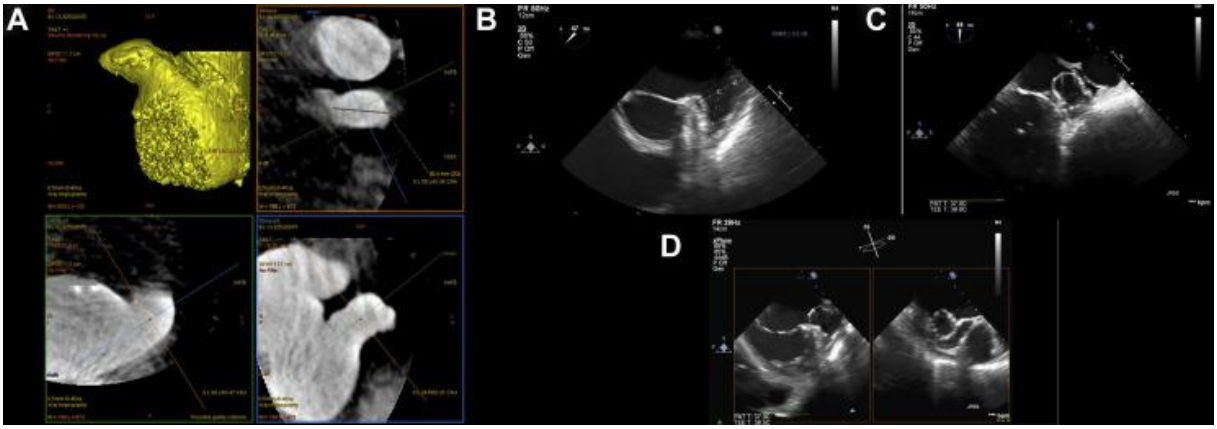

Chapter 17

Endoscopic mitral valve repair of atrial functional mitral regurgitation in non-ischemic heart failure with preserved ejection fraction

Introduction:

In patients with heart failure and preserved ejection fraction (HFpEF), even mild atrial functional mitral regurgitation (AFMR) has been associated with poor outcome.

Objective:

To describe long-term effects of endoscopic mitral valve (MV) repair on outcome in patients with HFpEF and AFMR.

Methods:

The study population consisted of consecutive patients with HFpEF (LVEF ≥50%, H2FPEF score ≥ 5) and at least mild AFMR, who underwent isolated, minimally invasive (endoscopic), MV repair (MVRepair group) (n=131; 72 ± 7 years, 21% males) or remained on standard of care (StanCare group) (n=139; 78 ± 9 years, 28% males). Patients with coronary artery disease or organic MR were excluded. A complete (100%) follow up of all-cause mortality and HFpEF readmissions was obtained.

Results:

In the MVRepair group, the median follow up was 7.8 years (IQR 5.0-9.4 years). The perioperative, 30-day, 1- and 5-year mortality was 0, 1%, 1% and 12%, respectively. Additional 13 (10%) patients were readmitted for worsening HfpEF, while 2 (1%) individuals underwent redo MV surgery for recurrent MR. In different propensity matching analyses, MVRepair compared with StanCare showed 21-29% (SE 6-8%) and 19-26% (SE 6-8%) absolute risk reduction of all-cause mortality and HFpEF readmissions, respectively (all $p<0.05$).

MVRepair emerged as the strongest independent predictor of all-cause mortality (HR 0.16, 95% CI 0.07-0.34, $p<0.001$) and HFpEF readmissions (HR 0.21, 95% CI 0.09-0.51, $p<0.001$). At 5-year follow-up, in the MVRepair group, a total of 88% were alive and 80% were alive without readmission for HFpEF.

Conclusions:

In patients with HFpEF and AFMR, endoscopic MV repair is associated with low perioperative mortality and high long-term efficacy to treat AFMR. MV repair seems to reduce excess mortality associated with HFpEF and AFMR.

Introduction

Atrial functional mitral regurgitation (AFMR) shows high prevalence in heart failure patients with preserved ejection fraction (HFpEF) and atrial fibrillation (AF), where its presence is associated with worse outcome (1-5). The optimal treatment strategy of AFMR is not known. Two small studies have reported good short-term effects of undersized mitral valve (MV) annuloplasty using open chest sternotomy (6,7). However, long-term effects of MV intervention on survival are not available. Moreover, patients with HFpEF and AFMR are usually elderly with frequent comorbidities, in whom, a minimally invasive technique may provide a distinct safety advantage over the sternotomy (1,2).

Video-assisted endoscoscopic MV repair is a minimally invasive surgical approach using the right chest while avoiding sternotomy (8). The endoscopic technique shows comparable results as the open-chest MV surgery but with less postoperative morbidity (8). In ventricular FMR, endoscopic MV annuloplasty had conferred an independent long-term survival benefit compared with the guidelines directed therapy (9). However, its prognostic impact in AFMR is not known. Therefore, the aim of the present study was to describe long-term effects of endoscopic MV repair on outcome in patients with HFpEF and AFMR.

Methods

Study design A retrospective, single-center study.

Study population The study population consisted of consecutive patients with HFpEF and at least mild AFMR, who underwent isolated, minimally invasive (endoscopic), MV repair (MVRepair group) between 2003 and 2017 (n=406; age 69±12 years, 32.5% males) or remained on standard of care (StanCare group) (n=354, age 77±10 years, 36.4% males). The diagnosis of HFpEF was based on clinical presentation and the H2FPEF score (10). The H2FPEF score is a validated and robust algorithm, which relies on simple clinical and Doppler echocardiographic characteristics (age, body mass index, history of hypertension or atrial fibrillation, pulmonary artery systolic pressure and mitral E/e') allowing discriminating of HFpEF from non-cardiac causes of dyspnea (10).

AFMR was defined by structurally normal valve or with only minimal structural alteration, and with normal leaflet motion. All individual files and available images were reviewed by an experienced echocardiographer (ZB), who was blinded to clinical outcome. To be eligible for the study, patients had to fulfill the following criteria: [1] LV ejection fraction ≥ 50%; [2] H2FPEF score ≥ 5 suggesting > 80% probability of HFpEF; [3] Non ischemic etiology of HFpEF; and [4] at least mild AFMR (≥ 1/4 grade). Patients were excluded if they had reduced LV ejection fraction (<50%), history of myocardial infarction, previous heart surgery including

myocardial revascularization, suspected ischemic heart disease, need for concomitant myocardial revascularization or aortic valve surgery, congenital heart disease, hypertrophic or restrictive cardiomyopathy, metastatic cancer or other significant comorbidities likely to limit survival, and unavailable or poor quality echocardiographic images (Figure 1). The MVRepair group consisted of 131 patients (72 ± 7 years, 21% males) undergoing endoscopic MV repair using undersized semi-rigid annuloplasty ring on an elective basis. No patient underwent myocardial revascularization. Concomitant tricuspid valve annuloplasty or MAZE was not an exclusion criterion. The StanCare group consisted of 139 patients (78 ± 9 years, 28% males) hospitalized for de novo HFpEF who showed at least mild AFMR at fully compensated state at discharge.

The study protocol was performed in accordance with the Ethics Committee of our institution. The need for consent to participate in this research study was waived in view of its observational and anonymous nature. Demographic data, medical history, laboratory results, imaging findings, periprocedural, and follow-up data were collected for the analysis. In all patients, survival status at the end of follow-up was verified using the national population registry. The cause of each readmission was reviewed in patient's records and if needed validated with the patient or family doctor.

Statistical analysis

Data are expressed as mean ± SD for continuous variables and as percentages for categorical variables. The unpaired or paired Student t-test and the Pearson correlation coefficient were used as appropriate. The Fisher's exact test was used to compare categorical variables in 2× 2 contingency tables. Cumulative survival curves were derived according to the Kaplan-Meier method, and differences between curves were analyzed by log-rank test.

Several analyses were performed to estimate effect of MVRepair on all-cause mortality, HFpEF readmissions and their composite. [1] Propensity score to match for perioperative risk (EuroSCORE II) or for clinically relevant baseline characteristics (age, gender, NYHA class, body mass index, hypertension, diabetes mellitus, LV end-diastolic diameter, tricuspid regurgitation grade and pulmonary artery pressure).

Score was used for appropriate local optimal 1:1 caliber matching without replacement using 0.20 caliper width of the logit of the standard deviation of the calculated score to balance the baseline covariates; [2] Kaplan-Meier-derived survival analysis using inverse probability weighting;]3] Cox regression modelling adjusted for propensity score. Care was taken to avoid overfitting. For all tests, values of $p < 0.05$ were considered significant. For statistical analysis, R 3.5.0 was used.

Results

Baseline characteristics in Table 1 shows baseline clinical and echocardiographic characteristics in both groups. Per eligibility criteria, all patients had a non-dilated LV with

preserved LV ejection fraction. The average H2FPEF score was > 6 in both groups. The majority of patients had a history of AF. The StandCare individuals were significantly older and had higher prevalence of comorbidities compared with the MVRepair group ($p<0.01$). Despite being low in both groups, the EuroSCORE II was significantly higher in the StanCare versus the MVRepair group ($p<0.001$). The majority of patients (71%) undergoing MV repair had NYHA class III/IV symptoms. We observed significantly larger left atrial diameter, greater degree of AFMR and tricuspid regurgitation in patients undergoing MVRepair compared with StanCare (all $p < 0.001$).

Periprocedural and 30-day outcome in the MVRepair group The MV repair was successful in all patients and no individual died during surgery (intraoperative mortality=0). Concomitant tricuspid valve annuloplasty and MAZE was performed in 68 (49%) and in 97 patients (70%), respectively. The average cardiopulmonary bypass and myocardial ischemic time was 136 ± 37 minutes and 93 ± 30 minutes, respectively. One patient died during index hospitalization from multiorgan failure (hospital and 30-day mortality = 1%). Major surgical complications were observed in a total of 13 (9%) individuals, out of whom 9 patients (6%) showed total AV-block requiring implantation of permanent pacemaker, 1 (1%) had multiorgan failure, 2 (2%) had stroke, and 1 (1%) had sepsis. All these patients recovered and were discharged to ambulatory care.

Long-term outcome

Follow-up for all-cause mortality and HFpEF readmission was obtained in 100% of patients. During median follow up of 5.03 years (IQR 2.6-7.9 years) a total of 86 (32%) patients died from any cause and 61 (23%) ones were readmitted for worsening HFpEF. In MVRepair group, two patients (1.4%) had redo MV surgery for recurrent MR. In the StanCare group, no patient had MV intervention during follow up. As expected, both groups showed significantly higher all-cause mortality compared to expected mortality in age- and sex-matched general population (Figure 2A, 2B). Yet, in the MVRepair group, significant separation of the survival curves was observed only after 3 years following MV intervention. In contrast, in the StanCare group, the separation of the survival curves started immediately after index admission. Patients in the StanCare group had significantly higher 1-year (9% vs. 1%, $p=0.002$) and 5-year (40% vs. 12%, $p<0.001$) mortality from any cause and 1-year (17% vs. 4%, $p=0.006$) and 5-year (34% vs. 10%, $p<0.002$) readmissions for worsening HFpEF, respectively. The total number of HFpEF readmissions was significantly higher in the StanCare versus the MVRepair group (56% vs. 13%, $p<0.001$). Movies 1 shows individual examples of two patients with HFpEF and significant AFMR: a long-term survivor (Movie 1AB), who underwent successful MVRepair, and a non-survivor (Movie 1C), who remained on Standard of Care. Several different propensity-score models were constructed to account for baseline differences between groups in term of perioperative risk or other relevant characteristics. In all these analyses, MVRepair compared with StanCare showed significant

absolute risk reduction of all-cause mortality (21-29%), HFpEF readmissions (19-26%), and their composite (32-38%) (all $p < 0.05$) (Figures 3-5).

Predictors of outcome

MV repair was the strongest independent predictor of all-cause mortality, HFpEF readmissions and their composite (all $p < 0.001$). The other independent predictors were age and body mass index for of all-cause mortality, tricuspid regurgitation grade and diabetes mellitus for HFpEF readmissions, and age for their composite (Table 2).

Discussion

In the present study, in patients with HFpEF and AF, endoscopic MV repair of AFMR has been associated with: [1] low perioperative and 30-day mortality; [2] high long-term efficacy with low rate of recurrent AFMR; and [3] reduction of excessive mortality and HFpEF readmissions during follow-up.

Prevalence and outcome of AFMR

AFMR has emerged as a distinct type of mitral regurgitation, which is characterized by structurally normal MV with normal leaflet motion (1,3). The major underlying mechanism has been proposed to be mitral annulus dilatation stand alone or in some cases, combined with an insufficient compensatory leaflet growth, impairment of atrial and annular dynamics (1,3,11-15). AFMR shows high prevalence in patients with HFpEF and AF (1,2,5). HFpEF leads to increase in left atrial pressure, thus, left atrial remodeling, AF, mitral annulus dilatation and AFMR, which in turns worsens symptoms and outcome (1,2,5). As the prevalence of both HFpEF and AF is steadily increasing, AMFR may become the most frequent type of MR in the near future (1,16,17). In the ATTEND registry including 1825 patients with HFpEF, a total of 71% of subjects had at least mild AFMR before discharge following admission for acute decompensation (5). Presence of even mild “ischemic” AFMR at discharge has been independently associated with higher occurrence of the composite of all-cause death and HFpEF readmissions (4,5). In the community patients with isolated moderate-to-severe MR, AFMR accounted for 27% of cases (2). It is noteworthy, that, despite having relatively small effective regurgitant orifice area (0.2±0.08 cm^2), AFMR has been associated with excess 5-year mortality (50%) compared with expected mortality in general population (HR 1.88) (2).This suggests that even small amount of regurgitant volume may have prognostic impact in non-dilated and non-compliant LV alluding to the recently proposed concept of disproportionate FMR (18). In the present study, we have observed even higher prevalence of moderate to severe AFMR (37%) than in the previous studies, which may be related to inclusion of patients with high H2FPEF score, AF and at least mild AFMR into the present study (2,5). In the StanCare group, we have observed slightly better 5-year survival than in the Mayo clinic cohort, which may be explained by exclusion of ischemic AFMR from the present study (2).

Management of AFMR

Despite being associated with poor outcome, optimal therapeutic strategy in AFMR has not been determined (19). Diuretics and early restoration of sinus rhythm may reduce left atrial pressure and mitral annular area and, hence, the severity of AFMR. However, frequently associated renal impairment and persistence of AF makes this approach challenging for a large proportion of HFpEF patients (20). Undersized MV annuloplasty targets the major underlying mechanism of AFMR, i.e. annulus dilatation. Two smaller studies totaling 57 patients with permanent AF and preserved LV ejection fraction have reported good mid-term effects of MV annuloplasty using open chest technique (6,7,21). During median follow up of 932 days, the rates of composite of freedom from cardiac death and HFpEF readmissions was 64% (21). In our study, we report the long-term outcome in the largest cohort of HFpEF undergoing MVRepair for AFMR so far. At 5-year follow-up, a total of 88% of patients were alive and 80% ones were alive without HFpEF readmission, i.e. significantly better outcome than in the previous study (21). Moreover, in our study, MVRepair remained to be associated with improved survival compared with standard of care even after propensity matching. The more favorable outcome in the current study may be related to minimally invasive approach, which may present an important safety advantage in these frail patients.

Limitations

The present study was retrospective with all inherent limitations. However, all files and images were carefully examined by an experienced echocardiographer and patients with insufficient data or poor image quality were excluded. Moreover, in all patients, follow-up for mortality and HFpEF readmissions was obtained.

Conclusions

AFMR shows high prevalence in HFpEF patients, where it is associated with poor outcome. The results of the present study suggest that isolated MV repair is safe and provides long-term freedom from recurrent AFMR in the majority of patients. Moreover, MV repair seems to reduce excess mortality associated with HFpEF and AFMR. These results may encourage future studies using MitraClip in this population.

Table 1. Baseline clinical and echocardiography characteristics

Variables	MVRepair n=131	StanCare n=139	p
Age, y	71.99 (7.26)	77.71 (8.92)	<0.001
Gender, n (%)	28 (21.4)	39 (28.1)	0.259
Hypertension, n (%)	75 (60.5)	90 (64.7)	0.558
Diabetes mellitus, n (%)	1 (0.8)	13 (9.5)	0.003
COPD, n (%)	13 (10.0)	22 (15.8)	0.216
MDRD < 50 ml /min/1.73 m^2, n (%)	29 (22)	46 (33)	0.057
Stroke, n (%)	3 (2.3)	16 (11.5)	0.007
EuroSCORE II, %	2 (1)	3 (2)	<0.001
History of AF, n (%)	122 (93.1)	133 (95.7)	0.516
NYHA, n (%)			Not applicable
I, II	38 (29.0)	0	
III, IV	93 (71.0)	139 (100)	
Body mass index, kg/m^2	27.44 (4.30)	29.00 (7.48)	0.040
H_2FPEF	6.34 (1.14)	6.79 (1.27)	0.003
LVEDd, mm	49.80 (6.44)	48.48 (5.95)	0.093
LVEF, %	59.05 (5.55)	55.94 (4.13)	<0.001
LA diameter, mm	47.16 (7.10)	44.10 (5.96)	<0.001
AFMR	2.76 (0.67)	1.30 (0.63)	<0.001
Tricuspid regurgitation	2.14 (1.03)	1.68 (0.94)	<0.001
Systolic PAP, mmHg	42.04 (10.52)	44.22 (13.62)	0.150

Abbreviations: AF = atrial fibrillation, AFMR = atrial functional mitral regurgitation, COPD = chronic obstructive pulmonary disease, LA = left atrial, LVEDd = left ventricular end-diastolic diameter, LVEF = left ventricular ejection fraction, MDRD = The Modification on Diet in Renal Disease, MVA = mitral valve annuloplasty, NYHA = New York Heart Association, PAP = pulmonary artery pressure.

Table 2: Predictors of all-cause mortality, HFpEF readmissions and their composite

	Multivariable Analysis	
	HR (95% CI)	p value
All-cause mortality		
Age	1.05 (1.01-1.10)	0.031
Body mass index	0.93 (0.87-0.99)	0.023
MV repair	0.16 (0.07-0.34)	< 0.001
HFpEF readmissions	1.38 (0.97-1.97)	0.071
Diabetes mellitus	5.14 (1.16-22.73)	0.031
TR grade	2.14 (1.00-4.58)	0.050
MV repair	0.21 (0.09-0.51)	< 0.001
Mortality and HFpEF readmissions		
Age	1.03 (1.00-1.07)	0.050
MV repair	0.22 (1.13-1.41)	< 0.001

CI = confidence interval, HR = hazard ratio

Abbreviations: HFpEF = heart failure with preserved ejection fraction, MV = mitral valve

Figure 1: Identification of the study group. All patients labeled as HFpEF with at least mild FMR have been considered for the study. Abbreviations: AFMR = atrial functional mitral regurgitation, AR = aortic regurgitation, AS = aortic stenosis; HFpEF = heart failure with preserved ejection fraction, LVEF = left ventricular ejection fraction, MR = mitral regurgitation, MVRepair = mitral valve repair group, StanCare = standard of care group

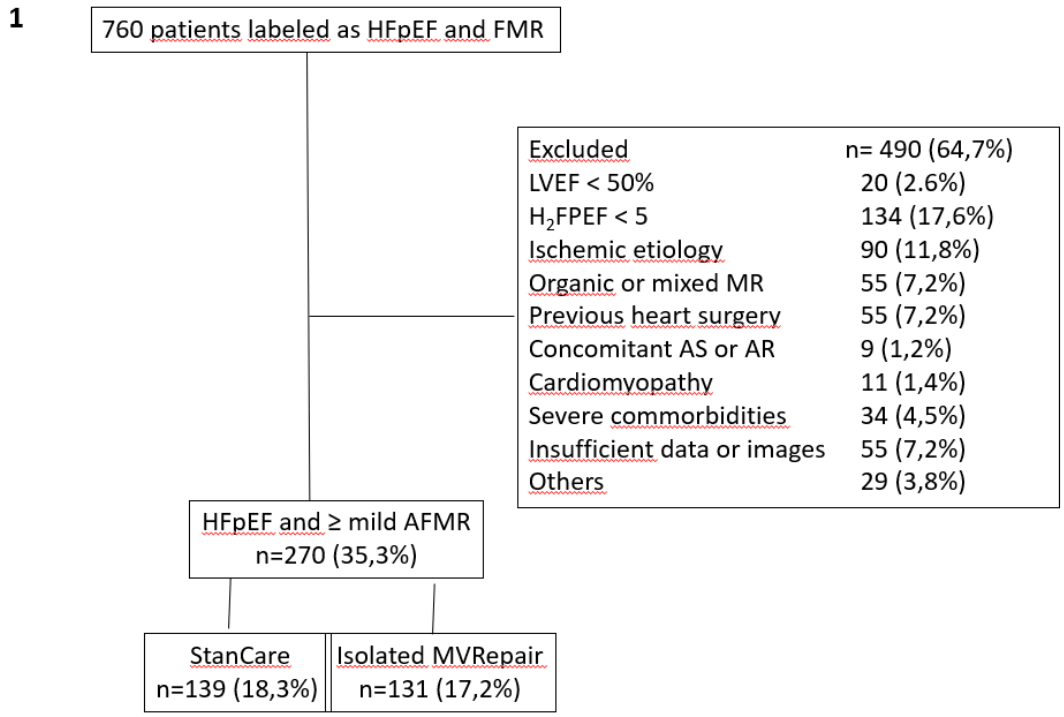

Figure 2: Observed versus expected survival in the MVRepair (2A) and StanCare (2B) group.

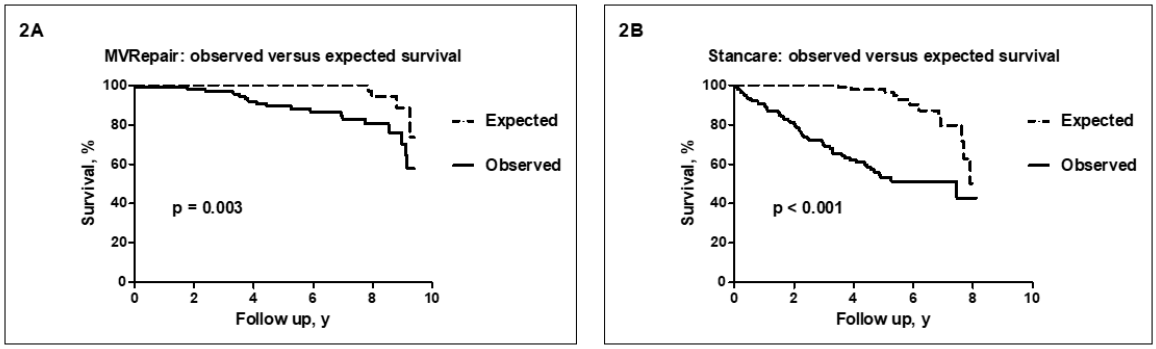

Figure 3: Estimating effect of MVRepair using propensity score matching at 5-year follow up.

3

Model	Variables	P value
No-adjustment	Mortality	<0.001
	Rehospitalization	<0.001
	Composite outcome	<0.001
Adjusted by Euroscore	Mortality	<0.001
	Rehospitalization	<0.001
	Composite outcome	<0.001
Adjusted by Euroscore, sex and age	Mortality	0.027
	Rehospitalization	<0.001
	Composite outcome	<0.001
Adjusted by Euroscore, age and NYHA at baseline	Mortality	0.001
	Rehospitalization	0.016
	Composite outcome	<0.001

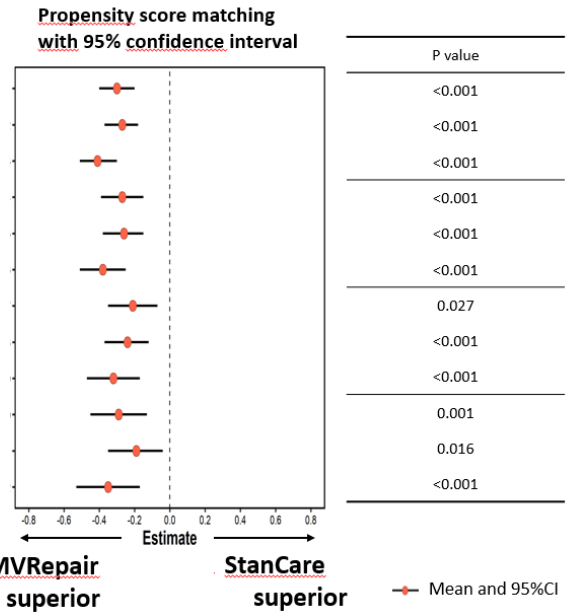

Figure 4: Survival analysis using inverse probability weighting. All-cause mortality (4A), HFpEF readmissions (4B) and their composite (4C) after propensity matching for baseline perioperative risk (EurSCOR II, age and HYHA class) at 5 years. Unadjusted (dashed lines) and adjusted (solid lines) in the MVRepair (red color) versus the StanCare (black color) groups. Propensity matching resulted in 52 matched pairs.

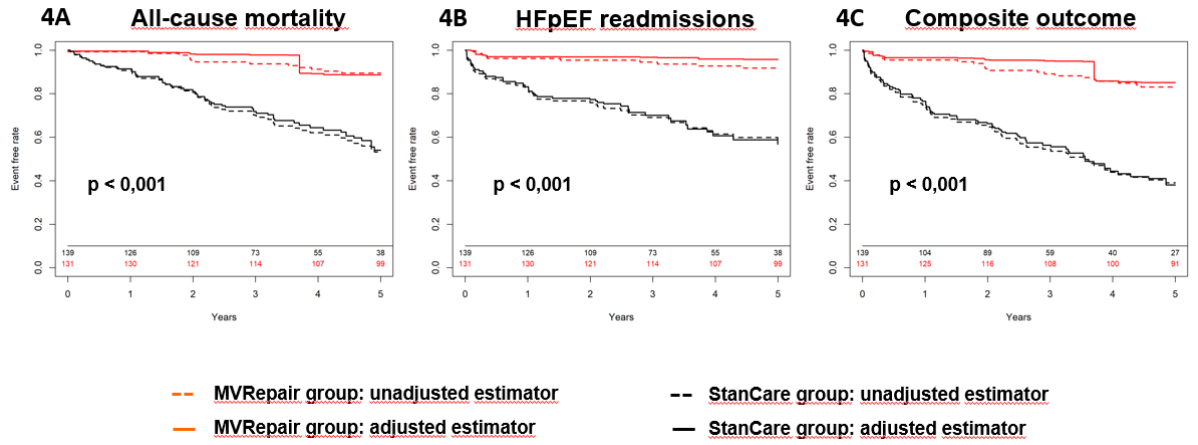

Figure 5: All-cause mortality (5A), HFpEF readmissions (5B) and their composite (5C) following propensity matching for clinically relevant baseline characteristics. The MVRepair group is shown in red color while the StanCare group in black color. Propensity matching resulted in 56 matched pairs.

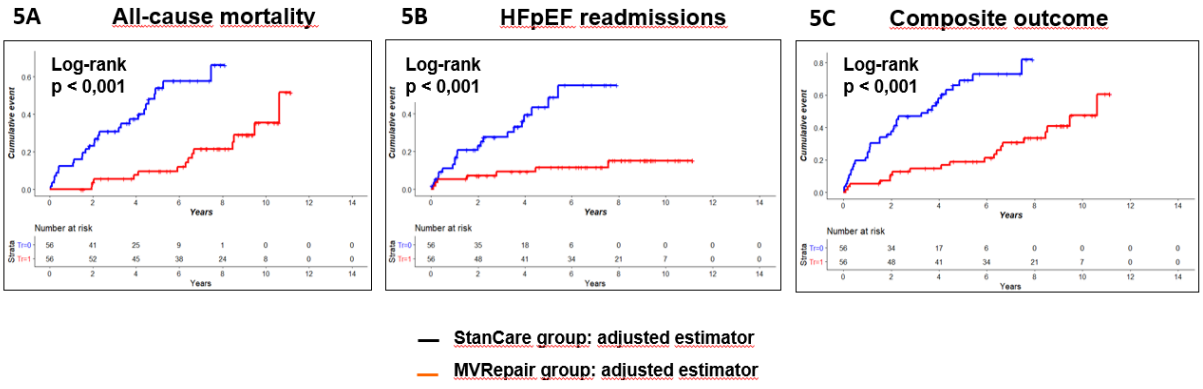

Chapter 18

Long-term outcome of minimally invasive mitral valve annuloplasty in disproportionate mitral regurgitation

Background:

Hypothetical concept of disproportionate secondary mitral regurgitation (SMR) has been recently introduced to facilitate patient's selection for mitral valve intervention. However, real world data validating this concept are unavailable.

Purpose:

To investigate long-term effects of minimally invasive mitral valve annuloplasty (MVA) in patients with disproportionate (dSMR) versus proportionate SMR.

Methods:

The study population consisted of 44 consecutive patients (age 67±9,5 years; 64% males) on guidelines-directed therapy with advanced heart failure (HF), reduced LV ejection fraction (EF) (32 ± 9,7%) and SMR undergoing isolated mini-invasive MVA. Patients with organic mitral regurgitation or concomitant myocardial revascularization were excluded. To assess SMR disproportionality, the PISA-derived effective regurgitant orifice area (EROA) and regurgitant volume (RV) were compared to the estimated EROA and RV by using Gorlin formula and pooled real-world data.

Results:

According to EROA, a total of 20 (46%) and 24 (54%) patients, respectively, had dSMR and proportionate SMR (pSMR). According to RV, a total of 17 (39%) had dSMR and 27 (61%) had pSMR. Patients with dSMR showed significantly lower prevalence of male gender and higher prevalence of diabetes mellitus than patients with pSMR (p<0,001). Moreover, we observed smaller LV end-diastolic volume, larger EROA and RV (both p<0,01) and higher LV EF (p=0,02) in the dSMR versus the pSMR group. Other baseline characteristics were similar. During median follow up of 4.39 y (IQR 2,2-9,96y), a total of 25 (56%) patients died from any cause while 21 (47%) individuals were readmitted for worsening HF. Patients with dSMR versus pSMR according to both EROA and RV showed significantly lower rate of HF readmissions (both p < 0.05) (Figure 1, 2). In Cox regression analysis combining clinical and imaging parameters, dSMR was the only independent predictor of HF readmissions (HR 0.20, 95% CI 0.07-0.60, p=0.004). In contrast, mortality was similar between dSMR and pSMR (NS) with

age as the only independent predictor (HR 1,10; 95% CI 1,03-1,18, p=0,003).

Conclusion:

Minimally invasive MVA is associated with significant reduction of HF readmissions in patients with dSMR versus pSMR while the mortality is similar. This suggests the importance of other parameters, i.e. age and degree of LV remodeling, to guide clinical management in SMR.

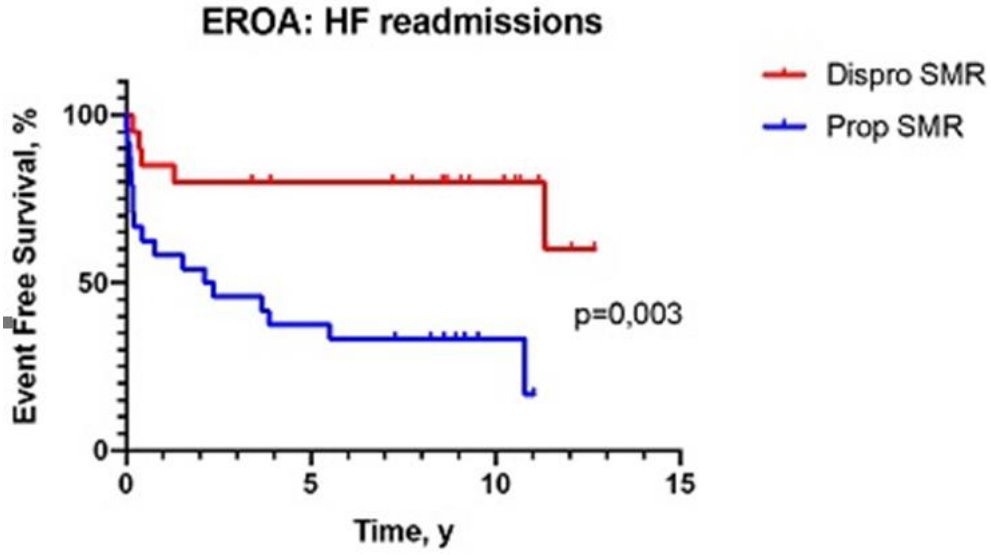

Figure 1

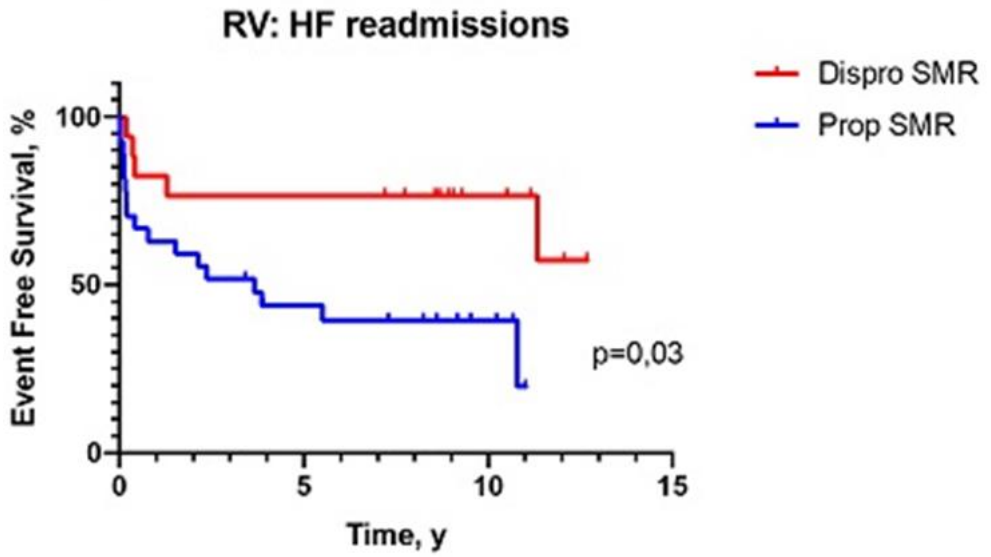

Figure 2

Part 4

Left ventricular performance projects

Chapter 19

Imaging of Myocardial Fibrosis and Its Functional Correlates in Aortic Stenosis: A Review and Clinical Potential

Abstract

Patients with severe aortic stenosis (AS) show progressive fibrotic changes in the myocardium, which may impair cardiac function and patient outcomes even after successful aortic valve replacement. Detection of patients who need an early operation remains a diagnostic challenge as myocardial functional changes may be subtle. In recent years, speckle tracking echocardiography (STE) and cardiac magnetic resonance mapping have been shown to provide complementary information for the assessment of left ventricular mechanics and identification of subtle damage by focal or diffuse myocardial fibrosis, respectively. Little is known, however, about how focal and diffuse myocardial fibrosis occurring in severe AS are related to measurable functional changes by echocardiography and to which extent both parameters have prognostic and diagnostic value. The aims of this review are to discuss the occurrence of focal and diffuse myocardial fibrosis in patients with severe AS and to explore their relation with myocardial function, determined by STE, as well as the prognostic and diagnostic potential of both parameters.

Introduction

The appropriate timing of aortic valve replacement (AVR) in asymptomatic patients with severe aortic stenosis (AS) remains challenging [1, 2]. Several of these patients show progressive fibrosis of the left ventricular (LV) myocardium, which may impair cardiac function and clinical outcomes even after successful AVR [3-5]. These individuals may benefit from early AVR before the development of irreversible myocardial fibrosis. The identification of myocardial damage at an early stage remains challenging. Indices provided by standard echocardiography show a low sensitivity as myocardial structural and functional changes may be subtle. Cardiac magnetic resonance (CMR) and speckle tracking echocardiography (STE) have been recently shown to provide complementary information in the assessment of myocardial fibrosis and its functional consequences, respectively [6-9]. However, information on the clinical value of the use of these cardiac imaging techniques in valvular heart disease is scant. Moreover, little is known about the relationship between myocardial fibrosis and measurable LV systolic function by STE. Accordingly, the aim of the present paper is to review the existing scientific literature on the relation between myocardial fibrosis and LV dysfunction and its possible impact on clinical outcomes in patients with AS.

Pathophysiology of LV Dysfunction in AS

Obstruction of the LV outflow tract due to AS is associated with a gradual increase in the LV afterload, which ultimately leads to the development of LV hypertrophy. Until recently, LV hypertrophy in AS had been considered a compensatory mechanism of the left ventricle muscle to face the high-pressure overload. Hypertrophied LV is capable of generating greater forces and higher pressures, while the increased wall thickness maintains a normal wall stress and sustains LV contractions. However, this original view of LV hypertrophy as a solely compensatory process has changed in the last decades. Focused papers have in fact demonstrated a significant relationship between LV hypertrophy and increased LV stiffness, diastolic dysfunction, and increased LV filling pressure [10-12]. Thanks to recent advances in cardiac imaging, a close association has been observed between the development of LV hypertrophy and myocardial fibrosis [13]. It has been postulated that, while originally being a compensatory process, LV hypertrophy ultimately becomes maladaptive and leads to myocyte apoptosis and diffuse interstitial myocardial fibrosis. These changes make the cardiac muscle less compliant and are responsible for the progression of LV hypertrophy towards overt heart failure [14-16]. Cardiac fibrocyte cells normally produce collagen to provide structural support for the heart. When overactivated in response to pressure overload, this process causes excessive accumulation of fibrosis and damages myocardial muscles. In histology, 2 types of myocardial fibrosis have been described: diffuse myocardial fibrosis (DMF), an early form of fibrosis believed to be reversible, and focal myocardial fibrosis (FMF), a later form that is irreversible [17]. AS is characterized by a significant increase in DMF, with a large variation in interindividual values [6, 17]. The extent of DMF has been shown to be an independent predictor of adverse clinical outcomes both before and after AVR as well [15, 18, 19]. Notably, patients with paradoxical low-flow low-gradient AS have a higher degree of myocardial fibrosis and LV longitudinal dysfunction than patients with normal-flow high-gradient AS [16, 20]. It has been hypothesized that not only a reduced LV cavity but also LV functional changes as a consequence of myocardial fibrosis contribute to a reduction in the LV stroke volume and production of a low transvalvular gradient, thus leading to a poor outcome [20, 21]. This suggests that DMF may be one of the critical mechanisms underlying the transition of LV hypertrophy to heart failure with an unfavorable clinical course. Accordingly, an accurate diagnostic technique, able to assess DMF or its functional correlates, may be crucial in patients experiencing AS.

Imaging of Diffuse Myocardial Fibrosis in AS

LV myocardial biopsy has been the gold standard for evaluation of DMF for a long time. However, the invasiveness, susceptibility to sampling errors, and inability to assess the fibrotic burden of the whole LV myocardium hamper its clinical utility in daily practice. CMR has emerged as a reference noninvasive method to assess both FMF and DMF [6, 15, 26]. Late gadolinium enhancement (LGE) at CMR is an established technique for assessing FMR (replacement fibrosis, scar). In symptomatic patients with severe AS, FMF occurs mainly in the subendocardial layer of the LV and its degree decreases from the base to the apex [15, 16]. Patients with a larger extent of FMF had a significantly lower freedom from cardiac

death at 10 years (42 ± 19% vs. 89 ± 6%, *p* = 0.002), with congestive heart failure being the most common cause of death [3]. In another study, the presence of FMF was significantly associated with poor postoperative outcomes [17]. However, FMF develops later in the disease course and, therefore, CMR-derived LGE is not sensitive enough to detect the early stage of myocardial damage. Accordingly, in our previous studies which used CMR-derived T1 mapping (CMR-T1), a total of 25% of patients had extensive (> 30%) DMF and a focal scar was not observed in any of them [23, 24]. Using the MOLLI sequence, CMR-T1 was in fact recently shown to allow accurate detection and quantification of DMF with excellent precision, reproducibility, and scan-rescan stability [22]. The T1 mapping technique measures the myocardial T1 relaxation time before or after contrast administration. An increased collagen content with expansion of the extracellular space causes prolongation of the native T1 relaxation time and an extracellular volume (ECV) fraction increase in comparison with normal myocardium. Both native T1 relaxation time and ECV have been significantly associated with DMF at myocardial histology [25-27]. We recently reported the high accuracy of both native T1 relaxation time with a cut-off value ≥1,010 ms (Ss = 90%, Sp = 73%, AUC = 0.82) and ECV with a cut-off value ≥0.315 (Ss = 80%, Sp = 90%, AUC = 0.85) to identify extensive (> 30%) DMF at histology [24]. Moreover, correlations between both native T1 and ECV with prognostic markers such as NT-pro-BNP or troponin have been reported [28, 29]. CMR-T1 has therefore been proposed as a promising technique to identify early structural changes in patients with AS. The advantages and limitations of CMR in AS assessment are shown in Table 1.

Table 1: Advantages and limitations of STE and CMR mapping in AS assessment

	STE	CMR mapping
Advantages	Low cost, more availability, rapid measurement offline after adequate image acquisition	Ability to image on any plane, full visualization of the myocardium, valve inflow/outflow tracts
	Non-Doppler, angle-independent, myocardial deformation evaluated in 2-D and 3-D, good reproducibility	Direct measurement of the valve area and characterization of the associated great vessel anatomy
	Objective quantification of myocardial systolic dynamics	Gold standard to quantify valve flow, cardiac volumes, and mass
	Recent data support GLS derived by STE as a sensitive marker to detect subclinical myocardial dysfunction in AS patients	CMR techniques such as LGE and T1 mapping are promising markers to detect focal and diffuse myocardial fibrosis, respectively
Limitations	Lower temporal resolution, need for good image quality	High cost, limited availability
	Tracking affected by out-of-plane cardiac motion	Adverse reaction to gadolinium
	Intervendor variability	Relative complexity of acquisitions, time-consuming image analysis

AS, aortic stenosis; CMR, cardiac magnetic resonance; DMF, diffuse myocardial fibrosis; ECV, extracellular volume; GLS, global longitudinal strain; LGE, late gadolinium enhancement; STE, speckle tracking echocardiography.

Imaging of Early LV Dysfunction in AS

LV ejection fraction by echocardiography is routinely used to assess LV systolic chamber function in patients with AS. However, increasing evidence demonstrates that irreversible myocardial damage might occur before changes in the ejection fraction become apparent [8]. It is noteworthy that AS-induced DMF starts at the subendocardial level, affecting mainly

longitudinal LV function. Since it is predominantly determined by radial function, the LV ejection fraction can be normal for a long time even in the presence of extensive subendocardial fibrosis [6, 15, 19]. Accordingly, the LV ejection fraction, i.e., the class I guideline recommendation for AVR, cannot be used for early risk stratification in asymptomatic AS patients. In contrast, STE-derived 2-D global longitudinal strain (GLS) is a validated and sensitive parameter to quantify LV longitudinal systolic function [8, 9]. Several studies have demonstrated a reduced magnitude of GLS in AS patients compared to controls despite a preserved LV ejection fraction [16-18, 31-33]. In asymptomatic AS, GLS at rest has been shown to be independently associated with development of symptoms, an abnormal exercise tolerance, a need for AVR, and mortality [34-37]. Furthermore, a magnitude of the longitudinal strain of LV basal segments below −13% has been found to be associated with a higher rate of cardiac events at follow-up [32]. It has also been shown that a GLS below −18% predicts an abnormal exercise response with a sensitivity of 68% and a specificity of 77% [38]. In another study, the assessment of GLS during exercise had a higher accuracy than the LV ejection fraction to detect latent LV systolic dysfunction [39]. Finally, even the decrease in circumferential strain may be a marker of advanced disease with unfavorable course, particularly when it is associated with a low-flow state in AS patients [40]. These findings suggest that both regional and GLS have a greater and earlier diagnostic power than the LV ejection fraction in this clinical setting [41]. The advantages and limitations of the STE-derived GLS assessment are summarized in Table 1.

Relationship between Myocardial Fibrosis and LV Systolic Function

Different kinds of observations have shown that GLS is a functional marker of myocardial fibrosis. First of all, GLS was found to be related to biomarkers of myocardial fibrosis such as those expressing calcification, collagen formation, or breakdown and inflammation [42, 43]. Several studies have also reported significant associations between LV systolic function and both FMF and DMF at CMR or myocardial histology [3, 14, 15, 18, 19, 24, 29, 44-46] (Table 2). Former studies have investigated the relationship between FMF and LV contractile function [14, 44, 45]. It has been shown that both the presence and the extent of FMF are inversely related to echocardiographic parameters such as relative wall thickness, LV fractional shortening, and ejection fraction and to STE-derived indices of LV myocardial function [18, 28, 44]. A GLS ≤−11.6% showed a sensitivity of 65% and a specificity of 75% to predict significant FMF (LGE > 10%) [43]. The majority of studies dealing with this issue have focused on DMF [15, 19, 24, 46, 47]. Of the conventional echocardiography-derived parameters, DMF seems to show a significant, though weak, correlation only with LV mass and the LV mass index [23, 24]. In contrast to FMF, none of the other conventional parameters including LV ejection fraction or aortic valve area had a significant association with the degree of DMF [39]. This emphasizes the need to use a highly sensitive technique to assess DMF. Recent investigations have reported a significant relationship among DMF at histology, the CMR-T1-derived native T1 relaxation time or ECV, and STE-derived deformation indices [15, 18, 45]. In our study, a GLS <–15% showed excellent accuracy to

predict extensive (> 30%) DMF (Fig. 1, 2) [23, 24]. Moreover, we observed a significant correlation between GLS during exercise and native T1 relaxation time (Fig. 3) [23, 24]. Finally, the native T1 relaxation time showed a high accuracy in predicting the limited LV contractile reserve [23, 24]. All together these results strongly support the concept that GLS could be considered as an accurate functional marker of DMF in AS.

Table 2: Studies showing relationships between myocardial fibrosis and LV systolic function assessed by different methods.

Study	Patients, *n*	MF type	Methods	Study results
Weidemann et al. [14]	85	FMF	LGE CMR, histology, GLS	The extent of histologically determined that cardiac fibrosis at baseline correlated closely with markers of LS function (all $p < 0.001$) but not global LVEF
Milano et al. [3]	99	FMF	Histology, LVEF	MF was inversely related to LV fractional shortening ($r = -0.64$, $p < 0.001$), LVEF ($r = -0.53$, $p < 0.001$), and LV relative wall thickness ($r = -0.70$, $p < 0.001$)
Treibel et al. [15]	133	FMF, DMF	LGE CMR, ECV, histology	High ECV was associated with worse LV remodeling, LVEF, and functional capacity
Dweck et al. [18]	143	MF	LGE CMR, LVEF	Midwall fibrosis has an incremental prognostic value to LVEF and may provide a useful method of risk stratification
Chin et al. [19]	166	FMF, DMF	LGE CMR, ECV, histology	Index ECV demonstrated a good correlation with DMF on myocardial biopsies; there was evidence of increasing hypertrophy, myocardial injury, diastolic dysfunction, and LS dysfunction consistent with progressive LV decompensation (all $p < 0.05$)
Kockova et al. [24]	40	DMF	CMR T1, ECV, histology,	Both native T1 relaxation time with a cutoff value ≥1,010 ms and ECV with a cutoff value ≥0.32 showed a high accuracy in identifying severe (>30%) DMF Native T1 relaxation time showed a significant correlation with LV mass ($p < 0.01$)
Fabiani et al. [29]	36	MF	Histology, GLS	MF is associated with alterations of regional and GLS Plasmatic miRNA-21 is directly related to MF and associated with LV structural and functional impairment
Hoffmann et al. [44]	30	FMF	LGE CMR, GLS	There was a negative correlation between the amount of MF determined by LGE CMR and peak systolic longitudinal strain for the total LV ($r = -0.538$, $p = 0.007$)
Lee et al. [45]	80	DMF	CMR T1, GLS	Native T1 correlated significantly with GLS measured with 2-D STE ($r = 0.598$, $p < 0.001$)
Bull et al. [46]	109	DMF	CMR T1, histology	T1 values increased with greater LV mass indices and correlated with the degree of biopsy-quantified fibrosis ($r = 0.36$, $p = 0.008$)

LVEF, left ventricle ejection fraction; STE, speckle tracking echocardiography; GLS, global longitudinal strain; LS, longitudinal systolic; CMR, cardiac magnetic resonance; MF, nonspecific myocardial fibrosis; DMF, diffuse myocardial fibrosis; FMF, focal myocardial fibrosis; LGE, late gadolinium enhancement; ECV, extracellular volume.

Figure 1: Examples of resting 2-D GLS compared with the extent of DMF on myocardial histology. a Patient with a preserved magnitude of 2-D GLS (–21.1%) and a negligible extent of DMF (7.4%). b Patient with a reduced magnitude of 2-D GLS (–14.9%) and extensive DMF (31.2%). DMF, diffuse myocardial fibrosis; GLS, global longitudinal strain. The images are shown with permission from the research work group of the Cardiovascular Center Aalst (Belgium) [23, 24].

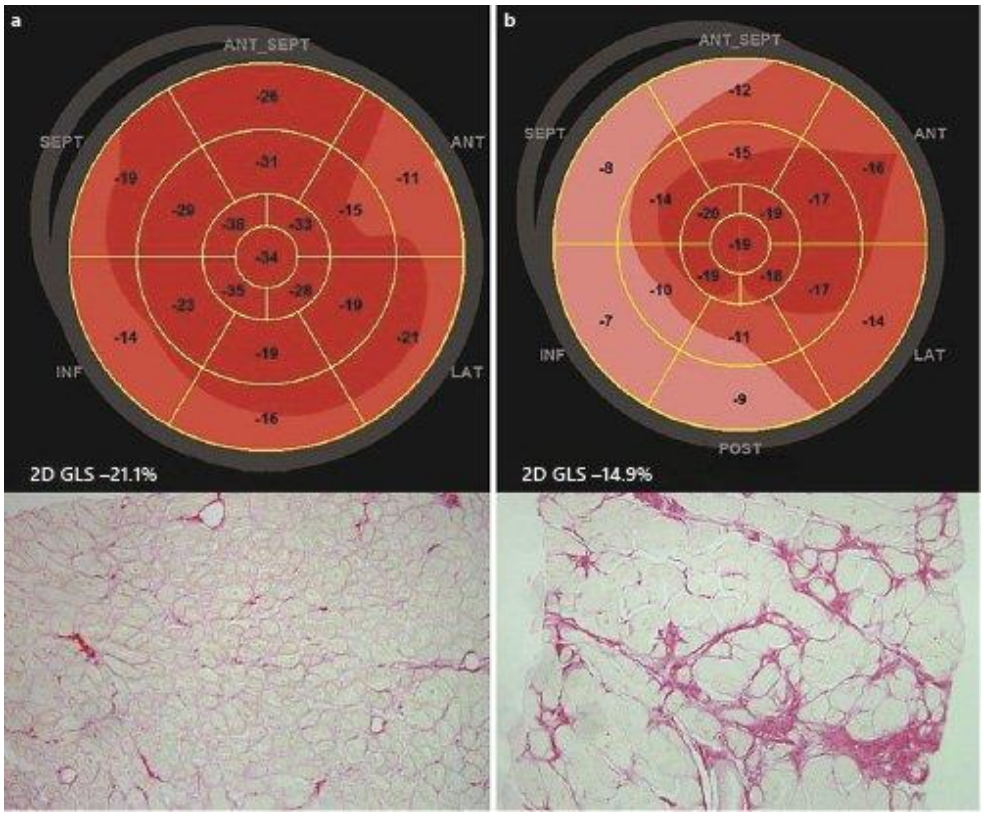

Figure 2: a Correlation between 2-D GLS and the percentage of myocardial collagen on myocardial histology. b Accuracy of resting 2-D GLS to identify extensive (> 30%) DMF on myocardial histology. DMF, diffuse myocardial fibrosis; GLS, global longitudinal strain. The images are shown w permission from the research work group of the Cardiovascular Center Aalst [23, 24].

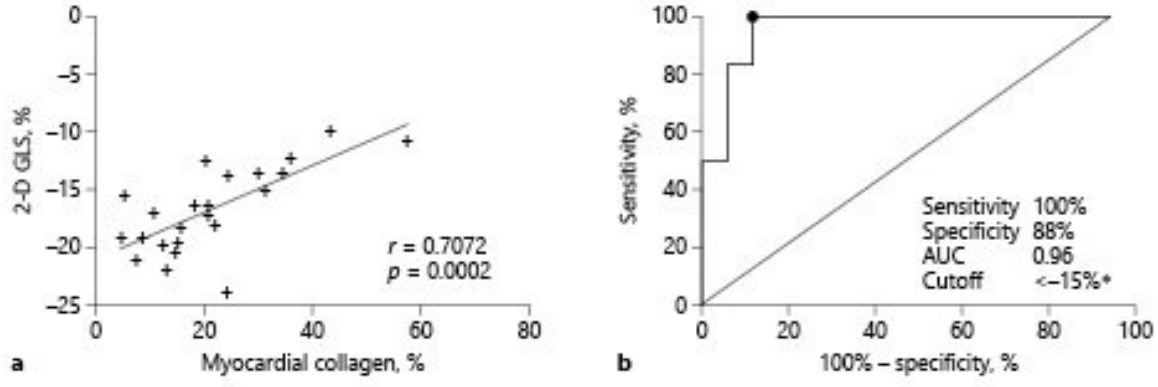

Figure 3: a Correlation between exercise-induced Δ 2-D GLS and native T1 relaxation time on a 3-T scan. b Accuracy of native T1 relaxation time on a 3-T scan to predict a reduced LV contractile reserve. DMF, diffuse myocardial fibrosis; GLS, global longitudinal strain. The images are shown with permission from research work group of the Cardiovascular Center Aalst [23, 24].

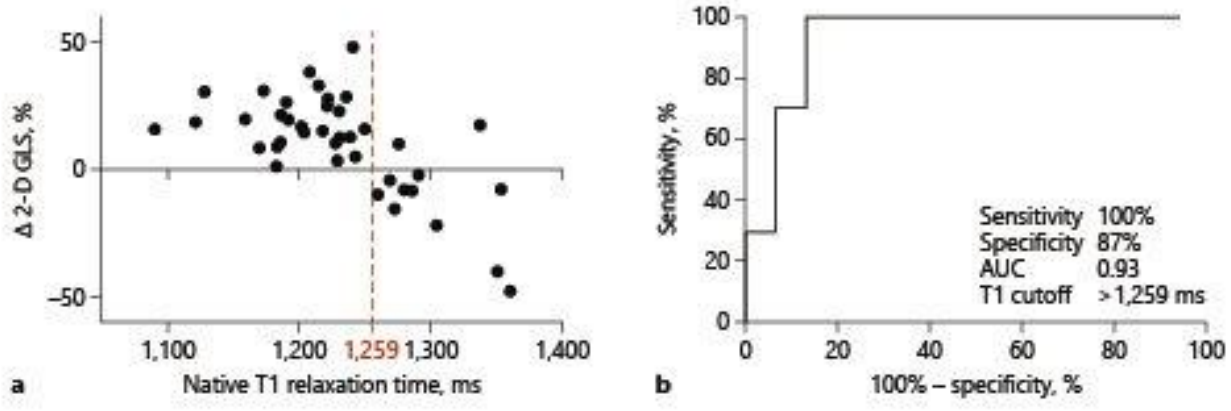

Limitations

Although both CMR-T1 and STE seem to have great clinical potential in various cardiovascular diseases, these techniques also have several limitations (Table 1). One of the major shortcomings of both methods is the great interscanner or intervendor variability of normal values. This disadvantage requires definition of normal values for each individual scanner or echo device when assessing healthy subjects. This procedure should be repeated after each major update of equipment or hardware. Other limitations need also mentioned. First of all, CMR-derived assessment of FMF using LGE has a wide interobserver variability, depends on the technical setting of the scanner, and does not allow detection of DMF [47]. The CMR-T1-derived T1 relaxation time and ECV are dependent on a specific CMR-T1 sequence, magnetic field strength, and homogeneity. In addition, there is a significant overlap between T1 mapping values in healthy and diseased myocardia, making the interpretation challenging [15, 30, 39, 40]. Other limitations of CMR include the limited availability of equipment and expertise, the associated high costs, and the need to administer a contrast agent. In contrast, echocardiography is more widely available, faster, and cheaper than CMR. GLS, a relatively operator-independent parameter, has a higher reproducibility compared to LV ejection fraction and other echocardiographic parameters of LV systolic function [6]. However, due to the difference among different vendors, the same software should be used in individual patients over time [48-50]. The load dependency of the STE-derived indices may represent another challenge for routine clinical use in AS, as they are largely influenced by both preload and afterload changes [27, 38, 39, 51].

According to recent published studies in animal models, STE-derived indices correlate strongly with pressure-volume loop-derived contractility indices and the STE-derived strain cannot predict load-independent contractility [51, 52]. Accordingly, to bypass this limitation in the chronic overloaded LV, the pressure-strain loop-based method is a promising tool for assessment and monitoring of myocardial function in patients with AS, but this method is still under investigation. Recently, novel techniques of derived tissue tracking by CMR cine acquisitions, such as CMR tagging and feature tracking, have provided a detailed characterization of LV global and regional contractility and reasonable agreement in the

assessment of myocardial deformation in patients with AS [53-55]. However, several technical limitations may affect quantitative results and lead to variability among different readers [56-58]. Finally, the role of tissue tracking by CMR in detection of the extent and types of myocardial fibrosis could be compromised by the coexistence of other comorbidities, such as hypertension, amyloidosis, or ischemic heart disease, which may play a role in disease phenotyping [59, 60]. Thus, the accuracy of these emerging methods for characterization of LV performance and quantification of myocardial fibrosis in patients with isolated AS or a concomitant comorbidity is still not adequately identified [61-64].

Conclusions

There is growing evidence that myocardial fibrosis plays an important role in the pathophysiology of AS and its complications. Recent advances in cardiac imaging technology allow noninvasive detection of myocardial fibrosis and the associated impairment of LV systolic function. It has been demonstrated that evaluation of myocardial fibrosis by CMR and of its functional consequences highlighted by GLS provides a more accurate assessment of early myocardial damage than LV ejection fraction. Despite its great diagnostic potential, further improvement of the current technology is needed to homogenize CMR-T1- and STE-derived indices across different vendors and scanners.

Future advances in noninvasive cardiac imaging might improve our understating of the interplay between myocardial fibrosis and LV function. The real clinical value of these parameters reflecting early myocardial injury needs to be validated in multicenter prospective studies. However, the encouraging results derived from different studies provide clinical perspectives on the use of these techniques for guidance in clinical decision making and improvement of the management of patients with AS.

Chapter 20

Cardiac Resynchronization Therapy Optimization: A Comprehensive Approach.

Abstract

Since the first report on biventricular pacing in 1994, cardiac resynchronization therapy (CRT) has become standard for patients with advanced heart failure (HF) and ventricular conduction delay. CRT improves myocardial function by resynchronizing myocardial contraction, which results in reverse left ventricular remodeling and improves symptoms and clinical outcomes. Despite the accelerated development of CRT device technology and its increased application in treating HF patients, almost one-third of these patients do not respond to the therapy or gain any clinical benefit from device implantation. Over the last decade, multiple cardiac imaging modalities have provided a deeper understanding of myocardial pathophysiology, thereby improving HF treatment management. However, the optimal strategy for improving the CRT response remains debatable. This article provides an updated overview of the electropathophysiology of myocardial dysfunction in ventricular conduction delay and the diagnostic approaches involving the use of multiple modalities.

Introduction

The selection of patients with heart failure (HF) and ventricular conduction delay who will benefit from cardiac resynchronization therapy (CRT) requires both an accurate assessment of myocardial structure and function and a clinical evaluation. According to recent guidelines, patients are considered candidates for CRT if they have HF symptoms of New York Heart Association (NYHA) class II–IV, left ventricular (LV) ejection fraction (LVEF) ≤35%, and a QRS duration >130 ms on ECG [1, 2]. Despite the selection criteria, 30–35% of patients are nonresponders with no symptomatic improvement or reverse LV remodeling [3, 4]. Some individuals even experience a clinical deterioration following device implantation [3, 4]. In addition, the parameters used to predict CRT response have not been significantly associated with an increase in the responder rate. Of note, left bundle branch block (LBBB) morphology, a QRS duration of ≥150 ms, and adequate coronary sinus anatomy have been most closely associated with a favorable CRT response [3, 4]; mitral valve regurgitation (MR), right ventricular (RV) dysfunction, and atrial fibrillation (AF) have been shown to have a negative impact on patient response [5–7]. However, all these conditions are highly and concomitantly prevalent in patients undergoing CRT, which makes their use challenging. Finally, CRT-device programing parameters that delay the progression of myocardial damage have largely remained unidentified.

During the past 2 decades, several echocardiography- or ECG-derived strategies to improve outcomes in CRT patients have been proposed [8, 9]. However, the exact cut-off values to predict the response and clinical outcome post-CRT are not yet established. Studies are ongoing to improve the role of imaging in predicting CRT response, including EuroCRT, a large European multicenter prospective observational study [10]. Furthermore, several CRT-device programming approaches for CRT optimization have emerged [11]. It has become clear that the development of appropriate strategies to improve CRT response will require answering a range of both clinical and technological questions. Novel bio-imaging markers associated with myocardial function restoration post-CRT are still to be identified and the available CRT technology needs further adjustment. This review provides an updated overview of the pathophysiology of myocardial dysfunction in ventricular conduction delay and the diagnostic approaches for CRT that involve multiple modalities.

Pathophysiology of Myocardial Dysfunction in LV Conduction Delay

Mechanical contractility is a consequence of electrical activation of the heart. Hence, early detection of abnormal electrical-mechanical patterns is important. LV systolic function is inversely correlated with electrical width and vector of the QRS complex on ECG. However, in clinical practice, electrical reverse remodeling is not always accompanied by mechanical reverse remodeling. Accordingly, CRT optimization focused on achieving the shortest-paced QRS duration has yielded mixed echocardiographic and clinical results [12]. The major determinants of myocardial performance and cardiac output are preload, myocardial contractility, and afterload [13, 14]. In the dyssynchrony pattern, the systolic stretching leaves the septum in a hibernation state characterized by switching metabolism from free fatty acids to glucose as the preferred substrate; consequently, the septum no longer contributes to LV systolic function and stroke volume [15]. The systolic stretching caused by LV free-wall shortening impairs the work performed by the septal segment and the septum absorbs energy. In LBBB, the abnormal early activation may result in a partial or complete loss of septum contribution. These changes in myocardial function can eventually lead to alterations in adrenergic density as well as the deterioration of the resting function, inotropic reserve, and function recovery [16]. In HF patients with ventricular conduction delay, impaired LV function has been considered a reversible process which can be improved by restoring the myocardial function using CRT, but the most favorable effects are observed in patients with significant myocardial viability and contractile reserve. Such patients have the potential to improve after CRT therapy [15, 17].

Patterns of Motion and Deformation

In patients with LBBB, the apex exhibits a pre-ejection rocking motion, due to active septal contraction unopposed by the absence of activation of LV lateral wall contraction. Many researchers suggested using visual markers of cardiac motion including apical rocking and septal flash as indicators for dyssynchrony [18, 19]. However, dyssynchrony is often subtle,

and so it cannot be quantified by visual assessment alone. Quantitative tools should be used to complement the visual description of myocardial deformation [18–20].

Since 2002, cardiac motion dyssynchrony has traditionally been described by parameters such as a septal-to-posterior wall motion delay ≥130 ms measured by M-mode echocardiography [21]. More recently, myocardial deformation has been assessed by imaging tools such as color-coded or pulsed tissue Doppler imaging, with dyssynchrony indicated by an opposing wall delay of ≥65 ms and a time to onset systolic velocity of ≥100 ms. However, these indicators have many technical limitations [21].

Speckle-tracking echocardiography (STE) imaging applied to routine echocardiography can provide higher accuracy to predict reverse LV remodeling post-CRT, as defined by an acute improvement of LVEF or LV end-systolic volume [22]. An acute increase in magnitude, together with more extensive synchronization of LV longitudinal strain, has been associated with improved functional capacity and NYHA class post-CRT [23]. This finding supports the use of STE to assess global longitudinal and radial strains to predict the extent of reverse LV remodeling following CRT (Fig. 1). Furthermore, regional strain patterns, particularly of septal strain, may help in assessing myocardial deformation in dyssynchronous HF, although the extent of acute change that predicts the clinical outcome remains unknown [24, 25].

Tissue tracking by using cine cardiac magnetic resonance (cine-CMR) has shown promising results, with recent studies reporting comparable results for radial dyssynchrony between cine-CMR and STE [26]; CMR can also be used to identify and evaluate mechanical dyssynchrony in patients with LBBB [27]. However, CMR has technical limitations in HF patients with LBBB, and further evaluation is needed before it can be clinically implemented [27]. Other limitations are high costs and limited availability.

Figure 1. Speckle-tracking echocardiography showing global longitudinal strain of the left ventricle in a patient with heart failure treated by cardiac resynchronization therapy (CRT). Left, before implanting CRT; right, echocardiography-based CRT optimization at 3 months.

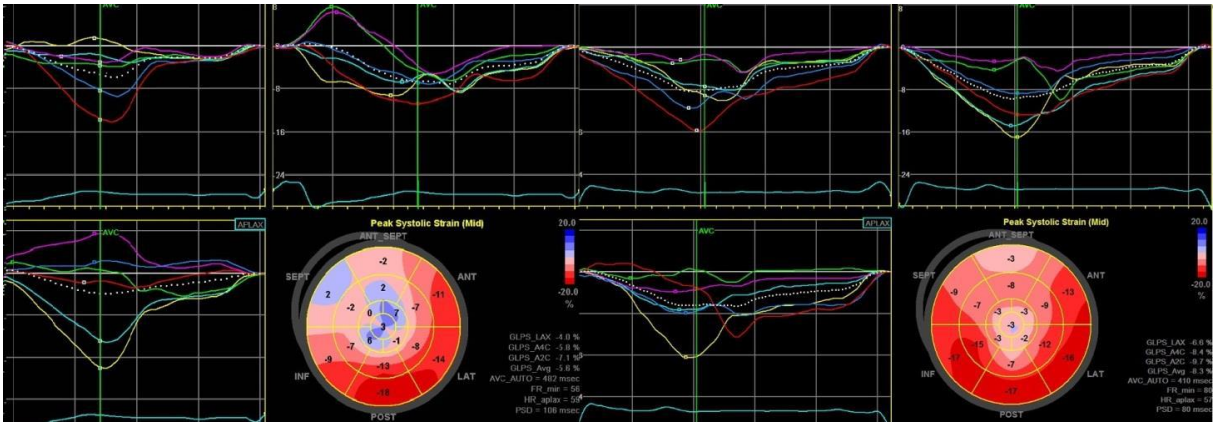

Myocardial Viability and Fibrosis

CRT response may be reduced by diminished myocardial viability associated with extensive LV scarring [28]. Moreover, CRT electrodes should not be placed in segments with scar tissue which can be easily identified on CMR [29, 30]. Patients with ischemic LV dysfunction and LBBB may have various amounts of focal myocardial fibrosis including in the interventricular septum. In contrast, patients with nonischemic cardiomyopathy may have a high level of diffuse fibrosis in the septum. A detailed description of regional myocardial fibrosis in dyssynchrony is needed (Fig. 2).

Figure 2. Examples of resting global longitudinal strain (GLS) of the left ventricle compared with the extent of hypoperfusion and the distribution of myocardial fibrosis in a patient with complete left bundle branch block and significantly reduced biventricular function. The figure A shows late gadolinium enhancement image by cardiac magnetic resonance imaging demonstrating a dense septal scar in the LV septal wall. Figure B shows scintigraphy image of a very large area of severe myocardial hypoperfusion and extensive transmural infarction in the septum. Figures C and D show a tissue Doppler image of myocardial dyssynchrony with a reduced magnitude of 2D GLS measured by speckle tracing echocardiography.

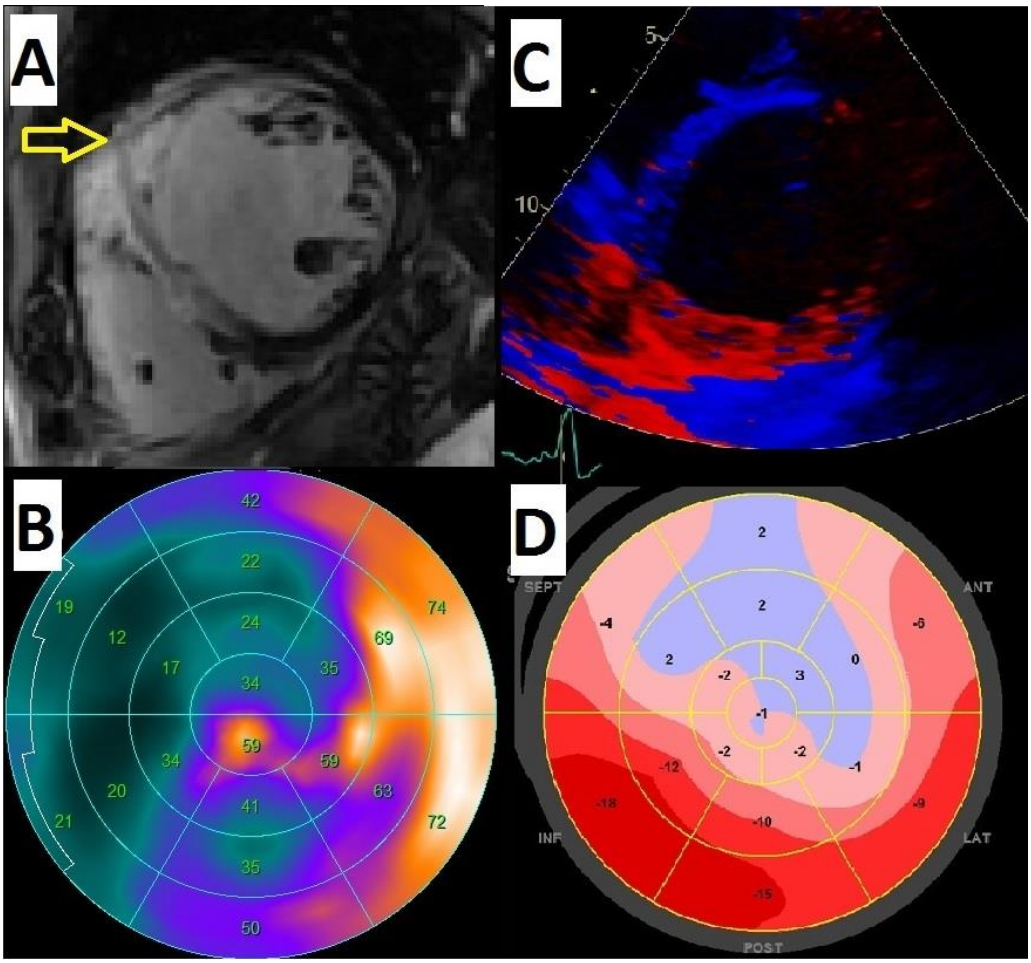

Advanced imaging methods, such as CMR, allow quantitative assessment of focal and diffuse myocardial fibrosis, but they do have limitations. CMR with late gadolinium enhancement, in particular, shows wide variation in quantifying focal fibrosis and cannot detect diffuse fibrosis [31, 32]. Other CMR approaches, such as T1 mapping and extracellular volume mapping, are affected by specific CMR techniques and magnetic field strength; they lack reference ranges, and there is a significant overlap of T1 mapping values of healthy and disease states [31, 32].

Using innovative imaging tools in this field is key to understanding the disease of the myocardial muscle, in terms of cellular and tissue abnormalities. Nuclear imaging, including positron emission tomography (PET), demonstrates reduced myocardial perfusion, glucose uptake, and oxidative metabolism in the septum of LBBB patients [33]. CRT partially normalizes these changes; therefore, measuring these radionuclide parameters may offer an improved approach for selecting CRT candidates [33]. Similarly, single-photon emission computed tomography (CT) supplies information about perfusion and is complementary to PET, which reflects metabolism. Radiation dose and the limited availability of PET may hamper routine clinical use. The advantages and limitations of different imaging techniques are summarized in Table 1.

Table 1. Cardiovascular imaging modalities and their advantages and limitations for the selection of cardiac resynchronization therapy candidates and optimizing therapy

	Advantages	Limitations
Echocardiography	Widely used; safe after CRT implantation	Relative subjectivity in quantifying myocardial dynamics
Tissue tracking with STE	Non-Doppler angle-independent evaluation of myocardial deformation evaluation; good reproducibility	Tracking affected by out-of-plane cardiac motion; intervendor variability
CMR mapping	More objective quantification of myocardial systolic dynamics; LGE and T1 mapping are promising methods for detecting focal and diffuse myocardial fibrosis, respectively	High cost and limited availability; adverse reaction to gadolinium; relative complexity of acquisition
Tissue tracking with CMR	Imaging possible in any plane; complete myocardium visualization	Technical limitations in HF patients with LBBB; time-consuming
PET and SPECT	Complementary assessment of CRT candidate with ischemic cardiomyopathy	Not widely used
X-ray fluoroscopy	Guides the position of the CRT leads by contrast injection through the right heart cavity and coronary sinus	Limited used for guiding the CRT leads during the procedure
MSCT	Visualization of cardiac veins; evaluation of structural remodeling in patients with inadequate echocardiographic images and CMR contraindications	High radiation dose

CRT, cardiac resynchronization therapy; STE, speckle-tracking echocardiography; CMR, cardiac magnetic resonance; LGE, late gadolinium enhancement; HF, heart failure; LBBB, left bundle branch block; PET, positron emission tomography; SPECT, single-photon emission computed tomography; MDCT, multidetector computed tomography.

Concomitant Cardiac Conditions

RV dysfunction is associated with a poor prognosis for HF patients [34]. Its role in CRT candidates is controversial. Impaired RV function pre-CRT, similar to HF, is associated with worse survival post-CRT [35], but a study has shown that CRT may improve RV function and

prognosis in patients with RV dysfunction [36]. A previous meta-analysis revealed that echocardiographic parameters of RV function do not predict CRT response-related changes in LVEF [37]. In contrast, a recent study reported that RV systolic dysfunction before CRT implantation could identify patients that might not benefit from CRT [38], and a prospective study concluded that CRT induces RV reverse remodeling and improves RV function with improved interventricular dependence [39]. Furthermore, a higher baseline RV-pulmonary artery (PA) coupling is associated with improved LV reverse remodeling and independently associated with a better prognosis [40]. Of note, the response to CRT was strongly associated with RV-PA coupling in both studies [39, 40]. However, using the RV-to-PA ratio as a potential guide for CRT in patients with diseases in whom RV failure predominates needs further investigation [39, 40].

Patients with congenital heart disease (CHD) may benefit from CRT. A recent German registry revealed that CRT can be used as an adjunct in the HF treatment of selected CHD patients [41]. A retrospective review on 20 patients with congenitally corrected transposition of the great arteries reported that CRT implantation is feasible, and that the long-term outcome is favorable but linked to systematic morphologic RV dysfunction in some patients [42]. Since most of the studies available are retrospective in nature, the impact of CRT on long-term prognosis in this population is still unknown [43, 44].

Several studies have shown that CRT improves secondary MR [45, 46]. A less favorable effect on MR has been reported in ischemic LV dysfunction with extensive scarring. Larger residual MR (an effective orifice area ≥0.20 cm2) following CRT has been associated with increased mortality and HF hospitalizations [47]. A recent study on 277 HF patients observed that MR severity at 6 months decreased in 48 (42%), remained stable in 42 (37%), and worsened in 24 (21%). Four-year adverse event rates were strongly predicted by the presence of at least moderate MR after, but not before, CRT [48]. On the other hand, a prospective study on 198 patients demonstrated that significant secondary MR after CRT is associated with higher morbidity and mortality, i.e., MR despite CRT provides important prognostic information beyond LV reverse remodeling [49].

Patients with AF before and after CRT represent a challenging cohort with insufficient data to guide clinical decision-making. CRT is recommended in patients with AF and ≤35 LVEF who meet the CRT criteria and in whom atrioventricular (AV) node ablation or pharmacological rate control allow approximately 100% ventricular pacing with CRT [50]. Although CRT improves some risk factors for AF, such as atrial size and LV systolic function, it does not reduce AF recurrence [50]. It is of note that, in HF with AF, pulmonary vein isolation may result in a better control of symptoms at short-term follow-up compared than CRT plus AV node ablation [51]. However, because the long-term effects remain unknown, pulmonary vein isolation should be only performed in selected individuals, taking into account patients' preference [51]. Further data on these patients are needed for developing a standardized approach.

Noncardiac Comorbidities

Many noncardiac comorbidities, e.g., diabetes, hypertension, dyslipidemia, obesity, respiratory insufficiency, and renal dysfunction, negatively affect myocardial contractility. CRT response is associated with the stabilization or improvement of renal function, which, in turn, is associated with lower mortality [52, 53]. A meta-analysis suggested that diabetic patients with advanced HF who received CRT exhibited higher total mortality than nondiabetic patients [54]. However, the increased mortality might have been attributable to insulin administration [54]. In the same context, another retrospective analysis showed that coexisting chronic obstructive pulmonary disease was an independent predictor of a nonresponse to CRT [55]. Cardiac disease but also noncardiac concomitant diseases should be taken into consideration when selecting patients for CRT [56].

Blood Biomarkers

Blood biomarkers, such as N-terminal pro-B-type natriuretic peptide (NT-proBNP), troponin T, galectin-3, and plasma miRNA-21, reflect myocardium status in HF patients. A reduction in the levels of these markers is mostly associated with a favorable CRT response [57]. The BIOCRT study revealed that NT-proBNP levels were 20% higher in the coronary sinus than in the peripheral veins [58]. It suggested that the coronary sinus sampling of HF biomarkers is more accurate than the peripheral venous blood sampling for predicting CRT outcomes. This study also reported that elevated galectin-3 levels during CRT device implantation are associated with the absence of MR improvement after CRT [59]. Thus, high circulating levels of these markers at the coronary sinus or peripheral veins may predict the CRT response and could therefore be used to document therapy success.

AV and Ventriculoventricular Time Interval

Prolonged PR intervals may impair AV mechanical coupling and the restoration of AV mechanical coupling with CRT may improve survival [60]. Following CRT implantation, AV interval optimization is of crucial importance to allow the completion of the atrial contribution to diastolic filling, resulting in the most favorable preload before ventricular contraction [61]. Several approaches have been used to optimize AV time interval. The CRT device's AV interval time setting has been considered the cornerstone for restoring myocardial contractility and performance. Doppler echocardiography-derived AV optimization has been associated with an improvement in both LV systolic function and presystolic MR. In brief, AV delay is programmed so that the end of atrial contraction is timed to coincide with the onset of ventricular contraction [62]. Because AV dyssynchrony is common and modifiable, Doppler echocardiography-guided AV optimization after CRT is warranted, particularly in nonresponders with a fused or truncated LV filling pattern [63]. The clinical efficacy of AV optimization has yet to be established.

The ventriculoventricular (VV) interval optimization, which is affected by LV and RV function, is rarely performed because it is time-consuming and without proven clinical benefit [64].

The methods used for VV optimization may be suboptimal to achieve adequate inter- and intraventricular resynchronization. However, it is still necessary to demonstrate its clinical relevance, and VV interval modification may be proposed to reduce the persistent asynchrony in nonresponders [65]. In summary, in clinical practice, CRT system parameters are often set empirically, using a shortened AV interval (90–120 ms) and simultaneous biventricular (BiV) pacing, with no further optimization during follow-up.

Mechanical Work

To assess myocardial reverse remodeling which directly affects the cardiac output following CRT, previously, studies used simple visual patterns such as apical rocking and septal flash to predict CRT responders [19, 20, 66]. Furthermore, it was reported that the correction of mechanical dyssynchrony versus the volumetric response was associated with long-term survival [67]. Recently, the calculation of the systolic dyssynchrony index (SDI) via real-time 3D echocardiography showed a superiority in the assessment of LV performance following CRT [68]. In contrast to a previous small study which reported that CRT optimization of interventricular delay by using SDI (vs. QRS width) assessment did not reveal any significant difference in terms of volumetric and clinical response at the 12-month follow-up [69], recent large studies have demonstrated that a more pronounced reduction in SDI immediately after CRT is independently associated with a superior long-term outcome [70], and that SDI derived by 3D speckle-area tracking shows a good correlation with the reduction of end-systolic volume post-CRT [71]. However, there is no consensus regarding the feasibility of using SDI to optimize the CRT.

Recently, noninvasive methods of calculating myocardial work have been applied in research into CRT response. Recent studies focused on mechanical dyssynchrony by taking into account the wasted and constructive myocardial work by means of strain analyses and hemodynamic data [72, 73]. The assessment of regional distribution to myocardial work based on different hemodynamics patterns can be used to determine the impact of elevated load on myocardial performance in HF patients that qualify for CRT [74]. These myocardial work indices derived from pressure-strain loops may provide comparable beneficial effects to serial evaluation of LV function (Fig. 3). At present, it is reasonable to consider these indices as semiquantitative novel tools to aid in guiding CRT, but caution is needed until this is validated in larger prospective studies. Echocardiography-based CRT candidate selection criteria and response optimization are summarized in Table 2.

Table 2. Echocardiography-based cardiac resynchronization therapy candidate selection criteria and response optimization

Method	Useful markers and parameters	Comments
M-mode	Septal-to-posterior wall motion delay of ≥130 ms	Limited assessment in clinical practice
B-mode	LVEF improvement and ≥15% ESV reduction relative to baseline	Standard parameters for predicting CRT response
Color-coded tissue Doppler imaging	Opposing wall delay of ≥65 ms	Many technical limitations
Pulsed tissue Doppler imaging	Delay in time-to-onset systolic velocity of ≥100 ms	Many limitations
Standard views based on LV mechanical description	Apical rocking and septal flash introduced to describe myocardial dyssynchrony	Relatively subjective
STE-derived strain	STE-derived regional strain and global strain measurement to determine LV reverse remodeling	Non-Doppler; angle-independent; underutilized
Area tracking using 3D STE	Area strain dyssynchrony index may enable a more objective quantification of myocardial systolic dynamics	Good image quality required for 3D STE; debatable STE standardization
Assessment of wasted myocardial work	Pressure-strain loops describe strain dispersion due to load change	Further investigation required

CRT, cardiac resynchronization therapy; LVEF, left ventricular ejection fraction; ESV, end-systolic volume; LV, left ventricular; STE, speckle-tracking echocardiography.

Figure 3. Regional and global myocardial work in a heart failure patient responded to cardiac resynchronization therapy (CRT). Left, before implanting CRT; regional work was inhomogeneous in the septal segments. Right, after 12 months; CRT increases the global myocardial work and this inhomogeneity disappeared.

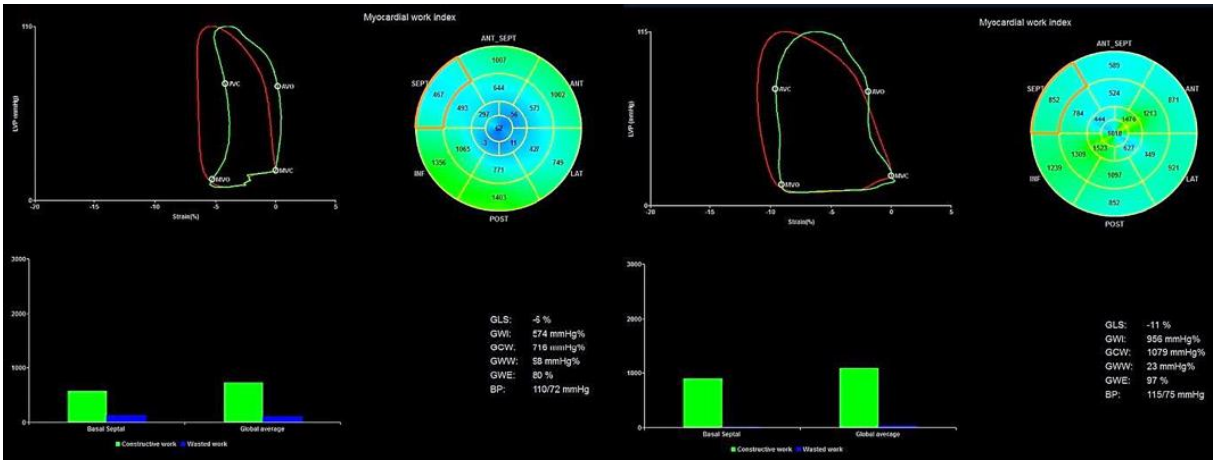

The assessment of BiV performance by echocardiography stress test should be interpreted to identify pathways and targets, so that we can address different phase patterns of ventricular remodeling and determine the degree of residual dyssynchrony, particularly in nonresponders [75]. On the other hand, cardiopulmonary exercise testing (CPET) might be helpful to assess the exercise capacity of HF patients with diseases of heart muscle and other significant diseases underestimated by rest evaluation [76]. Contemporary trends suggest that combined CPET imaging stress test can be implemented in clinical practice to assess BiV dysfunction in different HF phenotypes not detectable with rest evaluation [77].

Lead Placement

Optimal LV lead placement is crucial for a favorable CRT response. Accumulated evidence suggested that mechanical resynchronization is the primary mechanism underlying CRT response. Accordingly, in the absence of scarring, the optimal LV lead position is generally lateral or posterolateral because this is often the latest segment to contract in the presence of LBBB [78]. In contrast, apical pacing and pacing in a densely scarred region should be avoided when tailoring the therapy and to prevent adverse events [78, 79]. A multimodality complementary approach is ideal to establish the optimal CRT lead placement precisely. Multidetector CT can be used for preoperative mapping of the cardiac veins to assess the availability of suitable veins in potential target segments prior to CRT implantation [80]. The CRT outcome can be predicted by analyzing the 3D coronary sinus lead-tip trajectory and optimizing its placement based on advanced imaging methods [81]. Clearly, the introduction of a LV quadripolar lead provides multiple ways to pace the ventricle, and thus more options to avoid negative workload of the LV segments and achieve CRT optimization [82].

Maximal electric separation-guided placement of the RV defibrillation lead during CRT should be considered. The results of recent studies clearly show the benefits, in terms of reverse LV remodeling and clinical response, that can be obtained with optimization of the RV lead pacing position; the placement of the RV lead guided by maximal electric separation compared with standard apical placement not only improves cardiac function but can also reduce the risk of ventricular arrhythmia [83, 84]. For CRT therapy, multipoint pacing, guided by noninvasive hemodynamics, shows a positive LV structural remodeling [85]. However, many limitations in LV lead implantation, due to anatomical or other constraints, need to be considered. At present, permanent His-bundle pacing is a feasible alternative for patients in whom BiV pacing provided no clinical response. His-bundle pacing allows for the recruitment of BBB disease and ventricular activation in a more physiological fashion, specifically in patients with right BBB and those with AV block [86].

Emerging Optimization Strategy

A timely upgrade to BiV- or His-bundle-pacing devices needs to be considered in patients with CRT. A single-center registry involving 304 patients demonstrated that daily remote monitoring can be useful to identify the percentage of BiV pacing, and that a higher percentage improves the long-term prognosis after CRT [87]. Moreover, a recent study including 201 candidates reported that a higher percentage of BiV pacing (>98% at 6 months after CRT) is essential for patients to become superresponders [88]. However, the real clinical value of BiV-pacing percentage still needs to be validated in multicenter prospective studies.

Sensor-derived approaches are rapidly developing in modern cardiology. In CRT patients, the SonR sensor, which is embedded in the right atrial lead and picks up the intensity of the first heart sound as a surrogate for cardiac contractility, has been used to optimize CRT settings

[89]. It provides the opportunity for continuous reading of myocardial contractility during rest and exercise. This allows continuous adaptation of the AV and VV interval setting of the CRT device according to the instantaneous needs of the patient [89]. A comparative study demonstrated that automatic optimization with the SonR sensor is as effective as echo-guided optimization, allowing the primary efficacy end point to be met with a 35% significant reduction in HF hospitalization rates during long-term follow-up [90].

Advanced Computer Modeling

Advanced computer modeling combined with machine learning may provide mechanistic insights into CRT efficacy. It may help to solve complex problems involving big data by identifying interaction patterns among multiple variables in potential CRT candidates [91, 92]. The application of neural networks and deep learning in cardiovascular medicine plays a crucial role in imaging accusation, reconstruction, quantification, and analysis [93]. A combined deep-learning and deformable-model approach is a promising tool for fully automatic segmentation of the myocardium in CMR [94].

Thanks to recent advances in addictive manufacturing technologies, computational modeling and 3D printing have become powerful tools to describe the heart structure and the properties of myocardial tissue [95]. The encouraging results highlight clinical perspectives on the use of computer-aided design models to monitor myocardial structural changes following CRT and ultimately shape a favorable remodeling response to CRT [96, 97]. Certainly, the integration of imaging and nonimaging information based on computer-aided diagnosis will allow us to determine not only the effect of CRT on myocardial performance in the different phenotypes of cardiomyopathy, but also the long-term impact of CRT on the different symptomatic classes of HF patients [98].

Conclusion

CRT has shown significant clinical benefits for patients with HF refractory to medical therapy. Despite the great advances in CRT technology over the past decade, a further improvement of device settings, lead placement, and imaging tools is needed to improve the efficacy of CRT. However, programming devices to optimize the delivery of CRT remains challenging, and there are still no parameters that are routinely indicated to predict CRT response or guide CRT optimization. At present, multivariate computational models are promising tools used in the assessment of electromechanical dyssynchrony, and the latent strength of these methods to optimize CRT has shown great promise. Future advances will hopefully facilitate the identification of new bio-imaging markers and technical approaches to increase the responder rate. The promising results of pilot studies to date need to be validated in a multicenter, prospective setting.

Part 5

Case reports:

The role of imaging in valvular intervention

Chapter 21

Case report: transapical valve-in-valve implantation for bioprosthetic mitral valve failure secondary to endocarditis using a balloon-expandable device

Abstract:

Transcatheter valve-in-valve (VinV) implantation is an alternative to redo surgery for bioprosthetic valve failure in high risk patients. According to recent guidelines, transcatheter valve-in-valve procedure at a center with expertise in this procedure maybe considered in patients at high or greater risk for open surgical therapy. The patient with multi morbidities described here developed a rapid deterioration of mitral valve bioprosthesis function due to a serious condition of infective endocarditis. In this challenging case where there are no guidelines which specifically address the management, multidisciplinary team approach was the corner stone to make the right medical decision.

Case report:

A 71-year-old female patient with history of multi-morbidities was referred for bioprosthetic mitral valve repair. Her past medical history included hypertension, diabetes mellitus type 2, hyperlipidemia, cholecystectomy, lung fibrosis secondary to Tuberculosis and recurrent pulmonary infections. She also had history of coronary artery disease treated by bypass surgery (venous graft on left anterior descending artery) and postoperative moderate mitral valve insufficiency. Three years ago, the patient had symptomatic severe mitral valve insufficiency, so the mitral valve was replaced by mitral valve bioprosthesis type Mozaik size 27. Two years ago, the patient was admitted for diagnosis of hemolytic anemia and transient acute renal insufficiency and in April 2017, she was admitted to the hospital with diagnosis of bioprosthetic mitral valve endocarditis and blood cultures were positive for Streptococcus gallolyticus which has a high affinity for adherence to damaged endothelium. The patient was referred to our hospital for further evaluation after endocarditis treatment by antibiotics for a total duration of 6 weeks. On physical examination, a harsh systolic murmur in the heart apex radiating to the left sternal border. The transthoracic echocardiogram (TTE) revealed concentric hypertrophy with preserved systolic function (LVEF = 50%). The mitral valve bioprosthesis was shown with significant leaflets destruction and severe regurgitation. Transesophageal echocardiogram (TEE) showed a massive mobile mass on the atrial side of the bioprosthesis leaflet [figure 1]. Despite the treated endocarditis and the inflammatory biochemical parameters remained low, the pedunculated structure on atrial side of the mitral valve bioprosthesis, with comparison with previous studies, was unclear whether it corresponded to a vegetation or fibrotic mass. In August 2017, a successful PCI of the proximal and mid right coronary artery by implantation of drug eluting stent (Ultimaster 3.00

x 33 mm) had been performed and severe pulmonary artery hypertension and high elevated LV filling pressure had been reported. The patient was discharged on dual anti platelet therapy and prepared for bioprosthetic mitral valve repair after six weeks. After heart valve team discussion, she was prepared for percutaneous implantation of balloon expandable prosthetic valve. The patient was NYHA grade 4 before the procedure and arrived in shock on the table. The structural heart intervention team implanted the trans-apical 26-mm Sapien XT inside the mitral prosthesis by TEE guiding. After the procedure, the ECG showed sinus rhythm with normal AV conduction and the valve evaluation by fluoroscopy and echocardiography revealed trivial paravalvular leak and acceptable flow gradient through the implanted valve [figure 2]. A small mobile structure attached to the valve strut along the ventricular side was mentioned but without LVOT obstruction. After few days post-procedure, the patient was discharged and followed up in the heart valve clinic. She was perfectly fine a couple of weeks later at the outpatient clinic. Her clinical symptoms were improved (NYHA class 1) but TTE revealed an acute angle between the aortic and mitral valve planes with septal hypertrophy and with mild residual LVOT space. Although the device protrusion toward LVOT, the flow though LVOT was acceptable. The maximum and minimum gradient across the valve were 9.7 mmHg and 4.7 mmHg respectively [figure 3]. After 6 months follow-up, echocardiography showed no change in the structure and the function of the implanted valve with preserved myocardial function.

Discussion:

Prosthetic valve endocarditis (PVE) is the most severe form of infective endocarditis, accounting for 10-30% of all cases [1,2]. Risk factors for PVE include younger age, male sex, history of diabetes, presence of chronic obstructive pulmonary disease, post-procedure hemorrhage requiring transfusion, postoperative stroke, and moderate to severe residual valvular regurgitation [3,4]. Furthermore, the in-hospital mortality rate of PVE is 21-28.4% and preoperative status and complications are strongly related to the early mortality [3,4]. The indications for surgery in PVE include heart failure due to acute valve regurgitation, vegetation size, persistent sepsis and embolism [5,6]. A multidisciplinary team approach is essential for optimal treatment of patients with endocarditis and joint operating by appropriately trained surgeons should be considered for challenging cases [5,6]. Furthermore, follow up of the patient in comprehensive heart valve clinic/center has been shown to improve the clinical outcome [7,8].

A review of published data about VinV transcatheter implantation for failed bioprosthetic valves showed that most of the successful VinV implantations were for the treatment of failed degenerated bioprosthetic valve [9-12]. According to recent study including 61 patients, the transapical mitral VinV can be performed safely with results comparable with those of surgical therapy [13]. Only in a multicenter registry included 53 patients who suffered PVE after TAVI of 7944 patients, 6 underwent valve intervention (valve explanation and VinV procedure in 4 and 2 patients, respectively) [14]. According to a recent study, the

rate of PVE within the year following TAVI has ranged from 0.5 to 3.1% and patients who developed endocarditis had high rates of in-hospital mortality and 2-year mortality [15]. Regarding the technical aspects of VinV implantation, a recent published paper reported that VinV procedure can be associated with device malposition (including delayed malposition) and elevated post-procedural gradients (especially when performed inside small surgical valves) [16].

In our patient, the rapid deterioration of mitral valve bioprosthesis malfunction was mentioned by echocardiography secondary to PVE although multiple antibiotics treatment. After completion of the antibiotic treatment and verification of the absence of persistent infection, valve-in-valve procedure was selected for the treatment of severe mitral bioprosthetic regurgitation even though the residual vegetation on the destroyed valve. Optimal positioning of the transcatheter valve was achieved with rapid ventricular pacing immediately prior to valve deployment. TEE was used during the procedure to optimize the implanted valve position and to rule out LVOT obstruction or any residual post-procedural regurgitation which increases the risk of endocarditis recurrence. Although our consider of the technical aspects of this procedure, the meticulous evaluation of patient anatomy and the careful device selection, the 1-month post-procedural echocardiography revealed delayed malposition and elevated post-procedural gradients, that will have potential effect on device durability and increase the risk of the embolization. On the other hand, the existence of infected tissues and masses without surgical debridement increases the risk of endocarditis recurrence as well.

Conclusion:

Treatment of PVE remains a challenge and early diagnosis with a multidisciplinary team approach is essential to improve outcomes. This case report highlights that although the valve in valve procedure is not the optimal treatment for patients with failed valve bioprosthesis secondary to endocarditis, it probably remains a reasonable alternative for high surgical risk patients.

Figure 1: Pre-procedure 2D and 3D TEE showed a massive vegetation on the atrial side of the mitral bioprosthesis leaflet with severe regurgitation.

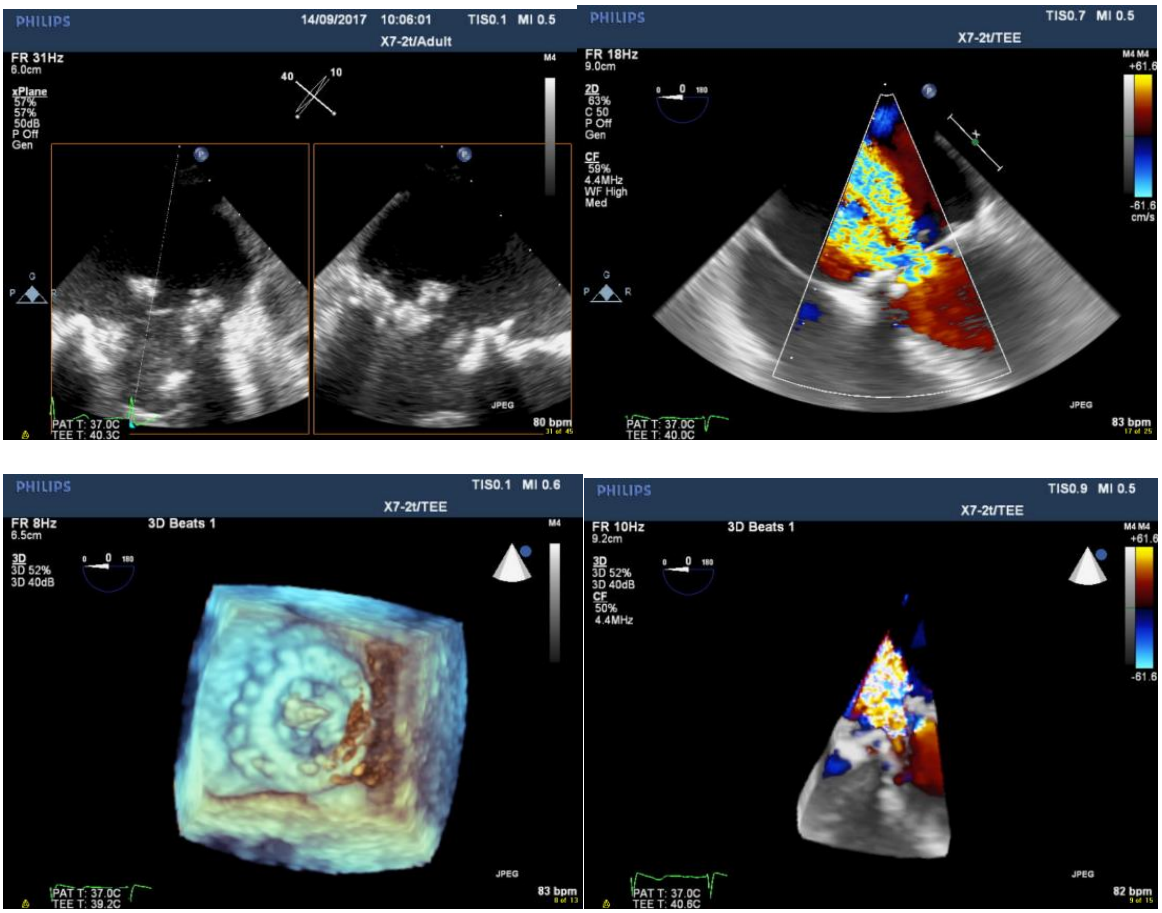

Figure 2: Transcatheter implantation of a 26-mm SAPIEN XT prosthesis in a failed mitral bioprosthesis. Via a transapical route, the SAPIEN XT prosthesis is positioned and deployment inside the mitral bioprosthesis.

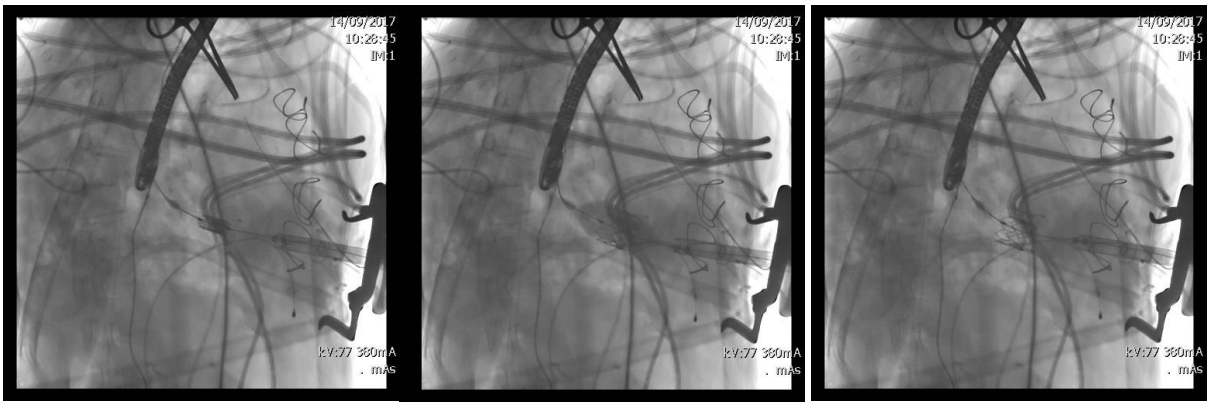

Figure 3: 3-month post-procedure TTE showed 26-mm Sapien XT inside the mitral prosthesis with maximum and mean gradient 9.3 and 4.7 mmHg respectively. It revealed an acute angle between the aortic and mitral valve planes with septal hypertrophy and with mild residual LVOT space.

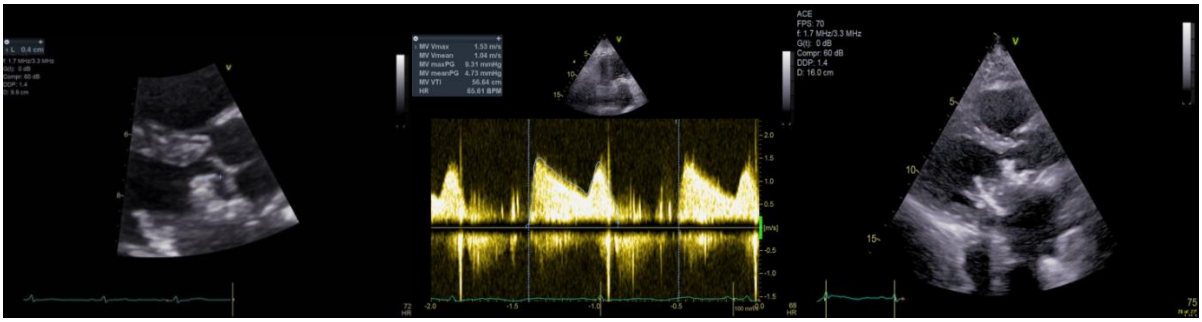

Chapter 22

Transfemoral TAVI valve-in-valve for xenograft valve failure of valved dacron conduit: imaging-based case report

Background:

Patients undergoing a root replacement with a xenograft aortic valve conduit may require a re-operation due to the structural deterioration of the bioprosthesis. Bioprosthetic heart valve failure represents a particularly serious complicated case to treat by redo surgery. Valve-in-valve (VIV) transcatheter aortic valve implantation (TAVI) is an alternative to surgery for patients with surgical high risk.

Clinical presentation:

A 83 year old female patient, with medical history of hypertension and hyperlipidemia, had undergone in 2002 surgical implantation of aortic Dacron conduit with a stented porcine xenograft valve (type Shellhigh 27) and re-implantation of coronary arteries. She was referred for evaluation of her functional deterioration of daily life physical abilities during the last year. She was admitted to the hospital with progressive dyspnea (functional NYHA class 4/4). A Grade 3-4/6 diastolic and systolic murmurs were heard over the area of the conduit valve. Electrocardiography showed left ventricular hypertrophy. Chest X-ray showed cardiomegaly with increased pulmonary venous congestion. In trans-thoracic echocardiography, the left ventricle (LV) showed concentric hypertrophy with preserved systolic function (EF:50%, GLS: -16.4), no regional wall motion abnormalities. The bioprosthetic valve was shown with degenerative significantly thickened cusps and with severe eccentric regurgitation. The maximum aortic gradient was 20 mmHg and the mean gradient was 10 mmHg (Figure 1). The patient was referred to TEE that showed the bioprosthetic leaflets were degenerated with pannus growth over prolapsed leaflet with perivalvular eccentric severe regurgitation along the anterior mitral leaflet (figure 1). Pre-procedure computed tomography (CT) revealed focal ectasia in the wall of the aortic arch (about 3.5 cm distal to the left subclavian artery) with a type B aortic dissection characterized by an interruption of the intima over a length of 27 mm and formation of a false lumen with a length of 39 mm and a thickness of 17 mm (figure 2). Coronary angiography revealed atherosclerotic coronary arteries with mild stenosis in the mid and distal right coronary artery with preserved fractional flow reserve (FFR:0.95). After heart team discussion, trans-catheter implantation of new prosthetic valve across femoral artery was indicated. The TAVI team suggested Edwards SAPIEN 3 as the delivery system of relatively low profile seems particularly suitable for use on a transfemoral route in this patient. The Sapien 3 valve and related delivery system were smoothly advanced through the right femoral artery up to the ascending aorta without problems. The bioprosthesis

Edwards SAPIEN 3 (size: 29 mm) valve was released during controlled ventricular pacing at 140 ppm inside the failed aortic bioprosthesis under TEE guidance (figure 3). After the valve was implanted, a significant leak was observed necessitating balloon post-dilation inside the new bioprosthesis. After post dilation, the paravalvular leak was trivial by echocardiography and angiography evaluation. On the sixth day after the operation, the patient was discharged uneventfully on a regimen of Aspirin and Clopidogrel. The patient was followed after the procedure, her clinical symptoms were improved and TTE showed preserved LV function and normal bioprosthetic valve function (Gmax: 15.9 mmHg, Gmean: 7.36 mmHg, EOR: 2.36 cm^2, EORI: 1.5 cm^2/m^2, trivial paravalvualr leak) (figure 4). After 6 months follow-up, echocardiography showed no change in the structure and the function of the implanted valve with preserved myocardial function.

Discussion:

Aortic root and valve replacement with a xenograft aortic valve conduit results in excellent hemodynamics but has limited durability [1]. The valve failure occurs for a variety of reasons, some of which are infectious, leaflet degeneration, and deterioration due to age [2]. Similar to other types of bioprosthesis valvular disease, the deterioration of the xenograft bioprosthesis of aortic conduit occurs much more frequently after a period of 12 to 15 years [3]. According to the recent valvular disease guidelines, the indications for surgery include the structural bioprosthesis degeneration with clinically relevant valve stenosis or/and valve regurgitation [4,5]. A multidisciplinary team approach is essential for optimal treatment of patients with bioprosthesis valve failure and joint operating by appropriately trained surgeons should be considered for challenging cases [4,5]. Furthermore, the follow up of the patient in comprehensive heart valve clinic/center has been shown to improve the clinical outcome [6,7].

Recently, the replacement of the degenerated aortic valve using trans-catheter valve-in-valve technique is an alternative to redo surgery for patients with a failing bioprosthetic aortic valve [8-11], but most of these cases were with a dominant stenotic valvular disease. With regard to safety of VIV procedure for stentless bioprosthesis, a previous study showed VIV TAVI after previous stentless aortic valve replacement is technically demanding but a safe and feasible approach. On the other hand, a recent published paper of multicenter propensity score analysis revealed patients with aortic bioprosthesis failure treated with either redo-SAVR or TAV-in-SAV have similar 30-day and one-year clinical outcomes [12]. Regarding the valvular replacement following the deterioration of a failed xenograft aortic valve conduit, recent papers reported cases of surgical aortic valve implantation following surgical deterioration of a biological valve composite conduit [13,14]. However, transfemoral TAVI valve-in-valve for xenograft valve failure of valved dacron conduit in adults had never been reported.

In this reported case of TAVI valve in valve for a failing xenograft bioprosthesis, the dominant valvular dysfunction was the valve insufficiency and the new implanted valve is inserted

through transfemoral access and the aortic conduit. During the stages of the assessment and management of the bioprosthesis failure, many anatomical and technical aspects had been emphasized using multi-modality imaging according to appropriateness criteria of European society of cardiology [14]. Before the procedure, the echocardiography was the reference imaging modality for the hemodynamic valvular assessment and the detection of its functional deterioration. While the multi-slice computed tomography (MSCT) can't determine the functional status of the failed valve, the severity of the valvular calcification description and the annulus size measurement were optimized by MSCT. The MSCT assessment of the vascular access, aortic angulation and conduit structure was very important to choose the femoral access and successful insert of the equipment through the conduit.

During the procedure, even the treatment of pure aortic regurgitation has carried the risk of the malposition or the embolization, the xenograft bioprosthesis profile and the leaflets characters were seemed sufficient to the new implanted bioprosthesis fixation to the annulus. Considering the difficult cross through the conduit, the Sapien 3 Commander System was used because of its low-profile and technically easy deployment. On the other hand, it is noticeable that the lack of correspondence between the stented part of the graft and the usual anatomical annulus we are used as marker to position and release the TAVI, in the case of the Shellhigh the stented segment is somewhat lower as compared to the normal position of the anatomic annulus, which has resulted in a slight lower TAVI implant. This later is currently performed with a ratio of 70:30 or even 80:20, while in this case we implanted with a ratio of 50:50 (meaning with this ration the portion of the deflated valve that goes on the aortic and ventricular side respectively). Although the risk of annulus rupture and coronary obstruction, a post-dilation balloon was inflated inside the new implanted bioprosthesis to optimize the valve development. TEE was the reference standard modality for the evaluation of the new implanted bioprosthesis position and its function as well. Furthermore, we depended on TEE in the assessment of the chronic dissection in the aortic arch directly after the procedure. Before the patient discharge, TTE assessment of the hemodynamic performance of the effective orifice aortic bioprosthesis was very important to exclude any patient-prosthetic mismatch, and sequentially, to guide the medical decision making during the follow-up.

Conclusion:

This present case shows the feasibility of implanting a transcatheter valve within xenograft aortic valve conduit, and it suggests that TAVI could be a valid therapeutic alternative to redo surgery in case of failed xenograft bioprosthesis. Furthermore, imaging-guided VIV TAVI appears to be a safe treatment option.

Figure 1: TTE and TEE showed the bioprosthetic valve with degenerative significantly thickened cusps and with severe eccentric regurgitation. The maximum aortic gradient was 20 mmHg and the mean gradient was 10 mmHg. The heart muscle function is reserved with global longitudinal strain -17.4%.

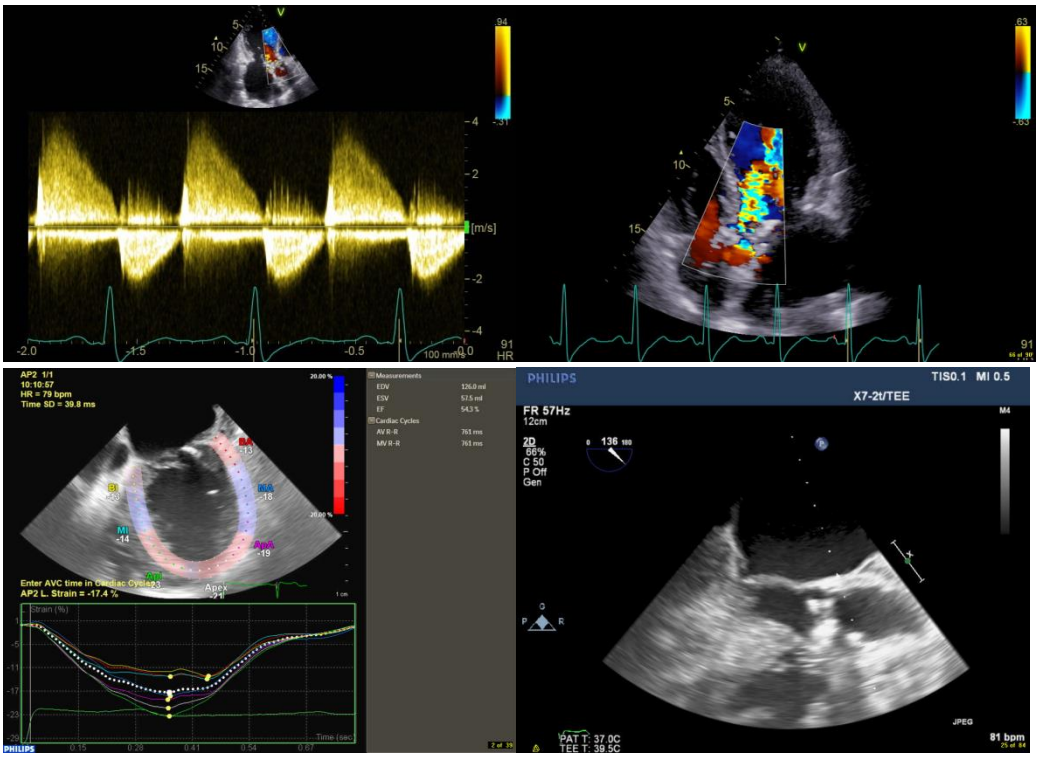

Figure 2: Computed tomography and TEE revealed focal ectasia in the wall of the aortic arch (about 3.5 cm distal to the left subclavian artery) with a type B aortic dissection characterized by an interruption of the intima over a length of 27 mm and formation of a false lumen with a length of 39 mm and a thickness of 17 mm.

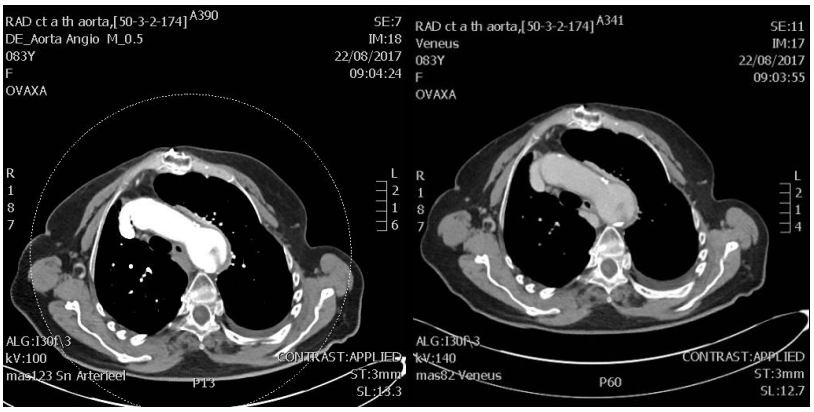

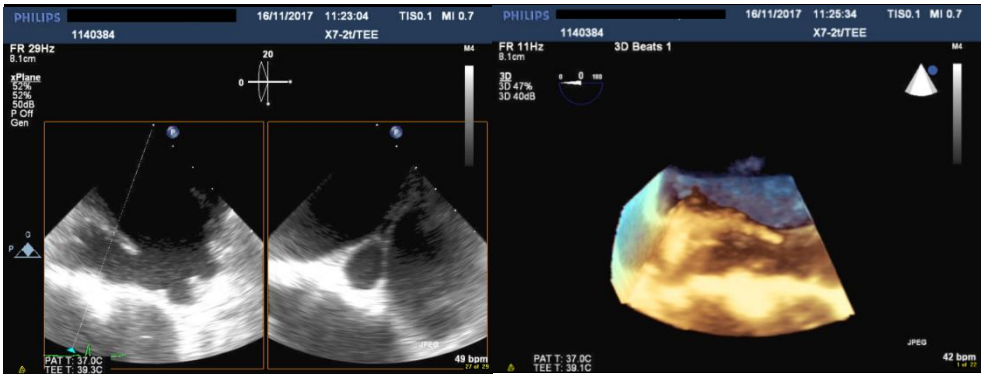

Figure 3: Transcatheter implantation of a SAPIEN XT prosthesis in xenograft aortic valve. During the procedure TEE showed the wire inside the left ventricle and the bioprosthesis aortic valve.

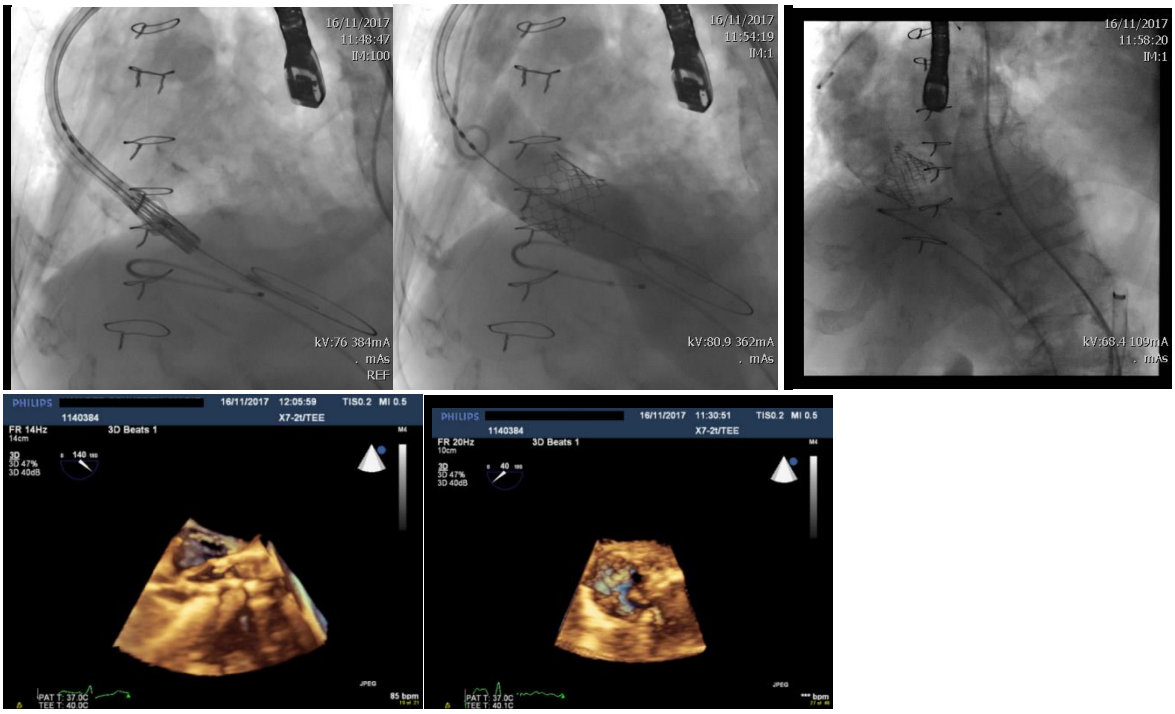

Figure 4: TTE showed preserved LV function and normal bioprosthetic valve function (Gmax: 15.9 mmHg, Gmean: 7.36 mmHg, EOR: 2.36 cm², EORI: 1.5 cm²/m², trivial paravalvualr leak).

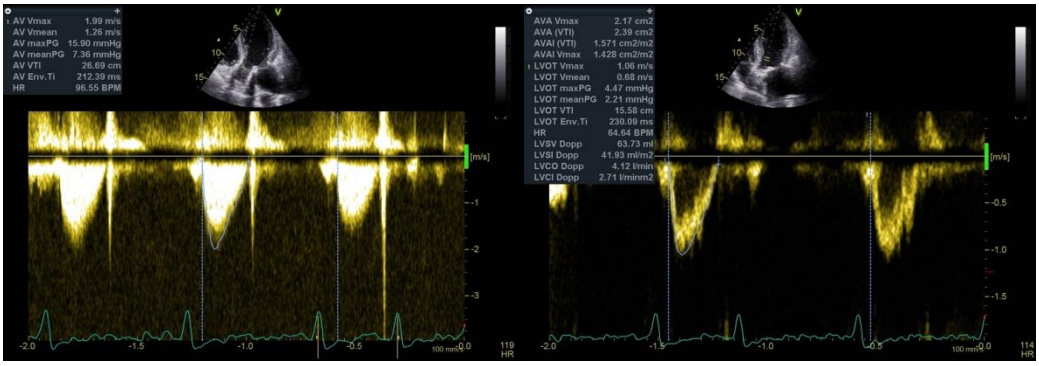

References

Introduction

1. Lüscher TF. Atrial fibrillation and arrhythmias: novel risk assessment, proper anticoagulation, and ablation. Eur Heart J. 2018 Apr 21;39(16):1317-1321.

2. Chugh SS, Havmoeller R, Narayanan K, Singh D, Rienstra M, Benjamin EJ, et al. Worldwide epidemiology of atrial fibrillation: a global burden of disease 2010 study. Circulation 2014;129:837–847.

3. Zoni-Berisso M, Lercari F, Carazza T, Domenicucci S. Epidemiology of atrial fibrillation: European perspective. Clin Epidemiol 2014;6:213–220.

4. Hill JA, Olson EN. Cardiac plasticity. N. Engl. J. Med. 2008 Mar 27;358(13):1370-80.

5. Ghzally Y, Gerasimon G. Treasure Island (FL): StatPearls Publishing; 2019-. 2019 Mar 1.

6. Calkins H, Kuck KH, Cappato R, Brugada J, Camm AJ, Chen SA, et al. 2012 HRS/EHRA/ECAS expert consensus statement on catheter and surgical ablation of atrial fibrillation: recommendations for patient selection, procedural techniques, patient management and follow-up, definitions, endpoints, and research trial design: a report of the Heart Rhythm Society (HRS) Task Force on Catheter and Surgical Ablation of Atrial Fibrillation. Heart Rhythm. 2012 Apr;9(4):632-696.e21.

7. Guichard JB, Nattel S. Atrial Cardiomyopathy: A Useful Notion in Cardiac Disease Management or a Passing Fad?. J Am Coll Cardiol. 2017 Aug 8;70(6):756-765.

8. Mondillo S, Galderisi M, Mele D, et al. Speckle-tracking echocardiography: a new technique for assessing myocardial function. J Ultrasound Med. 2011 Jan;30(1):71-83.

9. Cameli M, Caputo M, Mondillo S, et al. Feasibility and reference values of left atrial longitudinal strain imaging by two-dimensional speckle tracking. Cardiovasc ultrasound. 2009;7:6.

10. Quinones MA, Otto CM, Stoddard M, et al. Recommendations for quantification of Doppler echocardiography: a report from the Doppler Quantification Task Force of the Nomenclature and Standards Committee of the American Society of Echocardiography. J Am Soc Echocardiogr. 2002;15:167-84.

11. Hirose T, Kawasaki M, Tanaka R, et al. Left atrial function assessed by speckle tracking echocardiography as a predictor of newonset non-valvular atrial fibrillation: results from a prospective study in 580 adults. Eur Heart J Cardiovasc Imaging 2012;13:243–50.

12. Russo C, Jin Z, Sera F, Lee ES, Homma S, Rundek T, et al. Left ventricular systolic dysfunction by longitudinal strain is an independent predictor of incident atrial fibrillation: a community-based cohort study. Circ Cardiovasc Imaging 2015;8:e003520.

13. Olsen FJ, Christensen LM, Krieger DW, Højberg S, Høst N, Karlsen FM, et al. Relationship between left atrial strain, diastolic dysfunction and subclinical atrial fibrillation in patients with cryptogenic stroke: the SURPRISE echo substudy. Int J Cardiovasc Imaging. 2019 Oct 8.

14. Richter S, Di Biase L, Hindricks G. Atrial fibrillation ablation in heart failure. Eur Heart J. 2019 Feb 21;40(8):663-671.

15. Genovese D, Singh A, Volpato V, et al. Load Dependency of Left Atrial Strain in Normal Subjects. J Am Soc Echocardiogr. 2018 Nov;31(11):1221-1228.

16. Kawakami H, Ramkumar S, Pathan F, Wright L, Marwick TH. Use of echocardiography to stratify the risk of atrial fibrillation: comparison of left atrial and ventricular strain. Eur Heart J Cardiovasc Imaging. 2019 Oct 3.

17. Ocaranza MP, Bambs C, Salinas M, Matamala C, Garcia L, Troncoso R, et al. Early left atrial dysfunction is associated with suboptimal cardiovascular health. Echocardiography. 2019 Dec 18.

18. Carluccio E, Biagioli P, Mengoni A, et al. Left atrial reservoir function and outcome in heart failure with reduced ejection fraction. Circ Cardiovasc Imaging. 2018 Nov;11(11):e007696.

19. Andersen OS, Gude E, Skulstad H, Broch K, Andreassen AK, Smiseth OA et al. Peak left atrial strain is determined by left ventricular systolic function and filling pressure. Eur Heart J 2016;37(suppl_1):829, doi:10.1093/eurheartj/ehw433.

20. Daniel A Morris, Mudather Gailani, Amalia Vaz Pérez, et al. Left atrial systolic and diastolic dysfunction in heart failure with normal left ventricular ejection fraction. J Am Soc Echocardiogr . 2011 Jun;24(6):651-62.

21. Cameli M, Sparla S, Losito M, et al. Correlation of Left Atrial Strain and Doppler Measurements with Invasive Measurement of Left Ventricular End-Diastolic Pressure in Patients Stratified for Different Values of Ejection Fraction.

22. Jia-Li Fan, Bo Su, Xin Zhao, Bing-Yuan Zhou, Chang-Sheng Ma, Hai-Peng Wang, et al. Correlation of left atrial strain with left ventricular end-diastolic pressure in patients with normal left ventricular ejection fraction. Int J Cardiovasc Imaging. 2020 Sep;36(9):1659-1666.

23. Beltrami M, Palazzuoli A, Padeletti L, et al. The importance of integrated left atrial evaluation: From hypertension to heart failure with preserved ejection fraction. Int J Clin Pract. 2018 Feb;72(2).

24. Jens-Uwe Voigt, Marta Cvijic. 2- and 3-Dimensional Myocardial Strain in Cardiac Health and Disease. JACC Cardiovasc Imaging. 2019 Sep;12(9):1849-1863.

25. Sugumar H, Nanayakkara S, Prabhu S, Voskoboinik A, Kaye DM, Ling LH, Kistler PM. Pathophysiology of Atrial Fibrillation and Heart Failure: Dangerous Interactions. Cardiol Clin. 2019 May;37(2):131-138.

26. Soulat-Dufour L, Lang S, Ederhy S, Ancedy Y, Beraud AS, Adavane-Scheuble S, et al. Biatrial remodelling in atrial fibrillation: A three-dimensional and strain echocardiography insight. Arch Cardiovasc Dis. 2019 Oct;112(10):585-593.

27. Tsujiuchi M, Yamauchi T, Ebato M, Maezawa H, Nogi A, Ikeda N, et al. Prognostic Value of Left Atrial Size and Functional Indices Measured by 3-Dimensional Speckle-Tracking Analysis. Circ J. 2019 Mar 25;83(4):801-808.

28. Montserrat S, Gabrielli L, Bijnens B, Borràs R, Berruezo A, Poyatos S, et al. Left atrial deformation predicts success of first and second percutaneous atrial fibrillation ablation. Heart Rhythm. 2015;12:11–8.

29. Spethmann S, Stüer K, Diaz I, Althoff T, Hewing B, Baumann G, et al. Left atrial mechanics predict the success of pulmonary vein isolation in patients with atrial fibrillation. J Interv Card Electrophysiol. 2014;40:53–62.

30. Koca H, Demirtas A, Kaypakl O, et al. Decreased left atrial global longitudinal strain predicts the risk of atrial fibrillation recurrence after cryoablation in paroxysmal atrial fibrillation. J Interv Card Electrophysiol. 2020 Jun;58(1):51-59.

31. D'Ascenzo F, Corleto A, Biondi-Zoccai G, Anselmino M, Ferraris F, di Biase L, et al. Which are the most reliable predictors of recurrence of atrial fibrillation after transcatheter ablation?: A meta-analysis. Int J Cardiol 2013; 167: 1984 – 1989.

32. Left atrial structure and function predictors of recurrent fibrillation after catheter ablation: a systematic review and meta-analysis. Bajraktari G, Bytyçi I, Henein M. Clin Physiol Funct Imaging. 2020 Jan;40(1):1-13.

33. Motoki H, Negishi K, Kusunose K, et al. (2014) Global left atrial strain in the prediction of sinus rhythm maintenance after catheter ablation for atrial fibrillation. J Am Soc Echocardiogr 27(11):1184–1192.

34. Sarvari SI, Haugaa KH, Stokke TM, et al. (2016) Strain echocardiographic assessment of left atrial function predicts recurrence of atrial fibrillation. Eur Heart J Cardiovasc Imaging 17(6):660–667.

35. Hammerstingl C, Schwekendiek M, Momcilovic D, et al. (2012) Left atrial deformation imaging with ultrasound based two-dimensional speckle-tracking predicts the rate of

recurrence of paroxysmal and persistent atrial fibrillation after successful ablation procedures. J Cardiovasc Electrophysiol 23(3):247–255.

36. Sarvari S, Haugaa K, Stokke T, et al. Strain echocardiographic assessment of left atrial function predicts recurrence of atrial fibrillation. Eur Heart J Cardiovasc Imaging. 2016 Jun;17(6):660-7.

37. Sugimoto T, Robinet S, Dulgheru R, Bernard A, Ilardi F, Contu L, et al. Echocardiographic reference ranges for normal left atrial function parameters: results from the EACVI NORRE study. Eur Heart J Cardiovasc Imaging. 2018 Jun 1;19(6):630-638.

38. Pathan F, D'Elia N, Nolan MT, Marwick TH, Negishi K. Normal Ranges of Left Atrial Strain by Speckle-Tracking Echocardiography: A Systematic Review and Meta-Analysis. J Am Soc Echocardiogr. 2017 Jan;30(1):59-70.e8.

39. Brand A, Bathe M, Hübscher A, Baldenhofer G, Hättasch R, Seeland U, et al. Normative reference data, determinants, and clinical implications of right atrial reservoir function in women assessed by 2D speckle-tracking echocardiography. Echocardiography. 2018 Oct;35(10):1542-1549.

40. Wang Y, Li Z, Fei H, Yu Y, Ren S, Lin Q, et al. Left atrial strain reproducibility using vendor-dependent and vendor-independent software. Cardiovasc Ultrasound. 2019 May 15;17(1):9.

41. Rausch K, Shiino K, Putrino A, Lam AK, Scalia GM, Chan J. Reproducibility of global left atrial strain and strain rate between novice and expert using multi-vendor analysis software. Int J Cardiovasc Imaging. 2019 Mar;35(3):419-426.

Study background

1. Kirchhof P, Benussi S, Kotecha D, Ahlsson A, Atar D, Casadei B, et al. 2016 ESC Guidelines for the management of atrial fibrillation developed in collaboration with EACTS. Eur J Cardiothorac Surg. 2016 Nov;50(5):e1-e88. Epub 2016 Sep 23.

2. January CT, Wann LS, Alpert JS, Calkins H, Cigarroa JE, Cleveland JC Jr, et el. 2014 AHA/ACC/HRS guideline for the management of patients with atrial fibrillation: a report of the American College of Cardiology/American Heart Association Task Force on Practice Guidelines and the Heart Rhythm Society. J Am Coll Cardiol. 2014 Dec 2;64(21):e1-76

3. Kirchhof P, Calkins H. Catheter ablation in patients with persistent atrial fibrillation. Eur Heart J. 2017 Jan 1;38(1):20-26.

4. Andrew E Darby. Recurrent Atrial Fibrillation After Catheter Ablation: Considerations For Repeat Ablation And Strategies To Optimize Success. J Atr Fibrillation. 2016 Jun-Jul; 9(1): 1427.

5. Hakalahti A, Biancari F, Nielsen JC, Raatikainen MJ. Radiofrequency ablation vs. antiarrhythmic drug therapy as first line treatment of symptomatic atrial fibrillation: systematic review and meta-analysis. Europace. 2015 Mar;17(3):370-8.

6. Verma A, Champagne J, Sapp J, Essebag V, Novak P, Skanes A, et al. Discerning the incidence of symptomatic and asymptomatic episodes of atrial fibrillation before and after catheter ablation (DISCERN AF): a prospective, multicenter study. JAMA Intern Med 2013 ; 173 : 149 – 156.

7. Friberg L, Tabrizi F, Englund A. Catheter ablation for atrial fibrillation is associated with lower incidence of stroke and death: data from Swedish health registries. Eur Heart J. 2016 Aug;37(31):2478-87.

8. Lin YJ, Chao TF, Tsao HM, Chang SL, Lo LW, Chiang CE, et al. Successful catheter ablation reduces the risk of cardiovascular events in atrial fibrillation patients with CHA2DS2-VASc risk score of 1 and higher. Europace. 2013 May;15(5):676-84.

9. Bunch TJ, May HT, Bair TL, Johnson DL, Weiss JP, Crandall BG, et al. Increasing time between first diagnosis of atrial fibrillation and catheter ablation adversely affects long-term outcomes. Heart Rhythm. 2013 Sep;10(9):1257-62.

10. Lang RM, Badano LP, Mor-Avi V, Afilalo J, Armstrong A, Ernande L, et al. Recommendations for cardiac chamber quantification by echocardiography in adults: an update from the American Society of Echocardiography and the European Association of Cardiovascular Imaging. J Am Soc Echocardiogr. 2015 Jan;28(1):1-39.e14.

11. Lang RM, Badano LP, Tsang W, Adams DH, Agricola E, Buck T, et al. EAE/ASE recommendations for image acquisition and display using three-dimensional echocardiography. J Am Soc Echocardiogr. 2012 Jan;25(1):3-46.

12. Mor-Avi V, Lang RM, Badano LP, Belohlavek M, Cardim NM, Derumeaux G, et al. Current and evolving echocardiographic techniques for the quantitative evaluation of cardiac mechanics: ASE/EAE consensus statement on methodology and indications endorsed by the Japanese Society of Echocardiography. Eur J Echocardiogr. 2011 Mar;12(3):167-205.

13. Sareban M, Perz T, Macholz F, Reich B, Schmidt P, Fried S, et al. Reliability of echocardiographic speckle-tracking derived bi-atrial strain assessment under different hemodynamic conditions. Int J Cardiovasc Imaging. 2017 May 12. doi: 10.1007/s10554-017-1154-7.

14. Rosca M, Lancellotti P, Popescu BA, Pierard LA. Left atrial function: pathophysiology, echocardiographic assessment, and clinical applications. Heart 2011; 97:1982–9.

15. Madry W, Karolczak MA. Physiological basis in the assessment of myocardial mechanics using speckle-tracking echocardiography 2D. J Ultrason. 2016 Jun;16(65):135-44.

16. Olsen FJ. Assessment of left atrial mechanical function and synchrony in paroxysmal atrial fibrillation with two-dimensional speckle tracking echocardiography-utility of left atrial speckle tracking without left ventricular speckle tracking?. Echocardiography. 2017 Jul;34(7):1112.

17. Oikonomou E, Zografos T, Papamikroulis GA, Siasos G, Vogiatzi G, Theofilis P, et al. Biomarkers in atrial fibrillation and heart failure. Curr Med Chem. 2017 Aug 29.

18. Shang Z, Su D, Cong T, Sun Y, Liu Y, Chen N, et al. Assessment of left atrial mechanical function and synchrony in paroxysmal atrial fibrillation with two-dimensional speckle tracking echocardiography. Echocardiography. 2017 Feb;34(2):176-183.

19. Walters TE, Nisbet A, Morris GM, Tan G, Mearns M, Teo E, et al. Progression of atrial remodeling in patients with high-burden atrial fibrillation: Implications for early ablative intervention. Heart Rhythm. 2016 Feb;13(2):331-9.

20. Ma XX, Zhang YL, Hu B, Zhu MR, Jiang WJ, Wang M, et al. The usefulness of global left atrial strain for predicting atrial fibrillation recurrence after catheter ablation in patients with persistent and paroxysmal atrial fibrillation. Arch Cardiovasc Dis. 2017 Aug - Sep;110(8-9):447-455.

21. Nagueh SF, Smiseth OA, Appleton CP, Byrd BF 3rd, Dokainish H, Edvardsen T, et el. Recommendations for the Evaluation of Left Ventricular Diastolic Function by Echocardiography: An Update from the American Society of Echocardiography and the European Association of Cardiovascular Imaging. Eur Heart J Cardiovasc Imaging. 2016 Dec;17(12):1321-1360.

22. Cameli M, Lisi M, Mondillo S, Padeletti M, Ballo P, Tsioulpas C, et al. Left atrial longitudinal strain by speckle tracking echocardiography correlates well with left ventricular filling pressures in patients with heart failure. Cardiovasc Ultrasound 2010; 8:14.

Left atrial performance in patients undergoing catheter ablation

1. Kirchhof P, Benussi S, Kotecha D, et al. 2016 ESC Guidelines for the management of atrial fibrillation developed in collaboration with EACTS. Eur Heart J. 2016 Oct 7;37(38):2893-2962.

2. Rosca M, Lancellotti P, Popescu BA, Pierard LA. Left atrial function: pathophysiology, echocardiographic assessment, and clinical applications. Heart. 2011 Dec;97(23):1982-9.

3. Walters TE, Nisbet A, Morris GM, et al. Progression of atrial remodeling in patients with high-burden atrial fibrillation: Implications for early ablative intervention. Heart Rhythm. 2016 Feb;13(2):331-9.

4. Lang RM, Badano LP, Mor-Avi V, et al. Recommendations for cardiac chamber quantification by echocardiography in adults: an update from the American Society of

Echocardiography and the European Association of Cardiovascular Imaging. Eur Heart J Cardiovasc Imaging. 2016 Apr;17(4):412.

5. Todaro MC, Choudhuri I, Belohlavek M, et al. New echocardiographic techniques for evaluation of left atrial mechanics. Eur Heart J Cardiovasc Imaging. 2012 Dec;13(12):973-84.

6. Cameli M, Caputo M, Mondillo S, et al. Feasibility and reference values of left atrial longitudinal strain imaging by two-dimensional speckle tracking. Cardiovasc Ultrasound. 2009 Feb 8;7:6.

7. Donal E, Lip GY, Galderisi M, et al. EACVI/EHRA Expert Consensus Document on the role of multi-modality imaging for the evaluation of patients with atrial fibrillation. Eur Heart J Cardiovasc Imaging. 2016 Apr;17(4):355-83.

8. Hwang HJ, Choi EY, Rhee SJ, et al. Left atrial strain as predictor of successful outcomes in catheter ablation for atrial fibrillation: a two-dimensional myocardial imaging study. J Interv Card Electrophysiol. 2009 Nov;26(2):127-32.

9. Mirza M, Caracciolo G, Khan U, et al. Left atrial reservoir function predicts atrial fibrillation recurrence after catheter ablation: a two-dimensional speckle strain study. J Interv Card Electrophysiol. 2011 Sep;31(3):197-206.

10. Montserrat S, Gabrielli L, Bijnens B, et al. Left atrial deformation predicts success of first and second percutaneous atrial fibrillation ablation. Heart Rhythm. 2015 Jan;12(1):11-8.

11. Parwani AS, Morris DA, Blaschke F, et al. Left atrial strain predicts recurrence of atrial arrhythmias after catheter ablation of persistent atrial fibrillation. Open Heart. 2017 Apr 28;4(1):e000572.

12. Yasuda R, Murata M, Roberts R, et al. Left atrial strain is a powerful predictor of atrial fibrillation recurrence after catheter ablation: study of a heterogeneous population with sinus rhythm or atrial fibrillation. Eur Heart J Cardiovasc Imaging. 2015 Sep;16(9):1008-14.

13. Kuppahally SS, Akoum N, Burgon NS, et al. Left atrial strain and strain rate in patients with paroxysmal and persistent atrial fibrillation: relationship to left atrial structural remodeling detected by delayed-enhancement MRI. Circ Cardiovasc Imaging. 2010 May;3(3):231-9.

14. Pilichowska-Paszkiet E, Baran J, Sygitowicz G, et al. Noninvasive assessment of left atrial fibrosis. Correlation between echocardiography, biomarkers, and electroanatomical mapping. Echocardiography. 2018 Sep;35(9):1326-1334.

15. Habibi M, Lima JA, Khurram IM, et al. Association of left atrial function and left atrial enhancement in patients with atrial fibrillation: cardiac magnetic resonance study. Circ Cardiovasc Imaging. 2015 Feb;8(2):e002769.

16. Calkins H, Kuck KH, Cappato R, et al. 2012 HRS/EHRA/ECAS Expert Consensus Statement on Catheter and Surgical Ablation of Atrial Fibrillation: recommendations for patient selection, procedural techniques, patient management and follow-up, definitions, endpoints, and research trial design. Europace. 2012 Apr;14(4):528-606.

17. Badano LP, Kolias TJ, Muraru D, et al. Standardization of left atrial, right ventricular, and right atrial deformation imaging using two-dimensional speckle tracking echocardiography: a consensus document of the EACVI/ASE/Industry Task Force to standardize deformation imaging. Eur Heart J Cardiovasc Imaging. 2018 Jun 1;19(6):591-600.

18. Ciuffo L, Inoue YY, Tao S, et al. Mechanical dyssynchrony of the left atrium during sinus rhythm is associated with history of stroke in patients with atrial fibrillation. Eur Heart J Cardiovasc Imaging. 2018 Apr 1;19(4):433-441.

19. Vieira MJ, Teixeira R, Goncalves L, Gersh BJ. Left atrial mechanics: echocardiographic assessment and clinical implications. J Am Soc Echocardiogr. 2014 May;27(5):463-78.

20. Cichon M, Wieczorek J, Wybraniec M, et al. Left atrial function in obese and non-obese patients undergoing percutaneous pulmonary vein isolation. Heart Vessels. 2019 Feb;34(2):343-351.

21. Sugimoto T, Robinet S, Dulgheru R, et al. Echocardiographic reference ranges for normal left atrial function parameters: results from the EACVI NORRE study. Eur Heart J Cardiovasc Imaging. 2018 Jun 1;19(6):630-638.

22. Fung MJ, Thomas L, Leung DY. Left atrial function: Correlation with left ventricular function and contractile reserve in patients with hypertension. Echocardiography. 2018 Oct;35(10):1596-1605.

23. Wakami K, Ohte N, Asada K, et al. Correlation between left ventricular end-diastolic pressure and peak left atrial wall strain during left ventricular systole. J Am Soc Echocardiogr. 2009 Jul;22(7):847-51.

24. Sarvari SI, Haugaa KH, Stokke TM, et al. Strain echocardiographic assessment of left atrial function predicts recurrence of atrial fibrillation. Eur Heart J Cardiovasc Imaging. 2016 Jun;17(6):660-7.

25. Khan IA. Atrial stunning: basics and clinical considerations. Int J Cardiol. 2003 Dec;92(2-3):113-28.

26. Gasparovic H, Cikes M, Kopjar T, et al. Atrial apoptosis and fibrosis adversely affect atrial conduit, reservoir and contractile functions. Interact Cardiovasc Interact Cardiovasc Thorac Surg. 2014 Aug;19(2):223-30; discussion 230.

Effects of catheter ablation on left atrial performance in different types of atrial fibrillation

1. Sugumar H, Prabhu S, Voskoboinik A, Young S, Gutman SJ, Wong GR, et al. Atrial Remodeling Following Catheter Ablation for Atrial Fibrillation-Mediated Cardiomyopathy: Long-Term Follow-Up of CAMERA-MRI Study. JACC Clin Electrophysiol. 2019 Jun;5(6):681-688.

2. Toplisek J, Pernat A, Ruzic N, Robic B, Sinkovec M, Cvijic M, et al. Improvement of Atrial and Ventricular Remodeling with Low Atrial Fibrillation Burden after Hybrid Ablation of Persistent Atrial Fibrillation. Pacing Clin Electrophysiol. 2016 Mar;39(3):216-24.

3. Walters TE, Nisbet A, Morris GM, Tan G, Mearns M, Teo E, et al. Progression of atrial remodeling in patients with high-burden atrial fibrillation: Implications for early ablative intervention. Heart Rhythm. 2016 Feb;13(2):331-9.

4. Liżewska-Springer A, Dąbrowska-Kugacka A, Lewicka E, Królak T, Drelich Ł, Kozłowski D, et al. Echocardiographic assessment in patients with atrial fibrillation (AF) and normal systolic left ventricular function before and after catheter ablation: If AF begets AF, does pulmonary vein isolation terminate the vicious circle?. Cardiol J. 2019 Jan 31. doi: 10.5603/CJ.a2019.0004.

5. Wen S, Liu N, Bai R, Tang RB, Yu RH, Long DY, et al. Right atrial diameter and outcome of catheter ablation of atrial fibrillation. J Interv Card Electrophysiol. 2017 Aug;49(2):157-164.

6. Donal E, Galli E, Lederlin M, Martins R, Schnell F. Multimodality Imaging for Best Dealing With Patients in Atrial Arrhythmias. JACC Cardiovasc Imaging. 2019 Mar 8. pii: S1936-878X(19)30168-8.

7. Lang RM, Badano LP, Mor-Avi V, et al. Recommendations for cardiac chamber quantification by echocardiography in adults: an update from the American Society of Echocardiography and the European Association of Cardiovascular Imaging. Eur Heart J Cardiovasc Imaging. 2016 Apr;17(4):412.

8. Sareban M, Perz T, Macholz F, Reich B, Schmidt P, Fried S, et al. Reliability of echocardiographic speckle-tracking derived bi-atrial strain assessment under different hemodynamic conditions. Int J Cardiovasc Imaging. 2017 Nov;33(11):1685-1692.

9. Kuppahally SS, Akoum N, Burgon NS, Badger TJ, Kholmovski EG, Vijayakumar S, et al. Left atrial strain and strain rate in patients with paroxysmal and persistent atrial fibrillation: relationship to left atrial structural remodeling detected by delayed-enhancement MRI. Circ Cardiovasc Imaging. 2010 May;3(3):231-9.

10. Cameli M, Lisi M, Mondillo S, Padeletti M, Ballo P, Tsioulpas C, et al. Left atrial longitudinal strain by speckle tracking echocardiography correlates well with left ventricular filling pressures in patients with heart failure. Cardiovasc Ultrasound 2010; 8:14.

11. Calkins H, Kuck KH, Cappato R, Brugada J, Camm AJ, Chen SA, et al. 2012 HRS/EHRA/ECAS Expert Consensus Statement on Catheter and Surgical Ablation of Atrial Fibrillation: recommendations for patient selection, procedural techniques, patient management and follow-up, definitions, endpoints, and research trial design. Europace. 2012 Apr;14(4):528-606.

12. Badano LP, Kolias TJ, Muraru D, Abraham TP, Aurigemma G, Edvardsen T, et al. Standardization of left atrial, right ventricular, and right atrial deformation imaging using two-dimensional speckle tracking echocardiography: a consensus document of the EACVI/ASE/Industry Task Force to standardize deformation imaging. Eur Heart J Cardiovasc Imaging. 2018 Jun 1;19(6):591-600.

13. Park JW, Yu HT, Kim TH, Uhm JS, Joung B, Lee MH, et al. Atrial Fibrillation Catheter Ablation Increases the Left Atrial Pressure. Circ Arrhythm Electrophysiol. 2019 Apr;12(4):e007073.

14. Xie R, Yang Y, Cui W, Yin H, Zheng H, Zhang J, et al. Atorvastatin can ameliorate left atrial stunning induced by radiofrequency ablation for atrial fibrillation. Can J Physiol Pharmacol. 2017 Sep;95(9):985-992.

15. Škňouřil L, Havránek Š, Bulková V, Dorda M, Paleček T, Šimek J, et al. Disparity between two-dimensional echocardiographic and electroanatomic left and right atrial volumes in patients undergoing catheter ablation for long-standing persistent atrial fibrillation. Physiol Res. 2017 May 4;66(2):241-249.

16. Shang Z, Su D, Cong T, Sun Y, Liu Y, Chen N, et al. Assessment of left atrial mechanical function and synchrony in paroxysmal atrial fibrillation with two-dimensional speckle tracking echocardiography. Echocardiography. 2017 Feb;34(2):176-183.

17. Correia ETO, Barbetta LMDS, Silva OMPD, Mesquita ET. Left Atrial Stiffness: A Predictor of Atrial Fibrillation Recurrence after Radiofrequency Catheter Ablation - A Systematic Review and Meta-Analysis. Arq Bras Cardiol. 2019 May;112(5):501-508.

18. Gorter TM, van Melle JP, Rienstra M, Borlaug BA, Hummel YM, van Gelder IC, et al. Right Heart Dysfunction in Heart Failure With Preserved Ejection Fraction: The Impact of Atrial Fibrillation. J Card Fail. 2018 Mar;24(3):177-185.

19. Olsen FJ. Assessment of left atrial mechanical function and synchrony in paroxysmal atrial fibrillation with two-dimensional speckle tracking echocardiography-utility of left atrial speckle tracking without left ventricular speckle tracking?. Echocardiography. 2017 Jul;34(7):1112.

20. Thomas L, Marwick TH, Popescu BA, Donal E, Badano LP. Left Atrial Structure and Function, and Left Ventricular Diastolic Dysfunction: JACC State-of-the-Art Review. J Am Coll Cardiol. 2019 Apr 23;73(15):1961-1977.

21. Tops LF, Den Uijl DW, Delgado V, Marsan NA, Zeppenfeld K, Holman E, et al. Long-term improvement in left ventricular strain after successful catheter ablation for atrial fibrillation in patients with preserved left ventricular systolic function. Circ Arrhythm Electrophysiol. 2009 Jun;2(3):249-57.

22. Ollivier R, Donal E, Veillard D, Pavin D, Hamonic S, Daubert JC, et al. Early and late cardiac ventricular reverse remodeling after catheter ablation for lone paroxysmal atrial fibrillation. Ann Cardiol Angeiol (Paris). 2011 Feb;60(1):1-8.

23. Olsen FJ. Assessment of left atrial mechanical function and synchrony in paroxysmal atrial fibrillation with two-dimensional speckle tracking echocardiography-utility of left atrial speckle tracking without left ventricular speckle tracking?. Echocardiography. 2017 Jul;34(7):1112.

24. Packer M. Effect of catheter ablation on pre-existing abnormalities of left atrial systolic, diastolic, and neurohormonal functions in patients with chronic heart failure and atrial fibrillation. Eur Heart J. 2019 Jun 14;40(23):1873-1879.

25. You L, Yao L, Zhou B, Jin L, Yin H, Wu J, et al. Effects of different ablation strategies on long-term left atrial function in patients with paroxysmal atrial fibrillation: a single-blind randomized controlled trial. Sci Rep. 2019 May 22;9(1):7695.

26. Ollivier R, Donal E, Veillard D, Pavin D, Hamonic S, Daubert JC, et al. Early and late cardiac ventricular reverse remodeling after catheter ablation for lone paroxysmal atrial fibrillation. Ann Cardiol Angeiol (Paris). 2011 Feb;60(1):1-8.

Echocardiography markers of myocardial tissue deformation as independent predictors of sinus rhythm maintenance after catheter ablation for paroxysmal atrial fibrillation

1. Hakalahti A, Biancari F, Nielsen JC, Raatikainen MJ. Radiofrequency ablation vs. antiarrhythmic drug therapy as first line treatment of symptomatic atrial fibrillation: systematic review and meta-analysis. Europace. 2015 Mar;17(3):370-8.

2. Verma A, Champagne J, Sapp J, Essebag V, Novak P, Skanes A, et al. Discerning the incidence of symptomatic and asymptomatic episodes of atrial fibrillation before and after catheter ablation (DISCERN AF): a prospective, multicenter study. JAMA Intern Med 2013 ; 173 : 149 – 156.

3. Lin YJ, Chao TF, Tsao HM, Chang SL, Lo LW, Chiang CE, et al. Successful catheter ablation reduces the risk of cardiovascular events in atrial fibrillation patients with CHA2DS2-VASc risk score of 1 and higher. Europace. 2013 May;15(5):676-84.

4. Bunch TJ, May HT, Bair TL, Johnson DL, Weiss JP, Crandall BG, et al. Increasing time between first diagnosis of atrial fibrillation and catheter ablation adversely affects long-term outcomes. Heart Rhythm. 2013 Sep;10(9):1257-62.

5. Rosca M, Lancellotti P, Popescu BA, Pierard LA. Left atrial function: pathophysiology, echocardiographic assessment, and clinical applications. Heart 2011; 97:1982–9.

6. Olsen FJ. Assessment of left atrial mechanical function and synchrony in paroxysmal atrial fibrillation with two-dimensional speckle tracking echocardiography-utility of left atrial speckle tracking without left ventricular speckle tracking?. Echocardiography. 2017 Jul;34(7):1112.

7. Lang RM, Badano LP, Mor-Avi V, Afilalo J, Armstrong A, Ernande L, et al. Recommendations for cardiac chamber quantification by echocardiography in adults: an update from the American Society of Echocardiography and the European Association of Cardiovascular Imaging. J Am Soc Echocardiogr. 2015 Jan;28(1):1-39.e14.

8. Lang RM, Badano LP, Tsang W, Adams DH, Agricola E, Buck T, et al. EAE/ASE recommendations for image acquisition and display using three-dimensional echocardiography. J Am Soc Echocardiogr. 2012 Jan;25(1):3-46.

9. Sareban M, Perz T, Macholz F, Reich B, Schmidt P, Fried S, et al. Reliability of echocardiographic speckle-tracking derived bi-atrial strain assessment under different hemodynamic conditions. Int J Cardiovasc Imaging. 2017 May 12. doi: 10.1007/s10554-017-1154-7.

10. Badano LP, Kolias TJ, Muraru D, Abraham TP, Aurigemma G, Edvardsen T, et al. Standardization of left atrial, right ventricular, and right atrial deformation imaging using two-dimensional speckle tracking echocardiography: a consensus document of the EACVI/ASE/Industry Task Force to standardize deformation imaging. Eur Heart J Cardiovasc Imaging. 2018 Jun 1;19(6):591-600.

11. Shang Z, Su D, Cong T, Sun Y, Liu Y, Chen N, et al. Assessment of left atrial mechanical function and synchrony in paroxysmal atrial fibrillation with two-dimensional speckle tracking echocardiography. Echocardiography. 2017 Feb;34(2):176-183.

12. Walters TE, Nisbet A, Morris GM, Tan G, Mearns M, Teo E, et al. Progression of atrial remodeling in patients with high-burden atrial fibrillation: Implications for early ablative intervention. Heart Rhythm. 2016 Feb;13(2):331-9.

13. Cameli M, Lisi M, Mondillo S, Padeletti M, Ballo P, Tsioulpas C, et al. Left atrial longitudinal strain by speckle tracking echocardiography correlates well with left ventricular filling pressures in patients with heart failure. Cardiovasc Ultrasound 2010; 8:14.

14. Calkins H, Kuck KH, Cappato R, Brugada J, Camm AJ, Chen SA, et al. 2012 HRS/EHRA/ECAS Expert Consensus Statement on Catheter and Surgical Ablation of Atrial Fibrillation: recommendations for patient selection, procedural techniques, patient management and follow-up, definitions, endpoints, and research trial design. Europace. 2012 Apr;14(4):528-606.

15. Hammerstingl C, Schwekendiek M, Momcilovic D, Schueler R, Sinning JM, Schrickel JW, Mittmann-Braun E, Nickenig G, Lickfett L. Left atrial deformation imaging with ultrasound based two-dimensional speckle-tracking predicts the rate of recurrence of paroxysmal and persistent atrial fibrillation after successful ablation procedures. J Cardiovasc Electrophysiol. 2012 Mar;23(3):247-55.

16. Sarvari SI, Haugaa KH, Stokke TM, Ansari HZ, Leren IS, Hegbom F, Smiseth OA, Edvardsen T. Strain echocardiographic assessment of left atrial function predicts recurrence of atrial fibrillation. Eur Heart J Cardiovasc Imaging. 2016 Jun;17(6):660-7.

17. Ma XX, Zhang YL, Hu B, Zhu MR, Jiang WJ, Wang M, et al. The usefulness of global left atrial strain for predicting atrial fibrillation recurrence after catheter ablation in patients with persistent and paroxysmal atrial fibrillation. Arch Cardiovasc Dis. 2017 Aug - Sep;110(8-9):447-455.

18. Mirza M, Caracciolo G, Khan U, Mori N, Saha SK, Srivathsan K, et al. Left atrial reservoir function predicts atrial fibrillation recurrence after catheter ablation: a two-dimensional speckle strain study. J Interv Card Electrophysiol. 2011;31:197–206.

19. Motoki H, Negishi K, Kusunose K, Popović ZB, Bhargava M, Wazni OM, Saliba WI, Chung MK, Marwick TH, Klein AL. Global left atrial strain in the prediction of sinus rhythm maintenance after catheter ablation for atrial fibrillation. J Am Soc Echocardiogr. 2014 Nov;27(11):1184-92.

20. Kagawa Y, Fujii E, Fujita S, and Ito M. Association between left atrial reverse remodeling and maintenance of sinus rhythm after catheter ablation of persistent atrial fibrillation. Heart Vessels. 2020; 35(2): 239–245.

21. Machino-Ohtsuka T, Seo Y, Ishizu T, Yamamoto M, Hamada-Harimura Y, Machino T, et al. Relationships Between Maintenance of Sinus Rhythm and Clinical Outcomes in Patients With Heart Failure With Preserved Ejection Fraction and Atrial Fibrillation. J Cardiol . 2019 Sep;74(3):235-244.

22. Bajraktari G, Bytyçi I, Henein MY. Left Atrial Structure and Function Predictors of Recurrent Fibrillation After Catheter Ablation: A Systematic Review and Meta-Analysis. Clin Physiol Funct Imaging. 2020 Jan;40(1):1-13.

23. Miyazaki S, Kuwahara T, Kobori A, Takahashi Y, Takei A, Sato A, et al. Preprocedural predictors of atrial fibrillation recurrence following pulmonary vein antrum isolation in patients with paroxysmal atrial fibrillation: long-term follow-up results. J Cardiovasc Electrophysiol (2011); 22: 621-625.

24. Khan M, Memon M, Murad M, Vaduganathan M, Greene S, Hall M, et al. Left atrial function in heart failure with preserved ejection fraction: a systematic review and meta-analysis., Eur J Heart Fail. 22 (2020) 472–485. doi:10.1002/ejhf.1643.

25. Kawakami H, Ramkumar S, Pathan F, Wright L, Marwick T. Use of echocardiography to stratify the risk of atrial fibrillation: comparison of left atrial and ventricular strain. Eur Heart J Cardiovasc Imaging. 2020 Apr 1;21(4):399-407.

26. Russo C, Jin Z, Sera F, Lee ES, Homma S, Rundek T, et al. Left ventricular systolic dysfunction by longitudinal strain is an independent predictor of incident atrial fibrillation: a community-based cohort study. Circ Cardiovasc Imaging. 2015 Aug;8(8):e003520.

Heart failure with preserved ejection fraction or non-cardiac dyspnea in paroxysmal atrial fibrillation: the role of left atrial strain

1. Reddy YNV, Carter RE, Obokata M, Redfield MM, Borlaug BA. A Simple, Evidence-Based Approach to Help Guide Diagnosis of Heart Failure With Preserved Ejection Fraction. Circulation. 2018 Aug 28;138(9):861-870.

2. Pieske B, Tschöpe C, de Boer RA, Fraser AG, Anker SD, Donal E, Edelmann F, Fu M, Guazzi M, Lam CSP, Lancellotti P, Melenovsky V, Morris DA, Nagel E, Pieske-Kraigher E, Ponikowski P, Solomon SD, Vasan RS, Rutten FH, Voors AA, Ruschitzka F, Paulus WJ, Seferovic P, Filippatos G. How to diagnose heart failure with preserved ejection fraction: the HFA-PEFF diagnostic algorithm: a consensus recommendation from the Heart Failure Association (HFA) of the European Society of Cardiology (ESC). Eur Heart J. 2019 Oct 21;40(40):3297-3317.

3. Thomas L, Marwick T, Popescu B, Donal E, Badano L. Left atrial structure and function, and left ventricular diastolic dysfunction. J Am Coll Cardiol. 2019; 15:1961-1977.

4. Cleland JGF, Lyon AR, McDonagh T, McMurray JJV. The year in cardiology: heart failure. Eur Heart J. 2020 Jan 6. pii: ehz949. doi: 10.1093/eurheartj/ehz949.

5. Ponikowski P, Voors AA, Anker SD, Bueno H, Cleland JGF, Coats AJS, Falk V, González-Juanatey JR, Harjola VP, Jankowska EA, Jessup M, Linde C, Nihoyannopoulos P, Parissis JT, Pieske B, Riley JP, Rosano GMC, Ruilope LM, Ruschitzka F, Rutten FH, van der Meer P; ESC Scientific Document Group. 2016 ESC Guidelines for the diagnosis and treatment of acute and chronic heart failure: The Task Force for the diagnosis and treatment of acute and chronic heart failure of the European Society of Cardiology (ESC) developed with the special contribution of the Heart Failure Association (HFA) of the ESC. Eur Heart J. 2016 Jul 14;37(27):2129-2200.

6. Reddy YNV, Obokata M, Egbe A, Yang JH, Pislaru S, Lin G, Carter R, Borlaug BA. Left atrial strain and compliance in the diagnostic evaluation of heart failure with preserved ejection fraction. Eur J Heart Fail. 2019 Jul;21(7):891-900.

7. Carlisle MA, Fudim M, DeVore AD, Piccini JP. Heart Failure and Atrial Fibrillation, Like Fire and Fury. JACC Heart Fail. 2019 Jun;7(6):447-456.

8. Sugumar H, Nanayakkara S, Prabhu S, Voskoboinik A, Kaye DM, Ling LH, Kistler PM. Pathophysiology of Atrial Fibrillation and Heart Failure: Dangerous Interactions. Cardiol Clin. 2019 May;37(2):131-138.

9. Bisbal F, Baranchuk A, Braunwald E, Bayés de Luna A, Bayés-Genís A. Atrial Failure as a Clinical Entity. J Am Coll Cardiol. 2020. DOI: 10.1016/j.jacc.2019.11.013.

10. Patel RB, Alenezi F, Sun JL, Alhanti B, Vaduganathan M, Oh JK, Redfield MM, Butler J, Hernandez AF, Velazquez EJ, Shah SJ. Biomarker Profile of Left Atrial Myopathy in Heart Failure with Preserved Ejection Fraction: Insights from the RELAX Trial. J Card Fail. 2019 Dec 16.

11. Singh A, Addetia K, Maffessanti F, Mor-Avi V, Lang RM. LA Strain for Categorization of LV Diastolic Dysfunction. JACC Cardiovasc Imaging. 2017 Jul;10(7):735-743.

12. Reddy YNV, Borlaug BA, O'Connor CM, Gersh BJ. Novel approaches to the management of chronic systolic heart failure: future directions and unanswered questions. Eur Heart J. 2019 Jun 14. pii: ehz364.

13. Kurt M, Wang J, Torre-Amione G, Nagueh SF. Left atrial function in diastolic heart failure. Circ Cardiovasc Imaging. 2009 Jan;2(1):10-5.

14. Obokata M, Negishi K, Kurosawa K, Arima H, Tateno R, Ui G, Tange S, Arai M, Kurabayashi M. Incremental diagnostic value of la strain with leg lifts in heart failure with preserved ejection fraction. JACC Cardiovasc Imaging. 2013 Jul;6(7):749-58.

15. Nagy AI, Hage C, Merkely B, Donal E, Daubert JC, Linde C, Lund LH, Manouras A. Left atrial rather than left ventricular impaired mechanics are associated with the pro-fibrotic ST2 marker and outcomes in heart failure with preserved ejection fraction. J Intern Med. 2018 Apr;283(4):380-391.

16. Lang RM, Badano LP, Mor-Avi V, et al. Recommendations for cardiac chamber quantification by echocardiography in adults: an update from the American Society of Echocardiography and the European Association of Cardiovascular Imaging. Eur Heart J Cardiovasc Imaging. 2016 Apr;17(4):412.

17. Badano LP, Kolias TJ, Muraru D, Abraham TP, Aurigemma G, Edvardsen T, D'Hooge J, Donal E, Fraser AG, Marwick T, Mertens L, Popescu BA, Sengupta PP, Lancellotti P, Thomas JD, Voigt JU. Standardization of left atrial, right ventricular, and right atrial deformation imaging using two-dimensional speckle tracking echocardiography: a consensus document of the EACVI/ASE/Industry Task Force to standardize deformation imaging. Eur Heart J Cardiovasc Imaging. 2018 Jun 1;19(6):591-600.

18. Nagueh SF, Smiseth OA, Appleton CP, Byrd BF, Dokainish H, Edvardsen T, Flachskampf FA, Gillebert TC, Klein AL, Lancellotti P, Marino P, Oh JK, Alexandru Popescu B, Waggoner AD.

Recommendations for the Evaluation of Left Ventricular Diastolic Function by Echocardiography: An Update from the American Society of Echocardiography and the European Association of Cardiovascular Imaging. Eur Heart J Cardiovasc Imaging. 2016 Dec;17(12):1321-1360.

19. Yoshida Y, Nakanishi K, Daimon M, Ishiwata J, Sawada N, Hirokawa M, Kaneko H, Nakao T, Mizuno Y, Morita H, Di Tullio MR, Homma S, Komuro I. Alteration of Cardiac Performance and Serum B-Type Natriuretic Peptide Level in Healthy Aging. J Am Coll Cardiol. 2019 Oct 8;74(14):1789-1800.

20. Morris DA, Belyavskiy E, Aravind-Kumar R, Kropf M, Frydas A, Braunauer K, Marquez E, Krisper M, Lindhorst R, Osmanoglou E, Boldt LH, Blaschke F, Haverkamp W, Tschöpe C, Edelmann F, Pieske B, Pieske-Kraigher E. Potential Usefulness and Clinical Relevance of Adding Left Atrial Strain to Left Atrial Volume Index in the Detection of Left Ventricular Diastolic Dysfunction. JACC Cardiovasc Imaging. 2018 Oct;11(10):1405-1415.

21. Cameli M, Sparla S, Losito M, Righini FM, Menci D, Lisi M, D'Ascenzi F, Focardi M, Favilli R, Pierli C, Fineschi M, Mondillo S. Correlation of Left Atrial Strain and Doppler Measurements with Invasive Measurement of Left Ventricular End-Diastolic Pressure in Patients Stratified for Different Values of Ejection Fraction. Echocardiography. 2016 Mar;33(3):398-405.

22. Telles F, Nanayakkara S, Evans S, Patel HC, Mariani JA, Vizi D, William J, Marwick TH, Kaye DM. Impaired left atrial strain predicts abnormal exercise haemodynamics in heart failure with preserved ejection fraction. Eur J Heart Fail. 2019 Apr;21(4):495-505.

23. Santos AB, Roca GQ, Claggett B, Sweitzer NK, Shah SJ, Anand IS, Fang JC, Zile MR, Pitt B, Solomon SD, Shah AM. Prognostic Relevance of Left Atrial Dysfunction in Heart Failure With Preserved Ejection Fraction. Circ Heart Fail. 2016 Apr;9(4):e002763.

24. Freed BH, Daruwalla V, Cheng JY, Aguilar FG, Beussink L, Choi A, Klein DA, Dixon D, Baldridge A, Rasmussen-Torvik LJ, Maganti K, Shah SJ. Prognostic utility and clinical significance of cardiac mechanics in heart failure with preserved ejection fraction. Circ Cardiovasc Imaging. 2016 Mar;9(3).

25. Kawakami H, Ramkumar S, Pathan F, Wright L, Marwick TH. Use of echocardiography to stratify the risk of atrial fibrillation: comparison of left atrial and ventricular strain. Eur Heart J Cardiovasc Imaging. 2019 Oct 3. pii: jez240.

26. Liu S, Guan Z, Zheng X, Meng P, Wang Y, Li Y, et al. Impaired left atrial systolic function and inter-atrial dyssynchrony may contribute to symptoms of heart failure with preserved left ventricular ejection fraction: A comprehensive assessment by echocardiography. Int J Cardiol. 2018 Apr 15;257:177-181.

27. Aung SM, Güler A, Güler Y, Huraibat A, Karabay CY, Akdemir I. Left atrial strain in heart failure with preserved ejection fraction. Herz. 2017 Apr;42(2):194-199.

28. Sugumar H, Nanayakkara S, Prabhu S, Voskoboinik A, Kaye DM, Ling LH, et al. Pathophysiology of Atrial Fibrillation and Heart Failure: Dangerous Interactions. Cardiol Clin. 2019 May;37(2):131-138.

29. Singh A, Addetia K, Maffessanti F, Mor-Avi V, Lang RM. LA Strain for Categorization of LV Diastolic Dysfunction. JACC Cardiovasc Imaging. 2017 Jul;10(7):735-743.

30. Santos AB, Roca GQ, Claggett B, Sweitzer NK, Shah SJ, Anand IS, et al. Prognostic Relevance of Left Atrial Dysfunction in Heart Failure With Preserved Ejection Fraction. Circ Heart Fail. 2016 Apr;9(4):e002763.

31. Al Saikhan L, Hughes AD, Chung WS, Alsharqi M, Nihoyannopoulos P. Left atrial function in heart failure with mid-range ejection fraction differs from that of heart failure with preserved ejection fraction: a 2D speckle-tracking echocardiographic study. Eur Heart J Cardiovasc Imaging. 2019 Mar 1;20(3):279-290.

32. Santos AB, Kraigher-Krainer E, Gupta DK, Claggett B, Zile MR, Pieske B, et al. Impaired left atrial function in heart failure with preserved ejection fraction. Eur J Heart Fail. 2014 Oct;16(10):1096-103.

33. Morris DA, Belyavskiy E, Aravind-Kumar R, Kropf M, Frydas A, Braunauer K, et al. Potential Usefulness and Clinical Relevance of Adding Left Atrial Strain to Left Atrial Volume Index in the Detection of Left Ventricular Diastolic Dysfunction. JACC Cardiovasc Imaging. 2018 Oct;11(10):1405-1415.

34. Yoshida Y, Nakanishi K, Daimon M, Ishiwata J, Sawada N, Hirokawa M, et al. Alteration of Cardiac Performance and Serum B-Type Natriuretic Peptide Level in Healthy Aging. J Am Coll Cardiol. 2019 Oct 8;74(14):1789-1800.

Left atrial mechanics and functional capacity in heart failure patients with paroxysmal atrial fibrillation

1. T. Owan, D. Hodge, R. Herges, S. Jacobsen, V. Roger, M. Redfield, Trends in Prevalence and Outcome of Heart Failure with Preserved Ejection Fraction. New Engl J Med. 355 (2006) 251–259.

2. R. Zakeri, A. Chamberlain, V. Roger, M. Redfield, Temporal Relationship and Prognostic Significance of Atrial Fibrillation in Heart Failure Patients With Preserved Ejection Fraction. Circulation. 128 (2013) 1085–1093.

3. M. Khan, M. Memon, M. Murad, M. Vaduganathan, S. Greene, M. Hall, F. Triposkiadis, C. Lam, A. Shah, J. Butler, S. Shah, Left atrial function in heart failure with preserved ejection fraction: a systematic review and meta-analysis. Eur J Heart Fail. 22 (2020) 472–485.

4. M. Obokata, K. Negishi, K. Kurosawa, H. Arima, R. Tateno, G. Ui, S. Tange, M. Arai, M. Kurabayashi, Incremental Diagnostic Value of LA Strain With Leg Lifts in Heart Failure With Preserved Ejection Fraction. Jacc Cardiovasc Imaging. 6 (2013) 749–758.

5. A. Singh, K. Addetia, F. Maffessanti, V. Mor-Avi, R. Lang, LA Strain Categorization of LV Diastolic Dysfunction. Jacc Cardiovasc Imaging. 10 (2016) 735–743.

6. F. Triposkiadis, B. Pieske, J. Butler, J. Parissis, G. Giamouzis, J. Skoularigis, D. Brutsaert, H. Boudoulas, Global left atrial failure in heart failure. Eur J Heart Fail. 18 (2016) 1307–1320.

7. D. Morris, H.- Dungen, L.- Boldt, Normal values and clinical relevance of left atrial myocardial function analysed by speckle-tracking echocardiography: multicentre study. European Hear J - Cardiovasc Imaging. 16 (2014) 364–372.

8. T. Sugimoto, S. Robinet, R. Dulgheru, A. Bernard, F. Ilardi, L. Contu, K. Addetia, L. Caballero, G. Kacharava, G. Athanassopoulos, D. Barone, M. Baroni, N. Cardim, A. Hagendorff, K. Hristova, T. Lopez, G. Morena, B. Popescu, M. Penicka, T. Ozyigit, J. Carbonero, N. Veire, R. Bardeleben, D. Vinereanu, J. Zamorano, Y. Go, S. Marchetta, A. Nchimi, M. Rosca, A. Calin, M. Moonen, S. Cimino, J. Magne, B. Cosyns, E. Galli, E. Donal, G. Habib, R. Esposito, M. Galderisi, L. Badano, R. Lang, P. Lancellotti, N. Study, Echocardiographic reference ranges for normal left atrial function parameters: results from the EACVI NORRE study. European Hear J Cardiovasc Imaging. 19 (2018) 630–638.

9. F. Telles, S. Nanayakkara, S. Evans, H. Patel, J. Mariani, D. Vizi, J. William, T. Marwick, D. Kaye, Impaired left atrial strain predicts abnormal exercise haemodynamics in heart failure with preserved ejection fraction. Eur J Heart Fail. 21 (2019) 495–505.

10. R. Malhotra, K. Bakken, E. D'Elia, G. Lewis, Cardiopulmonary Exercise Testing in Heart Failure, Jacc Hear Fail. 4 (2016) 607–616.

11. Y. Reddy, R. Carter, M. Obokata, M. Redfield, B. Borlaug, A Simple, Evidence-Based Approach to Help Guide Diagnosis of Heart Failure with Preserved Ejection Fraction. Circulation (2018).

12. R. Lang, L. Badano, V. Mor-Avi, J. Afilalo, A. Armstrong, L. Ernande, F. Flachskampf, E. Foster, S. Goldstein, T. Kuznetsova, P. Lancellotti, D. Muraru, M. Picard, E. Rietzschel, L. Rudski, K. Spencer, W. Tsang, J. Voigt, Recommendations for Cardiac Chamber Quantification by Echocardiography in Adults: An Update from the American Society of Echocardiography and the European Association of Cardiovascular Imaging, European Hear J - Cardiovasc Imaging. 16 (2015) 233–271.

13. R. Lang, L. Badano, V. Mor-Avi, J. Afilalo, A. Armstrong, L. Ernande, F. Flachskampf, E. Foster, S. Goldstein, T. Kuznetsova, P. Lancellotti, D. Muraru, M. Picard, E. Rietzschel, L. Rudski, K. Spencer, W. Tsang, J. Voigt, Recommendations for Cardiac Chamber Quantification by Echocardiography in Adults: An Update from the American Society of Echocardiography

and the European Association of Cardiovascular Imaging, J Am Soc Echocardiog. 28 (2015) 1-39.e14.

14. L. Badano, T. Kolias, D. Muraru, et al. Standardization of left atrial, right ventricular, and right atrial deformation imaging using two-dimensional speckle tracking echocardiography: a consensus document of the EACVI/ASE/Industry Task Force to standardize deformation imaging. European Hear J Cardiovasc Imaging. 19 (2018) 591–600.

15. V. Mor-Avi, R. Lang, L. Badano, M. Belohlavek, N. Cardim, G. Derumeaux, M. Galderisi, T. Marwick, S. Nagueh, P. Sengupta, R. Sicari, O. Smiseth, B. Smulevitz, M. Takeuchi, J. Thomas, M. Vannan, J. Voigt, J. Zamorano, Current and Evolving Echocardiographic Techniques for the Quantitative Evaluation of Cardiac Mechanics: ASE/EAE Consensus Statement on Methodology and Indications. J Am Soc Echocardiog. 24 (2011) 277–313.

16. M. Obokata, B.A. Borlaug, Left atrial dysfunction: the next key target in heart failure with preserved ejection fraction. Eur J Heart Fail. 21 (2019) 506–508.

17. M. Obokata, Y.N.V. Reddy, B.A. Borlaug, Diastolic Dysfunction and Heart Failure With Preserved Ejection Fraction: Understanding Mechanisms by Using Noninvasive Methods. Jacc Cardiovasc Imaging. 13 (2019) 245–257.

18. B.H. Freed, V. Daruwalla, J.Y. Cheng, F.G. Aguilar, L. Beussink, A. Choi, D.A. Klein, D. Dixon, A. Baldridge, L.J. Rasmussen-Torvik, K. Maganti, S.J. Shah, Prognostic Utility and Clinical Significance of Cardiac Mechanics in Heart Failure With Preserved Ejection Fraction, Circulation Cardiovasc Imaging. 9 (2016) e003754.

19. V. Melenovsky, B.A. Borlaug, B. Rosen, I. Hay, L. Ferruci, C.H. Morell, E.G. Lakatta, S.S. Najjar, D.A. Kass, Cardiovascular Features of Heart Failure With Preserved Ejection Fraction Versus Nonfailing Hypertensive Left Ventricular Hypertrophy in the Urban Baltimore Community The Role of Atrial Remodeling/Dysfunction, J Am Coll Cardiol. 49 (2007) 198–207.

20. M. Obokata, B.A. Borlaug, Left Ventricular Filling Pressures in Heart Failure With Preserved Ejection Fraction: Is the Tail Now Wagging the Dog?, JACC. Heart Failure. 5 (2017) 802–804.

21. G. Hasenfuß, C. Hayward, D. Burkhoff, F. Silvestry, S. McKenzie, F. Gustafsson, F. Malek, Jv. Heyden, I. Lang, M. Petrie, J. Cleland, M. Leon, D. Kaye, Rl. investigators, A transcatheter intracardiac shunt device for heart failure with preserved ejection fraction (REDUCE LAP-HF): a multicentre, open-label, single-arm, phase 1 trial., Lancet Lond Engl. 387 (2016) 1298–304.

Multicentric atrial strain comparison between two different modalities

1. Blume GG, McLeod CJ, Barnes ME, Seward JB, Pellikka PA, Bastiansen PM, et al. Left atrial function: physiology, assessment, and clinical implications. Eur J Echocardiogr. 2011;12:421-30.

2. Cameli M, Mandoli GE, Sciaccaluga C, Mondillo S. More than 10 years of speckle tracking echocardiography: Still a novel technique or a definite tool for clinical practice? Echocardiography. 2019;36:958-70.

3. Mor-Avi V, Lang RM, Badano LP, Belohlavek M, Cardim NM, Derumeaux G, et al. Current and evolving echocardiographic techniques for the quantitative evaluation of cardiac mechanics: ASE/EAE consensus statement on methodology and indications endorsed by the Japanese Society of Echocardiography. Eur J Echocardiogr. 2011;12:167-205.

4. Saraiva RM, Demirkol S, Buakhamsri A, Greenberg N, Popovic ZB, Thomas JD, et al. Left atrial strain measured by two-dimensional speckle tracking represents a new tool to evaluate left atrial function. J Am Soc Echocardiogr. 2010;23:172-80.

5. Badano LP, Kolias TJ, Muraru D, Abraham TP, Aurigemma G, Edvardsen T, et al. Standardization of left atrial, right ventricular, and right atrial deformation imaging using two-dimensional speckle tracking echocardiography: a consensus document of the EACVI/ASE/Industry Task Force to standardize deformation imaging. Eur Heart J Cardiovasc Imaging. 2018;19:591-600.

6. Mancia G, Fagard R, Narkiewicz K, Redon J, Zanchetti A, Bohm M, et al. 2013 ESH/ESC guidelines for the management of arterial hypertension: the Task Force for the Management of Arterial Hypertension of the European Society of Hypertension (ESH) and of the European Society of Cardiology (ESC). Eur Heart J. 2013;34:2159-219.

7. Lang RM, Badano LP, Mor-Avi V, Afilalo J, Armstrong A, Ernande L, et al. Recommendations for cardiac chamber quantification by echocardiography in adults: an update from the American Society of Echocardiography and the European Association of Cardiovascular Imaging. Eur Heart J Cardiovasc Imaging. 2015;16:233-70.

8. Nagueh SF, Smiseth OA, Appleton CP, Byrd BF, 3rd, Dokainish H, Edvardsen T, et al. Recommendations for the Evaluation of Left Ventricular Diastolic Function by Echocardiography: An Update from the American Society of Echocardiography and the European Association of Cardiovascular Imaging. Eur Heart J Cardiovasc Imaging. 2016;17:1321-60.

9. Rudski LG, Lai WW, Afilalo J, Hua L, Handschumacher MD, Chandrasekaran K, et al. Guidelines for the echocardiographic assessment of the right heart in adults: a report from the American Society of Echocardiography endorsed by the European Association of Echocardiography, a registered branch of the European Society of Cardiology, and the Canadian Society of Echocardiography. J Am Soc Echocardiogr. 2010;23:685-713

10. Baumgartner H, Falk V, Bax JJ, De Bonis M, Hamm C, Holm PJ, et al. 2017 ESC/EACTS Guidelines for the management of valvular heart disease. Eur Heart J. 2017;38:2739-91.

11. Voigt JU, Pedrizzetti G, Lysyansky P, Marwick TH, Houle H, Baumann R et al. Definitions for a common standard for 2D speckle tracking echocardiography: consensus document of the EACVI/ASE/Industry Task Force to standardize deformation imaging. Eur Heart J Cardiovasc Imaging. 2015;16:1-11.

12. Donal E, Behagel A, Feneon D. Value of left atrial strain: a highly promising field of investigation. Eur Heart J Cardiovasc Imaging. 2015;16:356-7.

13. Thomas L, Marwick TH, Popescu BA, Donal E, Badano LP. Left Atrial Structure and Function, and Left Ventricular Diastolic Dysfunction: JACC State-of-the-Art Review. J Am Coll Cardiol. 2019;73:1961-77.

14. Sugimoto T, Robinet S, Dulgheru R, Bernard A, Ilardi F, Contu L, et al. Echocardiographic reference ranges for normal left atrial function parameters: results from the EACVI NORRE study. Eur Heart J Cardiovasc Imaging. 2018;19:630-8.

15. Galli E, Fournet M, Chabanne C, Lelong B, Leguerrier A, Flecher E, et al. Prognostic value of left atrial reservoir function in patients with severe aortic stenosis: a 2D speckle-tracking echocardiographic study. Eur Heart J Cardiovasc Imaging. 2016;17:533-41.

16. Pernigo M, Benfari G, Geremia G, Noni M, Borio G, Mazzali G, et al. Atrial Function as an Independent Predictor of Postoperative Atrial Fibrillation in Patients Undergoing Aortic Valve Surgery for Severe Aortic Stenosis J Am Soc Echocardiogr. 2017;30:956-65 e1.

17. Cameli M, Pastore MC, Righini FM, Mandoli GE, D'Ascenzi F, Lisi M, et al. Prognostic value of left atrial strain in patients with moderate asymptomatic mitral regurgitation. Int J Cardiovasc Imaging. 2019;35:1597-1604.

18. Yang LT, Liu YW, Shih JY, Li YH, Tsai LM, Luo CY, et al. Predictive value of left atrial deformation on prognosis in severe primary mitral regurgitation. J Am Soc Echocardiogr. 2015;28:1309-17 e4.

19. Miyoshi H, Oishi Y, Mizuguchi Y, Iuchi A, Nagase N, Ara N, et al. Effect of an increase in left ventricular pressure overload on left atrial-left ventricular coupling in patients with hypertension: a two-dimensional speckle tracking echocardiographic study. Echocardiography. 2013;30:658-66.

20. Miyoshi H, Oishi Y, Mizuguchi Y, Iuchi A, Nagase N, Ara N, et al. Early predictors of alterations in left atrial structure and function related to left ventricular dysfunction in asymptomatic patients with hypertension. J Am Soc Hypertens. 2013;7:206-15.

21. Cameli M, Sciaccaluga C, Loiacono F, Simova I, Miglioranza MH, Nistor D, et al. The analysis of left atrial function predicts the severity of functional impairment in chronic heart failure: The FLASH multicenter study. Int J Cardiol. 2019;286:87-91.

22. Freed BH, Daruwalla V, Cheng JY, Aguilar FG, Beussink L, Choi A, et al. Prognostic Utility and Clinical Significance of Cardiac Mechanics in Heart Failure With Preserved Ejection Fraction: Importance of Left Atrial Strain. Circ Cardiovasc Imaging. 2016;9.

23. Rosca M, Popescu BA, Beladan CC, Calin A, Muraru D, Popa EC, et al. Left atrial dysfunction as a correlate of heart failure symptoms in hypertrophic cardiomyopathy. J Am Soc Echocardiogr. 2010;23:1090-8.

24. Al Saikhan L, Hughes AD, Chung WS, Alsharqi M, Nihoyannopoulos P. Left atrial function in heart failure with mid-range ejection fraction differs from that of heart failure with preserved ejection fraction: a 2D speckle-tracking echocardiographic study. Eur Heart J Cardiovasc Imaging. 2019;20:279-90.

25. Hayashi S, Yamada H, Bando M, Saijo Y, Nishio S, Hirata Y, et al. Optimal Analysis of Left Atrial Strain by Speckle Tracking Echocardiography: P-wave versus R-wave Trigger. Echocardiography. 2015;32:1241-9.

26. Wakami K, Ohte N, Asada K, Fukuta H, Goto T, Mukai S, et al. Correlation between left ventricular end-diastolic pressure and peak left atrial wall strain during left ventricular systole. J Am Soc Echocardiogr. 2009;22:847-51.

Inter-center reproducibility of standard and advanced echocardiographic parameters in the EACVI AFib Echocardiographic Registry

1. Galderisi M, Donal E, Magne J, Lo Iudice F, Agricola E, Sade LE, et al. Rationale and design of the EACVI AFib Echo Europe Registry for assessing relationships of echocardiographic parameters with clinical thrombo-embolic and bleeding risk profile in non-valvular atrial fibrillation. Eur Heart J Cardiovasc Imaging 2018;19:245-252.

2. Galderisi M, Henein MY, D'Hooge J, Sicari R, Badano LP, Zamorano JL, et al; European Association of Echocardiography. Recommendations of the European Association of Echocardiography: how to use echo-Doppler in clinical trials: different modalities for different purposes. Eur J Echocardiogr 2011;12:339-353.

3. Lang RM, Badano LP, Mor-Avi V, Afilalo J, Armstrong A, Ernande L, et al. Recommendations for cardiac chamber quantification by echocardiography in adults: an update from the American Society of Echocardiography and the European Association of Cardiovascular Imaging. Eur Heart J Cardiovasc Imaging 2015;16:233-270.

4. Mor-Avi V, Lang RM, Badano LP, Belohlavek M, Cardim NM, Derumeaux G, et al. Current and evolving echocardiographic techniques for the quantitative evaluation of cardiac

mechanics: ASE/EAE consensus statement on methodology and indications endorsed by the Japanese Society of Echocardiography. Eur J Echocardiogr 2011;12:167-205.

5.Nagueh SF, Smiseth OA, Appleton CP, Byrd BF 3rd, Dokainish H, Edvardsen T, et al. Recommendations for the evaluation of left ventricular diastolic function by echocardiography: An Update from the American Society of Echocardiography and the European Association of Cardiovascular Imaging. Eur Heart J Cardiovasc Imaging 2016;17:1321-1360.

6.Voigt JU, Pedrizzetti G, Lysyansky P, Marwick TH, Houle H, Baumann R, et al. Definitions for a common standard for 2D speckle tracking echocardiography: consensus document of the EACVI/ASE/Industry Task Force to standardize deformation imaging. Eur Heart J Cardiovasc Imaging 2015;16:1-11.

7. Badano LP, Kolias TJ, Muraru D, Abraham TP, Aurigemma G, Edvardsen T, et al. Standardization of left atrial, right ventricular, and right atrial deformation imaging using two-dimensional speckle tracking echocardiography: a consensus document of the EACVI/ASE/Industry Task Force to standardize deformation imaging. Eur Heart J Cardiovasc Imaging 2018;19:591-600.

8. Donal E, Coisne D, Pham B, Ragot S, Herpin D, Thomas JD. Anatomic M-mode, a pertinent tool for the daily practice of transthoracic echocardiography. J Am Soc Echocardiogr 2004;17:962-967.

10. Gottdiener JS, Livengood SV, Meyer PS, Chase GA. Should echocardiography be performed to assess effects of antihypertensive therapy? Test-retest reliability of echocardiography for measurement of left ventricular mass and function. J Am Coll Cardiol 1995;25:424–430.

10. de Simone G, Muiesan ML, Ganau A, Longhini C, Verdecchia P, Palmieri V, et al. Reliability and limitations of echocardiographic measurement of left ventricular mass for risk stratification and follow-up in single patients: the RES trial. Working Group on Heart and Hypertension of the Italian Society of Hypertension. Reliability of M-mode echocardiographic studies. J Hypertens 1999;17: 1955–1963.

11. Himelman RB, Cassidy MM, Landzberg JS, Schiller NB. Reproducibility of quantitative two-dimensional echocardiography. Am Heart J 1988;115:425–431.

12. Farsalinos KE, Daraban AM, Unlu S, Thomas JD, Badano LP, Voigt JU. Head-to-head comparison of global longitudinal strain measurements among nine different vendors: the EACVI/ASE Inter-vendor comparison study. J Am Soc Echocardiogr 2015;28:1171-1181.

13. Palmieri V, Innocenti F, Pini R, Celentano A. Reproducibility of Doppler echocardiographic assessment of left ventricular diastolic function in multicenter setting. J Am Soc Echocardiogr 2005;18:99-106.

14. Palmieri V, Arezzi E, Sabbatella M, Celentano A. Interstudy reproducibility of parameters of left ventricular diastolic function: a Doppler echocardiographic study. J Am Soc Echocardiogr 2003;16:1128-1135.

15. Galderisi M, Benjamin EJ, Evans JC, D'Agostino RB, Fuller DL, et al. Intra-and inter-observer reproducibility of Doppler-assessed indexes of left ventricular diastolic function in a population-based study (the Framingham Heart Study). Am J Cardiol 1992;70:1341-1346.

16. Coiro S, Huttin O, Bozec E, Selton-Suty C, Lamiral Z, Carluccio E, et al. Reproducibility of echocardiographic assessment of 2D derived longitudinal strain parameters in a population-based study (the STANILAS cohort Study). Int J Cardiovasc Imaging 2017;33:1361-1369.

17. Cheng S, Larson MG, McCabe EL, Osypiuk E, Lehman BT, Stanchev P, et al. Reproducibility of speckle-tracking-based strain measures of left ventricular function in a community-based community. J Am Soc Echocardiogr 2013;26:1258-1266.

18.Thavendiranathan P, Grant AD, Negishi T, Plana JC, Popović ZB, Marwick TH. Reproducibility of echocardiographic techniques for sequential assessment of left ventricular ejection fraction and volumes: application to patients undergoing cancer chemotherapy. J Am Coll Cardiol 2013;61:77-84.

19. Negishi T, Negishi K, Thavendiranathan P, Popescu BA, Vinereaunu D, Kurosawa K, SUCCOUR Investigators, et al. Effect of Experience and training on the concordance and precision of strain measurements. JACC Cardiovasc Imaging 2017;10:518-522.

20. Galderisi M, Cosyns B, Edvardsen T, Cardim N, Delgado V, Di Salvo G, et al. Standardization of adult transthoracic echocardiography reporting in agreement with recent chamber quantification, diastolic function, and heart disease recommendations: an expert consensus document of the European Association of Cardiovascular Imaging. Eur Heart J Cardiovasc Imaging 2017;18:1301-1310.

21. Kim DG, Lee KJ, Lee S, Jeong SY, Lee YS, Vhoi YJ, et al. Feasibility of two-dimensional global longitudinal strain and strain rate for the assessment of left atrial function: a study in subjects with a low probability of cardiovascular disease and normal exercise capacity. Echocardiography 2009;26:1179-1187.

22. Cameli M, Caputo M, Mondillo S, Ballo P, Palmerini E, Lisi M, et al. Feasibility and reference values of left atrial longitudinal strain imaging by two-dimensional speckle tracking. Cardiovasc Ultrasound 2009 Feb 8;7:6.

23. Oxborough D, George K, Birch KM. Interobserver reliability of two-dimensional derived strain imaging in the assessment of the left ventricle, right ventricle, and left atrium of healthy human hearts. Echocardiography 2012;29:793-802.

1. Timóteo AT, Moura Branco L, Filipe F, Galrinho A, Rio P, Portugal G, et al. Cardiotoxicity in breast cancer treatment: What about left ventricular diastolic function and left atrial function?. Echocardiography. 2019 Oct;36(10):1806-1813.

2. Tadic M, Genger M, Cuspidi C, Belyavskiy E, Frydas A, Dordevic A, et al. Phasic Left Atrial Function in Cancer Patients Before Initiation of Anti-Cancer Therapy. J Clin Med. 2019 Mar 27;8(4). pii: E421.

3. Yaylali YT, Saricopur A, Yurtdas M, Senol H, Gokoz-Dogu G. Atrial Function in Patients with Breast Cancer After Treatment with Anthracyclines. Arq Bras Cardiol. 2016 Nov;107(5):411-419.

4. Moreno J, García-Sáez JA, Clavero M, Manganaro R, Moreno F, López J, et al. Effect of breast cancer cardiotoxic drugs on left atrial myocardium mechanics. Searching for an early cardiotoxicity marker. Int J Cardiol. 2016 May 1;210:32-4.

5. Milks MW, Velez MR, Mehta N, Ishola A, Van Houten T, Yildiz VO, et al. Usefulness of Integrating Heart Failure Risk Factors Into Impairment of Global Longitudinal Strain to Predict Anthracycline-Related Cardiac Dysfunction. Am J Cardiol. 2018 Apr 1;121(7):867-873.

Comparison between echocardiography and rotational angiography in left atrial appendage closure

1. A.J. Camm, G.Y. Lip, R. De Caterina, et al. 2012 focused update of the ESC Guidelines for the management of atrial fibrillation: an update of the 2010 ESC Guidelines for the management of atrial fibrillation. Developed with the special contribution of the European Heart Rhythm Association. Eur Heart J, 33 (2012), pp. 2719-2747.

2. L. Pison, T.S. Potpara, J. Chen, et al. Left atrial appendage closure-indications, techniques, and outcomes: results of the European Heart Rhythm Association Survey. Europace, 17 (20

3. N.C. Wunderlich, R. Beigel, M.J. Swaans, S.Y. Ho, R.J. Siegel. Percutaneous interventions for left atrial appendage exclusion: options, assessment, and imaging using 2D and 3D echocardiography. J Am Coll Cardiol Img, 8 (2015), pp. 472-48815), pp. 642-646.

4. M.V. Orlov, P. Hoffmeister, G.M. Chaudhry, et al. Three-dimensional rotational angiography of the left atrium and esophagus: a virtual computed tomography scan in the electrophysiology lab?. Heart Rhythm, 4 (2007), pp. 37-43.

5. T. De Potter Jr., G. Bardhaj, A. Viggiano, K. Morrice, P. Geelen. Three-dimensional rotational angiography as a periprocedural imaging tool in atrial fibrillation ablation Arrhythm Electrophysiol Rev, 3 (2014), pp. 173-176.

Endoscopic mitral valve repair of atrial functional mitral regurgitation in non-ischemic heart failure with preserved ejection fraction

1. Deferm S, Bertrand PB, Verbrugge FH, et al. Atrial Functional Mitral Regurgitation: JACC Review Topic of the Week. J Am Coll Cardiol;73:2465-2476.

2. Dziadzko V, Dziadzko M, Medina-Inojosa JR, et al. Causes and mechanisms of isolated mitral regurgitation in the community: clinical context and outcome. Eur Heart J;40:2194-2202.

3. Kagiyama N, Mondillo S, Yoshida K, Mandoli GE, Cameli M. Subtypes of Atrial Functional Mitral Regurgitation: Imaging Insights Into Their Mechanisms and Therapeutic Implications. JACC Cardiovasc Imaging.

4. Kajimoto K, Minami Y, Otsubo S, Sato N. Ischemic or Nonischemic Functional Mitral Regurgitation and Outcomes in Patients With Acute Decompensated Heart Failure With Preserved or Reduced Ejection Fraction. Am J Cardiol;120:809-816.

5. Kajimoto K, Sato N, Takano T. Functional mitral regurgitation at discharge and outcomes in patients hospitalized for acute decompensated heart failure with a preserved or reduced ejection fraction. Eur J Heart Fail;18:1051-9.

6. Kihara T, Gillinov AM, Takasaki K, et al. Mitral regurgitation associated with mitral annular dilation in patients with lone atrial fibrillation: an echocardiographic study. Echocardiography 2009;26:885-9.

7. Takahashi Y, Abe Y, Sasaki Y, et al. Mitral valve repair for atrial functional mitral regurgitation in patients with chronic atrial fibrillation. Interact Cardiovasc Thorac Surg;21:163-8.

8. Casselman FP, Van Slycke S, Wellens F, et al. Mitral valve surgery can now routinely be performed endoscopically. Circulation 2003;108 Suppl 1:II48-54.

9. Penicka M, Kotrc M, Ondrus T, et al. Minimally invasive mitral valve annuloplasty confers a long-term survival benefit compared with state-of-the-art treatment in heart failure with functional mitral regurgitation. Int J Cardiol;244:235-241.

10. Reddy YNV, Carter RE, Obokata M, Redfield MM, Borlaug BA. A Simple, Evidence-Based Approach to Help Guide Diagnosis of Heart Failure With Preserved Ejection Fraction. Circulation;138:861-870.

11. Ito K, Abe Y, Takahashi Y, et al. Mechanism of atrial functional mitral regurgitation in patients with atrial fibrillation: A study using three-dimensional transesophageal echocardiography. J Cardiol;70:584-590.

12. Kagiyama N, Hayashida A, Toki M, et al. Insufficient Leaflet Remodeling in Patients With Atrial Fibrillation: Association With the Severity of Mitral Regurgitation. Circ Cardiovasc Imaging;10.

13. Kim DH, Heo R, Handschumacher MD, et al. Mitral Valve Adaptation to Isolated Annular Dilation: Insights Into the Mechanism of Atrial Functional Mitral Regurgitation. JACC Cardiovasc Imaging;12:665-677.

14. Nishino S, Watanabe N, Ashikaga K, et al. Reverse Remodeling of the Mitral Valve Complex After Radiofrequency Catheter Ablation for Atrial Fibrillation: A Serial 3-Dimensional Echocardiographic Study. Circ Cardiovasc Imaging;12:e009317.

15. Ring L, Dutka DP, Wells FC, Fynn SP, Shapiro LM, Rana BS. Mechanisms of atrial mitral regurgitation: insights using 3D transoesophageal echo. Eur Heart J Cardiovasc Imaging;15:500-8.

16. Chugh SS, Havmoeller R, Narayanan K, et al. Worldwide epidemiology of atrial fibrillation: a Global Burden of Disease 2010 Study. Circulation;129:837-47.

17. Dunlay SM, Roger VL, Redfield MM. Epidemiology of heart failure with preserved ejection fraction. Nat Rev Cardiol;14:591-602.

18. Grayburn PA, Sannino A, Packer M. Proportionate and Disproportionate Functional Mitral Regurgitation: A New Conceptual Framework That Reconciles the Results of the MITRA-FR and COAPT Trials. JACC Cardiovasc Imaging;12:353-362.

19. Baumgartner H. The 2017 ESC/EACTS guidelines on the management of valvular heart disease : What is new and what has changed compared to the 2012 guidelines? Wien Klin Wochenschr;130:168-171.

20. Agrawal A, Naranjo M, Kanjanahattakij N, Rangaswami J, Gupta S. Cardiorenal syndrome in heart failure with preserved ejection fraction-an under-recognized clinical entity. Heart Fail Rev;24:421-437.

21. Takahashi Y, Abe Y, Takashi M, et al. Mid-term results of valve repairs for atrial functional mitral and tricuspid regurgitations. Gen Thorac Cardiovasc Surg.

Imaging of Myocardial Fibrosis and Its Functional Correlates in Aortic Stenosis

1. Baumgartner H, Falk V, Bax JJ, De Bonis M, Hamm C, Holm PJ, et al.; ESC Scientific Document Group. 2017 ESC/EACTS Guidelines for the management of valvular heart disease. Eur Heart J. 2017 Sep;38(36):2739–91.

2. Nishimura RA, Otto CM, Bonow RO, Carabello BA, Erwin JP 3rd, Fleisher LA, et al. 2017 AHA/ACC Focused Update of the 2014 AHA/ACC Guideline for the Management of Patients With Valvular Heart Disease: A Report of the American College of Cardiology/American Heart Association Task Force on Clinical Practice Guidelines. J Am Coll Cardiol. 2017 Jul;70(2):252–89.

3. Milano AD, Faggian G, Dodonov M, Golia G, Tomezzoli A, Bortolotti U, et al. Prognostic value of myocardial fibrosis in patients with severe aortic valve stenosis. J Thorac Cardiovasc Surg. 2012 Oct;144(4):830–7.

4. Treibel TA, Kozor R, Schofield R, Benedetti G, Fontana M, Bhuva AN, et al. Reverse Myocardial Remodeling Following Valve Replacement in Patients With Aortic Stenosis. J Am Coll Cardiol. 2018 Feb;71(8):860–71.

5. Kwiecinski J, Chin CW, Everett RJ, White AC, Semple S, Yeung E, et al. Adverse prognosis associated with asymmetric myocardial thickening in aortic stenosis. Eur Heart J Cardiovasc Imaging. 2018 Mar;19(3):347–56.

6. Kvernby S, Rönnerfalk M, Warntjes M, Carlhäll CJ, Nylander E, Engvall J, et al. Longitudinal changes in myocardial T1 and T2 relaxation times related to diffuse myocardial fibrosis in aortic stenosis; before and after aortic valve replacement. J Magn Reson Imaging. 2018 Feb;48(3):799–807.

7. Podlesnikar T, Delgado V, Bax JJ. Cardiovascular magnetic resonance imaging to assess myocardial fibrosis in valvular heart disease. Int J Cardiovasc Imaging. 2018 Jan;34(1):97–112.

8. Kempny A, Diller GP, Kaleschke G, Orwat S, Funke A, Radke R, et al. Longitudinal left ventricular 2D strain is superior to ejection fraction in predicting myocardial recovery and symptomatic improvement after aortic valve implantation. Int J Cardiol. 2013 Sep;167(5):2239–43.

9. Cengiz B, Şahin ŞT, Yurdakul S, Kahraman S, Bozkurt A, Aytekin S. Subclinical left ventricular systolic dysfunction in patients with severe aortic stenosis: A speckle-tracking echocardiography study. Turk Kardiyol Dern Ars. 2018 Jan;46(1):18–24.

10. Rader F, Sachdev E, Arsanjani R, Siegel RJ. Left ventricular hypertrophy in valvular aortic stenosis: mechanisms and clinical implications. Am J Med. 2015 Apr;128(4):344–52.

11. Dweck MR, Joshi S, Murigu T, Gulati A, Alpendurada F, Jabbour A, et al. Left ventricular remodeling and hypertrophy in patients with aortic stenosis: insights from cardiovascular magnetic resonance. J Cardiovasc Magn Reson. 2012 Jul;14(1):50.

12. Dahl JS, Christensen NL, Videbæk L, Poulsen MK, Carter-Storch R, Hey TM, et al. Left ventricular diastolic function is associated with symptom status in severe aortic valve stenosis. Circ Cardiovasc Imaging. 2014 Jan;7(1):142–8.

13. Golia G, Milano AD, Dodonov M, Bergamini C, Faggian G, Tomezzoli A, et al. Influence of myocardial fibrosis on left ventricular hypertrophy in patients with symptomatic severe aortic stenosis. Cardiology. 2011;120(3):139–45.

14. Weidemann F, Herrmann S, Störk S, Niemann M, Frantz S, Lange V, et al. Impact of myocardial fibrosis in patients with symptomatic severe aortic stenosis. Circulation. 2009 Aug;120(7):577–84.

15. Treibel TA, López B, González A, Menacho K, Schofield RS, Ravassa S, et al. Reappraising myocardial fibrosis in severe aortic stenosis: an invasive and non-invasive study in 133 patients. Eur Heart J. 2018 Feb;39(8):699–709.

16. Azevedo CF, Nigri M, Higuchi ML, Pomerantzeff PM, Spina GS, Sampaio RO, et al. Prognostic significance of myocardial fibrosis quantification by histopathology and magnetic resonance imaging in patients with severe aortic valve disease. J Am Coll Cardiol. 2010 Jul;56(4):278–87.

17. Jellis C, Martin J, Narula J, Marwick TH. Assessment of nonischemic myocardial fibrosis. J Am Coll Cardiol. 2010 Jul;56(2):89–97.

18. Dweck MR, Joshi S, Murigu T, Alpendurada F, Jabbour A, Melina G, et al. Midwall fibrosis is an independent predictor of mortality in patients with aortic stenosis. J Am Coll Cardiol. 2011 Sep;58(12):1271–9.

19. Chin CW, Everett RJ, Kwiecinski J, Vesey AT, Yeung E, Esson G, et al. Myocardial fibrosis and cardiac decompensation in aortic stenosis. JACC Cardiovasc Imaging. 2017 Nov;10(11):1320–33.

20. Adda J, Mielot C, Giorgi R, Cransac F, Zirphile X, Donal E, et al. Low-flow, low-gradient severe aortic stenosis despite normal ejection fraction is associated with severe left ventricular dysfunction as assessed by speckle-tracking echocardiography: a multicenter study. Circ Cardiovasc Imaging. 2012 Jan;5(1):27–35.

21. Hachicha Z, Dumesnil JG, Bogaty P, Pibarot P. Paradoxical low-flow, low-gradient severe aortic stenosis despite preserved ejection fraction is associated with higher afterload and reduced survival. Circulation. 2007 Jun;115(22):2856–64.

22. Fontana M, White SK, Banypersad SM, Sado DM, Maestrini V, Flett AS, et al. Comparison of T1 mapping techniques for ECV quantification. Histological validation and reproducibility of ShMOLLI versus multibreath-hold T1 quantification equilibrium contrast CMR. J Cardiovasc Magn Reson. 2012 Dec;14(1):88.

23. Kockova R, Kacer P, Pirk J, Maly J, Vsianska M, Sukupova L, et al. Magnetic resonance-derived pre-contrast T1 relaxation time is the accurate marker of diffuse myocardial fibrosis in severe aortic valve disease: a comparison with left ventricular myocardial biopsy. Circulation. 2015;132:A13596.

24. Kockova R, Kacer P, Pirk J, Maly J, Sukupova L, Sikula V, et al. Native T1 Relaxation Time and Extracellular Volume Fraction as Accurate Markers of Diffuse Myocardial Fibrosis in

Heart Valve Disease – Comparison With Targeted Left Ventricular Myocardial Biopsy. Circ J. 2016 Apr;80(5):1202–9.

25. Sibley CT, Noureldin RA, Gai N, Nacif MS, Liu S, Turkbey EB, et al. T1 Mapping in cardiomyopathy at cardiac MR: comparison with endomyocardial biopsy. Radiology. 2012 Dec;265(3):724–32.

26. Puntmann VO, Voigt T, Chen Z, Mayr M, Karim R, Rhode K, et al. Native T1 mapping in differentiation of normal myocardium from diffuse disease in hypertrophic and dilated cardiomyopathy. JACC Cardiovasc Imaging. 2013 Apr;6(4):475–84.

27. Ugander M, Oki AJ, Hsu LY, Kellman P, Greiser A, Aletras AH, et al. Extracellular volume imaging by magnetic resonance imaging provides insights into overt and sub-clinical myocardial pathology. Eur Heart J. 2012 May;33(10):1268–78.

28. Treibel TA, Fontana M, Reant P, Espinosa MA, Castelletti S, Herrey AS, et al. T1 mapping in severe aortic stenosis: insights into LV remodeling. J Cardiovasc Magn Reson. 2015;17 Suppl 1:17.

29. Fabiani I, Scatena C, Mazzanti CM, Conte L, Pugliese NR, Franceschi S, et al. Micro-RNA-21 (biomarker) and global longitudinal strain (functional marker) in detection of myocardial fibrotic burden in severe aortic valve stenosis: a pilot study. J Transl Med. 2016 Aug;14(1):248.

30. Chin CW, Semple S, Malley T, White AC, Mirsadraee S, Weale PJ, et al. Optimization and comparison of myocardial T1 techniques at 3T in patients with aortic stenosis. Eur Heart J Cardiovasc Imaging. 2014 May;15(5):556–65.

31. Delgado V, Tops LF, van Bommel RJ, van der Kley F, Marsan NA, Klautz RJ, et al. Strain analysis in patients with severe aortic stenosis and preserved left ventricular ejection fraction undergoing surgical valve replacement. Eur Heart J. 2009 Dec;30(24):3037–47.

32. Kearney LG, Lu K, Ord M, Patel SK, Profitis K, Matalanis G, et al. Global longitudinal strain is a strong independent predictor of all-cause mortality in patients with aortic stenosis. Eur Heart J Cardiovasc Imaging. 2012 Oct;13(10):827–33.

33. Kusunose K, Goodman A, Parikh R, Barr T, Agarwal S, Popovic ZB, et al. Incremental prognostic value of left ventricular global longitudinal strain in patients with aortic stenosis and preserved ejection fraction. Circ Cardiovasc Imaging. 2014 Nov;7(6):938–45.

34. Carstensen HG, Larsen LH, Hassager C, Kofoed KF, Jensen JS, Mogelvang R. Basal longitudinal strain predicts future aortic valve replacement in asymptomatic patients with aortic stenosis. Eur Heart J Cardiovasc Imaging. 2016 Mar;17(3):283–92.

35. Dulgheru R, Magne J, Davin L, Nchimi A, Oury C, Pierard LA, et al. Left ventricular regional function and maximal exercise capacity in aortic stenosis. Eur Heart J Cardiovasc Imaging. 2016 Feb;17(2):217–24.

36. Lafitte S, Perlant M, Reant P, Serri K, Douard H, DeMaria A, et al. Impact of impaired myocardial deformations on exercise tolerance and prognosis in patients with asymptomatic aortic stenosis. Eur J Echocardiogr. 2009 May;10(3):414–9.

37. Yingchoncharoen T, Gibby C, Rodriguez LL, Grimm RA, Marwick TH. Association of myocardial deformation with outcome in asymptomatic aortic stenosis with normal ejection fraction. Circ Cardiovasc Imaging. 2012 Nov;5(6):719–25.

38. Călin A, Roşca M, Beladan CC, Enache R, Mateescu AD, Ginghină C, et al. The left ventricle in aortic stenosis—imaging assessment and clinical implications. Cardiovasc Ultrasound. 2015 Apr;13(1):22.

39. Donal E, Thebault C, O'Connor K, Veillard D, Rosca M, Pierard L, et al. Impact of aortic stenosis on longitudinal myocardial deformation during exercise. Eur J Echocardiogr. 2011 Mar;12(3):235–41.

40. Ng AC, Delgado V, Bertini M, Antoni ML, van Bommel RJ, van Rijnsoever EP, et al. Alterations in multidirectional myocardial functions in patients with aortic stenosis and preserved ejection fraction: a two-dimensional speckle tracking analysis. Eur Heart J. 2011 Jun;32(12):1542–50.

41. Bruch C, Stypmann J, Grude M, Gradaus R, Breithardt G, Wichter T. Tissue Doppler imaging in patients with moderate to severe aortic valve stenosis: clinical usefulness and diagnostic accuracy. Am Heart J. 2004 Oct;148(4):696–702.

42. Kang SJ, Lim HS, Choi BJ, Choi SY, Hwang GS, Yoon MH, et al. Longitudinal strain and torsion assessed by two-dimensional speckle tracking correlate with the serum level of tissue inhibitor of matrix metalloproteinase-1, a marker of myocardial fibrosis, in patients with hypertension. J Am Soc Echocardiogr. 2008 Aug;21(8):907–11.

43. Kapelouzou A, Tsourelis L, Kaklamanis L, Degiannis D, Kogerakis N, Cokkinos DV. Serum and tissue biomarkers in aortic stenosis. Glob Cardiol Sci Pract. 2015 Nov;2015(4):49.

44. Hoffmann R, Altiok E, Friedman Z, Becker M, Frick M. Myocardial deformation imaging by two-dimensional speckle-tracking echocardiography in comparison to late gadolinium enhancement cardiac magnetic resonance for analysis of myocardial fibrosis in severe aortic stenosis. Am J Cardiol. 2014 Oct;114(7):1083–8.

45. Lee SP, Lee W, Lee JM, Park EA, Kim HK, Kim YJ, et al. Assessment of diffuse myocardial fibrosis by using MR imaging in asymptomatic patients with aortic stenosis. Radiology. 2015 Feb;274(2):359–69.

46. Bull S, White SK, Piechnik SK, Flett AS, Ferreira VM, Loudon M, et al. Human non-contrast T1 values and correlation with histology in diffuse fibrosis. Heart. 2013 Jul;99(13):932–7.

47. Bluemke DA, Pattanayak P. Tissue characterization of the myocardium by MR and CT imaging. Radiol Clin North Am. 2015 Mar;53(2):413–23.

48. Mądry W, Karolczak MA. Physiological basis in the assessment of myocardial mechanics using speckle-tracking echocardiography 2D. Part I. J Ultrason. 2016 Jun;16(65):135–44.

49. Farsalinos KE, Daraban AM, Ünlü S, Thomas JD, Badano LP, Voigt JU. Head-to-Head Comparison of Global Longitudinal Strain Measurements among Nine Different Vendors: The EACVI/ASE Inter-Vendor Comparison Study. J Am Soc Echocardiogr. 2015 Oct;28(10):1171–1181.e2.

50. Ünlü S, Mirea O, Duchenne J, Pagourelias ED, Bézy S, Thomas JD, et al. Comparison of Feasibility, Accuracy, and Reproducibility of Layer-Specific Global Longitudinal Strain Measurements Among Five Different Vendors: A Report from the EACVI-ASE Strain Standardization Task Force. J Am Soc Echocardiogr. 2018 Mar;31(3):374–380.e1.

51. Bauer F, Bénigno S, Lemercier M, Tapiéro S, Eltchaninoff H, Tron C, et al. Early improvement of left ventricular function after implantation of a transcutaneous aortic valve: a tissue Doppler ultrasound study. Arch Cardiovasc Dis. 2009 Apr;102(4):311–8.

52. Kovács A, Oláh A, Lux Á, Mátyás C, Németh BT, Kellermayer D, et al. Strain and strain rate by speckle-tracking echocardiography correlate with pressure-volume loop-derived contractility indices in a rat model of athlete's heart. Am J Physiol Heart Circ Physiol. 2015 Apr;308(7):H743–8.

53. Dahle GO, Stangeland L, Moen CA, Salminen PR, Haaverstad R, Matre K, et al. The influence of acute unloading on left ventricular strain and strain rate by speckle tracking echocardiography in a porcine model. Am J Physiol Heart Circ Physiol. 2016 May;310(10):H1330–9.

54. Nagel E, Stuber M, Burkhard B, Fischer SE, Scheidegger MB, Boesiger P, et al. Cardiac rotation and relaxation in patients with aortic valve stenosis. Eur Heart J. 2000 Apr;21(7):582–9.

55. Sandstede JJ, Johnson T, Harre K, Beer M, Hofmann S, Pabst T, et al. Cardiac systolic rotation and contraction before and after valve replacement for aortic stenosis: a myocardial tagging study using MR imaging. AJR Am J Roentgenol. 2002 Apr;178(4):953–8.

56. Al Musa T, Uddin A, Swoboda PP, Garg P, Fairbairn TA, Dobson LE, et al. Myocardial strain and symptom severity in severe aortic stenosis: insights from cardiovascular magnetic resonance. Quant Imaging Med Surg. 2017 Feb;7(1):38–47.

57. Schneeweis C, Lapinskas T, Schnackenburg B, Berger A, Hucko T, Kelle S, et al. Comparison of myocardial tagging and feature tracking in patients with severe aortic stenosis. J Heart Valve Dis. 2014 Jul;23(4):432–40.

58. Singh A, Steadman CD, Khan JN, Horsfield MA, Bekele S, Nazir SA, et al. Intertechnique agreement and interstudy reproducibility of strain and diastolic strain rate at 1.5 and 3 Tesla: a comparison of feature-tracking and tagging in patients with aortic stenosis. J Magn Reson Imaging. 2015 Apr;41(4):1129–37.

59. Chin CW, Messika-Zeitoun D, Shah AS, Lefevre G, Bailleul S, Yeung EN, et al. A clinical risk score of myocardial fibrosis predicts adverse outcomes in aortic stenosis. Eur Heart J. 2016 Feb;37(8):713–23.

60. Treibel TA, Kozor R, Fontana M, Torlasco C, Reant P, Badiani S, et al. Sex Dimorphism in the Myocardial Response to Aortic Stenosis. JACC Cardiovasc Imaging. 2017 Nov.

61. Bax JJ, Delgado V. Advanced imaging in valvular heart disease. Nat Rev Cardiol. 2017 Apr;14(4):209–23.

62. Muraru D, Niero A, Rodriguez-Zanella H, Cherata D, Badano L. Three-dimensional speckle-tracking echocardiography: benefits and limitations of integrating myocardial mechanics with three-dimensional imaging. Cardiovasc Diagn Ther. 2018 Feb;8(1):101–17.

63. Dulgheru R, Pibarot P, Sengupta PP, Piérard LA, Rosenhek R, Magne J, et al.; Viewpoint of the Heart Valve Clinic International Database (HAVEC) Group. Multimodality Imaging Strategies for the Assessment of Aortic Stenosis: Viewpoint of the Heart Valve Clinic International Database (HAVEC) Group. Circ Cardiovasc Imaging. 2016 Feb;9(2):e004352.

64. Scully PR, Bastarrika G, Moon JC, Treibel TA. Myocardial Extracellular Volume Quantification by Cardiovascular Magnetic Resonance and Computed Tomography. Curr Cardiol Rep. 2018 Mar;20(3):15.

Cardiac resynchronization therapy optimization

1. Brignole M, Auricchio A, Baron-Esquivias G, Bordachar P, Boriani G, Breithardt OA, et al.; Document Reviewers. 2013 ESC Guidelines on cardiac pacing and cardiac resynchronization therapy: the Task Force on cardiac pacing and resynchronization therapy of the European Society of Cardiology (ESC). Developed in collaboration with the European Heart Rhythm Association (EHRA). Eur Heart J. 2013 Aug;34(29):2281–329.

2. Epstein AE, DiMarco JP, Ellenbogen KA, Estes NA 3rd, Freedman RA, Gettes LS, et al. 2012 ACCF/AHA/HRS focused update incorporated into the ACCF/AHA/HRS 2008 guidelines for device-based therapy of cardiac rhythm abnormalities: a report of the American College of Cardiology Foundation/American Heart Association Task Force on Practice Guidelines and the Heart Rhythm Society. J Am Coll Cardiol. 2013 Jan;61(3):e6–75.

3. Goldenberg I, Kutyifa V, Klein HU, Cannom DS, Brown MW, Dan A, et al. Survival with cardiac-resynchronization therapy in mild heart failure. N Engl J Med. 2014 May;370(18):1694–701.

4. Jarcho JA. Biventricular pacing. N Engl J Med. 2006;355(3):288–94.

5. Upadhyay GA, Chatterjee NA, Kandala J, Friedman DJ, Park MY, Tabtabai SR, et al. Assessing mitral regurgitation in the prediction of clinical outcome after cardiac resynchronization therapy. Heart Rhythm. 2015 Jun;12(6):1201–8.

6. Leong DP, Höke U, Delgado V, Auger D, Witkowski T, Thijssen J, et al. Right ventricular function and survival following cardiac resynchronisation therapy. Heart. 2013 May;99(10):722–8.

7. Barold SS, Herweg B. Cardiac resynchronization in patients with atrial fibrillation. J Atr Fibrillation. 2015 Dec;8(4):1383.

8. Gorcsan J 3rd, Abraham T, Agler DA, Bax JJ, Derumeaux G, Grimm RA, et al.; American Society of Echocardiography Dyssynchrony Writing Group. Echocardiography for cardiac resynchronization therapy: recommendations for performance and reporting—a report from the American Society of Echocardiography Dyssynchrony Writing Group endorsed by the Heart Rhythm Society. J Am Soc Echocardiogr. 2008 Mar;21(3):191–213.

9. Assadian Rad M, Tabarzan Baboli N, Barzigar A, Keirkhah J, Soltanipour S, Bonakdar HR, et al. The role of the fragmented QRS complexes on a routine 12-lead ECG in predicting non-responsiveness to cardiac resynchronization therapy. Anatol J Cardiol. 2015 Mar;15(3):204–8.

10. Donal E, Delgado V, Magne J, Bucciarelli-Ducci C, Leclercq C, Cosyns B, et al. Rational and design of EuroCRT: an international observational study on multi-modality imaging and cardiac resynchronization therapy. Eur Heart J Cardiovasc Imaging. 2017 Oct;18(10):1120–7.

11. Kloppe A, Lemke B, Zarse M. New technologies in the optimization of CRT programming. Herzschrittmacherther Elektrophysiol. 2008 Mar;19(1):19–29. German.

12. Exner DV, Auricchio A, Singh JP. Contemporary and future trends in cardiac resynchronization therapy to enhance response. Heart Rhythm. 2012 Aug;9(8 Suppl):S27–35.

13. Chiariello M, Perrone-Filardi P. Pathophysiology of heart failure. Miner Electrolyte Metab. 1999 Jan-Apr;25(1-2):6–10.

14. Gjesdal O, Remme EW, Opdahl A, Skulstad H, Russell K, Kongsgaard E, et al. Mechanisms of abnormal systolic motion of the interventricular septum during left bundle-branch block. Circ Cardiovasc Imaging. 2011 May;4(3):264–73.

15. Thompson K, Saab G, Birnie D, Chow BJ, Ukkonen H, Ananthasubramaniam K, et al. Is septal glucose metabolism altered in patients with left bundle branch block and ischemic cardiomyopathy? J Nucl Med. 2006 Nov;47(11):1763–8.

16. Smiseth OA, Remme EW. Regional left ventricular electric and mechanical activation and relaxation. J Am Coll Cardiol. 2006 Jan;47(1):173–4.

17. Riedlbauchová L, Brunken R, Jaber WA, Popová L, Patel D, Lánská V, et al. The impact of myocardial viability on the clinical outcome of cardiac resynchronization therapy. J Cardiovasc Electrophysiol. 2009 Jan;20(1):50–7.

18. Szulik M, Tillekaerts M, Vangeel V, Ganame J, Willems R, Lenarczyk R, et al. Assessment of apical rocking: a new, integrative approach for selection of candidates for cardiac resynchronization therapy. Eur J Echocardiogr. 2010 Dec;11(10):863–9.

19. Haugaa KH, Edvardsen T, Smiseth OA. Mechanical dyssynchrony-resurrected as a flashing and rocking parameter to predict prognosis after cardiac resynchronization therapy. Eur Heart J Cardiovasc Imaging. 2017 Oct;18(10):1118–9.

20. Beela AS, Ünlü S, Duchenne J, Ciarka A, Daraban AM, Kotrc M, et al. Assessment of mechanical dyssynchrony can improve the prognostic value of guideline-based patient selection for cardiac resynchronization therapy. Eur Heart J Cardiovasc Imaging. 2019 Jan;20(1):66–74.

21. Gorcsan J 3rd, Abraham T, Agler DA, Bax JJ, Derumeaux G, Grimm RA, et al.; American Society of Echocardiography Dyssynchrony Writing Group. Echocardiography for cardiac resynchronization therapy: recommendations for performance and reporting—a report from the American Society of Echocardiography Dyssynchrony Writing Group endorsed by the Heart Rhythm Society. J Am Soc Echocardiogr. 2008 Mar;21(3):191–213.

22. Seo Y, Ishizu T, Machino-Ohtsuka T, Yamamoto M, Machino T, Kuroki K, et al. Incremental Value of Speckle Tracking Echocardiography to Predict Cardiac Resynchronization Therapy (CRT) Responders. J Am Heart Assoc. 2016 Oct;5(10):e003882.

23. Khan SG, Klettas D, Kapetanakis S, Monaghan MJ. Clinical utility of speckle-tracking echocardiography in cardiac resynchronisation therapy. Echo Res Pract. 2016 Mar;3(1):R1–11.

24. Van Everdingen WM, Paiman ML, van Deursen CJ, Cramer MJ, Vernooy K, Delhaas T, et al. Comparison of septal strain patterns in dyssynchronous heart failure between speckle tracking echocardiography vendor systems. J Electrocardiol. 2015 Jul-Aug;48(4):609–16.

25. Cvijic M, Duchenne J, Ünlü S, Michalski B, Aarones M, Winter S, et al. Timing of myocardial shortening determines left ventricular regional myocardial work and regional

remodelling in hearts with conduction delays. Eur Heart J Cardiovasc Imaging. 2018 Aug;19(8):941–949.

26. Onishi T, Saha SK, Ludwig DR, Onishi T, Marek JJ, Cavalcante JL, et al. Feature tracking measurement of dyssynchrony from cardiovascular magnetic resonance cine acquisitions: comparison with echocardiographic speckle tracking. J Cardiovasc Magn Reson. 2013 Oct;15(1):95.

27. Revah G, Wu V, Huntjens PR, Piekarski E, Chyou JY, Axel L. Cardiovascular magnetic resonance features of mechanical dyssynchrony in patients with left bundle branch block. Int J Cardiovasc Imaging. 2016 Sep;32(9):1427–38.

28. Ono S, Nohara R, Kambara H, Okuda K, Kawai C. Regional myocardial perfusion and glucose metabolism in experimental left bundle branch block. Circulation. 1992 Mar;85(3):1125–31.

29. Adelstein EC, Saba S. Scar burden by myocardial perfusion imaging predicts echocardiographic response to cardiac resynchronization therapy in ischemic cardiomyopathy. Am Heart J. 2007 Jan;153(1):105–12.

30. Sweeney MO, van Bommel RJ, Schalij MJ, Borleffs CJ, Hellkamp AS, Bax JJ. Analysis of ventricular activation using surface electrocardiography to predict left ventricular reverse volumetric remodeling during cardiac resynchronization therapy. Circulation. 2010 Feb;121(5):626–34.

31. Everett RJ, Stirrat CG, Semple SI, Newby DE, Dweck MR, Mirsadraee S. Assessment of myocardial fibrosis with T1 mapping MRI. Clin Radiol. 2016 Aug;71(8):768–78.

32. Krombach GA, Niendorf T, Günther RW, Mahnken AH. Tissue characterization of the myocardium: state of the art characterization by MR and CT imaging. Radiol Clin North Am. 2015 Mar;53(2):413–23.

33. Ukkonen H, Beanlands RS, Burwash IG, de Kemp RA, Nahmias C, Fallen E, et al. Effect of cardiac resynchronization on myocardial efficiency and regional oxidative metabolism. Circulation. 2003;107(1):28–31.

34. Sharma A, Bax JJ, Vallakati A, Goel S, Lavie CJ, Kassotis J, et al. Meta-analysis of the relation of baseline right ventricular function to response to cardiac resynchronization therapy. Am J Cardiol. 2016 Apr;117(8):1315–21.

35. Scuteri L, Rordorf R, Marsan NA, Landolina M, Magrini G, Klersy C, et al. Relevance of echocardiographic evaluation of right ventricular function in patients undergoing cardiac resynchronization therapy. Pacing Clin Electrophysiol. 2009 Aug;32(8):1040–9.

36. Damy T, Ghio S, Rigby AS, Hittinger L, Jacobs S, Leyva F, et al. Interplay between right ventricular function and cardiac resynchronization therapy: an analysis of the CARE-HF trial (Cardiac Resynchronization-Heart Failure). J Am Coll Cardiol. 2013 May;61(21):2153–60.

37. Sharma A, Bax JJ, Vallakati A, Goel S, Lavie CJ, Kassotis J, et al. Meta-Analysis of the Relation of Baseline Right Ventricular Function to Response to Cardiac Resynchronization Therapy. Am J Cardiol. 2016 Apr;117(8):1315–21.

38. Abdelhamid MA, Ghanem MT, Abdelmotaleb AM. Assessment of right ventriclular systolic function prior to cardiac resynchronization therapy: does it make any difference? Indian Heart J. 2017 Nov - Dec;69(6):731–5.

39. Schmeisser A, Rauwolf T, Ghanem A, Groscheck T, Adolf D, Grothues F, et al. Right heart function interacts with left ventricular remodeling after CRT: A pressure volume loop study. Int J Cardiol. 2018 Oct;268:156–61.

40. Martens P, Verbrugge FH, Bertrand PB, Verhaert D, Vandervoort P, Dupont M, et al. Effect of Cardiac Resynchronization Therapy on Exercise-Induced Pulmonary Hypertension and Right Ventricular-Arterial Coupling. Circ Cardiovasc Imaging. 2018 Sep;11(9):e007813.

41. Flügge AK, Wasmer K, Orwat S, Abdul-Khaliq H, Helm PC, Bauer U, et al.; German Competence Network for Congenital Heart Defects Investigators. Cardiac resynchronization therapy in congenital heart disease: Results from the German National Register for Congenital Heart Defects. Int J Cardiol. 2018 Dec;273:108–11.

42. Moore JP, Cho D, Lin JP, Lluri G, Reardon LC, Aboulhosn JA, et al. Implantation techniques and outcomes after cardiac resynchronization therapy for congenitally corrected transposition of the great arteries. Heart Rhythm. 2018 Dec;15(12):1808–15.

43. Karpawich PP, Bansal N, Samuel S, Sanil Y, Zelin K. 16 Years of Cardiac Resynchronization Pacing Among Congenital Heart Disease Patients: Direct Contractility (dP/dt-max) Screening When the Guidelines Do Not Apply. JACC Clin Electrophysiol. 2017 Aug;3(8):830–41.

44. Anjewierden S, Aziz PF. Resynchronization Therapy for Patients with Congenital Heart Disease: Are We Ready for Prime Time? Curr Cardiol Rep. 2018 Jul;20(9):75.

45. Breithardt OA, Sinha AM, Schwammenthal E, Bidaoui N, Markus KU, Franke A, et al. Acute effects of cardiac resynchronization therapy on functional mitral regurgitation in advanced systolic heart failure. J Am Coll Cardiol. 2003 Mar;41(5):765–70.

46. Cleland JG, Daubert JC, Erdmann E, Freemantle N, Gras D, Kappenberger L, et al. The effect of cardiac resynchronization on morbidity and mortality in heart failure. N Engl J Med. 2005;352(15):1539–49.

47. Cabrera-Bueno F, García-Pinilla JM, Peña-Hernández J, Jiménez-Navarro M, Gómez-Doblas JJ, Barrera-Cordero A, et al. Repercussion of functional mitral regurgitation on reverse remodelling in cardiac resynchronization therapy. Europace. 2007 Sep;9(9):757–61.

48. Onishi T, Onishi T, Marek JJ, Ahmed M, Haberman SC, Oyenuga O, et al. Mechanistic features associated with improvement in mitral regurgitation after cardiac resynchronization therapy and their relation to long-term patient outcome. Circ Heart Fail. 2013 Jul;6(4):685–93.

49. Binda C, Menet A, Appert L, Ennezat PV, Delelis F, Castel AL, et al. Time course of secondary mitral regurgitation in patients with heart failure receiving cardiac resynchronization therapy: impact on long-term outcome beyond left ventricular reverse remodelling. Arch Cardiovasc Dis. 2018 May;111(5):320–31.

50. Upadhyay GA, Steinberg JS. Managing atrial fibrillation in the CRT patient: controversy or consensus? Heart Rhythm. 2012 Aug;9(8 Suppl):S51–9.

51. Gianni C, Di Biase L, Mohanty S, Gökoğlan Y, Güneş MF, Al-Ahmad A, et al. How to improve cardiac resynchronization therapy benefit in atrial bibrillation patients: pulmonary vein isolation (and beyond). Heart Fail Clin. 2017 Jan;13(1):199–208.

52. Jeevanantham V, Turagam M, Shanberg D, Reddy M, Atoui M, Daubert JP, et al. Cardiac Resynchronization Therapy prevents progression of renal failure in heart failure patients. Indian Pacing Electrophysiol J. 2016 Jul - Aug;16(4):115–9.

53. Goldenberg I, Moss AJ, McNitt S, Barsheshet A, Gray D, Andrews ML, et al.; Multicenter Automatic Defibrillator Implantation Trial—Cardiac Resynchronization Therapy Investigators. Relation between renal function and response to cardiac resynchronization therapy in Multicenter Automatic Defibrillator Implantation Trial—Cardiac Resynchronization Therapy (MADIT-CRT). Heart Rhythm. 2010 Dec;7(12):1777–82.

54. Sun H, Guan Y, Wang L, Zhao Y, Lv H, Bi X, et al. Influence of diabetes on cardiac resynchronization therapy in heart failure patients: a meta-analysis. BMC Cardiovasc Disord. 2015 Mar;15(1):25.

55. Kirubakaran S, Ladwiniec A, Arujuna A, Ginks M, McPhail M, Bostock J, et al. Male gender and chronic obstructive pulmonary disease predict a poor clinical response in patients undergoing cardiac resynchronisation therapy. Int J Clin Pract. 2011 Mar;65(3):281–8.

56. Ruwald MH. Co-Morbidities and Cardiac Resynchronization Therapy: When Should They Modify Patient Selection? J Atr Fibrillation. 2015 Jun;8(1):1238.

57. Brouwers C, Versteeg H, Meine M, Heijnen CJ, Kavelaars AM, Pedersen SS, et al. Association between brain natriuretic peptide, markers of inflammation and the objective

and subjective response to cardiac resynchronization therapy. Brain Behav Immun. 2014 Aug;40:211–8.

58. Truong QA, Januzzi JL, Szymonifka J, Thai WE, Wai B, Lavender Z, et al. Coronary sinus biomarker sampling compared to peripheral venous blood for predicting outcomes in patients with severe heart failure undergoing cardiac resynchronization therapy: the BIOCRT study. Heart Rhythm. 2014 Dec;11(12):2167–75.

59. Beaudoin J, Singh JP, Szymonifka J, Zhou Q, Levine RA, Januzzi JL, et al. Novel heart failure biomarkers predict improvement of mitral regurgitation in patients receiving cardiac resynchronization therapy—the BIOCRT Study. Can J Cardiol. 2016 Dec;32(12):1478–84.

60. Lin J, Buhr KA, Kipp R. Effect of PR Interval on Outcomes Following Cardiac Resynchronization Therapy: A Secondary Analysis of the COMPANION Trial. J Cardiovasc Electrophysiol. 2017 Feb;28(2):185–91.

61. Hsing JM, Selzman KA, Leclercq C, Pires LA, McLaughlin MG, McRae SE, et al. Paced left ventricular QRS width and ECG parameters predict outcomes after cardiac resynchronization therapy: PROSPECT-ECG substudy. Circ Arrhythm Electrophysiol. 2011 Dec;4(6):851–7.

62. Sinner GJ, Gupta VA, Seratnahaei A, Charnigo RJ, Darrat YH, Elayi SC, et al. Atrioventricular dyssynchrony from empiric device settings is common in cardiac resynchronization therapy and adversely impacts left ventricular morphology and function. Echocardiography. 2017 Apr;34(4):496–503.

63. Meluzín J, Novák M, Müllerová J, Krejcí J, Hude P, Eisenberger M, et al. A fast and simple echocardiographic method of determination of the optimal atrioventricular delay in patients after biventricular stimulation. Pacing Clin Electrophysiol. 2004 Jan;27(1):58–64.

64. Van Gelder BM, Bracke FA, Meijer A, Lakerveld LJ, Pijls NH. Effect of optimizing the VV interval on left ventricular contractility in cardiac resynchronization therapy. Am J Cardiol. 2004 Jun;93(12):1500–3.

65. Bogaard MD, Meine M, Doevendans PA. Programmed versus effective VV delay during CRT optimization: when what you see is not what you get. Pacing Clin Electrophysiol. 2013 Apr;36(4):403–9.

66. Stankovic I, Belmans A, Prinz C, Ciarka A, Maria Daraban A, Kotrc M, et al. The association of volumetric response and long-term survival after cardiac resynchronization therapy. Eur Heart J Cardiovasc Imaging. 2017 Oct;18(10):1109–17.

67. Stankovic I, Prinz C, Ciarka A, Daraban AM, Mo Y, Aarones M, et al. Long-Term Outcome After CRT in the Presence of Mechanical Dyssynchrony Seen with Chronic RV Pacing or Intrinsic LBBB. JACC Cardiovasc Imaging. 2017 Oct;10(10 10 Pt A):1091–9.

68. Weigand S, Karl M, Brkić A, Lennerz C, Grebmer C, Blažek P, et al. The impact of multipole pacing on left ventricular function in patients with cardiac resynchronization therapy - A real-time three-dimensional echocardiography approach. Int J Cardiol. 2018 Dec;272:238–43.

69. Vondrak J, Marek D, Vecera J, et al. Cardiac resynchronisation therapy optimisation of interventricular delay by the systolic dyssynchrony index: a comparative, randomised, 12-month follow-up study. Hellenic J Cardiol. 2017. doi: 10.1016/j.hjc.2017.11.003.

70. Höke U, Bax JJ, Delgado V, Ajmone Marsan N. Assessment of left ventricular dyssynchrony by three-dimensional echocardiography: prognostic value in patients undergoing cardiac resynchronization therapy. J Cardiovasc Electrophysiol. 2018 May;29(5):780–7.

71. Tatsumi K, Tanaka H, Tsuji T, Kaneko A, Ryo K, Yamawaki K, et al. Strain dyssynchrony index determined by three-dimensional speckle area tracking can predict response to cardiac resynchronization therapy. Cardiovasc Ultrasound. 2011 Apr;9(1):11.

72. Vecera J, Penicka M, Eriksen M, Russell K, Bartunek J, Vanderheyden M, et al. Wasted septal work in left ventricular dyssynchrony: a novel principle to predict response to cardiac resynchronization therapy. Eur Heart J Cardiovasc Imaging. 2016 Jun;17(6):624–32.

73. Galli E, Leclercq C, Hubert A, Bernard A, Smiseth OA, Mabo P, et al. Role of myocardial constructive work in the identification of responders to CRT. Eur Heart J Cardiovasc Imaging. 2018 Sep;19(9):1010–8.

74. Galli E, Leclercq C, Fournet M, Hubert A, Bernard A, Smiseth OA, et al. Value of Myocardial Work Estimation in the Prediction of Response to Cardiac Resynchronization Therapy. J Am Soc Echocardiogr. 2018 Feb;31(2):220–30.

75. Gilewski W, Błażejewski J, Karasek D, Banach J, Wołowiec Ł, Płońska-Gościniak E, et al. Are changes in heart rate, observed during dobutamine stress echocardiography, associated with a response to cardiac resynchronisation therapy in patients with severe heart failure? Results of a multicentre ViaCRT study. Kardiol Pol. 2018;76(3):611–7.

76. Pugliese NR, Fabiani I, Mandoli GE, Guarini G, Galeotti GG, Miccoli M, et al. Echo-derived peak cardiac power output-to-left ventricular mass with cardiopulmonary exercise testing predicts outcome in patients with heart failure and depressed systolic function. Eur Heart J Cardiovasc Imaging. 2018 Nov. https://doi.org/10.1093/ehjci/jey172.

77. Guazzi M, Bandera F, Ozemek C, Systrom D, Arena R. Cardiopulmonary Exercise Testing: What Is its Value? J Am Coll Cardiol. 2017 Sep;70(13):1618–36.

78. Wong JA, Yee R, Stirrat J, Scholl D, Krahn AD, Gula LJ, et al. Influence of pacing site characteristics on response to cardiac resynchronization therapy. Circ Cardiovasc Imaging. 2013 Jul;6(4):542–50.

79. Antoniadis AP, Sieniewicz B, Gould J, Porter B, Webb J, Claridge S, et al. Updates in cardiac resynchronization therapy for chronic heart failure: review of multisite pacing. Curr Heart Fail Rep. 2017 Aug;14(5):376–83.

80. Markstad H, Bakos Z, Ostenfeld E, Geijer M, Carlsson M, Borgquist R. Preoperative CT of cardiac veins for planning left ventricular lead placement in cardiac resynchronization therapy. Acta Radiol. 2018. doi: 10.1177/0284185118803796.

81. Antoniadis AP, Behar JM, Sieniewicz B, Gould J, Niederer S, Rinaldi CA. A comparison of the different features of quadripolar left ventricular pacing leads to deliver cardiac resynchronization therapy. Expert Rev Med Devices. 2017 Sep;14(9):697–706.

82. Tomasi C, Corsi C, Turco D, Severi S. An exploratory study on coronary sinus lead tip three-dimensional trajectory changes in cardiac resynchronization therapy. Heart Rhythm. 2013 Sep;10(9):1360–7.

83. Miranda RI, Nault M, Johri A, Simpson CS, Michael KA, Abdollah H, et al. Maximal electric separation-guided placement of right ventricular lead improves responders in cardiac resynchronization defibrillator therapy. Circ Arrhythm Electrophysiol. 2012 Oct;5(5):927–32.

84. Su H, Bao P, Chen KY, Yan J, Xu J, Yu F, et al. Influence of the Right Ventricular Lead Location on Ventricular Arrhythmias in Cardiac Resynchronization Therapy. Chin Med J (Engl). 2018 Oct;131(20):2402–9.

85. Lercher P, Lunati M, Rordorf R, Landolina M, Badie N, Qu F, et al. Long-term reverse remodeling by cardiac resynchronization therapy with MultiPoint Pacing: a feasibility study of noninvasive hemodynamics-guided device programming. Heart Rhythm. 2018. doi: 10.1016/j.hrthm.2018.06.032.

86. Sharma PS, Vijayaraman P. His Bundle Pacing Or Biventricular Pacing For Cardiac Resynchronization Therapy In Heart Failure: Discovering New Methods For An Old Problem. J Atr Fibrillation. 2016 Dec;9(4):1501.

87. Mazurek M, Jędrzejczyk-Patej E, Lenarczyk R, Liberska A, Przybylska-Siedlecka K, Kozieł M, et al. Do we need to monitor the percentage of biventricular pacing day by day? Int J Cardiol. 2016 Oct;221:81–9.

88. Jin H, Gu M, Hua W, Fan XH, Niu HX, Ding LG, et al. Predictors of super-response to cardiac resynchronization therapy: the significance of heart failure medication, pre-implant left ventricular geometry and high percentage of biventricular pacing. J Geriatr Cardiol. 2017 Dec;14(12):737–42.

89. Duncker D, Delnoy PP, Nägele H, Mansourati J, Mont L, Anselme F, et al. First clinical evaluation of an atrial haemodynamic sensor lead for automatic optimization of cardiac resynchronization therapy. Europace. 2016 May;18(5):755–61.

90. Brugada J, Delnoy PP, Brachmann J, Reynolds D, Padeletti L, Noelker G, et al.; RESPOND CRT Investigators. Contractility sensor-guided optimization of cardiac resynchronization therapy: results from the RESPOND-CRT trial. Eur Heart J. 2017 Mar;38(10):730–8.

91. Sermesant M, Chabiniok R, Chinchapatnam P, Mansi T, Billet F, Moireau P, et al. Patient-specific electromechanical models of the heart for the prediction of pacing acute effects in CRT: a preliminary clinical validation. Med Image Anal. 2012 Jan;16(1):201–15.

92. Panthee N, Okada J, Washio T, Mochizuki Y, Suzuki R, Koyama H, et al. Tailor-made heart simulation predicts the effect of cardiac resynchronization therapy in a canine model of heart failure. Med Image Anal. 2016 Jul;31:46–62.

93. Østvik A, Smistad E, Aase SA, Haugen BO, Lovstakken L. Real-Time Standard View Classifcation in Transthoracic Echocardiography Using Convolutional Neural Networks. Ultrasound Med Biol. 2019 Feb;45(2):374-384.

94. Leng S, Yang X, Zhao X, Zeng Z, Su Y, Koh AS, et al. Computational Platform Based on Deep Learning for Segmenting Ventricular Endocardium in Long-axis Cardiac MR Imaging. Conf Proc IEEE Eng Med Biol Soc. 2018 Jul;2018:4500–3.

95. Vukicevic M, Mosadegh B, Min JK, Little SH. Cardiac 3D printing and its future directions. JACC Cardiovasc Imaging. 2017 Feb;10(2):171–84.

96. Chen Z, Niederer S, Shanmugam N, Sermesant M, Rinaldi CA. Cardiac computational modeling of ventricular tachycardia and cardiac resynchronization therapy: a clinical perspective. Minerva Cardioangiol. 2017 Aug;65(4):380–97.

97. Warriner DR, Jackson T, Zacur E, Sammut E, Sheridan P, Hose DR, et al. An Asymmetric Wall-Thickening Pattern Predicts Response to Cardiac Resynchronization Therapy. JACC Cardiovasc Imaging. 2018 Oct;11(10):1545–6.

98. Lumens J, Tayal B, Walmsley J, Delgado-Montero A, Huntjens PR, Schwartzman D, et al. Differentiating Electromechanical from Non-Electrical Substrates of Mechanical Discoordination to Identify Responders to Cardiac Resynchronization Therapy. Circ Cardiovasc Imaging. 2015 Sep;8(9):e003744.

Valve in Valve implantation for mitral valve failure

1. Habib G, Lancellotti P, Antunes MJ, Bongiorni MG, Casalta JP, Del Zotti F, et al. 2015 ESC Guidelines for the management of infective endocarditis: The Task Force for the Management of Infective Endocarditis of the European Society of Cardiology (ESC). Endorsed by: European Association for Cardio-Thoracic Surgery (EACTS), the European Association of Nuclear Medicine (EANM). Eur Heart J. 2015 Nov 21;36(44):3075-128.

2. Baddour LM, Wilson WR, Bayer AS, Fowler VG, Tleyjeh IM, Rybak MJ, et al. Infective Endocarditis in Adults: Diagnosis, Antimicrobial Therapy, and Management of Complications.

A Scientific Statement for Healthcare Professionals From the American Heart Association. Circulation. 2015 Sep 15.

3. Musci M, Hübler M, Amiri A, Stein J, Kosky S, Meyer R, et al. Surgical treatment for active infective prosthetic valve endocarditis: 22-year single-centre experience. Eur J Cardiothorac Surg. 2010, 38: 528-538.

4. Habib G, Tribouilloy C, Thuny F, Giorgi R, Brahim A, Amazouz M, et al. Prosthetic valve endocarditis: who needs surgery? A multicentre study of 104 cases. Heart. 2005, 91: 954-959.

5. Baumgartner H, Falk V, Bax JJ, De Bonis M, Hamm C, Holm PJ, et al. 2017 ESC/EACTS Guidelines for the management of valvular heart disease. The Task Force for the Management of Valvular Heart Disease of the European Society of Cardiology (ESC) and the European Association for Cardio-Thoracic Surgery (EACTS) Authors/Task Force Members. Eur Heart J. 2017 Aug 26.

6. Nishimura RA, Otto CM, Bonow RO, Carabello BA, Erwin JP 3rd, Fleisher LA, et el. 2017 AHA/ACC Focused Update of the 2014 AHA/ACC Guideline for the Management of Patients With Valvular Heart Disease: A Report of the American College of Cardiology/American Heart Association Task Force on Clinical Practice Guidelines. Circulation. 2017 Jun 20;135(25):e1159-e1195.

7. Lancellotti P, Rosenhek R, Pibarot P, Iung B, Otto CM, Tornos P, et al. ESC Working Group on Valvular Heart Disease position paper-heart valve clinics: organization, structure, and experiences. Eur Heart J. 2013 Jun;34(21):1597-606.

8. Chambers JB, Prendergast B, Iung B, Rosenhek R, Zamorano JL, Piérard LA, et al. Standards defining a 'Heart Valve Centre': ESC Working Group on Valvular Heart Disease and European Association for Cardiothoracic Surgery Viewpoint. Eur Heart J. 2017 Jul 21;38(28):2177-2183.

9. Cerillo AG, Chiaramonti F, Murzi M, Bevilacqua S, Cerone E, Palmieri C, et al. Transcatheter valve in valve implantation for failed mitral and tricuspid bioprosthesis. Catheter Cardiovasc Interv. 2011 Dec 1;78(7):987-95.

10. Schaefer A, Conradi L, Seiffert M, Lubos E, Blankenberg S, Reichenspurner H, et al. Valve-in-Valve Procedures in Failing Biological Xenografts Using a Novel Balloon-Expandable Device: Experience in Aortic, Mitral, and Tricuspid Positions. Thorac Cardiovasc Surg. 2016 Aug;64(5):366-73.

11. Ye J, Cheung A, Yamashita M, Wood D, Peng D, Gao M, et al. Transcatheter Aortic and Mitral Valve-in-Valve Implantation for Failed Surgical Bioprosthetic Valves: An 8-Year Single-Center Experience. JACC Cardiovasc Interv. 2015 Nov;8(13):1735-44.

12. Eggebrecht H, Schäfer U, Treede H, Boekstegers P, Babin-Ebell J, Ferrari M, et al. Valve-in-valve transcatheter aortic valve implantation for degenerated bioprosthetic heart valves. JACC Cardiovasc Interv. 2011 Nov;4(11):1218-27.

13. Murzi M, Berti S, Gasbarri T, Trianni G, Maffei S, Solinas M, et al. Transapical transcatheter mitral valve-in-valve implantation versus minimally invasive surgery for failed mitral bioprostheses. Interact Cardiovasc Thorac Surg. 2017;25(1):57.

14. Amat-Santos IJ, Messika-Zeitoun D, Eltchaninoff H, Kapadia S, Lerakis S, Cheema AN, et al. Infective endocarditis after transcatheter aortic valve implantation: results from a large multicenter registry. Circulation. 2015 May 5;131(18):1566-74.

15. Regueiro A, Linke A, Latib A, Ihlemann N, Urena M, Walther T, et al. Association Between Transcatheter Aortic Valve Replacement and Subsequent Infective Endocarditis and In-Hospital Death. JAMA. 2016 Sep 13;316(10):1083-92.

16. Dvir D, Webb J. Mitral valve-in-valve and valve-in-ring: technical aspects and procedural outcomes. EuroIntervention. 2016 Sep 18;12(Y):Y93-6.

Valve in valve for Dacron conduit

1. Rodriguez-Gabella T, Voisine P, Puri R, Pibarot P, Rodés-Cabau J. Aortic Bioprosthetic Valve Durability: Incidence, Mechanisms, Predictors, and Management of Surgical and Transcatheter Valve Degeneration. J Am Coll Cardiol. 2017 Aug 22;70(8):1013-1028.

2. Capodanno D, Petronio AS, Prendergast B, Eltchaninoff H, Vahanian A, Modine T, et al. Standardized definitions of structural deterioration and valve failure in assessing long-term durability of transcatheter and surgical aortic bioprosthetic valves: a consensus statement from the European Association of Percutaneous Cardiovascular Interventions (EAPCI) endorsed by the European Society of Cardiology (ESC) and the European Association for Cardio-Thoracic Surgery (EACTS). Eur J Cardiothorac Surg. 2017 Sep 1;52(3):408-417.

3. Etz CD, Girrbach FF, von Aspern K, Battellini R, Dohmen P, Hoyer A, et al. Longevity after aortic root replacement: is the mechanically valved conduit really the gold standard for quinquagenarians?. Circulation. 2013 Sep 10;128(11 Suppl 1):S253-62.

4. Baumgartner H, Falk V, Bax JJ, De Bonis M, Hamm C, Holm PJ, et al. 2017 ESC/EACTS Guidelines for the management of valvular heart disease. The Task Force for the Management of Valvular Heart Disease of the European Society of Cardiology (ESC) and the European Association for Cardio-Thoracic Surgery (EACTS) Authors/Task Force Members. Eur Heart J. 2017 Aug 26.

5. Nishimura RA, Otto CM, Bonow RO, Carabello BA, Erwin JP 3rd, Fleisher LA, et el. 2017 AHA/ACC Focused Update of the 2014 AHA/ACC Guideline for the Management of Patients With Valvular Heart Disease: A Report of the American College of Cardiology/American Heart

Association Task Force on Clinical Practice Guidelines. Circulation. 2017 Jun 20;135(25):e1159-e1195.

6. Lancellotti P, Rosenhek R, Pibarot P, Iung B, Otto CM, Tornos P, et al. ESC Working Group on Valvular Heart Disease position paper-heart valve clinics: organization, structure, and experiences. Eur Heart J. 2013 Jun;34(21):1597-606.

7. Chambers JB, Prendergast B, Iung B, Rosenhek R, Zamorano JL, Piérard LA, et al. Standards defining a 'Heart Valve Centre': ESC Working Group on Valvular Heart Disease and European Association for Cardiothoracic Surgery Viewpoint. Eur Heart J. 2017 Jul 21;38(28):2177-2183.

8. Dvir D, Webb J, Brecker S, Bleiziffer S, Hildick-Smith D, Colombo A, et al. Transcatheter aortic valve replacement for degenerative bioprosthetic surgical valves: results from the global valve-in-valve registry. Circulation. 2012 Nov 6;126(19):2335-44.

9. Schaefer A, Conradi L, Seiffert M, Lubos E, Blankenberg S, Reichenspurner H, et al. Valve-in-Valve Procedures in Failing Biological Xenografts Using a Novel Balloon-Expandable Device: Experience in Aortic, Mitral, and Tricuspid Positions. Thorac Cardiovasc Surg. 2016 Aug;64(5):366-73.

10. Ye J, Cheung A, Yamashita M, Wood D, Peng D, Gao M, et al. Transcatheter Aortic and Mitral Valve-in-Valve Implantation for Failed Surgical Bioprosthetic Valves: An 8-Year Single-Center Experience. JACC Cardiovasc Interv. 2015 Nov;8(13):1735-44.

11. Eggebrecht H, Schäfer U, Treede H, Boekstegers P, Babin-Ebell J, Ferrari M, et al. Valve-in-valve transcatheter aortic valve implantation for degenerated bioprosthetic heart valves. JACC Cardiovasc Interv. 2011 Nov;4(11):1218-27.

12. Spaziano M, Mylotte D, Thériault-Lauzier P, De Backer O, Søndergaard L, Bosmans J, et al. Transcatheter aortic valve implantation versus redo surgery for failing surgical aortic bioprostheses: a multicentre propensity score analysis. EuroIntervention. 2017 Nov 20;13(10):1149-1156.

13. Chiariello GA, Villa E, Messina A, Dalla Tomba M, Cirillo M, Brunelli F, et al. Perceval valve-in-valve implant for full root xenograft failure. J Card Surg. 2017 Sep;32(9):567-570.

14. Gatti G, Dell'Angela L, Pinamonti B, Moncada A, Minati A, Benussi B, et al. Aortic root replacement with a stented bioprosthetic valved conduit: mid-term results. J Heart Valve Dis. 2013 Jul;22(4):500-8.

15. Chambers JB, Garbi M, Nieman K, Myerson S, Pierard LA, Habib G, et al. Appropriateness criteria for the use of cardiovascular imaging in heart valve disease in adults: a European Association of Cardiovascular Imaging report of literature review and current practice. Eur Heart J Cardiovasc Imaging. 2017 May 1;18(5):489-498.

Publications

- Katbeh A, et al. Heart failure with preserved ejection fraction or non-cardiac dyspnea in paroxysmal atrial fibrillation: The role of left atrial strain. Int J Cardiol. 2020 Aug 31;S0167-5273(20)33720-7.

- Katbeh A, et al. Time course of left atrial performance in patients with paroxysmal atrial fibrillation undergoing radio-frequency catheter isolation of pulmonary veins. January 2020 EHJ Cardiovascular Imaging 21(Supplement_1) DOI: 10.1093/ehjci/jez319.631

- Katbeh A, et al. Atrial mechanical dispersion in patients with atrial fibrillation undergoing catheter ablation. January 2020 EHJ Cardiovascular Imaging 21(Supplement_1) DOI: 10.1093/ehjci/jez319.284

- Katbeh A, et al. The effect of hypertension and metabolic syndrome on left atrial function in patients with paroxysmal atrial fibrillation undergoing catheter ablation. European Heart Journal, Volume 40, Issue Supplement_1, October 2019, ehz747.0266

- Katbeh A, et al. Patterns of left atrial structural and functional remodeling after catheter ablation in paroxysmal and long-standing persistent atrial fibrillation. European Heart Journal, Volume 40, Issue Supplement_1, October 2019, ehz748.0783

- Katbeh A, et al. Cardiac Resynchronization Therapy Optimization: A Comprehensive Approach. Cardiology. 2019 May 22;142(2):116-127.

- Katbeh A, et al. Imaging of Myocardial Fibrosis and Its Functional Correlates in Aortic Stenosis: A Review and Clinical Potential. Cardiology. 2018;141(3):141-149.

-Katbeh A, et al. P651 Comparison between echocardiography and three-dimensional rotational angiography: the implication for successful percutaneous left atrial appendage closure. EHJ - Cardiovascular Imaging, Volume 20, Issue Supplement_1, January 2019, Pages i363–i381. https://doi.org/10.1093/ehjci/jey265

- Katbeh A, et al. Catheter ablation during sinus rhythm is associated with acute loss of left atrial contractile function in paroxysmal atrial fibrillation: a strain study. European Heart Journal, Volume 39, Issue suppl_1, August 2018, ehy566.P6469.

Posters

- Effects of catheter ablation on left atrial performance in different types of atrial fibrillation: a strain study. ESC congress 2020.

- Diagnosis of HFpEF in patients with dyspnea and paroxysmal atrial fibrillation: the role of left atrial strain. ESC congress 2020.

- Endoscopic repair of atrial functional mitral regurgitation in heart failure: long-term effects. ESC congress 2020.

- Long-term outcome of minimally invasive mitral valve annuloplasty in disproportionate mitral regurgitation. ESC congress 2020.

- Atrial strain performance in patients with paroxysmal atrial fibrillation undergoing successful radio-frequency catheter ablation. BSC congress 2020.

- Effects of catheter ablation on left atrial performance in different types of atrial fibrillation: a strain study. BSC congress 2020.

- Acute change in left atrial strain performance in patients with atrial fibrillation undergoing catheter ablation: A comparison of two vendors. BSC congress 2020.

- Minimally invasive surgical mitral valve repair of secondary mitral regurgitation improves outcome in non-ischemic heart failure with preserved ejection fraction. AHA congress 2019.

- Impact of obesity and age on left atrial function in patients with paroxysmal atrial fibrillation undergoing catheter ablation. ESC Heart Failure congress 2019.

- Impact of radiofrequency wide circumferential pulmonary vein isolation on left atrial geometry in patients with recurrent atrial fibrillation. EHRA congress 2019.

- Left atrial cardiotoxicity in breast cancer patients undergoing chemotherapy. BSC congress 2019.

- Comparison between echocardiography and three-dimensional rotational angiography: the implication for successful percutaneous left atrial appendage closure. EuroEcho 2018.

- How to assess left atrial function in patients with paroxysmal atrial fibrillation undergoing first or redo catheter ablation: what is the most promising parameter? EuroEcho 2018.

- Left atrial contractile function in breast cancer patients undergoing trastuzumab therapy. EuroEcho 2018.

- Left atrial contractile strain, left ventricular strain or ejection fraction to assess cardiotoxicity in breast cancer patients receiving trastuzumab therapy? EuroEcho 2018.

Case reports

- Transapical valve-in-valve implantation for bioprosthetic mitral valve failure secondary to endocarditis. ESC Clinical Case Gallery 2018. Euro PCR 2019.

- Transfemoral TAVI valve-in-valve for xenograft valve failure of valved dacron conduit: imaging-based case report. ESC Clinical Case Gallery 2018.

CV: Asim Katbeh. MD. FESC

DOB: 12/04/1983 Damascus, Syria

Email: asimkatbeh@yahoo.com

Clinical Experience

- PhD candidate at international PhD Program in cardiovascular pathophysiology and therapeutics at University of Naples Federico II, Italy from November 2016 to October 2020.

- Clinical research fellow in the Cardiovascular Centre Aalst, OLV Hospital, Belgium from October 2017 to September 2020.

- Clinical fellow in cardiovascular institute at Hospital Universitario Clinico San Carlos, Madrid, Spain from October 2014 to September 2016.

- Cardiologist at Damascus Heart Centre, Damascus, Syria from November 2013 to October 2014.

Medical Education

- Certification of Syrian Board of Cardiology with rate of very good, Damascus, Syria, October 2013.

- Cardiology fellowship at Damascus Heart Centre, Damascus, Syria from June 2011 to December 2014.

- Internal medicine residency in Syrian Health hospitals from July 2009 to June 2011.

- Medical Diploma with rate of very good, Damascus University, Damascus, Syria, March 2008.

- Internship in St Luke Episcopal hospital, Houston and John H. Stroger hospital of Cook County, Chicago, USA from April 2008 to March 2009.

- ECFMG Certification in United States of America, September 2008.

Research Experience

- Principal investigator in Cardiovascular Centre Aalst, OLV Hospital, Belgium since September 2017.

- Clinical research fellow in Hospital Clinico San Carlos, Madrid, Spain (ESC training grant 2015).

- Advanced imaging fellowship at University Hospital Leuven, Belgium (Autumn 2016).

Scientific Activities

- Co-chair of many sessions and evaluator of abstracts submitted for EuroPCR 2018-2019-2020.

- Grader of abstracts submitted for the World Congress of Cardiology 2018.

- Grader of clinical cases submitted for the ESC congress 2018-2019.

- JACC Cardiovascular imaging and Case Reports editorial board member.

Organizations

- EuroPCR faculty and EACVI-HIT member since 2017.

- ESC council on valvular heart disease and ESC council for cardiology practice member since 2018.

Grants and Awards

- EuroEcho Young Investigator Awards Clinical Science 2019.

- World Heart Federation Emerging Leaders Program 2018.

- European Society of Cardiology Training Grant 2015.

Languages

- Arabic (mother-language), English (fluent), Spanish (intermediate).

Acknowledgment

Thanksgiving to my supervisors; Dr. Martin Penicka and Dr. Guy Van Camp, for their guidance and insightful suggestions.

Special thanks to the coordinators of the PhD program; Dr. Bruno Trimarco and Dr. Emanuele Barbato, who have always supported me during the PhD course.

Apart from my mentors, I won't forget to express the gratitude to rest of the team: Dr. Jozef Bartunek and Dr. Marc Vanderheyden, Dr. Peter Geelen, Dr. Tom de Potter, for giving the encouragement and sharing research projects.

Warm thanks to all the nurses and the fellows in the Cardiovascular Center OLV Aalst with whom I have spent these years as one family.

I am grateful to my parents who remembered me in their prayers and to all my brothers and sister who always give me motivation and support.

In the end, this work was never done without support of Dr. Maurizio Galderisi who passed away last March. His generosity and leadership are hard to forget throughout my life.